Investigating Equine Host Barriers to Infection with Influenza A Viruses

Joanna Lorna Crispell

Submitted in fulfillment of the requirements for the Degree:

Doctor of Philosophy

School of Life Sciences

College of Medical, Veterinary, and Life Sciences

University of Glasgow

May 2018

Abstract

Influenza A viruses (IAVs) are significant pathogens of humans and animals whose main natural host is considered to be wild waterfowl. IAVs have jumped the species barrier on multiple occasions, sometimes with devastating consequences. Successful infection and onward transmission (i.e. viral emergence) requires highly specific interactions between virus and host proteins. However, how an avian virus adapts to a mammalian host to establish as a novel pathogen after initial interspecies transmission is not yet clear.

It was hypothesized that adaptation of an avian virus to mammals would involve changes in virus-host interactions that would result in more efficient viral replication and counteraction of immune responses. To test this hypothesis this thesis firstly describes the characterization of an equine dermal cell line (E.Derm) for the study of infection with EIVs. A panel of H3N8 AIVs was selected to investigate how equine host barriers affect the replication kinetics of distinct viruses. Finally, the transcriptome of the equine cells was investigated after infection with two evolutionary distinct H3N8 equine influenza viruses (H3N8 EIVs), and treatment with interferon-alpha (IFN-α). H3N8 EIV is an avian-origin virus that emerged in 1960s and has been circulating in horses for over 50 years, thus providing a natural model system to study the interspecies transmission and post-transfer adaptation of an avian influenza virus to a mammalian host.

To examine the cellular response to infection, equine dermal cells (E.Derm) were infected with either A/equine/Uruguay/63 or A/equine/Ohio/2003. Total RNA was extracted at 4 and 24 hours post-infection for RNA sequencing and downstream transcriptomics analysis. Mock-infected cells and interferon-treated cells were also included for comparison purposes. RNA-seq data were analysed using CuffDiff2 to identify differentially expressed (DE) genes between samples. Ingenuity Pathway Analysis was used to determine the intracellular pathways in which DE genes were involved. The results showed clear differences on the intracellular pathways affected between the viruses, which were especially evident during the eclipse phase of virus replication. Distinct intracellular pathways were identified as important for EIV adaptation to the horse, which in turn could be employed by other avian influenza viruses to establish in mammals.

Table of Contents

List of Figures

List of Tables

Acknowledgements

I would first of all like to thank my two PhD supervisors – Dr Pablo Murcia and Dr David Bhella – for guiding me through the PhD, and for inspiring me to work hard, as they both do. Thank you for all of your support throughout my time here.

I am very grateful to my two examiners – Professor Paul Digard and Dr Ed Hutchinson – for taking the time to read my thesis thoroughly, provide really helpful suggestions, and overall for putting in a lot of effort for my viva.

Thank you to all the members of the lab through the years: Fiona Thornburn, Alice Coburn, Caroline Chauché, Henan Zhu, Livia Patrono, Sema Nickbakhsh, Ilaria Piras and Julien Amat. I, of course, save Gaelle Gonzalez for last – not only because she was the best Postdoc ever, but also an amazing friend.

My time at the CVR was definitely made more-than-bearable thanks to the many wonderful people I met during my time there. For many helpful discussions, lending of reagents, teaching of methods, and general life sharing, thanks to Yasmin Parr, Eleonora Melzi, Idoia Busnadiego, Andrew Shaw, Swetha Vijayakrishnan, Filipe Nunes, Mariana Varela, Navapon Techakriengkrai, Matt Charman, Matthew Harris, Maxime Ratinier and so many more. I miss you all.

Also, a special thanks to Connor Bamford and Siobhan Petrie for facilitating all the public engagement opportunities, and helping me learn so many varying skills. It all eventually led me to where I am today.

Thank you to my family – for always checking in to see how I was doing, and for long phone calls while I plated cells. Mum, thanks for the "blue bag" full of goodies to open when I was feeling "blue". I still had some left at the end, either the PhD wasn't that bad or you just made too many.

Finally, thank you to the one person, who pushed me to finish this beast. I owe you so much, and I don't know how you put up with me over the years: always late meeting you after the lab, taking forever to write this thesis, eating far too much take-away... This PhD has been the most difficult thing I have ever done, but at least one good thing is I met you. Joe, it's finally over, let's go start life!

Author's Declaration

I, Joanna Lorna Crispell, declare that, with exception to where explicit reference has been made to the contribution of others, this thesis is the result of my own work and has not been submitted for any other degree as the University of Glasgow, or any other institution.

List of Abbreviations

Abbreviation	Meaning
IAV	Influenza A virus
H/HA	Haemagglutinin
N/NA	Neuraminidase
NP	Nucleoprotein
EIV	Equine Influenza Virus
CIV	Canine Influenza Virus
A549	Human alveolar epithelial
Vero	African green monkey kidney
DF-1	Chicken
MDCK	Madin-Darby Canine Kidney
E.Derm	Equine Dermal
IFN	Interferon
VSV-ΔG-GFP	Vesticular Stomatitus Virus - Δ Glycoprotein - Green Fluorescent Protein
DMEM	Dulbecco's Modified Eagle Medium
TPCK	Tosyl Phenylalanyl Choromethyl Ketone
AIV	Avian Influenza Virus
FACS	Fluorescence-Activated Cell Sorting
PBS	Phosphate Buffered Saline
DPBS	Dulbecco's PBS
ANOVA	ANalysis Of Variance
MOI	Multiplicity Of Infection
CPE	Cytophathic Effects
WSN	Influenza A/WSN/33
PFU	Plaque Forming Units
Mx1	Myxovirus Resistance Protein 1
BSA	Bovine Serum Albumin
HBLB	Horserace Betting Levy Board
SA	Sialic Acid
LPAI	Low Pathogenic Avian Influenza
NS1	Non-Structural
EIV/2003	A/equine/Ohio/1/03
CIV/2009	A/canine/New York/dog23/2009
EIV/1963	A/equine/Uruguay/1963
AIV/2009	A/ruddy shelduck/Mongolia/963V/2009
UI	International Units
FBS	Fetal Bovine Serum
NEAA	Non Essential Amino Acids
NGS	Normal Goat Serum
RPMI	Roswell Park Memorial Institute
ISG	IFN Stimulated Gene
DIPs	Defective Interfering Particles
RdRp	RNA-dependent RNA polymerase
RNA-seq	High-throughput RNA sequencing
DE	Differentially Expressed
FPKM	Fragments Per Kilobase of transcript per Million mapped reads
Log_2FC	Log_2FoldChange
RIN	RNA Integrity Number
MDS	Multidimensional Scaling
IPA	Ingenuity Pathway Analysis
eIF2	Eukaryotic Initiation Factor 2
PHH	Primary Human Hepatocytes
GO	Gene Ontology
PKR	Protein Kinase R
AFT	Activating Transcription Factor
ATCC	American Type Culture Collection
AHT	Animal Health Trust
L-glut	L-glutamine
RNA	Ribonucleic Acid
DNA	Deoxy Ribonucleic Acid
PAMPS	Pathogen Associated Molecular Patterns
HPV	Human Papilloma Virus

Publications

Contributed to, but not included in this thesis:

Gaelle Gonzalez, John F Marshall, Joanna Morrell (Crispell), David Robb, John W McCauley, Daniel R Perez, Colin R Parrish, Pablo R Murcia: *Infection and Pathogenesis of Canine, Equine, and Human Influenza Viruses in Canine Tracheas*. Journal of Virology, June 2014 **DOI:10.1128/JVI.00887-14**

Gaelle Gonzalez, Batchuluun Damdinjav, Henan Zhu, Livia Victoria Patrono, Humberto Ramirez-Mendoza, Joanna Crispell, Joseph Hughes, Toni-ann Hammond, Enkhtuvshin Shiilegdamba, Y.H. Connie Leung, Malik J. S. Peiris, John F. Marshall, Martin Gilbert, Pablo R. Murcia: Evolution hampers influenza emergence in horses despite frequent interspecies transmission from wild birds. (in preparation)

Chapter 1

1.General Introduction

1.1. Influenza A virus

There are three Influenza viruses that make up the *Orthomyxoviridae* family – A, B and C (classified based on the nucleoprotein and matrix segments). These viruses are enveloped, segmented, negative stranded with single-sense RNA genomes. The term *Orthomyxoviridae* actually comes from the word *orthos*, which means "standard, correct," and *myxa*, which means "mucus" (Cheung & Poon 2007).

Influenza was first identified as being the infectious agent of human influenza pandemics in 1933 (Smith *et al*. 1933), and has since continued to be a significant cause of disease within the human population. There are four types of influenza viruses – A, B, C and D. Influenza D virus was recently identified in 2011, and is found to infect sheep and cattle (Hause *et al*. 2014). Influenza B and C viruses primarily infect humans, but it is influenza A viruses (IAV) that are the most ubiquitous within both human and animal populations, and cause the more significant disease. This thesis will concentrate on IAVs and their interactions within one host in particular.

IAVs naturally find their hosts in wild birds, such as gulls and waterfowl and are the reservoir where most IAVs are thought to have emerged from. They are ubiquitously found in those populations, but often are non-pathogenic, meaning that they do not cause disease. In birds, IAVs normally replicate in cells lining the intestinal tract, and are excreted in high doses in faeces. This offers a source of infectivity to other animals via faecal pollution of water. Avian IAVs (AIVs) have evolved the ability to jump species barriers to infect mammals such as pigs, chickens, seals, whales, horses and humans (**Figure 1**).

IAVs are one of the most significant respiratory pathogens found in humans. There have been four major pandemics within the last 100 years, including the 1918 "Spanish flu", an H1N1 virus that is estimated to have led to the loss of as many as 50 million lives (Johnson & Mueller 2002), the 1957 H2N2 influenza, the 1968 Hong Kong H3N2 virus and, most recently, the H1N1 of swine-origin of 2009 (Morens & Fauci 2007). In conjunction with these pandemic strains, there are

always seasonal strains circulating within the human population, which currently are H3N2 and H1N1 subtypes. These influenza epidemics arise annually, occurring globally during the autumn and winter seasons for each region. One of the reasons that make IAVs such important pathogens is their ability to evade the host immune response to infection (Hay *et al*. 2001). This distinctive ability allows IAVs to cause pandemics as they are able to expand their host range and have much greater antigenic diversity. These influenza viruses are constantly undergoing antigenic shift and antigenic drift (explained in more detail later), and therefore require new vaccines every year (Salk & Suriano 1949; Kilbourne *et al*. 2002).

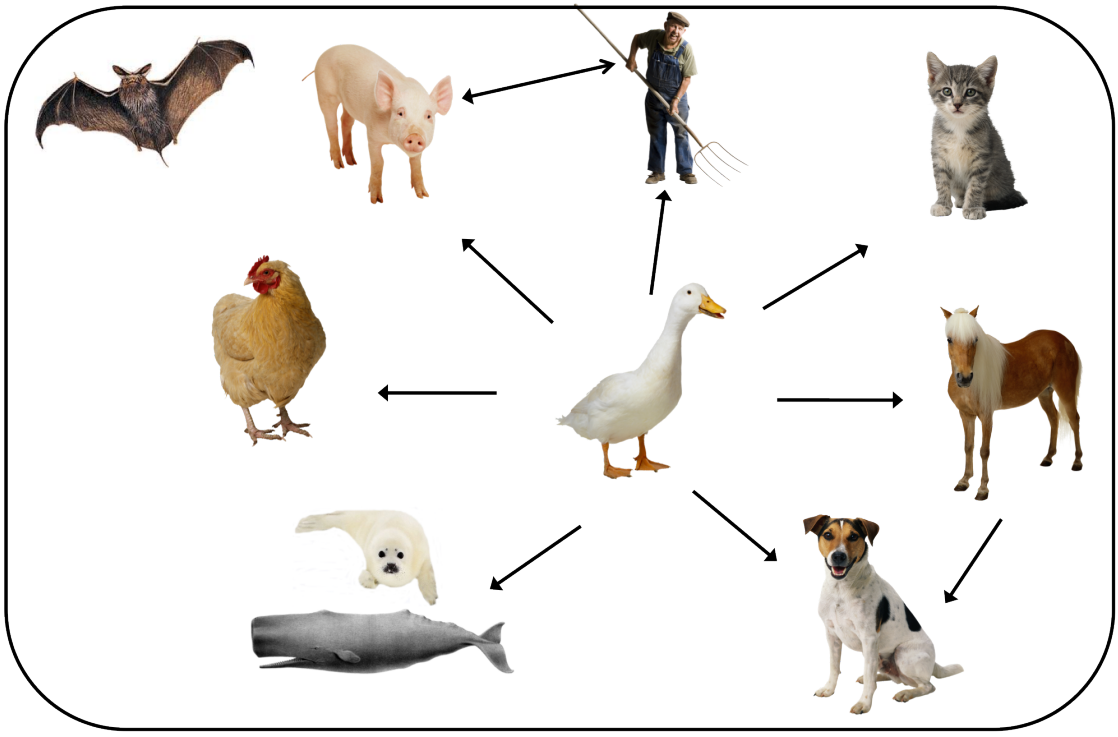

Figure 1: Schematic representation of IAV host range.

The antigenic differences within the glycoproteins Haemagglutinin (HA) and Neuraminidase (NA) of IAVs are used to classify them into subtypes. There have been 18 different haemagglutinin subtypes (H1-H18) documented, and 11 different neuraminidase subtypes (N1-N11) (Tong *et al*. 2013). Within the viruses that have sustained transmission within humans, only three HA (H1, H2 and H3) and two NA subtypes (N1 and N2) have been documented (Bouvier & Palese 2008). Avian influenza strains have been transmitted to humans on multiple

occasions, such as H5N1, H9N2 and H7N9 (Subbarao & Katz 2000; Gao *et al*. 2013).

1.2. Equine Influenza

It is believed that horses have been infected with Equine influenza viruses (EIV) for centuries, with the first EIV being isolated in 1956 of the H7N7 subtype. Consequently another H3N8 subtype crossed the species barrier from birds and was isolated in 1963. This new subtype became an established infection in horses, and within the next 15 years replaced the H7N7 subtype that had previously been circulating. The H7N7 EIV subtype is now assumed to be extinct among current horse populations as it has not been isolated since 1977, meaning H3N8 is the now the only circulating EIV within horses (Murcia *et al*. 2010). It is this H3N8 EIV that subsequently jumped the host species barrier and infected dogs (Daly *et al*. 2008; Payungporn *et al*. 2008). This phenomenon was recorded in the early 2000's, and was shown to be a whole virus jumping from horses to dogs.

There has been another documented incident of horses becoming infected with an H3N8 EIV (A/equine/Jilin/1/89). This outbreak occurred in 1989 in the Jilin and Heilongjiang provinces of Northeast China, with a high morbidity of 81%, and the mortality was as high as 20% in some herds (Guo et al. 1995). Another outbreak occurred in the following year of 1990 in Heilongjiang province with, 41% morbidity and no mortality. The viruses responsible for this outbreak were shown to be antigenically distinguishable from the circulating H3N8 subtype, and in fact the majority of the genes were shown to be of avian origin (Guo et al. 1992).

After much investment into vaccinating horses for EIV, it is still a virus that circulates globally and is constantly undergoing antigenic drift (discussed later in this chapter), meaning that the vaccine needs to constantly be updated. Therefore, this is a virus of importance due to the economic loss of racehorses not being able to perform when they are sick. The horse is also a good model to

investigate IAV evolution over time in a host, as the virus has been isolated since the beginning of the outbreak until present day.

1.3. Canine Influenza

The emergence of Canine Influenza Virus (CIV) dates back to 2004, when the virus was first isolated in racing dogs in Florida, US. This virus was shown to be an H3N8 EIV virus that had jumped the species barrier from racing horses to infect greyhounds (Crawford *et al*. 2005; Daly *et al*. 2008; Murcia *et al*. 2011).

The virus was shown to have a greater than 96% sequence identity with EIV and each of the eight segments were of equine origin, showing that the emergence of CIV had occurred as a result of direct transmission of the whole virus from horses to dogs, with no intermediate reassortment with other strains. The new CIV H3N8 continued to circulate in greyhounds and eventually spread to pet dogs mainly in shelters. H3N8 influenza virus has been also reported in Australia and the UK (Payungporn *et al*. 2008; Harder & Vahlenkamp 2010).

Transmission of a whole avian virus to a novel mammalian host is a rare event due to host species barriers. These include cell receptors for entry, the intracellular machinery necessary to replicate and spread successfully within host tissue, environmental barriers and host behaviour preventing contact between the two species (Kuiken *et al*. 2006). These barriers were overcome in 2006 when in South Korea an avian-origin IAV was first reported in dogs, which led to an outbreak in a small animal clinic that eventually showed 100% of animals to be seropositive for H3N2 (Song *et al*. 2008). This virus was experimentally shown to transmit to dogs that were contact-exposed to an infected H3N2 dog (Song *et al*., 2009). Four strains of avian-origin H3N2 CIV have now been shown to be prevalent in Southern China (Li *et al*. 2010) and recently a high seroprevalence of H3N2 was reported among dogs in North-eastern China (Su *et al*. 2013)

1.4. Structure of Influenza A Virus

Influenza A virions typically are 80-160 nm in diameter, with a genome that is around 13 kb in size. The genome exists as eight single-stranded negative-sense RNA segments that are encapsidated into ribonucleoproteins (RNPs), which consist of the viral RNA polymerase complex (PB1, PB2 and PA) and multiple copies of the viral nucleoprotein (NP). Each segment is numbered one through to eight depending upon its length (Noda *et al*. 2006). This genome encodes for at least 20 proteins that are currently known of (Pleschka 2013). The virion is composed of an outer lipid envelope that is formed from the host plasma membrane as the new virion exits the cell. Across the surface of the virion there are two glycoproteins: Haemagglutinin (HA) and Neuraminidase (NA), which are found in a ratio of approximately four to one (Lamb & Krug 2001). The membrane protein M2 is implanted within the lipid bi-layer, and the matrix protein (M1) is found underneath this layer and acts as a structural support for the virion. The M1 does this by interacting with the cytoplasmic tails of the glycoproteins in the plasma membrane, as well as the NP of the RNP (Rossman & Lamb 2011).

The proteins encoded by each of the segments are as follows: Segment 1 produces PB2 and PB2-S1 (encoded by a novel spliced mRNA (Yamayoshi *et al*. 2016)) ; Segment 2 encodes for PB1 but also has alternate open reading frames (ORFs) for the expression of PB1-F2 and PB1-N40; Segment 3 encodes for PA, PA-X (which has an alternative reading frame to PA) (Jagger *et al*. 2012), PA-N155 and PA-N182 produced by leaky ribosomal scanning and initiation from the 11th and 13th start codons, respectively; Segment 4 is HA, Segment 5 is NP; Segment 6 is NA; Segment 7 can undergo alternative splicing for protein expression and encode for five proteins M1, M2, M3, M4 and M42 (Jackson & Lamb 2008; Helen M. Wise *et al*. 2009); and finally Segment 8 contains two negative-sense ORFs encoding viral proteins NS1 and NEP, a novel donor splice site in NS1 which produces a novel influenza A viral protein NS3 (Selman *et al*. 2012), and an additional ORF in the positive-sense orientation that encodes a negative-sense protein (NSP/NEG8). However, all of these proteins are not expressed in all IAV strains (H. M. Wise *et al*. 2009). See **Figure 2** for virus structure.

Table 1: Summary of influenza A proteins (adapted from Pleschka 2013)

Segment Number	Protein	Function
Segment 1	Polymerase Basic 2 (PB2)	Cap-binding subunit of the viral RdRp; cap-binding
Segment 2	Polymerase Basic 1 (PB1)	Central location of the polymerase domain of the viral RdRp
	PB1-F2	Pro-apoptotic activity
	PB1-N40	Undefined
Segment 3	Polymerase Acidic (PA)	Cap-snatching endonuclease subunit of the viral RdRp
	PA-X	Endonuclease, cap-snatching
	PA-N155	Undefined, likely important in the replication cycle
	PA-N182	Undefined, likely important in the replication cycle
Segment 4	Haemagglutinin (HA)	Surface glycoprotein, receptor binding, membrane fusion, antigenic determinant
Segment 5	Nucleoprotein (NP)	Encapsidation of viral genomic and anti-genomic RNA
Segment 6	Neuraminidase (NA)	Surface glycoprotein, receptor destroying Neuraminidase

		activity, antigenic determinant
Segment 7	Matrix 1 (M1)	Matrix protein
	Matrix 2 (M2)	Ion channel activity, protecting HA conformation
	Matrix 3 (M3)	Undefined
	Matrix 4 (M4)	Undefined
	M42	Can functionally replace M2, differences in intracellular localisation
Segment 8	Non-Structural 1 (NS1)	Regulation of viral RdRp activity Interferon antagonist; Enhancer of viral mRNA translation; inhibition of (i) pre-mRNA splicing, (ii) cellular mRNApolyadenylation, (iii) PKR activity,
	Nuclear Export Protein (NEP), also referred to as NS2	Nuclear export factor
	Non-Structural 3 (NS3)	Provides replicative gain-of-function
	Negative Sense Protein (NSP/NEG8)	Undefined

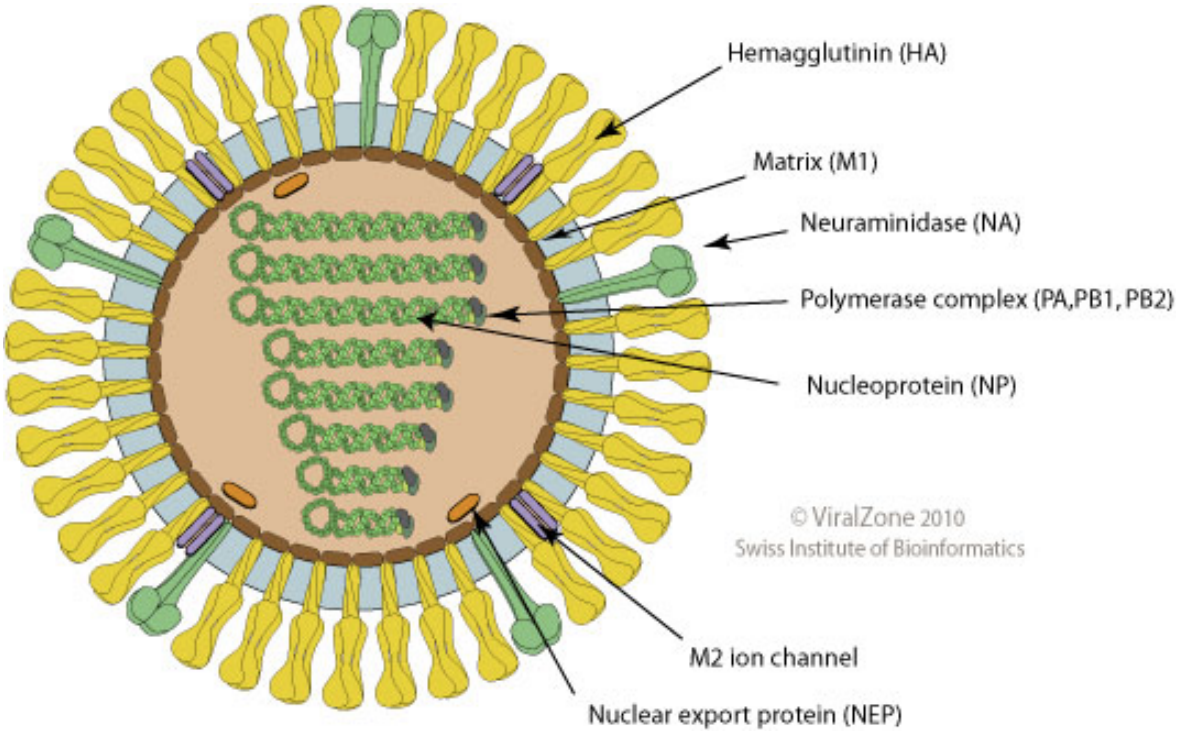

Figure 2: Influenza A virus structure. NS1 is not included in image, but may be a structural protein. (Source: ViralZone:www.expasy.org/viralzone, SIB Swiss Institute of Bioinformatic).

Influenza is a pleomorphic virus, meaning that it can either present itself in long filaments or small spherical particles. The functional explanation for both forms has not been discovered but filaments are usually observed for virus taken from clinical samples, whereas the spherical morphology is observed for virus of influenza strains that have been passaged in the laboratory (Choppin *et al*. 1960). The fact that filamentous influenza seems to be selected for in nature, but reverts to spherical or ovoid particles when passaged in culture suggests that filamentous forms have an advantage and are selected for. A recent paper (Seladi-Schulman *et al*. 2013) compared the serial passaging of filamentous virions, in both eggs and MDCK cells, with the spherical laboratory strain A/PR8/8/34 (PR8) in guinea pigs. They showed that the passaging of filamentous virus in culture led to a loss of filaments, while the virus serially passaged in guinea pigs resulted in a selection of the filamentous form. These findings imply that filamentous variants have a selective advantage in nature.

1.5. Influenza A virus replication

The IAV life cycle begins when the virus particles first bind to the apical surface of the target epithelial cells (**Figure 3**). This interaction occurs between the HA glycoprotein spike on the surface of the virus, and specific N-acetylneuraminic (sialic) acid residues found on the cell membrane (Whittaker & Digard 2006). Depending upon the virus these can either be α-2,3- or α-2,6-linkages (Cheung & Poon 2007; Bouvier & Palese 2008). AIVs preferentially bind to α-2,3-linkages, and for birds such as ducks and wild waterfowl, these are predominantly found in the gut epithelium. For human IAVs, the more commonly preferred linkages are α-2,6, which are found in the respiratory tract. However, α-2,3-linkages are present in the lower respiratory tract, meaning that if a human does get infected with an AIV the infection can be much more severe (Lee & Saif 2009; Neumann *et al*. 2009). Pigs are referred to as "mixing vessels", as the trachea of a pig contains both α-2,3 and α-2,6-linked sialic acids, meaning that there is a possibility they could be co-infected by human and avian IAVs potentially allowing for virus reassortment (Ito *et al*. 1998; Wright *et al*. 2007).

After the virus binds to the cell, the virus particle is internalised by receptor-mediated endocytosis (**Figure 3**). The resulting endosome has an increasingly low pH environment due to regulation by proton pumps. The HA glycoprotein undergoes a conformational change when it reaches a low enough pH. This change allows the fusion peptide to mediate the fusing of the endosomal membrane and viral envelope. At the same time the ion channel activity by M2, manages the flow of protons into the virion from the endosome to lower the pH (Pinto *et al*. 1992). This acidification of the inside of the virion disrupts the protein:protein interactions of the RNPs and M1, and at the same time disrupting the interaction of HA and M1. The dissociation of the proteins is what causes the passage of the RNPs into the cytoplasm (Lamb & Pinto 2006). The NP nuclear localization signal promotes the import of the vRNPs into the nucleus, which would have been inhibited by M1, and so dissociation from M1 is important. The RNPs are imported into the nucleus through the nuclear pore complexes, which is promoted by the nuclear localization signal (NLS) of NP.

Unusually, the synthesis of influenza virus RNA takes place in the nucleus of an infected cell. This nucleus-based synthesis is rare for most RNA viruses. An explanation for it could be that for viral mRNA synthesis, IAVs require the capped 5' ends of host mRNAs to act as primers to initiate viral mRNA synthesis (Plotch *et al*. 1981). However, *Bunyaviridae* are also RNA viruses with segmented, negative sense genomes, yet replicate in the cytoplasm. The reason for this is that they do not generate spliced mRNAs, unlike *Orthomixoviridae* that require localisation in the nucleus to facilitate splicing (Guu *et al*. 2012).

Viral replication involves three different types of viral RNAs: viral mRNA (mRNA), viral genomic RNA (vRNA), and complementary RNA (cRNA). The initial RNA is used as a template to produce complementary positive-sense cRNA and negative-sense vRNA. The negative-sense vRNA is used as a template to synthesize the cRNA, and from this the RNA polymerase transcribes negative-sense genomic vRNA.

The viral ribonucleoprotein (vRNP) is comprised of a core of NP copies, around which the vRNA is helically wrapped. Each vRNP is also made up of a heterotrimeric RNA polymerase complex, consisting of PB1, PB2 and PA. The synthesis of viral RNA is carried out by the RNP, which is made up of the four viral proteins PB2, PB1, PA and NP (Portela & Digard 2002). The viral RNA (vRNA) is transcribed to mRNA via the RNP, together with the acquisition of a 5' capped RNA that is snatched from the host (Plotch & Krug 1977). During mRNA synthesis, the polymerase binds to the 5' end of the vRNA segment and so induces the cap-snatching activity of PB2. This cap-snatching activity happens as the viral polymerase binds to host mRNAs, which triggers cleavage of the of the host mRNAs allowing for the retention of the 5' host cap structure (Li *et al.*, 2001). The snatched host cap performs as a primer for the initiation of viral transcription, which is mediated by the viral polymerases, more specifically the interaction of PB2 with the host cap structure, and elongation of the RNA by PB1 (Elton *et al.*, 2006).

The vRNPs are formed in the nucleus from the newly synthesised proteins and are transported into the cytoplasm. The vRNPs are exported out of the nucleus through the nuclear pores by the formation of a vRNP-M1 complex. The mRNA transcripts must be trafficked from the nucleus to the cytoplasm for translation into proteins by ribosomes. However, the segments that require splicing to produce more than one protein, for example NS1 and NEP, must be spliced before exiting the nucleus.

The encapsidation of the vRNPs is controlled by discrete packaging signals, and it has been revealed through electron microscopy that the segments are selectively incorporated into each budding particle as seven segments always surround one central segment (Noda *et al*. 2006). A new viral particle must contain all eight genome segments to be infectious.

HA, NA and M2 proteins are targeted to the plasma membrane, with HA and NA being incorporated into lipid raft structures on the cell membrane. Virus budding from these rafts means that the new virions contain HA and NA surface glycoproteins. The viral budding is initiated by M1 accumulating in the cytoplasm of the cell membrane via association with the tails of HA and NA.

After the viral replication is finished, the virus must exit the host cell. It does this through budding from the cellular membrane (**Figure 3**) by using lipid raft domains in the plasma membrane of infected cells. These are sites of virus assembly and budding, and are intrinsically linked to the glycoproteins HA and NA. The role of NA is very important in that it facilitates the cleavage of the sialic acids on the surface of the cell. Without the action of NA the budding viruses would stick to the infected cells, and each other, and wouldn't successfully infect neighbouring cells. The anti-influenza drug oseltamivir acts as a neuraminidase inhibitor and blocks this action, decreasing virus replication efficiency.

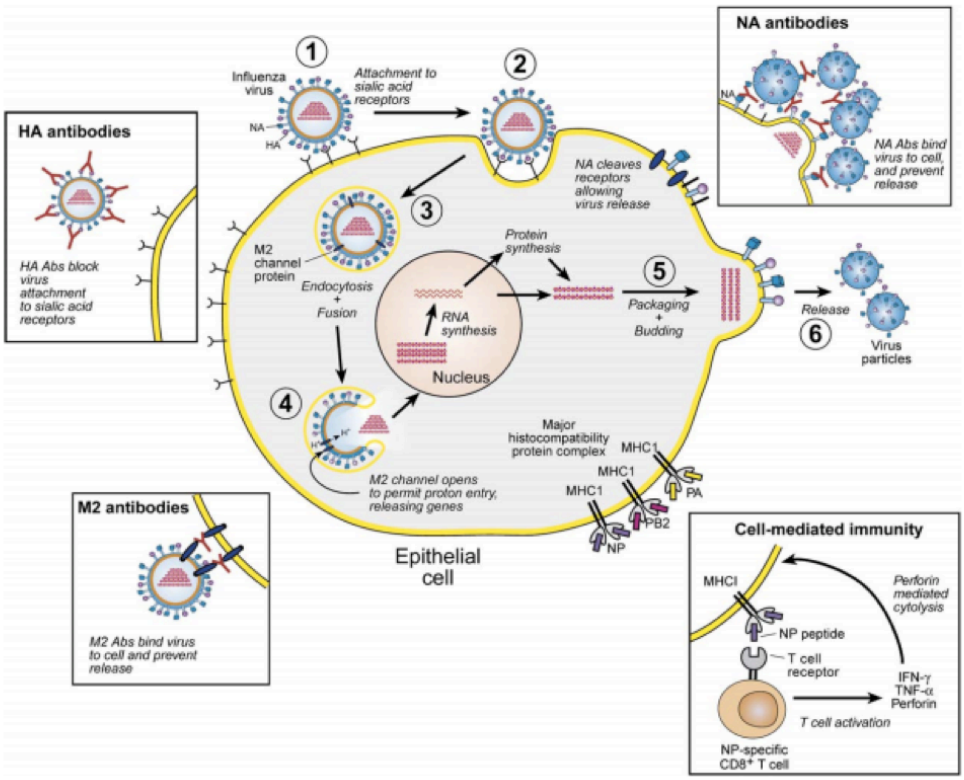

Figure 3: Life Cycle of Influenza A Virus. Adapted with permission (21).

1.6. NS1 protein and immune response

The non-structural protein 1 (NS1) of IAVs is not a structural component of the virion, as its name suggests (Marc 2014). It is expressed in high quantities in infected cells, and is a virulence factor with many different functions. NS1 acts by suppressing the host immune response (Lu et al. 1995; Krug et al. 2003) regulating viral RNA synthesis, and enhancing viral mRNA translation. Although NS1 is the main antagonist of the IFN response, studies have shown that other parts of the IAV genome also contribute to this function (Weber-Gerlach & Weber 2016).

The NS1 protein is ~26 kDa, and depending upon the strain of IAV the majority have a length varying from 230-237 amino acids, some, which will be discussed in more detail shortly, are shorter than this (Lamb & Krug 2001). For the other influenza A viral proteins (PB1, PB2, PA, NP, M, HA and NA), there isn't much difference between the charge for these proteins among different strains. However, avian and human NS1 proteins have different charges, with AIV NS1s

being principally acidic, whereas human NS1s are usually basic (Petri *et al*. 1982).

The structure of NS1 is composed of two structural domains: the N-terminal RNA-binding domain (residues 1–73) and the C-terminal effector domain (ED) (residues 74–230). The RNA-binding domain is involved in the inhibition of IFN induction, and its antiviral effects. The C-terminal contains a PDZ domain ligand while the ED controls interactions with host-cell proteins. The final 25 residues form a "disordered tail (Hale, Barclay, *et al*. 2008).

The NS1 is almost indispensable to the virus, as it has been shown that replication is greatly reduced when mutations are introduced into the NS1 gene, and this is especially apparent if these affect the RNA binding domain (Krug et al. 2003). The expression of NS1 by itself appears to have a negative affect on the host cell, which has been shown when trying to establish cell lines that constitutively express NS1 (van Wielink et al. 2011). However, NS1 also acts in very specific ways. The host IFN response is antagonised by NS1, through inhibition of the antiviral defences of infected cells. NS1 functions by limiting both the production and downstream effects of IFN. It does this by first preventing the activation of RIG-I, which would usually begin the cascade of the antiviral response after being activated by the presence of dsRNA (Randall & Goodbourn 2008). It also blocks the RIG-I signal transduction pathway by interacting with TRIM-25 and inhibiting RIG-I ubiquitination (Gack *et al*. 2010). NS1 also affects another important constituent of the immune response, protein kinase R (PKR), by preventing its activation (Gale & Katze 1998). These mechanisms lead to failings in the activation of the IFN system, which in turn prevents transcription factors such as NFkB and the family of IFN regulatory factors (IRFs) being translocated to the nucleus (Ulfert *et al*. 2014). NS1 has also been shown to limit IFN-β by inhibiting the post-transcriptional processing of cellular pre-mRNAs. This inhibition occurs through the binding of NS1 to the 30kDa subunit of cleavage and polyadenylation specificity factor (CPSF30), which stops cellular proteins from binding pre-mRNAs (Kochs *et al*. 2007). The binding of pre-mRNAs inhibits the correct cleavage and polyadenylation of the host

mRNAs. The pre-mRNAs can also be retained in the nucleus and can rapidly degrade, a process also controlled by NS1 (Katze & Krug 1984).

The other way that NS1 is able to antagonise the IFN response is through downstream action, by directly inhibiting the effects of the activated IFN system. NS1 sequesters the viral dsRNAs, which prevents the activation of the antiviral defences in the cell. The NS1 protein also has a role to play in the host apoptotic response to infection. IAVs induce cell death in two ways: by apoptosis and, depending on the cell type, by necrosis. Apoptosis can be triggered in infected cells by intrinsic responses within the cell, however neighbouring uninfected cells are also induced into a state of apoptosis. It is regarded that apoptosis is part of the antiviral defence to infection with a virus, as it prevents virus replication within the host cells. However, the role of apoptosis in IAV replication is complicated, as some pro-apoptotic molecules have been shown to allow for the replication of IAVs (Wurzer *et al*. 2003). It may that the virus requires a balance of the pro-apoptotic signals. If apoptosis occurs early during virus replication this may stop virus replication, however apoptosis later within the cycle may actually benefit the virus by clearing infected cells that would stimulate the host adaptive immune response. NS1 has been shown to both promote and prevent apoptosis, and may differ depending on viral strain. However, NS1 has been shown to interact with the phosphoinositide 3-kinase (PI3K) signalling pathway and delay apoptosis induced by viral infection (Hale *et al*. 2006).

The NS1 protein is most often composed of 230 amino acids, however there are viruses that exist as shorter or longer than this (Hale, Randall, et al. 2008). For example, the NS1 of the pandemic H1N1 of 2009, has only 219 aa, whereas the NS1 of human IAVS from the late 1940s until the mid-1980s had an additional 7 aa. The NS1 of EIVs has been shown to evolve over time during replication in its equine host (Barba & Daly 2016). One of the significant changes that occurred to EIV during its adaptation to the horse was the introduction of a stop codon, which introduced an 11 amino acid truncation in NS1. This truncation occurs in the C-terminal region, and leads to viral attenuation due to

lack of ability to block host gene expression, which allows for the presence of higher levels of type I IFN (Kochs *et al*. 2009; Solórzano *et al*. 2005). When looking at the early H3N8 CIV viruses, they had a truncated NS1, which is understandable as they were directly descent from the EIVs circulating at the same time. However, since 2005 all H3N8 CIV viruses have been shown to possess the full-length NS1 (Rivailler *et al*. 2010). The evolution of the canine NS1 may be as a direct result of the virus adapting to a new mammalian host.

1.7. Virus evolution

Influenza A viruses are viruses that can evolve rapidly due to the error prone RNA polymerase. Within wild aquatic birds, which is their natural reservoir, there doesn't seem to be such rapid evolution and in fact what could be termed as static (Robert G Webster *et al*. 1992). However, as an IAV infects a new host it will encounter host antibodies that target the surface glycoproteins. This can drive amino acid changes to the antigenic sites present within HA and NA (Wright *et al*. 2007). The accumulation of these point mutations leads to a process known as antigenic drift.

Antigenic drift happens due to the lack of proof reading by the RNA polymerase of the virus, leading to mutations such as substitutions, deletions and insertions (Robert G Webster *et al*. 1992). If these point mutations occur and affect the antigenic sites of the virus, they can eventually lead to the virus evolving until it cannot be recognised by the host immune response. This antigenic drift is the reason that the seasonal influenza vaccine needs to be constantly surveyed and updated. Historically, the influenza vaccine was a trivalent vaccine against the H3N2 and H1N1 influenza A subtypes, and an influenza B subtype. However, since 2012 a quadrivalent vaccine has been available that covers an extra influenza B subtype. The rationale behind this change was that with the inclusion of only one influenza B subtype, meant that people were left exposed to (Ambrose & Levin 2012).

Antigenic shift happens when reassortment occurs, due to the segmented nature of IAVs. When a single cell is infected with more than one type of IAV, the segments can assemble to produce a new virion during viral replication. The resulting virus consists of a mixture of genetic information from both parental viruses, and can expose a host to antigenic proteins for which there may be no pre-existing immunity. In the recent swine H1N1 pandemic virus, this is what occurred. Pigs, which are commonly referred to as "mixing vessels" due to the presence of both α-2,3 and α-2,6-linked sialic acids, are believed to have been the source of the swine pandemic H1N1 outbreak of 2009 when two viruses reassorted and produced a new virus to which the human population was antigenically naïve.

1.8. Interferon signaling

When a cell becomes infected with a virus, a vertebrate host has two countermeasures with which to defend itself: the innate and the adaptive immune systems. The adaptive immune system is highly specific to infection, contrary to the innate immune system that is non-specific. The other difference is that the adaptive immune response is much slower and can sometimes take up to a week to be effective, whereas the innate immune response can act immediately or within a few hours of cells becoming infected with a pathogen (Alberts *et al*. 2014). One of the most important aspects of the innate immune response is the interferon (IFN) system, which was first documented in 1957 as a substance, likely produced by cells, that interferes with influenza infection (Goodbourn *et al*. 2000; Randall & Goodbourn 2008; Isaacs & Lindenmann 1957). There are three types of IFN: type I, II and III, and in humans, type I IFNs include IFN-α, IFN-β, IFN-ε, IFN-κ, and IFN-ω to name a few. The roles of IFN-α and IFN-β have been shown to be induced in response to viral infections, whereas the other type I IFNs are less well known but have been thought to be associated as regulators of maternal recognition in pregnancy. It has been known for a long time that several genes control IFN-α and IFN-β, but it is still unclear how the genes are expressed differentially in separate cell types, and whether they are induced by distinct viruses or whether they are functionally specialized.

Type II IFN has a single type: IFN-γ, and the type III IFNs consist of three types of IFN-λ (Ank *et al*. 2006). The IFNs are not only responsible for the innate immunity, but also the adaptive immune response. The production of these cytokines begins when a cell recognizes that it has been infected by a foreign pathogen, by Pathogen Associated Molecular Patterns (PAMPs). The cells secrete these IFN cytokines, and when they reach other neighbouring cells initiate intracellular signaling cascades. The IFNs bind to specific receptors on the cell surfaces, which leads to the upregulation of many Interferon Stimulated Genes (ISGs) that have antiviral properties. The type III IFN receptor appears to be limited in its distribution in tissues (Zhou *et al*. 2007). Type I and type III IFNs lead to the same signaling pathways becoming upregulated, whereas type II IFN is different. Type III IFNs and their role remains to be completely established and so far there is limited evidence supporting whether they have an essential role for host response to infection. The signaling cascade caused by the IFNs leads the cells to develop into an antiviral state (Hoffmann *et al*. 2015). There also exists a number of ISGs that can be directly upregulated by viral infection in an IFN-independent fashion. This method offers certain protection to the primarily infected cells, although this is less effective than the full IFN response.

Some viruses, such as IAVs, consist of an RNA genome, and so host cells must consist of a way to discriminate and recognize foreign RNA from host RNA. Early studies suggested that IFN was induced by synthetic double-stranded (ds) RNAs (such as Poly(I:C)), leading to the conclusion that viral dsRNA could lead to the induction of IFN (Marcus & Sekellick, 1977; Marcus, 1983). The recognition of viral dsRNA as a host defence mechanism is effective as negative-stranded RNA viruses generate dsRNA upon transcription, positive-stranded RNA viruses generate dsRNA during replication, and even DNA viruses generate dsRNA as a result of convergent transcription. RNA viruses also produce 5′-triphosphorylated single-stranded (ss) uncapped RNAs during the replication of their viral genome. These PAMPs are detected by pattern recognition receptors (PRRs) as “non-self RNA”, for exampled Toll-like receptors (TLRs) and melanoma differentiation-associated gene-5 (MDA-5) or retinoic acid-inducible gene-I (RIG-I) (Goodbourn *et al*. 2000; Randall & Goodbourn 2008). TLR3, TLR7 and TLR9 are endosomal, allowing for the detection of dsRNA during virus endocytosis. The other TLRs are

largely found in antigen-presenting cells, such as dendritic cells (Schaefer *et al.*, 2004). RIG-I and MDA-5 are expressed in many different cell types, and can detect many different classes of RNA viruses as short and long dsRNA are recognized by each PRR respectively. When a cell is infected with an IAV, MDA-5 is less important, whereas RIG-I is critical (Kato *et al.*, 2006).

When RIG-I binds viral RNA this begins a process of activation, leading to the turning on of downstream signaling pathways. The N-terminus of RIG-I is polyubiquitinated by TRIM25 (tripartite motif-containing protein 25), which is an E3 ubiquitin ligase that is necessary for activation (Zeng *et al.*, 2009). When RIG-I binds to RNA it undergoes a conformational changed that exposes the tandem caspase activation and recruitment domains (CARD), which lead to multimerization and interaction of the CARD domains of MAVS (mitochondrial antiviral signaling protein) (Saito *et al.*, 2007). This leads to the activation of interferon regulatory factor 3 (IRF-3) and nuclear factor κ-lightchain-enhancer of activated B cells (NF-κB) and they translocate to the nucleus where they turn on the promoter of the IFN-α/β gene to initiate the synthesis of IFN-α/β (Randall & Goodbourn 2008).

IFN is also important for inducing a pro-apoptotic state within a target cell (Goodbourn *et al*. 2000) The apoptosis of an infected cell allows for its removal and attempts to stop the spread of infection. Viral dsRNA can activate genes such as PKR (Gale & Katze 1998), which can affect apoptosis. PKR can be involved in apoptosis through the eIF2α-dependent pathways (Scheuner *et al*. 2006). However, dsRNA alone can activate apoptosis through the formation of a complex that leads to the cleavage of procaspase-8 into its active form. The well-known apoptotic p53 gene can also be triggered by IFN, or can also be triggered directly by dsRNA or virus infection (Goodbourn *et al*. 2000). IFNs also induce a growth arrest within cells, causing suppression of cell growth.

When IFN binds to a receptor of a cell, a signal is transmitted through the membrane and into the cell, setting off a cascade of events. The changes within the cellular properties occurs strikingly quickly, and the reason for this is that many of the necessary components are already constitutively expressed and so

the synthesis of new proteins is not immediately required (Larner *et al*. 1986). All IFNs use the JAK-STAT pathway through which to signal. There are four known JAKs, of which three are ubiquitously expressed within the cell. The role of the JAKs is to bind receptor chains on the inner side of the membrane and to give the receptors stability, enable them to be localized to the cell surface and most importantly, they are crucial components of the signaling pathway (Ragimbeau *et al*. 2003). When the IFN receptors are not in the presence of a stimulus, the cytoplasmic domain of each chain is attached to a JAK protein in its inactive state. When IFN molecules bind with the receptors, the chains are brought close together causing the two JAKs to undergo transphosphorylation and activation. After activation, JAKs phosphorylate the IFN receptor chains and begins binding STAT proteins. Consequently, this leads to phosphorylation of the STATs and are released from the receptor. In mammals, there are seven STAT proteins that exist. However, it has been shown that STAT1 and STAT2 are the most important when it comes to IFN signaling through the receptor complexes. Type I and III IFN signaling leads to the phosphorylation of both STAT1 and STAT2, with heterodimerization and interaction with IFN regulatory factor (IRF) 9. Together they form the ISG factor 3 (ISGF3) complex, which translocates to the nucleus where it binds IFN-stimulated response elements (ISRE) present in the DNA upstream of ISGs and results in the transcription of many type I and type III IFN signaling ISGs. Those upregulated ISGs have many different roles, with some having direct antiviral activity such as interferon inducible transmembrane (IFITM) proteins. These work by inhibiting a virus from entering the cell by controlling membrane fluidity. However, some of the ISGs act on the IFN signaling pathways themselves and control them by positive or negative regulation. IRF3 and IRF7 lead to the induction of more IFN, and results in a positive feedback loop. Contrary to these ISGs, there are others that act as negative regulators if IFN induction, such as activating signal cointegrator complex 3 (ASCC3), which functions to modulate ISG expression in an IRF-3- and IRF-7-dependent manner (Li *et al*. 2013). It is important that there are ISGs modulating the IFN response, because an excessive induction of ISGs could eventually lead to damage of the host, as is apparent in patients who suffer from excessive immune activation, which occurred to some of those infected during the 2009 pandemic H1N1 outbreak.

1.9. Importance of cell lines

As IAVs are viruses, they are defined as obligate intracellular parasites, in that the requirement of a host cell for replication is essential. As has already been discussed in this chapter, there are many intrinsic antiviral defences that a virus has to overcome to replicate successfully. For example, viruses must first overcome physical barriers such as the presence of mucus within the respiratory tract before locating the cells with the correct receptors for virus binding. When the virus does enter the host cell, it is then faced with the innate immune response, including the production of IFN in response to pathogen invasion. It is critical that the virus has a way to antagonise this response to allow for replication, and in the case of IAVs the protein that is mainly important for this is NS1. The initiation of the IFN response is controlled by PRRs, that can respond to low-level infection. Therefore, only cells that comprise of intact antiviral pathways are able to respond to infection and mount an antiviral defence. It is possible that cells can retain the property of responding to IFN-I, and viruses that are potent IFN-I inducers (for example, Sendai virus (SeV), or synthetic dsRNA (such as polyinosinic-polycytidylic acid (Poly I:C)) but lose their ability to respond to low levels of viral infection.

It is important that an *in vitro* cell system should be convenient and physiologically representative of the cells infected *in vivo* (Hare *et al*. 2016). There are different methods to produce a cell line for *in vitro* studies, including using primary cells and immortalised cells. However, both of these methods have negative factors. Primary cells can better represent cell from the original tissue, because they have not been passaged continually in tissue culture leading to mutations and change of phenotype. However, they are a difficult system to work with as primary cells are limited in how many times they can be doubled, and close to senescence (when cells undergo replicative arrest) by the time the selection of the cell population is complete. There are also examples showing that cells at later passages produce a higher basal level of IFN-β, and therefore produce an unrealistic stronger IFN response when infected with a virus (Reddel 2010). Therefore, these changes can affect the results when studying virus-host interactions, and it makes it crucial to study experiments with cells at the same passage so as to account for these changes. Primary cells are also notoriously

difficult to transfect, making it difficult for experiments that require exogenous gene expression. Therefore, primary cells are problematic to work with and another system is usually required.

However, transforming cells leads to a continual culture of cells that don't necessarily resemble the phenotype of the original cell. Tumourigenesis and the process of continually culturing cells lead to a collection of mutations that change how the virus and host interact. The reason for this is that some of the cellular pathways that are involved in antiviral defence and tumour suppression are shared. It has been shown that cells that lack antiviral genes are easier to immortalise in cell culture, and so immortalisation of cells is often accompanied by a loss in response of virus invasion (Chen *et al*. 2009). The fact that tumour suppression and antiviral defences are linked, also leads to the fact that cells that are deficient for tumour suppressors are also more susceptible to virus infection (Munoz-Fontela *et al*. 2005).

The research described in this thesis explains the characterization of an equine cell line for the relevant study of influenza infection. It was important to find a cell line that was appropriate for the study of EIVs and their interaction with an equine host cellular response. MDCKs (Madin-Darby Canine Kidney Epithelial Cells) are the most widely used cell type for *in vitro* experiments with IAVs. However, they are not appropriate for studying the virus-host interactions for a number of reasons. When MDCKs were first shown to be infected by IAVs, it was discovered that they were permissive to infection with a wide range of influenza viruses (Gaush & Smith 1968). MDCK cells also require the addition of an exogenous protease to facilitate the cleavage of the glycoprotein HA in order to produce a mature virion (with the exception of WSN influenza virus). With the addition of an exogenous protease, it means that natural host protease barriers to infection cannot be investigated (Seitz *et al*. 2012). Another finding described in the literature is that in MDCK cells the IFN response is a weak restrictive factor for the replication of IAVs, which is partly caused by a deficiency of anti-influenza activity by the canine Mx proteins (Seitz *et al*. 2010).

Overall, while MDCK cells are very efficient at growing almost all IAVs, and producing very high virus titres, the cell line is not physiologically relevant to study host-virus interactions in relation to IAVs. Therefore, when studying the host barriers to infection, is it important to select a cell line that best reflects the composition of the host organism. Cells must have a preserved innate antiviral response, and be sufficiently sensitive to stimuli. One of the chapters in this thesis concentrates on characterizing an alternative cell line for the investigation of equine host barriers to infection with IAVs.

1.10. Ex-Vivo Organ Culture Systems

The most commonly used practice in laboratories are *in vitro* studies that attempt to study viral evolution, pathogenesis and the immune responses to the host in the artificial context of cells grown in wells. This allows for the discovery and research of many new areas but sometimes *in vivo* studies are necessary to provide the full scientific answers required for these questions. However it is crucial in the use *in vivo* studies to justify the use of animals in research and can often lead to the criticism from animal welfare groups.

Therefore the majority of experiments occur *in vitro*, which are not ideal models due to absence of cell polarity and pseudostratification of the cell layers. This becomes an issue when studying pathogens that infect pseudostratified epithelium such as Human Papilloma Virus (HPV) or, as in this study, influenza A virus. When studying the influenza infection, which naturally infects tracheal tissue, using *in vitro* methods sometimes means that cilia and microvilli can be absent, although they are ndpresent for cells such as MDCKs. A major contrast between *in vitro* and *in vivo* is that there is no air interface with the infected cells.

The other shortcomings of *in vitro* methods are also that the cell lines used have been severely mutated to become “immortalized” cell lines and so are abnormal. They may also be cells lines from an entirely different species,

not from the host species, and are usually located from a different type of tissue than that of which the virus normally infects.

An excellent alternative to these problems with *in vitro* methods is to use an *ex vivo* organ culture (EVOC) system, which takes the tissue of interest from the organism and keeps it as close to natural conditions as possible. These EVOC systems allow for the reduction of animals in research, as part of the 3Rs framework (Zurlo *et al*. 1996). In previous studies tracheal explants have been used to study swine influenza pathogenesis (Nunes *et al*. 2010). Each trachea is split into many small explants, meaning that numerous experiments can be carried out from the one animal, greatly reducing the number of animals used as compared to those needed for the same study using *in vivo* methods. It is also important to note that when experiments with pathogens are carried out *in vivo* in animals, the side effects of the infections can be unpleasant, whereas this can be avoided through use of EVOC. The variability between animals is also decreased as the same animal phenotype can be guaranteed.

The EVOC system therefore is a good alternative, providing the compromise between *in vitro* and *in vivo* methods, presenting tissue pseudo-stratification, along with important features like receptors and cilia, to be preserved for at least seven days. Another similar system that had been previously optimized by Jackson *et al*. (Jackson *et al*. 1996) was used to study human nasal turbinate tissue with an air interface, was able to keep the nasal tissue alive and healthy for 20 days. This was better than previous traditional methods that fully immersed the tissue in medium, which interfered with the natural processes of infection. These systems, along with many others (Jang *et al*. 2005; Priestnall *et al*. 2009), can be used as experimental platforms to bridge the gap between *in vitro* and *in vivo* methods. This thesis will only briefly look at an experiment within the EVOC system, but is worth noting as the future work expanding upon this thesis could make use of the system much more readily.

1.11. Transcriptomics

There has been a recent increase in the research field of "omics". This includes genomics, proteomics and transcriptomics. There are many positive and negative reasons to each technique. For example, proteomics provides a much more definite picture of what is happening inside a cell through the study of the proteins but is limited due to expense and availability of mass spectrometers. Transcriptomics studies the transcripts present within a cell, but that does not necessarily mean that these transcripts will be translated into proteins. However, as it is more readily available and is a reliable technique, this chapter will focus on the use of transcriptomics to study equine cellular pathways.

Transcriptomics used to be carried out most of the time using qPCR. However, as it has a limited output it isn't suitable for genome-wide studies. Microarrays followed after qPCR, as it allowed for the expansion to study thousands of genes using DNA probes. It is important to note that this can produce a more biased result than RNASeq, as the DNA probes can produce a level of selection for the genes that the researcher is interested in. On the other hand, RNASeq amplifies all of the RNA within a cell, and so allows for a more critical analysis of which genes are differentially expressed.

There are a few different tools that can be used for *in silica* analysis of RNASeq data, some of these being edgeR, DeqSeq and CuffDiff2 (Robinson *et al*. 2009; Trapnell *et al*. 2013). Each one runs with a slightly different pipeline, with edgeR and DeqSeq using count based methods to measure the level of expression of RNA. However, CuffDiff2 uses an alternative method of mapping the RNA-seq reads to a reference genome, and then calculates the transcript abundance to produce an output defined as: Fragments Per Kilobase of transcript per Million mapped reads (FPKM). The FPKM value for the combined replicates of each condition is compared to the FPKM value of the Mock-infected cells. This comparison allows the calculation of the fold change in the gene expression, which is reported as the Log_2FoldChange (Log_2FC). There should be less false positives when using CuffDiff2, as the pipeline controls for cross-replicate variability. Each differential expressed gene is given a statistical significance,

which allows for the creation of thresholds to decide upon what level of expression within the genes that should be studied. Studies have been carried out to compare the different pipelines, and depending upon the data available some will be more suitable than others (Zhang *et al*. 2014). However, as this is still a relatively novel technique, there is still a lot more research required into the different pipelines and how they are beneficial. For the purposes of this thesis, the CuffDiff2 pipeline was selected to study the RNASeq data.

1.12. Conclusion

Influenza A is a complex virus that has managed to evolve so as to overcome the species barrier and infect different hosts many times in history. The recent jump of EIV from horses to CIV in dogs shows how the virus is still constantly changing. The H3N8 subtype is especially interesting as it has managed to cross the host species barrier twice to infect horses, and has infected other mammals as well. As there was much surveillance of horses before this species jump, there is a unique opportunity to study influenza within this context to try and answer the questions of the requirements for the virus to infect a new host species. This thesis provides the opportunity to study H3N8 IAVs more closely to determine how host barriers interact with the viruses upon infection.

1.13. Objectives and Aims of Project

The overall objective of this project is to generate important new information on the pathogenesis of different IAVs in an equine host to better understand the process of viral emergence.

1. Characterization of an equine cell line for the *in vitro* study of EIV

As has been discussed in this chapter, it is essential to use a physiologically appropriate, IFN competent cell line when studying the host response to infection with a virus. It is also essential that the cell line is relevant to the host organism it has come from, and reflects the results seen in nature *in vivo*.

Therefore, one of the aims of this thesis was to find an equine cell line, and fully characterize it for the effective study of IAVs, and specifically EIV.

2. Explore equine host barriers to infection with different IAVs

The reason it was essential to have a relevant equine cell line in which to study IAVs, was that one of the primary aims of this thesis was to study how IAVs of different origins replicate within an equine host, and what the host barriers to infection may be.

3. Determine the cellular response to infection between two evolutionary distinct equine influenza viruses of the same lineage using transcriptomics

Using the new tool of transcriptomics, investigate how two evolutionary distinct EIVs (one from the beginning of the EIV H3N8 outbreak, and one after 40 years of adaptation to the equine host) differ in the way they control host cellular responses to infection.

Chapter 2

2.Characterization of an equine cell line for the in vitro study of equine influenza

2.1. Introduction

Influenza A virus (IAV) is a pathogen that has had a significant impact upon human health (World Health Organization 2018). There have been four major pandemics of influenza within the last 100 years, with the 1918 "Spanish flu" estimated to have caused 50 million deaths (Johnson & Mueller 2002). Seasonal strains of influenza, H3N2 and H1N1 (H for Haemagglutinin, and N for Neuraminidase), are constantly circulating, and evolving to escape host immunity. These circulating strains necessitate a costly vaccine, which requires annual updating to remain effective against antigenic drift and shift (Salk & Suriano 1949; Kilbourne *et al*. 2002).

As discussed in Chapter 1, IAVs have the potential to cross host species barriers and infect various hosts such as seals, pigs and humans (Anthony *et al*. 2012; Ito *et al*. 1998; Smith *et al*. 1933). A cross-species transmission event can either be deemed a "spillover" event, or if the virus maintains sustained transmission in the new host, an "emergence". There have been two documented subtypes of equine influenza emergence in horses. H7N7 was first identified in 1956, and H3N8 was reported in 1963 (Waddell *et al*. 1963). H7N7 has not been detected for the past 30 years, and is now thought to be extinct (Webster 1993; R G Webster *et al*. 1992). It is believed the only currently circulating equine influenza is of the H3N8 subtype.

Despite the availability of vaccines and investment in preventing transmission, H3N8 EIV (Equine Influenza Virus) is still circulating in many countries. Due to its high morbidity in horses, outbreaks can have high economic costs resulting from poor performance in racing. Therefore the study of its pathogenesis, and investigating its prevention, is important.

The lack of exchange of viral genes between EIV and influenza viruses from other species (Guo *et al*. 1991) had led to the assumption that horses were a 'dead-end' host. However, EIV jumped the species barrier and infected dogs in the early 2000's (Anderson *et al*. 2012). Canine Influenza Virus (CIV) was first isolated in 2004 in Florida, US (Crawford *et al*. 2005). CIV was shown to have a greater than 96% sequence identity with EIV, and each of the eight segments were of equine origin. This high sequence identity indicated that the emergence

of CIV was a result of direct transmission of the whole virus from horses to dogs, with no intermediate reassortment with other strains (Payungporn *et al*. 2008; Harder & Vahlenkamp 2010). Moreover, this is not the only documented case of EIV H3N8 inter-species transmission. EIV has been detected in pigs (Tu *et al*. 2009) and a Bactrian camel (Yondon *et al*. 2014). With EIV H3N8 seeming to have a high possibility of host expansion, it is important to study this virus to better understand IAV host-switching mechanisms and barriers.

There are many issues involved in the experimental study of influenza in horses. Apart from the great economic cost, the majority of horses are routinely vaccinated against influenza (Murcia *et al*. 2010), meaning that it is difficult to find suitable animals. Another issue is the ethical concern that horses can be viewed as companion animals. Therefore, even though it is of great importance to study EIV H3N8, *in vivo* experiments can prove very challenging.

When thinking about *in vitro* influenza experiments, the number of primary cells and cell lines that are able to maintain influenza virus replication is limited. Cell lines such as A549 (human alveolar epithelial), Vero (African green monkey kidney), DF-1 (chicken) and MDCK (Madin-Darby Canine Kidney) have all been used for the study of influenza (Lee *et al*. 2010; Kaverin & Webster 1995; Lee *et al*. 2008; Gaush & Smith 1968). Overall, MDCK cells are the most widely used for influenza isolation and propagation (Gaush & Smith 1968; Ilyushina *et al*. 2012; Gregersen *et al*. 2011; Audsley & Tannock 2004). However, for the successful replication of most influenza viruses in MDCK cells, the addition of exogenous trypsin is necessary (Tobita *et al*. 1975). It is also important to remember that MDCK cells are of canine-origin and therefore make it difficult to study specific equine host defence mechanisms to infection. A review by Hare *et al*. (Hare *et al*. 2016) discusses the importance of finding physiologically relevant cell lines to study host-virus interactions.

There has previously never been an equine cell line documented in the study of EIV. Equine primary respiratory epithelial cell cultures have been successfully generated, but have problems such as finite number of cell divisions (Lin *et al*. 2001). Therefore, a continuous equine cell line known as Equine Dermal (E.Derm) (Cullinane *et al*. 1988; Telford *et al*. 1992) was selected and

characterized specifically for the experimental investigation of EIVs. The current chapter describes an investigation into the potential susceptibility and permissibility of infection with EIV, and establishes if the results were consistent with what is observed *in vivo*. Once characterized the cell line was used for transcriptomic studies (described in Chapter 4 & 5). Therefore, it was important to assess their competency to produce and respond to interferon.

The aims of work described in this chapter were to find a continuous cell line for the study of EIV, characterising optimal infection conditions and susceptibility to influenza infection. It was important to determine IFN (Interferon) competency, so as to better understand the virus-host interactions (Hare *et al*. 2016). A reverse genetics virus of EIV from 2003 was used as the control virus throughout these experiments.

2.2. Results

2.2.1. E.Derm cells are susceptible to infection with equine influenza virus

To determine whether EIV is able to enter and infect E.Derm cells, monolayer cultures of E.Derm cells were first infected with EIV/2003 at a high MOI (MOI 3 based on MDCK titre). NP expression was determined at 4 hours post-infection, and a number of infected cells were observed by a strong fluorescence staining in comparison with mock-infections (**Figure 4, A**).

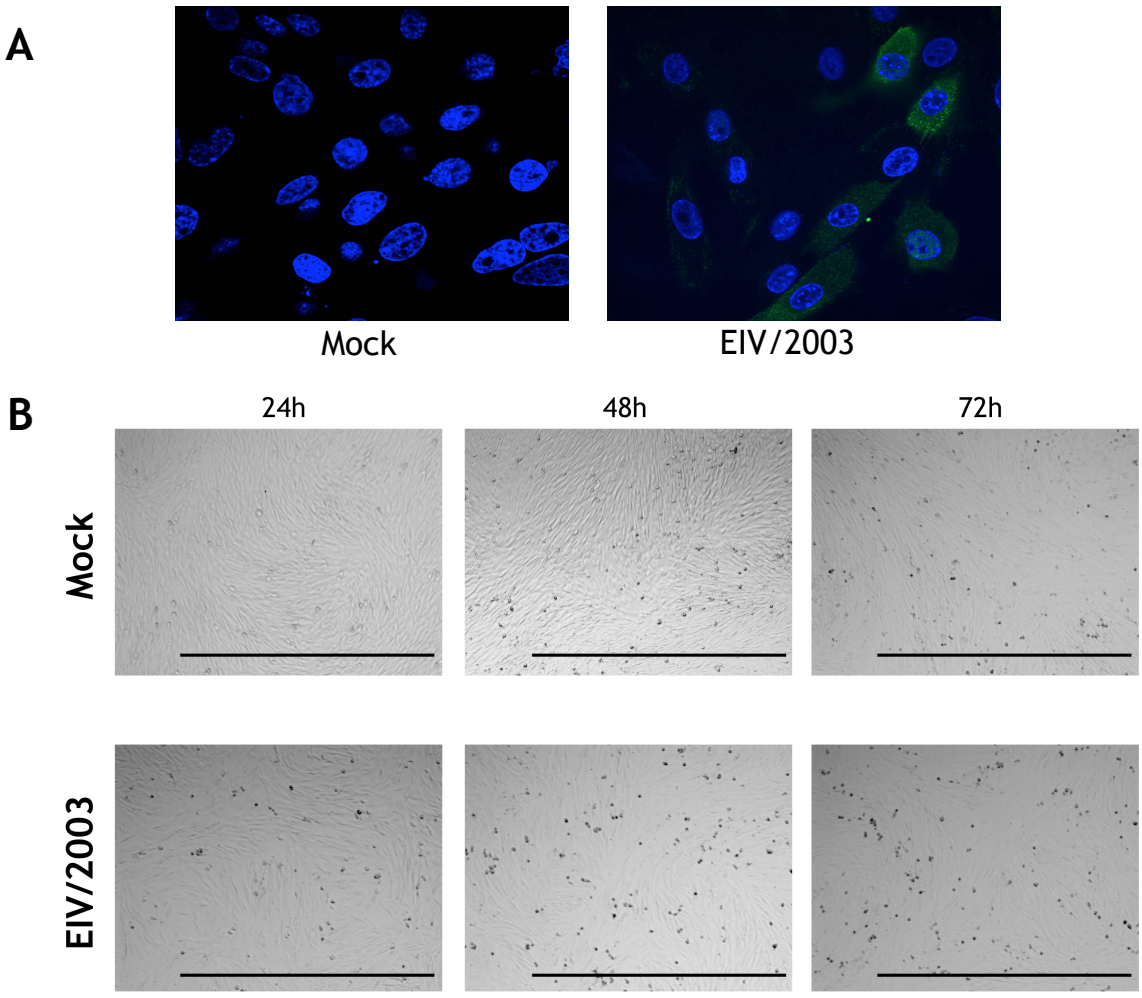

Figure 4: (A) E.Derm cells at 4 hours post-infection with EIV/2003 at an MOI of 3 (based on MDCK titre). Nuclei are stained blue, and NP is in green. (Magnification x63) (B) Light microscopy images of E.Derm cells Mock- and EIV/2003- infected at 24, 48 and 72 hours post-infection MOI 0.1 (based on MDCK titre). Horizontal bars represent 1,000 µm. (Magnification x4)

Using a low MOI (0.1 based on MDCK titre) E.Derm cells were infected and any changes were observed over 72 hours (**Figure 4, B**). Mock-infected cells showed almost no changes in morphology, whereas infected cells showed Cytopathic

Effects (CPE), such as cell shrinkage and rounding. Extensive cell death was not observed in infection with EIV/2003.

2.2.2. The eclipse phase of equine influenza in E.Derm cells is 7 hours

The eclipse phase is the period of time when the virus has entered the cell and is undergoing replication, but has not yet completed one cycle and exited the cell (White & Cheyne 1966). Researchers have previously reported eclipse times of 6 hours (Heldt *et al*. 2013). To determine the length of time of the eclipse phase in E.Derm cells, cell cultures were infected with an MOI of 3 (based on MDCK titre) and supernatant was collected every hour, up to 12 hours, and titrated. The curve of the graph began to increase after 7 hours of infection and it was determined that this was when the virus began exiting the cell (**Figure 5, A**). Furthermore, infected cells were also fluorescently labelled for the Haemagglutinin (HA) protein. Immunofluorescent staining of HA could be seen on the surface of the cell at 1 hour post-infection and slowly decreasing until 4 hours post-infection. At 6 hours post-infection HA staining could be observed distributed at the cell surface, ready for virus budding. Spherical HA staining could be seen on the surface of the cells from 7 hours post-infection (**Figure 5, B**).

It is very important to note that virus titrations throughout this thesis are affected by a methodological error, described in more details in the Materials and Methods section. Regrettably, it was not possible to repeat these experiments in the time available and, because the degree of systematic error might vary, the ability to make quantitative comparisons between these data is limited. However, it is still possible to describe changes in qualitative terms.

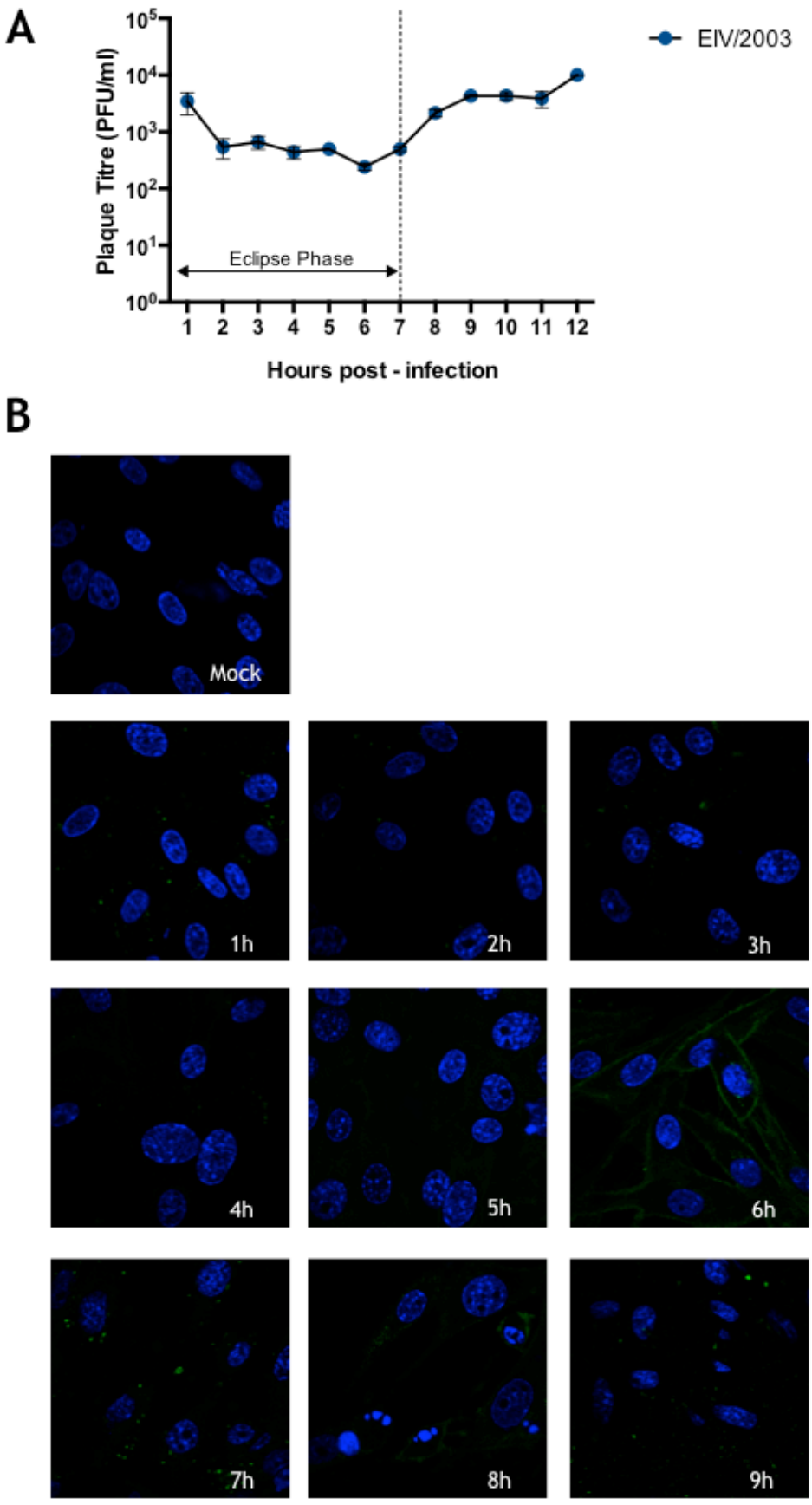

Figure 5: (A) Growth kinetics of E.Derm cells infected with EIV/2003 at an MOI of 3 (based on MDCK titre). Supernatant was collected every hour and titrated from three independent experiments; error bars indicate the standard error of the means. (B) Cells were grown on coverslips and infected at the same time as growth curves, fixed and stained. Nuclei are shown in blue, HA is in green. (Magnification x100)

2.2.3. Infection of E.Derm and MDCK cells with the same inoculation produces different percentage of infected cells

Throughout this thesis, cells will be collected and stained using an anti-NP antibody. A Guava Flow Cytometer was used to measure cells using Forward and Side Scatter. Live cells were sectioned off, and then of these cells a gate was created to quantify the percentage of fluorescently stained cells (**Figure 6**).

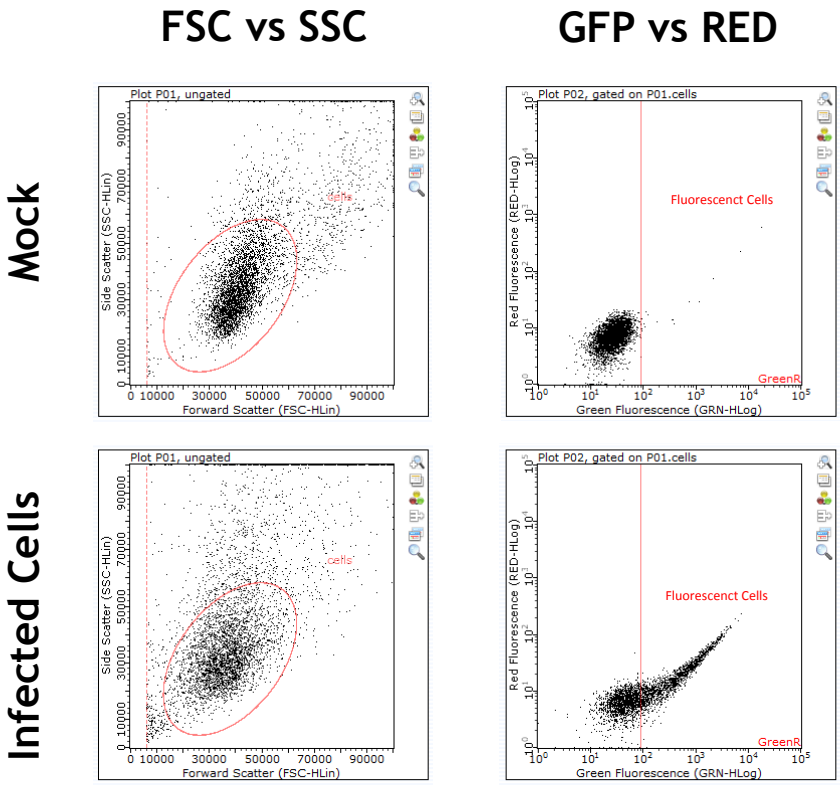

Figure 6: Guava Flow Cytometer gating. A Forward Scatter vs Side Scatter density plot was used to create a region of live cells (Plot P01). Subsequently these cells were separated into Green Fluorescence vs Red Fluorescence, and a gate was adjusted to the background fluorescence of the Mock-infected cells, which allowed for the quantification of infected cells (Plot P02).

To assess the entry efficiency of EIV in E.Derm, as compared to MDCK cells, both cell lines were infected with EIV/2003 at an MOI of 3 (based on MDCK titre). Intracellular virus levels were compared by staining the cells for the NP protein to give an indication of the percentage of cells infected (**Figure 7**). NP-positive cells were measured using a Guava Flow Cytometer. A significant difference was found, with ~55% of E.Derm cells and ~92% of MDCK cells infected at 4 hours post-infection (*). There was also a significant difference (*) between MDCK and E.Derm infected cells at 6, 8 and 10 hours post-infection. MDCK cells had a

maximum permissiveness of around 90%, whereas E.Derm cells peaked at ~80%. The percentage of cells infected became more similar at 12 to 20 hours post-infection, with a significant difference again at 24 hours post-infection (*).

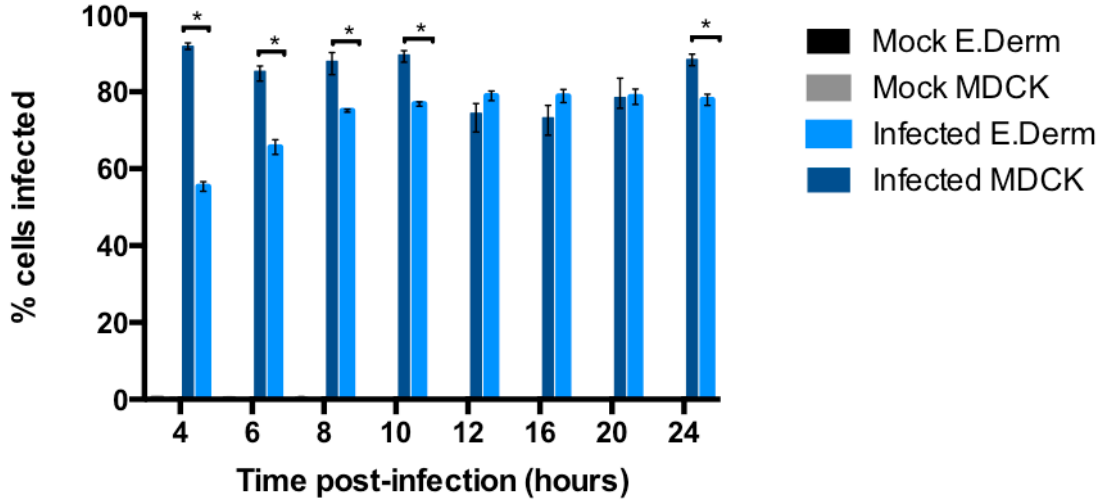

Figure 7: Percentage of NP-positive E.Derm and MDCK cells infected with EIV/2003 (MOI 3, based on MDCK titre). Infected cells were measured using the Guava Flow Cytometer. Experiments were repeated independently three times; error bars indicate the mean with range of the values. A statistical t-test was carried out, comparing the values in the infected E.Derm and MDCK cells. Significance is shown with * where $p \leq 0.05$.

2.2.4. Equine influenza can replicate in E.Derm cells without the presence of exogenous trypsin

For most influenza viruses replicating in MDCK cells (with the exception of WSN (Influenza A/WSN/33) virus), the addition of exogenous trypsin is required for multi-cycle infection. This is due to the necessity of a protease to cleave the HA of newly produced virions, leading to maturation and ability to infect another cell.

When EIV/2003 was grown in MDCK cells without the customary addition of TPCK trypsin there was a significant difference (*) at 48h and 72h post-infection between the percentage of cells infected with and without the presence of TPCK trypsin (respectively 48h: ~62% and ~32%, 72h: ~75% and ~35%) – as determined by examining the proportion of infected cells (NP-positive cells counted by FACS) (**Figure 8, A+B**). For the extracellular virus (titrated in the supernatant) titre,

there was a difference of around 4 logs at 48h and 5 logs at 72h (**Figure 8, A+B**).

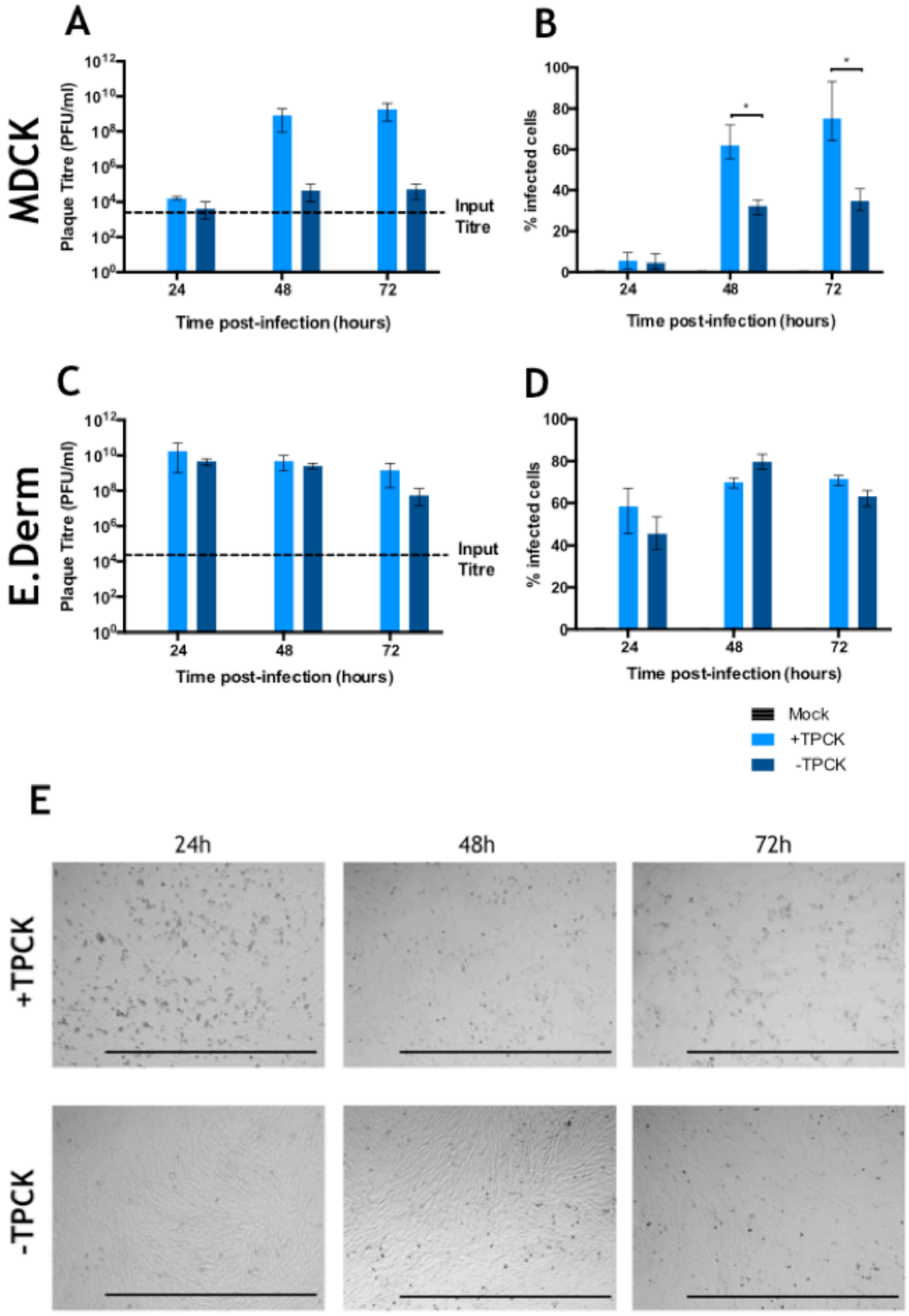

Figure 8: Growth curves of intracellular and extracellular EIV/2003, with and without the addition of exogenous TPCK trypsin in the infection media, in MDCK (A+B) and E.Derm cells (C+D). (E) E.Derm cells grown with and without exogenous TPCK trypsin in the media. MDCK cells were infected with MOI 0.01 (based on MDCK titre), and E.Derm cells were infected with MOI 0.1 (based on MDCK titre). Experiments were repeated independently three times; error bars indicate the mean with range of the values. For each figure a statistical t-test was carried out, comparing the values in the presence and absence of TPCK trypsin. Significance is shown with * where $p \leq 0.05$.

However, when EIV/2003 was grown in E.Derm cells either in the presence or absence of TPCK trypsin, no significant difference was found either in extracellular virus or intracellular virus (**Figure 8, C+D**).

The presence of TPCK trypsin appeared to effect E.Derm cells in a negative way, as can be seen from major CPE in the Mock-infected cells that contain exogenous TPCK in the medium (**Figure 8, E**). This negative effect was most apparent from 48 hours, with the rounding and detachment of cells from the culture plate. Therefore as TPCK trypsin was not necessary for the multi-cycle growth of EIV/2003, and was also harmful to the cells, future experiments were performed without its addition.

2.2.5. E.Derm cells are selective in susceptibility and propagation of influenza viruses

As well as investigating the infectivity of E.Derm cells with EIV, their ability to be selectively permissive for different influenza viruses was examined. One of the disadvantages of using MDCK cells is that they are susceptible to many influenza viruses and therefore it is hard to determine host barriers to infection.

To test whether the viruses examined had similar growth kinetics in a non-selective cell line, MDCK cells were infected with an MOI of 0.01 (based on MDCK titre). The growth kinetics were followed over 72 hours, by titrating the supernatant and quantifying the number of NP-positive cells using a Guava Flow Cytometer. ***Figure 9*** (A+B) shows that when EIV/2003 and CIV/2009 were grown in MDCK cells there was no significant difference in the growth kinetics, demonstrating that both viruses were able to replicate efficiently in this cell line.

It has been shown that EIV jumped species into dogs and evolved to become CIV and subsequently lost its ability to infect horses (Yamanaka *et al*. 2012). To test whether this phenotype was replicated in E.Derm cells, the cells were infected with both EIV/2003 and CIV/2009 at an MOI of 0.1 (based on MDCK titre), and the growth kinetics were observed over 72 hours. As can be seen from ***Figure 9***

(C+D), EIV/2003 grew to very high titres, with significant differences to CIV/2009 at 24 and 48 hours post-infection (*). EIV/2003 peaked at over 10^9 PFU/ml at 24 hours. In comparison CIV/2009 grew to titres that were 5 logs lower, to just less than 10^4 PFU/ml at 24 hours. The difference between the ability of EIV/2009 and CIV/2009 to infect the E.Derm cells was also evident in the number of NP-positive cells. There was a significant difference between both viruses at all time-points (*). Infection with EIV/2003 peaked with 80% of cells infected at 48 hours, whereas only 20% of cells were infected with CIV/2009 at 48h.

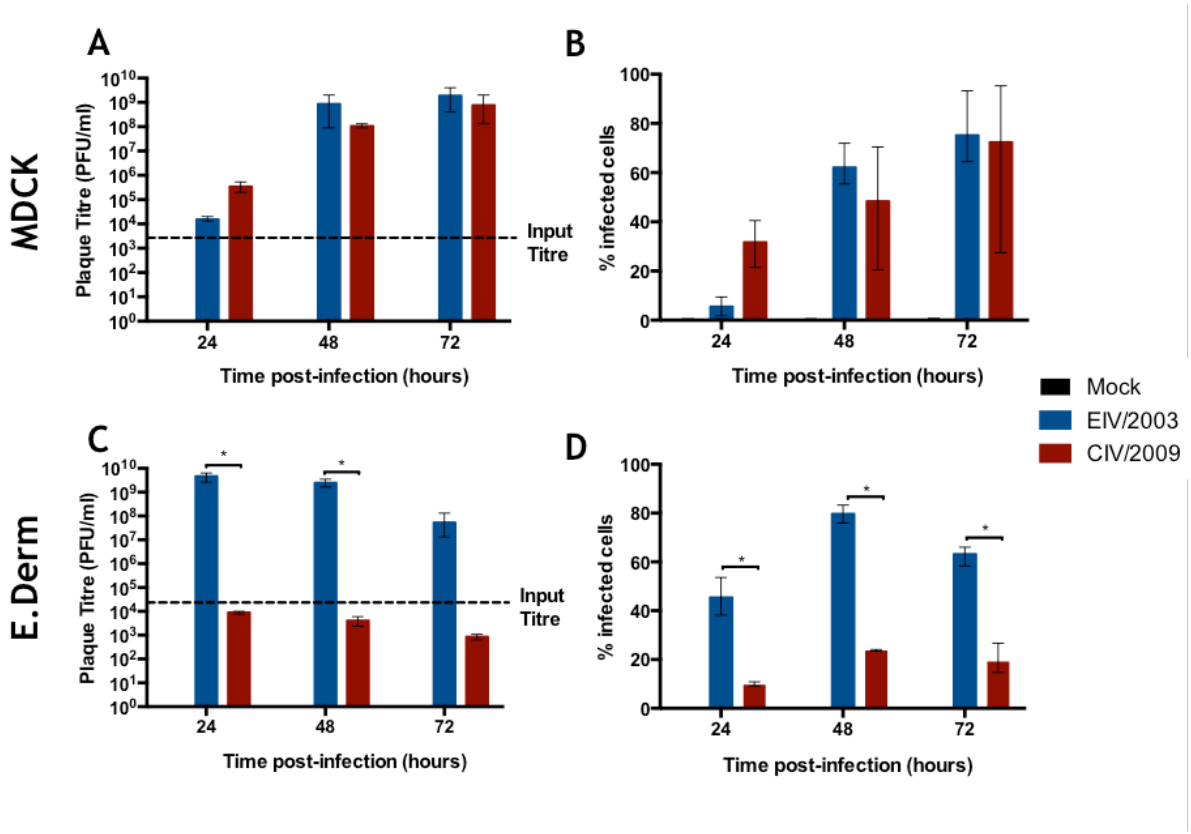

Figure 9: Growth kinetics of EIV/2003 and CIV/2009 in MDCK (A+B) and E.Derm (C+D) cells, infected with MOI 0.1 (based on MDCK titre). Infected cells were measured using the Guava Flow Cytometer. Experiments were repeated independently three times; error bars indicate the mean with range of the values. For each figure a statistical t-test was carried out, comparing the values in the EIV/2003 and CIV/2009 infected cells. Significance is shown with * where $p \leq 0.05$.

2.2.6. E.Derm cells both respond to and produce interferon

It was necessary to verify whether E.Derm cells were an interferon (IFN) competent cell line, i.e. that they were able to both respond to exogenous IFN and also produce IFN in response to stimuli. To this end E.Derm cells were

treated with increasing concentrations of Universal IFN-α (derived from Human IFN-α) for two time-points of treatment (4h and 24h). These cells were then challenged with a VSV-ΔG-GFP (a green fluorescent VSV virus lacking a glycoprotein, meaning it is replication incompetent) to determine the level of protection from infection, measured using a Guava Flow Cytometer. All concentrations of IFN-α treatment produced a significant difference (*). The protection level increased with the concentration of IFN-α, and there was slightly higher protection after pre-treating the cells for 24h (34% and 25% of relatively infected cells at 4h and 24h of 1000 UI/ml of IFN-α pre-treatment, respectively) (**Figure 10, A**).

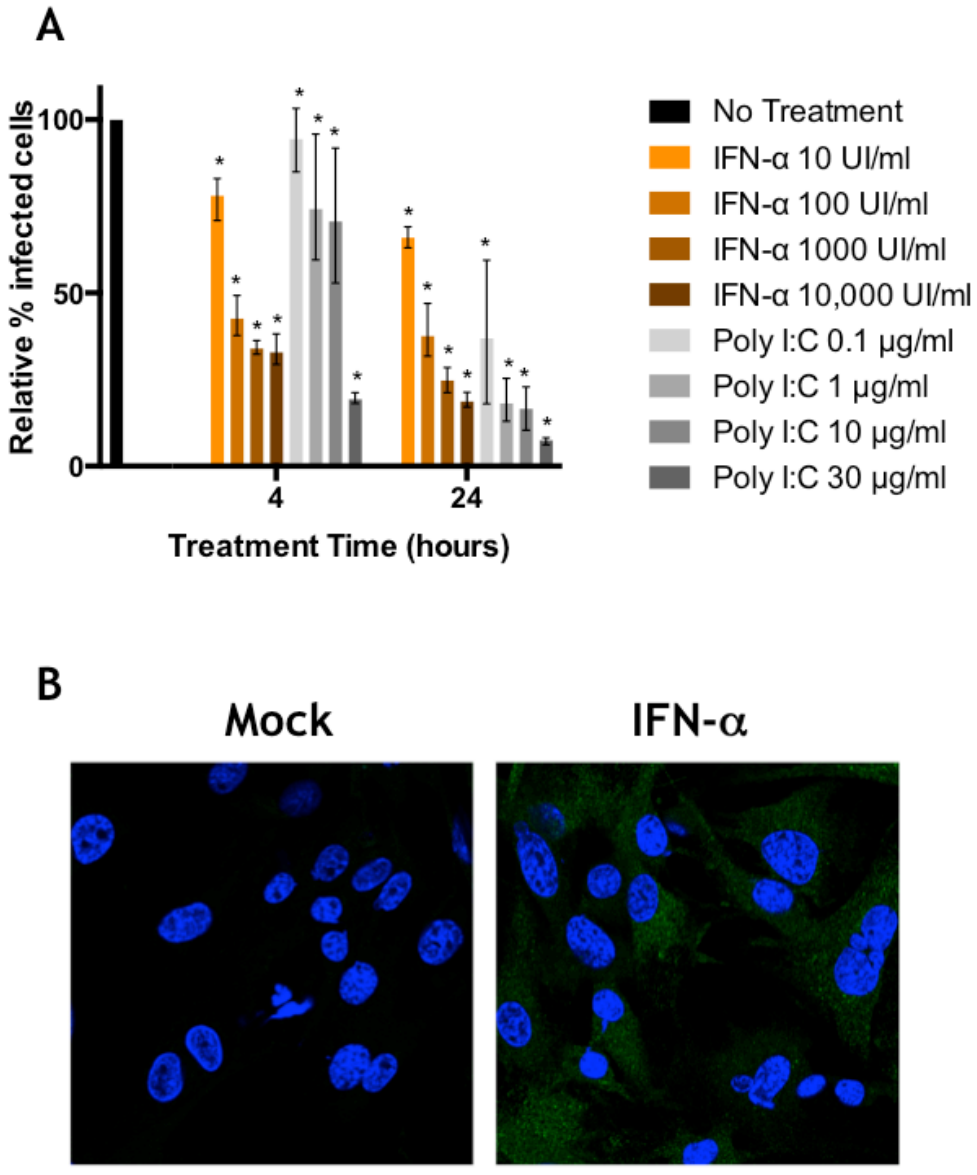

Figure 10: (A) E.Derm cells were treated for 4h and 24h with increasing concentrations of IFN-α or Poly I:C, and then challenged with a VSV-ΔG-GFP virus to assess the level of protected cells. (B) E.Derm cells treated for 24 hours with 1,000 UI/ml of IFN-α have a higher expression of Mx1 (in green). Experiments were repeated independently three times; error bars indicate the mean with range of the values. A statistical t-test was carried out, comparing the values to no treatment. Significance is shown with * where p≤0.05.

To determine how well E.Derm cells could produce their own IFN, a similar experiment was conducted. Cells were treated with increasing concentrations of Poly I:C for two lengths of time (4h and 24h). Poly I:C is a mimic of double-stranded (ds) RNA (a stimulus of the IFN pathway), and upon exposure the cells should produce IFN. To test the antiviral level the cells were challenged with VSV-ΔG-GFP infection, protection was measured using a Guava Flow Cytometer. The protection increased as the concentration of 4 hours of Poly I:C treatment increased, with all treatment concentrations showing a significant difference (*) to cells with no treatment. There was a greater difference observed between 4h and 24h pre-treatment than was seen for IFN-α pre-treatment (~71% and 17% of infected cells at 4h and 24h 10ng/ml Poly I:C pre-treatment, respectively) (**Figure 10, A**). All of the concentrations of Poly I:C produced a highly significant (*) difference compared to no treatment with 24 hours of treatment time.

Mx1 (Myxovirus Resistance Protein 1) is a well-characterized interferon-stimulated gene (ISGs) that has been shown to have antiviral activity against influenza (Staeheli *et al*. 1986). Therefore, the expression of Mx1 in E.Derm cells after IFN-α treatment was investigated. As can be seen from **Figure 10** (B), Mx1 was upregulated following pre-treatment with 1000 UI/ml of IFN-α for 24h.

2.3. Discussion

Equine influenza is a significant pathogen of the horse that requires more study, as it could shed light on cross-species transmission events. To date, an equine cell line has not been described for the *in vitro* experimental study of EIV. This chapter describes the full characterisation of the equine cell line E.Derm, derived from the dermis of a horse.

E.Derm cells were shown to be susceptible to infection with EIV, as shown by NP fluorescence positive cells after infection with EIV/2003 (**Figure 4**). When the virus was grown over the course of 72 hours, CPE was observed as the shrinking and rounding of cells. However, this CPE was not dramatic and certainly did not destroy the complete cell monolayer, as is normally observed for influenza infection in MDCK cells. This may be due to the existence of host barriers, or that the virus infects but does not lead to cell death.

For transcriptomic studies of infected E.Derm cells in Chapter 4, two separate time-points were examined. The first time-point was completed during the eclipse phase of the virus life cycle; and the next at 24h post-infection, when the virus will have undergone several replication cycles. It has been documented that one complete influenza replication cycle in MDCK cells takes 8 hours, which had yet to be characterized for E.Derm cells. To characterise the time taken to complete a single replication cycle, cells were infected with a high MOI (MOI 3, based on MDCK titre) and supernatant was collected every hour to observe when the growth curve began to increase its slope. As demonstrated in **Figure 5** (A) the slope begins to increase at 7 hours post-infection. Accompanying immunofluorescence images show that the viral HA begins to line the cell surface, in preparation for virus budding at 6 hours post-infection. At 7 hours HA, suggestive of virus budding, can be seen. This result was encouraging as the eclipse phase was very similar to other cell lines. Based on this information future "eclipse phase" time-points were taken at 4 hours post-infection.

During the characterization of E.Derm cells, the addition of TPCK trypsin to the growth media was observed to cause stress to the cells (**Figure 8**, **E**). TPCK trypsin is normally added in most *in vitro* influenza infections. It is needed

for the cleavage of HA to produce a mature virion and continue the replication cycle, which is normally carried out by cellular proteases *in vivo* (Kuiken *et al*. 2006). Decreased concentrations of TPCK trypsin to 0.1 ng/ml still resulted in CPE in control cells. Therefore, infections in E.Derm and MDCK were performed with and without the addition of TPCK trypsin. Viral growth in MDCK cells was inhibited significantly, confirming the requirement to add TPCK trypsin for successful replication (**Figure 8, A+B**). In contrast, the virus was still able to replicate in E.Derm cells, to a level only a little lower than with the addition of regular infectious media containing TPCK trypsin (**Figure 8, C+D**). Therefore, all further experiments carried out in E.Derm cells were carried out without the addition of TPCK trypsin (note, TPCK trypsin was still used in the infectious media for 1-hour inoculations so as to cleave any HA in immature virions produced in the virus stock grown in MDCKs). The absence of TPCK was especially important when investigating transcriptomic responses to infection, as stress responses to TPCK trypsin no longer need to be considered (please refer to Chapter 4 for transcriptomics work).

When E.Derm cells were infected with the same MOI (based on MDCK titre) as MDCK cells, they had a lower percentage of cells infected (**Figure 7**). There could be other factors involved in E.Derm cells, such as host barriers that are not present in MDCK cells. The interferon response of MDCK cells may well be inhibited after continual culturing (Masters & Stacey 2007). Canine Mx in MDCKs has been shown to be deficient (Seitz *et al*. 2010), which may explain why influenza viruses can grow to such high titres in these cells. Therefore, there may be host barriers in place in E.Derm cells that are combating infection with influenza. If these host barriers exist, it could indicate that more meaningful results can be concluded from *in vitro* studies using these cells, as opposed to MDCK cells. In addition, considering these potential barriers is important when looking at transcriptomic data, as there may be a higher number of active genes due to a higher capacity to block infection.

Unlike MDCK cells, which are highly susceptible to almost every influenza virus, E.Derm cells appear to be selective for which influenza viruses they can be infected by (***Figure 9***). This was shown by the low infectivity of CIV in E.Derm cells (C+D). There weren't a high number of new virions produced during

infection, whereas CIV grew to similar titres as EIV in MDCK cells (A+B). The contrasting growth of CIV in E.Derm and MDCK cells, is an important finding as it corroborates what is seen *in vivo*, that is, that CIV cannot go back along its evolutionary path and infect horses (Yamanaka *et al*. 2012). Recent research in Pablo Murcia's lab has demonstrated that this decrease in infectivity is due to the HA and NA proteins of the CIV virus. Work carried out by myself and Dr Gaelle Gonzalez showed that when we substituted the HA and NA of CIV with that of EIV, the infection phenotype is rescued. (My involvement in this work included: reverse genetics to produce different virus combinations, growth and titration of virus stocks, preparation of *ex vivo* tracheal explants, infection of tracheal explants, collection of data – infected explants and bead clearance, titration of virus from tracheal explants, immunohistochemistry staining of explants. Not involved in: taking images of immunohistochemistry). The reduced infectivity of CIV could be due to the sialic acid receptors distributed on the cell surface of E.Derm cells. MDCK cells have both SAα2, 3Gal and SAα2, 6Gal linked sialic acids (Ito *et al*. 1997). Collaborators at Cornell University are currently studying these receptors in E.Derm cells. Both EIV and CIV prefer SAα2, 3Gal linkages (Feng *et al*. 2015), although it has been shown that there may be additional glycan features at play that make sialic acid preferences more complex than previously believed (Gambaryan *et al*. 2005).

When looking at the transcriptome of a cell, it is important that the cell is IFN competent. Cells such as Vero cells have lost their ability to produce IFN, therefore these cells are very useful when it comes to growing up certain virus stocks, but they don't allow for the full picture of how a cell would try to combat a viral infection (Desmyter *et al*. 1968). To assess whether E.Derm cells were IFN competent, these cells were treated with Universal IFN (IFN-α) for 4 and 24 hours (the time-points that would later be used for transcriptomic analysis). Following the IFN-α treatment, these cells were challenged with a VSV-ΔG-GFP replication-incompetent virus. This challenge experiment was repeated, but the cells were treated with Poly I:C, a mimic of double-stranded RNA, and challenged them with VSV-ΔG-GFP. Protection from infection could be seen at 4 hours post-treatment, and increasing at 24 hours. The protection effect increased with treatment concentration for both IFN-α and Poly I:C (**Figure 10**). Future experiments, in agreement with the literature, will use IFN-

α at a concentration of 1,000 UI/ml, as there was very little difference by increasing the concentration to 10,000 UI/ml.

Overall an in-depth characterisation of an equine cell line was described, which can be used for the extensive *in vitro* analysis of EIV and other related influenza viruses. It was demonstrated that this cell line provided a good means to study the transcriptome response, as the equine E.Derm cells were IFN competent, as opposed to MDCK cells. The remaining chapters will describe infection with different influenza viruses, and detailed transcriptomic analyses.

Acknowledgements

This study was funded by grants from the Horserace Betting Levy Board (HBLB). The eclipse growth phase experiment was carried out with the help of Dr Gaelle Gonzalez and Caroline Chauché.

Chapter 3

3. Equine host barriers to influenza infection

3.1. Introduction

Some viruses are capable of crossing host species barriers to infect new animal and human hosts (Cheung & Poon 2007). A better understanding of what these barriers are, and how pathogens have evolved to overcome them, will enhance prediction and preparation for potential future outbreaks.

Influenza A viruses (IAVs) of animals are all believed to have their ancestry in wild aquatic birds (Kawaoka *et al*. 1988). There are only a limited number of influenza subtypes that have become established in mammals, for example H1N1 in pigs (Shope 1931), H3N8 in horses (Oxburgh *et al*. 1994), and H3N2 and H1N1 in humans (Rambaut *et al*. 2008). The horse appears to play an important role in influenza emergence. It has been documented as a natural host for sustained influenza transmission on at least three occasions. There was an outbreak in 1872 of an unknown Equine Influenza Virus (EIV) subtype (Morens & Taubenberger 2010), an H7N7 EIV was first isolated in 1956 (Sovinova *et al*. 1958), and an H3N8 EIV that was first identified in 1963 (Waddell *et al*. 1963).

Many within-host barriers exist to stop entry and replication of influenza viruses (Kuiken *et al*. 2006). The virus must first find the correct tissues in which it can replicate. Finding the correct tissues may require overcoming physical barriers such as mucus and cilia in the respiratory tract (Zanin *et al*. 2015). Once it reaches the correct tissue, the virus must use the appropriate receptors to bind to and enter a cell. These receptors will vary depending upon the haemagglutinin (HA) of the influenza virus. For example, avian influenza viruses (AIVs) preferentially bind to Sialic Acid (SA) -α-2,3-Gal-terminated saccharides, as do equine and canine influenza viruses (EIV and CIV, respectively) (Pecoraro *et al*. 2013). In contrast, human influenza viruses bind to SA-α-2,6-Gal-terminated saccharides (Couceiro *et al*. 1993). These distinctions in receptor binding result from different SA distributions within the host species. The trachea (the main site of influenza infection) in humans has a high distribution of SA-α-2,6-Gal-linkages, whereas equine tracheas are abundant with SA-α-2,3-Gal linkages (Suzuki *et al*. 2000). Different receptor distributions may explain why AIV replication in humans is limited, whereas AIVs have jumped the host-species barrier to infect horses on more than one occasion.

Once a virus enters a cell it must be able to replicate efficiently and continue to infect neighbouring cells. There are many factors that can affect the successful replication and dissemination of an IAV (Naffakh *et al*. 2000). Cleavage of HA by cellular proteases is an essential step of the replication cycle. Viruses that are not cleaved are not infectious, as cleaving of the glycoprotein enables the mature virus to bind to host cells. The HA of human influenza viruses and Low Pathogenic Avian Influenza (LPAI) are cleaved by trypsin-like proteases, thereby restricting virus tropism to where these proteases are present. For humans, these proteases are found in the respiratory tract, and for birds they are either found in the respiratory or intestinal tract, or both (Garten *et al*. 1981; Klenk *et al*. 1975).

An essential host barrier is the IFN response, which consists of a complex group of signalling proteins that are released in response to a pathogen, such as a virus, infecting a cell (Randall & Goodbourn 2008). These signalling proteins cause the cell to enter an antiviral state, and send signals to surrounding cells to heighten their viral defences. To overcome the IFN response, IAVs have adapted antagonists such as the non-structural (NS1) protein, which target the cellular response to infection (Hale, Randall, et al. 2008). However, the antagonistic protein can be host-specific and therefore it takes time for influenza viruses to adapt to new hosts.

As horses possess similar SA receptors as birds, there is a continual possibility that a new avian influenza sub-type could emerge in horses. In 1989 in Jilin, a Chinese province, such an event occurred. A cross-species transmission of an H3N8 influenza virus caused severe mortality, with up to 20% of horses dying in some herds (Guo *et al*. 1992). H3N8 viruses are a commonly isolated subtype from avian reservoirs (Sharp *et al*. 1997) and have crossed the host species barriers on multiple occasions to infect mammals such as seals and camels (Anthony *et al*. 2012). Therefore, it is important to study the ability of H3N8 AIVs to replicate in horses, and how they can overcome the host barriers described.

The horse is not a dead-end host for influenza H3N8. Two viruses isolated from pigs with respiratory disease in 2005 and 2006 were shown to be most

closely related to EIVs (Tu *et al*. 2009). In addition, EIV jumped into dogs on multiple occasions (Crawford *et al*. 2005; Daly *et al*. 2008) and established as canine influenza virus (CIV) infection in dogs in North America. Therefore, it is important to study influenza in the context of the horse in order understand how an IAV can switch hosts.

This chapter describes an analysis that aimed to investigate the host barriers to the emergence of an avian virus into an equine host, and the adaptation of the virus to the host. A panel of four distinct IAVs were selected: (a) an H3N8 AIV (AIV/2009) isolated during surveillance studies in Mongolia from wild birds (Gilbert *et al*. 2012), (b) an EIV first isolated in 1963 (EIV/1963) [the virus isolate was used for tracheal explant infections, the reverse genetics virus was used for *in vitro* experiments], (c) a reverse genetics virus of an EIV isolated after 40 years of adaptation to the horse (EIV/2003), and (d) a reverse genetics virus of a CIV isolate (CIV/2009). CIV is interesting to study, as it will provide a virus in the context of a virus departing from a host species and continuing to evolve.

In this chapter, both *ex vivo* equine tracheal explants, and *in vitro* equine dermal cells (E.Derm) were used for infections in order to investigate how evolutionary distinct viruses replicate in an equine host. The growth kinetics of each virus were compared using both systems and observing the infection characteristics. In order to assess correct protease availability as a restriction for influenza, the growth kinetics of the viruses were compared in cells treated with and without an exogenous trypsin protease. Finally, to characterize the ability of each of the selected viruses to overcome the equine IFN response, cells were induced into an antiviral state and then infected (Ronni *et al*. 1997).

3.2. Results

3.2.1. Ex vivo horse trachea explants are interferon competent

To establish whether *ex vivo* horse trachea explants would be a suitable future system to study influenza infections, it was first necessary to determine whether they could produce an IFN response. Horse tracheal explants were treated with increasing concentrations of IFN-α consisting of 10, 100, and 1000 units for 24 hours (**Figure 11**). The upregulation of the IFN response was investigated by targeting the well-known Interferon Stimulated Gene (ISG) Mx1 (Myxovirus Resistance Protein 1), using immunohistochemistry staining. Mx1 is constitutively expressed in the respiratory tract (Chang *et al*. 1990), and, consequently, a background level of Mx1 expression was present in the upper epithelial cells of the control tissue. The staining, and therefore the expression of Mx1, increased sharply with increasing concentration of IFN treatment – spreading to all the epithelial cells throughout the tissue. Treatment of 1000 units of IFN saw many additional cells in the lamina propria[1] expressing Mx1.

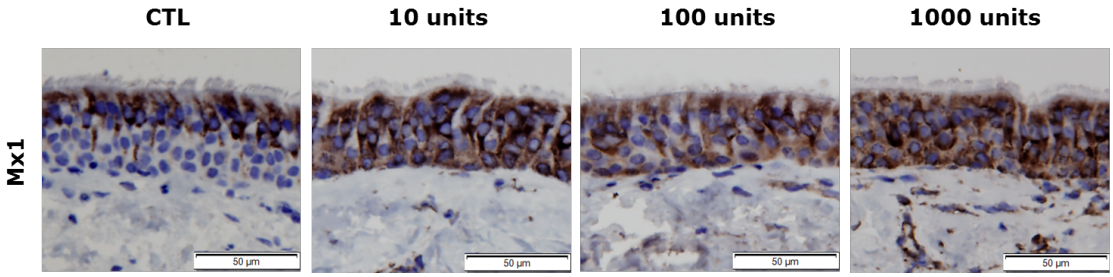

Figure 11: Immunohistochemistry staining of Mx1 in horse trachea explants treated with increasing concentrations of IFN-α for 24 hours. (Antibody: Mab143 anti-Mx1)

3.2.2. Influenza viruses have different infection phenotypes in ex vivo horse tracheal explants

Ex vivo horse tracheal explants were infected with the selected panel of influenza viruses. **Figure 12** (A) demonstrates that EIV/2003 grew to much higher titres than the other influenza A viruses (IAVs). The highest EIV/2003 titre was found at 5 days post-infection (~3.51×10^9 PFU/ml), with significant differences when compared to Mock-infected explants at 3 and 5 days post-

[1] A thin layer of loose connective tissue that lies beneath the epithelium.

infection (*). Infection with EIV/1963 resulted in lower titres, with a peak at 3 days post-infection of ~7.86x10^5 PFU/ml, four logs lower than EIV/2003 at the same time-point. Statistical analysis revealed there was a significant difference (*) between EIV/1863 and Mock-infected explants at 4 days post-infection. CIV/2009 also had very low replication kinetics, with a peak of infection at 2 days post-infection of 8.67x10^4 PFU/ml, four logs lower than EIV/2003 at the same time-point. The growth kinetics of AIV/2009 was very sporadic, with positive virus titres found only at 2 and 4 days post-infection, and no virus growth detected in between. However, day 4 post-infection was shown to be significantly different (*) than Mock-infected.

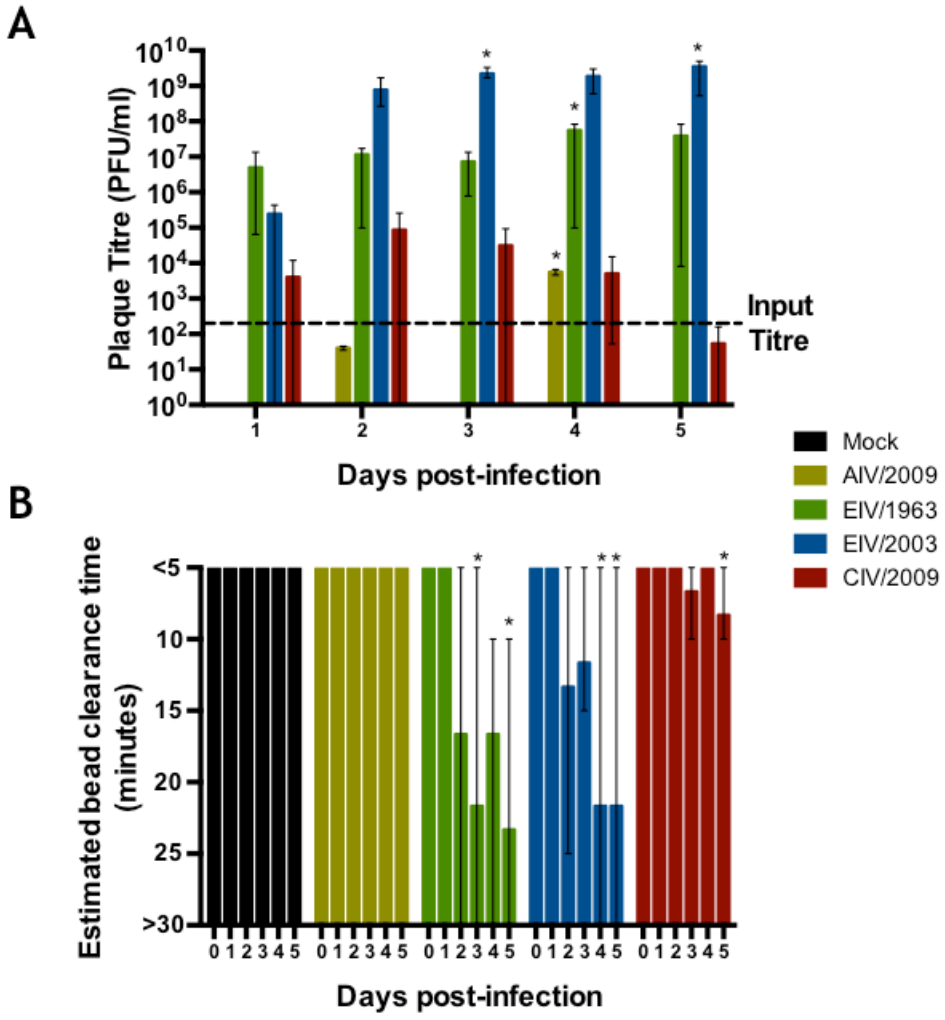

Figure 12: Equine tracheal explants were infected with AIV/2009, EIV/1963, EIV/2003 and CIV/2009 at 200 PFU (based on MDCK titre). (A) The virus growth kinetics. (B) Bead clearance assay, bars represent the average time for bead clearance. Experiments with AIV/2009 were repeated independently two times, experiments were the other viruses were repeated independently three times; error bars indicate the mean with range of the values. For each figure a statistical t-test was carried out, comparing the values to no treatment. Significance is shown with * where p≤0.05.

A coloured bead clearance assay was used to determine the ciliary function of the infected explants, and to ensure the healthiness of the Mock-infected controls (**Figure 12, B**). Explants infected with both EIVs showed impairment in bead clearance beginning at day 2 post-infection. For EIV/2003 the impairment was significantly different (*) at day 4 and 5 post-infection, as compared to the Mock-infected explants. The explants infected with EIV/1963 appeared to deteriorate faster, with a significant difference (*) shown earlier at 3 days post-infection, and again at 5 days post-infection with bead clearance time increasing to ~25 minutes. Infection with CIV/2009 leads to decrease in bead clearance time at day 3 post-infection onwards. Day 5 post-infection was the only time that showed a significant difference (*) when compared to the bead clearance of Mock-infected explants. The bead assay carried out on AIV/2009 infected explants did not show any decreased ciliary function, and so these virus infections were not significantly different from the Mock-infected explants.

3.2.3. In vitro infection with influenza viruses is similar to infections of ex vivo tracheal explants

To analyse potential host barriers to influenza infection, it was necessary to perform infections *in vitro* using an equine cell line. An equine dermal cell line (E.Derm) cell line was selected due to being permissive for infection with EIV. The infections using E.Derm cells were compared to infections in MDCK cells, which are considered permissive to most influenza viruses and therefore act as a control.

Infection with the panel of influenza viruses in MDCK cells demonstrated that EIV/1963, EIV/2003 and CIV/2009 grew to similar titres. AIV/2009 was lower, with a difference of around 3-4 logs at 72 hours post-infection (**Figure 13, A**). The only virus that showed a significant difference in viral titre when compared to Mock-infected cells was EIV/1963 at 72 hours post-infection (*). When looking at intracellular virus, AIV/2009 seemed to infect faster, with a significant difference (*) at 24 hours post-infection as opposed to the other viruses, which were not significantly different (**Figure 13, B**). This difference is also significant at 48 and 72 hours post-infection. The avian virus also had the highest percentage of infected cells at 72 hours post-infection (~90.4%). This is in

contradiction to the extracellular virus titrated using plaque assays, where AIV/2009 had the lowest titre of $8.2x10^5$ PFU/ml at 72 hours post infection (3-4 logs lower than the other influenza viruses). The high percentage of infected cells could be explained due to the fact that AIV/2009 appears to kill a large proportion of cells, leaving fewer alive cells that are infected. This complicates any discussion of the proportion of intracellular virus, and must be kept in mind when observing the high percentage of infected cells with AIV/2009.

CIV/2009 infected MDCK cells quickly, with ~31.7% of positive cells at 24 hours post-infected. The CIV/2009 virus titre was the highest of the viruses ($2.8x10^5$ PFU/ml) at this time-point. However, the growth slowed in comparison to both EIVs, which were about 0.4 logs higher at 72 hours post-infection. It was shown to be significantly different (*) at 48 and 72 hours post-infection when compared to Mock-infected cells. Both EIV/1963 and EIV/2003 also showed a significant difference (*) when compared to Mock-infected cells at 48 and 72 hours post-infection.

When the same panel of influenza viruses were used to infect E.Derm cells, EIV/2003 was significantly different in virus titre when compared to Mock-infected cells, reaching titres of $4.7x10^9$ PFU/ml and $2.5x10^9$ PFU/ml at 24 and 48 hours post-infection (*). All of the viruses had the same pattern of growth kinetics, peaking at 24 hours post-infection with significant difference (*), and decreasing at later time-points (**Figure 13, C**). Only CIV/2009 was also significantly different (*) at 48 hours post-infection when compared to Mock-infection, with a virus titre of $4.1x10^3$ PFU/ml.

In regards to intracellular virus, AIV/2009, EIV/1963 and EIV/2003 had similar proportions of infected cells, with CIV/2009 infecting fewer cells. Similarly to infection in MDCK cells, AIV/2009 infected a high proportion of cells, but produced a relatively low viral titre. The avian virus had the highest number of cells infected compared to the other viruses at 72 hours post-infection (~69.1% as opposed to the next highest ~63.1%, of EIV/2003) (**Figure 13, D**). All four viruses were significantly different (*) at 24, 48 and 72 hours post-infection when compared to Mock-infected cells.

MDCK and E.Derm cells were observed using a light microscope to assess cytopathic effects (CPE) of infection (**Figure 14**, **Figure 15**, and **Figure 16**). For both cell lines, the infection that caused the greatest CPE was when cells were infected with AIV/2009. The rounding of cells began much sooner and with a greater number than was found with the other viruses. By 72 hours post-infection, there were very few cells left attached to the plate. The other three viruses produced similar CPE in MDCK cells, with rounding of cells and detachment from the monolayer. In E.Derm cells, EIV/1963 induced a lot of CPE in comparison to EIV/2003 and CIV/2009. By 72 hours post-infection there were very few cells left of the monolayer and there were a lot of round cells. For EIV/2003 and CIV/2009, there wasn't very much CPE observed. There were slightly more rounded cells for infection with EIV/2003 when compared to CIV/2009.

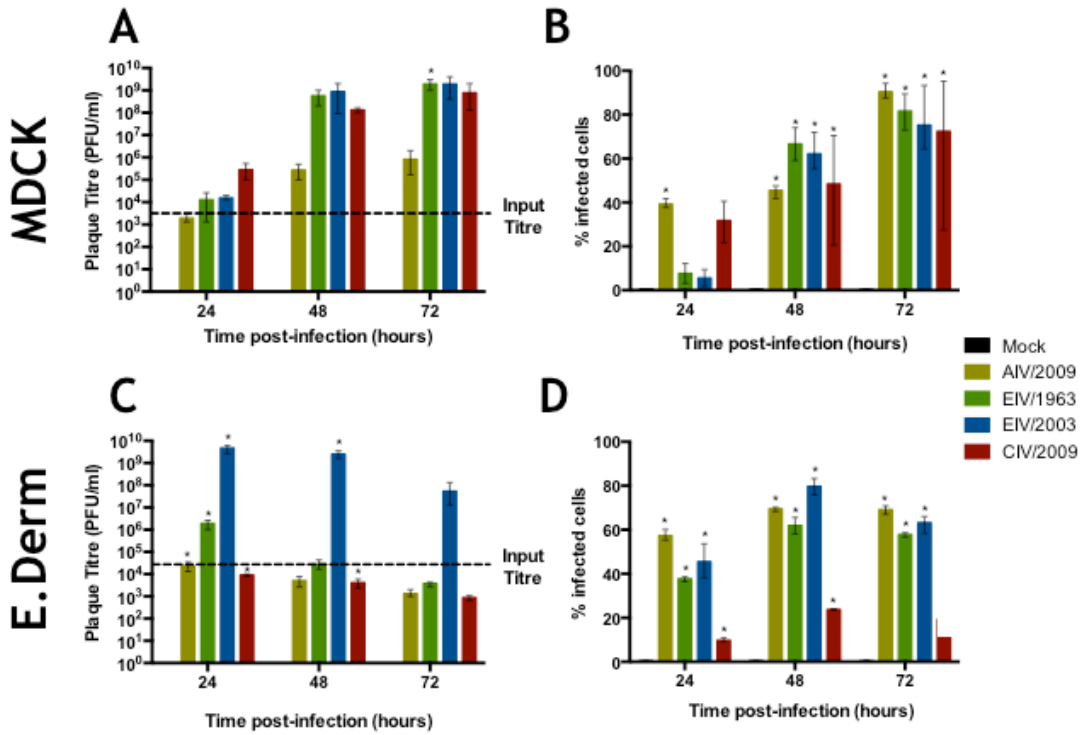

Figure 13: Growth curves of infections with AIV/2009, EIV/1963, EIV/2003 and CIV/2009, MOI 0.1 (based on MDCK titre). Intracellular and extracellular virus is shown for MDCK (A+B) and E.Derm cells (C+D). Infected cells were measured using the Guava Flow Cytometer. Experiments were repeated independently three times; error bars indicate the mean with range of the values. For each figure a statistical t-test was carried out, comparing the values of Mock-infected cells to each of the virus-infected cells. Significance is shown with * where $p \leq 0.05$.

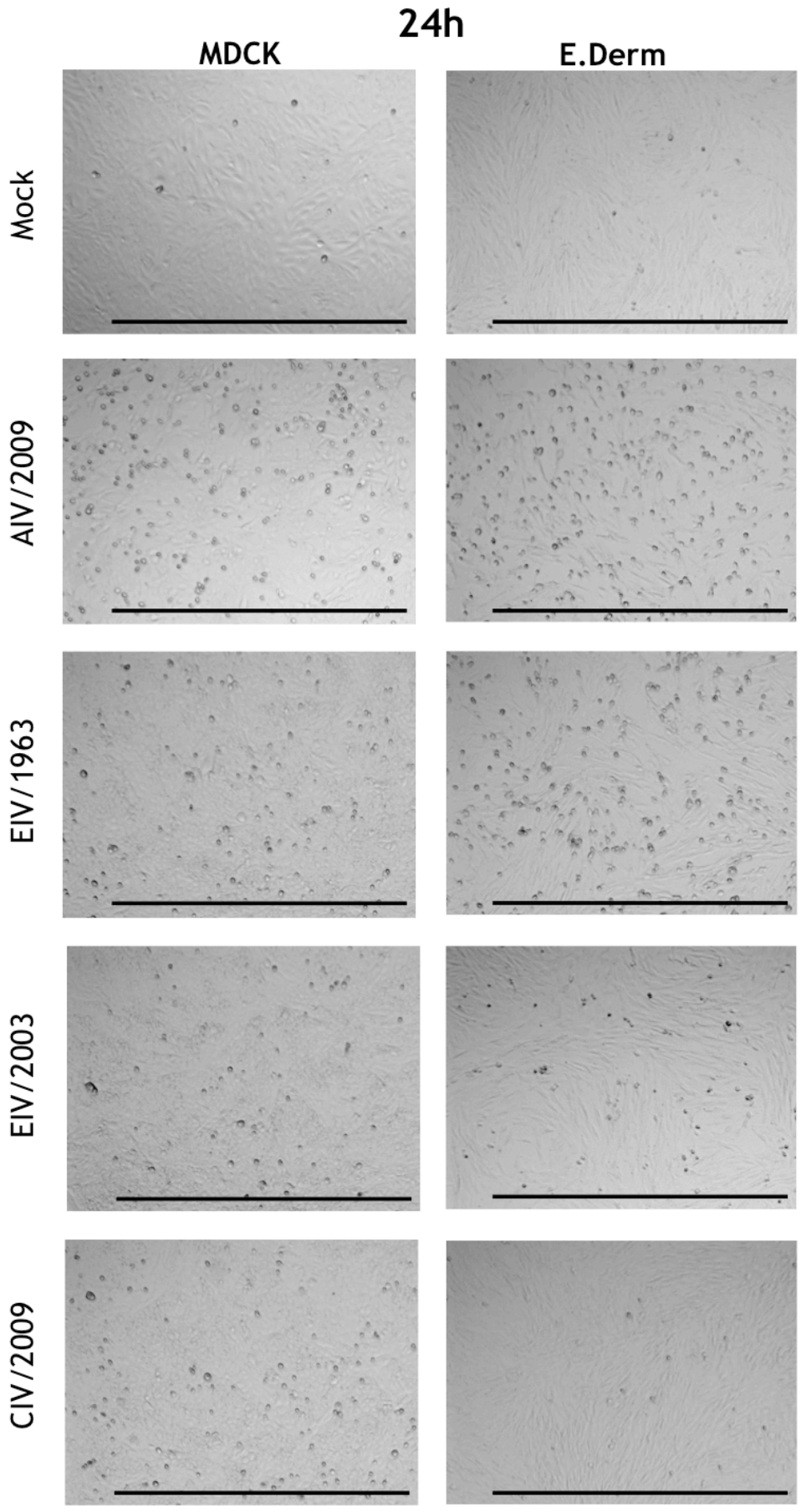

Figure 14: Light microscopy images of MDCK and E.Derm cells infected with AIV/2009, EIV/1963, EIV/2003 and CIV/2009 at 24 hours post-infection, MOI 0.1 (based on MDCK titre). Horizontal bars represent 1,000µm. (Magnification x4)

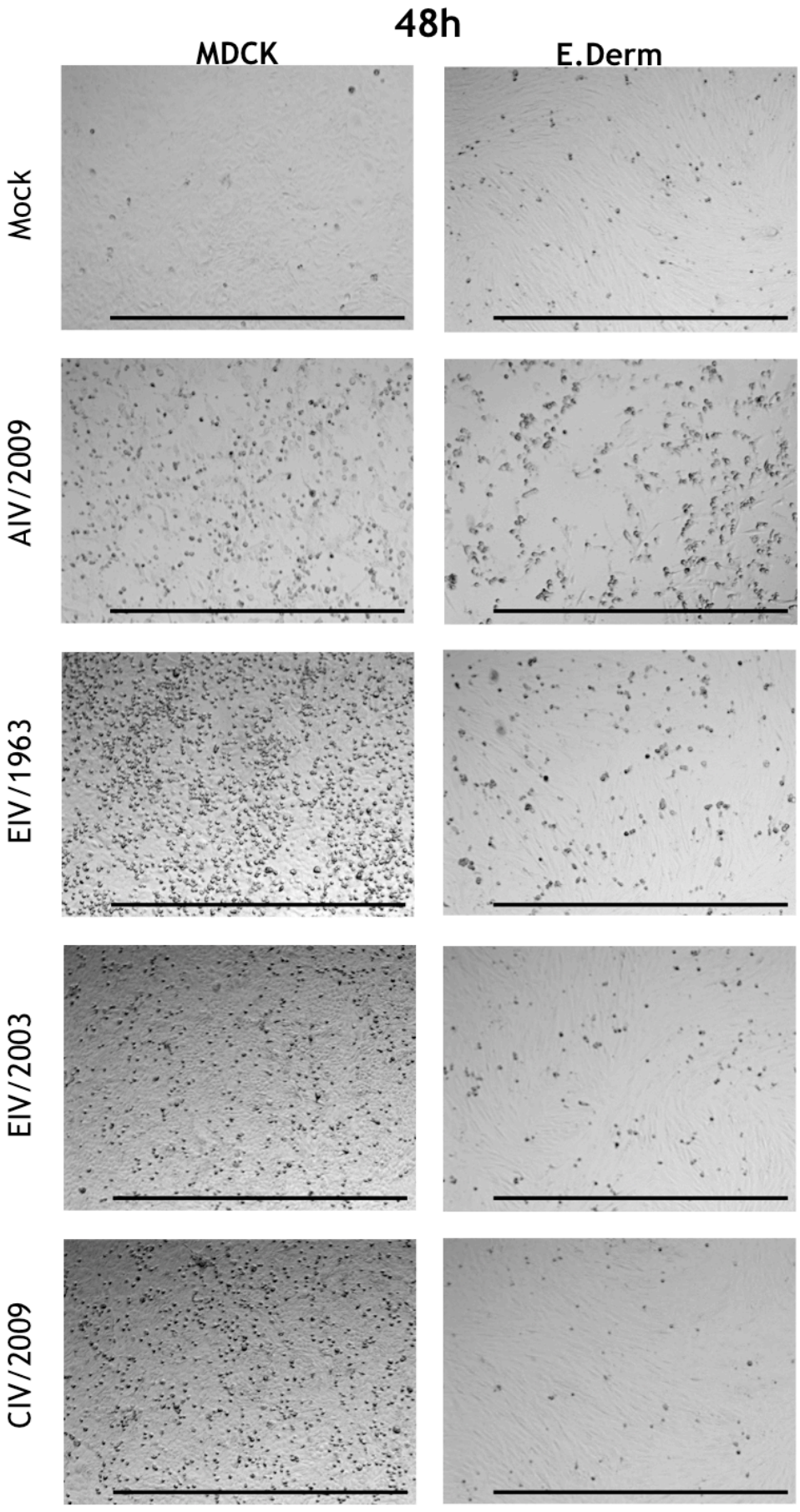

Figure 15: Light microscopy images of MDCK and E.Derm cells infected with AIV/2009, EIV/1963, EIV/2003 and CIV/2009 at 48 hours post-infection, MOI 0.1 (based on MDCK titre). Horizontal bars represent 1,000µm. (Magnification x4)

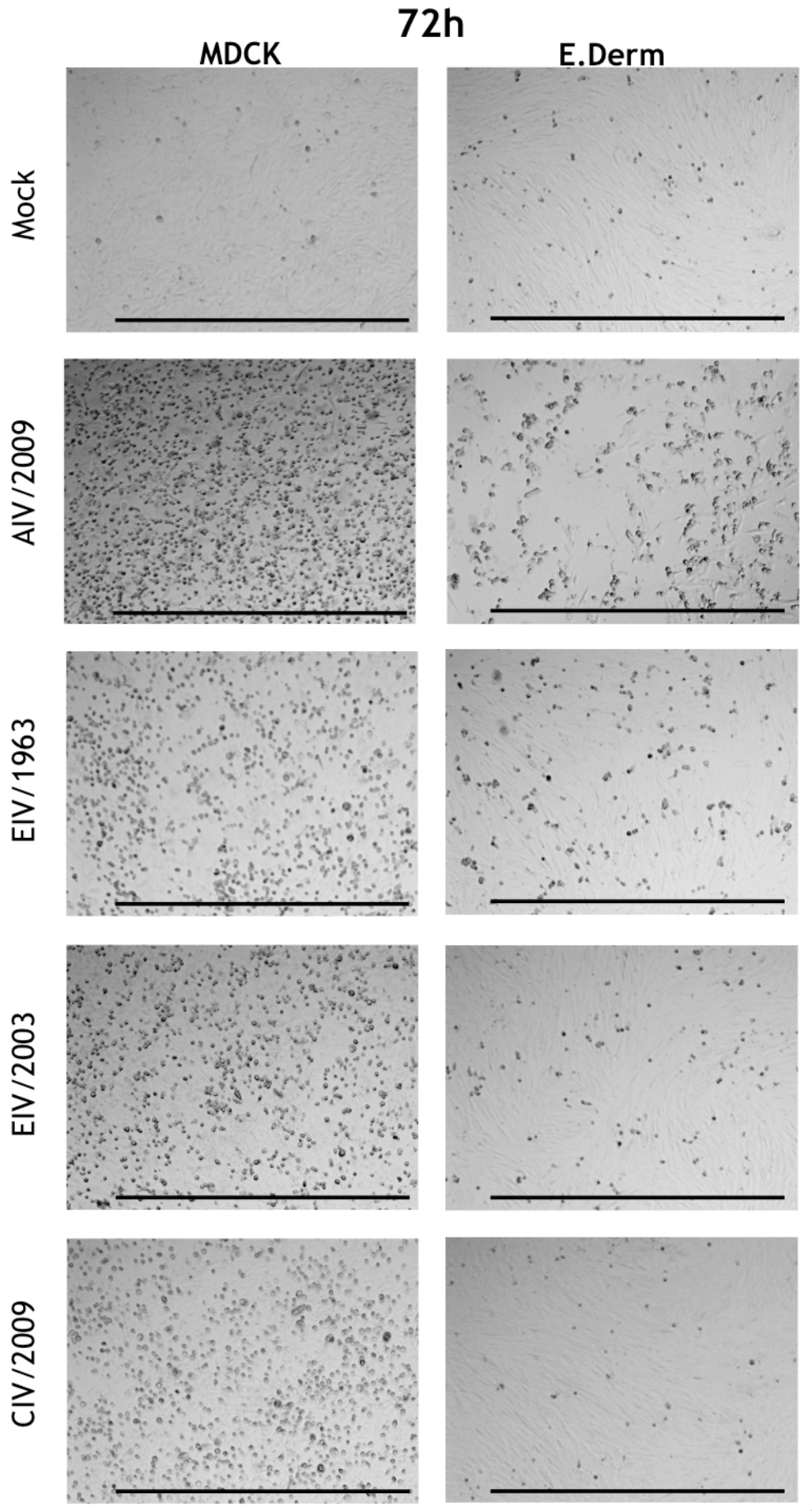

Figure 16: Light microscopy images of MDCK and E.Derm cells infected with AIV/2009, EIV/1963, EIV/2003 and CIV/2009 at 72 hours post-infection, MOI 0.1 (based on MDCK titre). Horizontal bars represent 1,000µm. (Magnification x4)

3.2.4. The addition of TPCK trypsin during replication increases the infection efficiency of less adapted influenza viruses

The addition of exogenous proteases is a requirement for most IAVs to replicate successfully in MDCK cells. To investigate whether the presence of exogenous proteases would increase infection kinetics of the viruses, the panel of IAVs were grown in E.Derm cells with and without the addition of an exogenous protease in the form of TPCK trypsin (**Figure 17, A**).

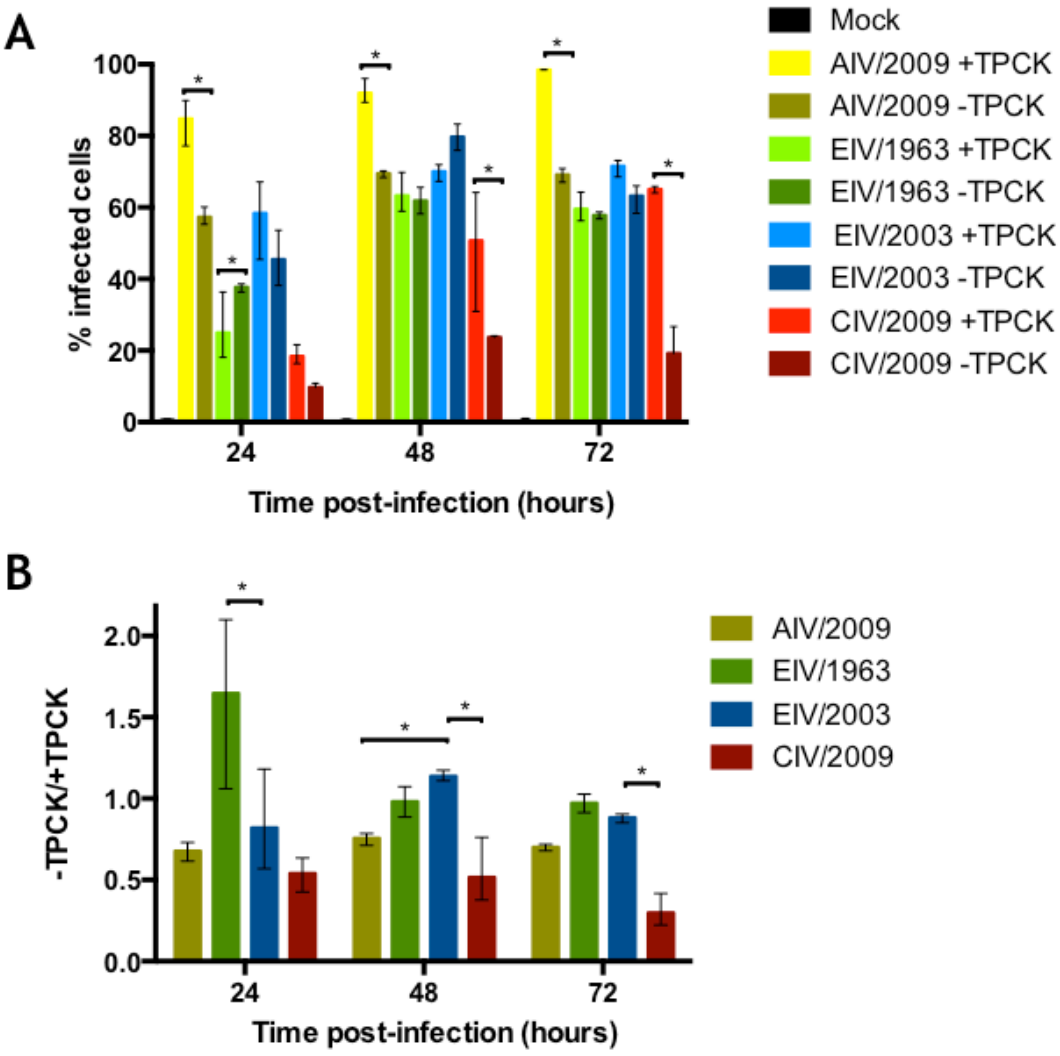

Figure 17: (A) Growth curves of intracellular virus in E.Derm cells infected with AIV/20009, EIV/1963, EIV/2003 and CIV/2009 with MOI 0.1 (based on MDCK titre), with and without the addition of exogenous TPCK trypsin in the infection media. (B) Ratio of percentage of infected cells without the addition of TPCK trypsin, divided by percentage of infected cells with the addition of TPCK trypsin. Infected cells were measured using the Guava Flow Cytometer. Experiments were repeated independently three times; error bars indicate the mean with range of the values. For each figure a statistical t-test was carried out, (A) comparing the values in the presence and absence of TPCK trypsin, (B) comparing the values to EIV/2003. Significance is shown with * where $p \leq 0.05$.

The virus that appeared to benefit the most from the addition of TPCK trypsin was AIV/20009, with significant differences (*) between virus grown in the presence of TPCK trypsin and virus grown in regular growth media at all time-points. The ratio (**Figure 17, B**) was calculated for the percentage of untreated infected cells divided by the percentage of TPCK trypsin treated infected cells. The closer the ratio is to 1, the less affected the virus is by the addition of an exogenous protease. For AIV/2009, this was ~0.69, ~0.76 and ~0.70 at 24, 48 and 72 hours post-infection, respectively. The ratio was shown to be significantly different (*) between AIV/2009 and EIV/2003 at 48 hours post-infection.

CIV/2009 was affected positively by the addition of TPCK trypsin. The percentage of cells infected showed significant differences at 48 hours and 72 hours post-infection (*), between the percentage of cells infected with and without the addition of TPCK trypsin to the infection media. CIV/2009 also had the lowest ratio when the percentage of cells infected in a regular infection, were divided by the percentage of cells infected in the presence of TPCK trypsin. At 24, 48 and 72 hours post-infection, this ratio was ~0.54, ~0.52 and ~0.30, respectively. There was a significant difference (*) when this ratio was compared to the ratio of EIV/2003, at 48 and 72 hours post- infection.

EIV/1963 showed a significant difference (*) in percentage of cells infected with and without the addition of TPCK trypsin at 24 hours post-infection - the percentage of cells infected in the presence of TPCK trypsin was less. For EIV/1963 this was ~1.65 at 24 hours post-infection, very high above the ratio of 1. In fact, as it was higher than 1, this means that EIV/1963 actually seemed to replicate more efficiently without the addition of TPCK. For 48 and 72 hours this decreased to ~0.98 and ~0.97, respectively. When compared to the ratio of EIV/2003, the only time-point where EIV/1963 was significantly different was at 24 hours post-infection (*).

The infection of EIV/2003 with and without TPCK trypsin also does not seem to be highly affected, similar to EIV/1963. The ratio of infection is ~0.82, ~1.14 and ~0.88 at 24, 48 and 72 hours post-infection. The higher ratio at 48 hours post-infection means the percentage of cells infected without the presence of TPCK trypsin was actually higher than with the addition of TPCK trypsin.

Light microscopy images were taken of the infections at each day post-infection (**Figure 18**, **Figure 19**, and **Figure 20**). It is important to note that it has been previously determined that TPCK trypsin is harmful to E.Derm cells. Therefore the images taken in the presence of TPCK trypsin naturally had a lot more CPE due to this effect. However, there did appear to be a marked increase in cell death between cells treated with and without TPCK trypsin in the case of infection with AIV/2009 and CIV/2009. The marked increased for AIV/2009 and CIV/2009 agreed with the findings that these were also the viruses that benefited the most from the addition of TPCK trypsin during infection.

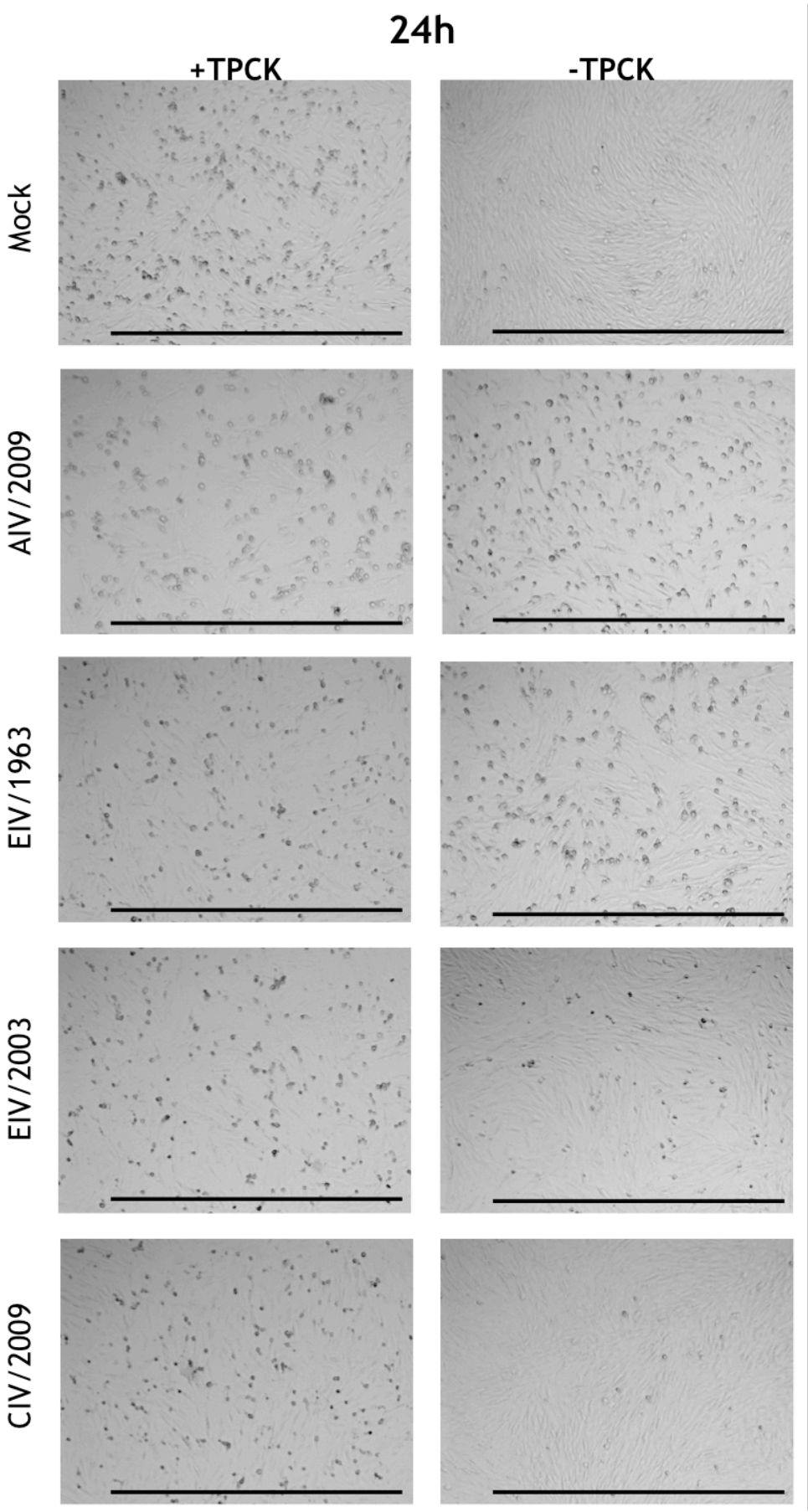

Figure 18: Light microscopy images of E.Derm cells infected in the presence or absence of TPCK trypsin. A panel of viruses were tested: AIV/2009, EIV/1963, EIV/2003 and CIV/2009 at 24 hours post-infection, MOI 0.1 (based on MDCK titre). Horizontal bars represent 1,000µm. (Magnification x4)

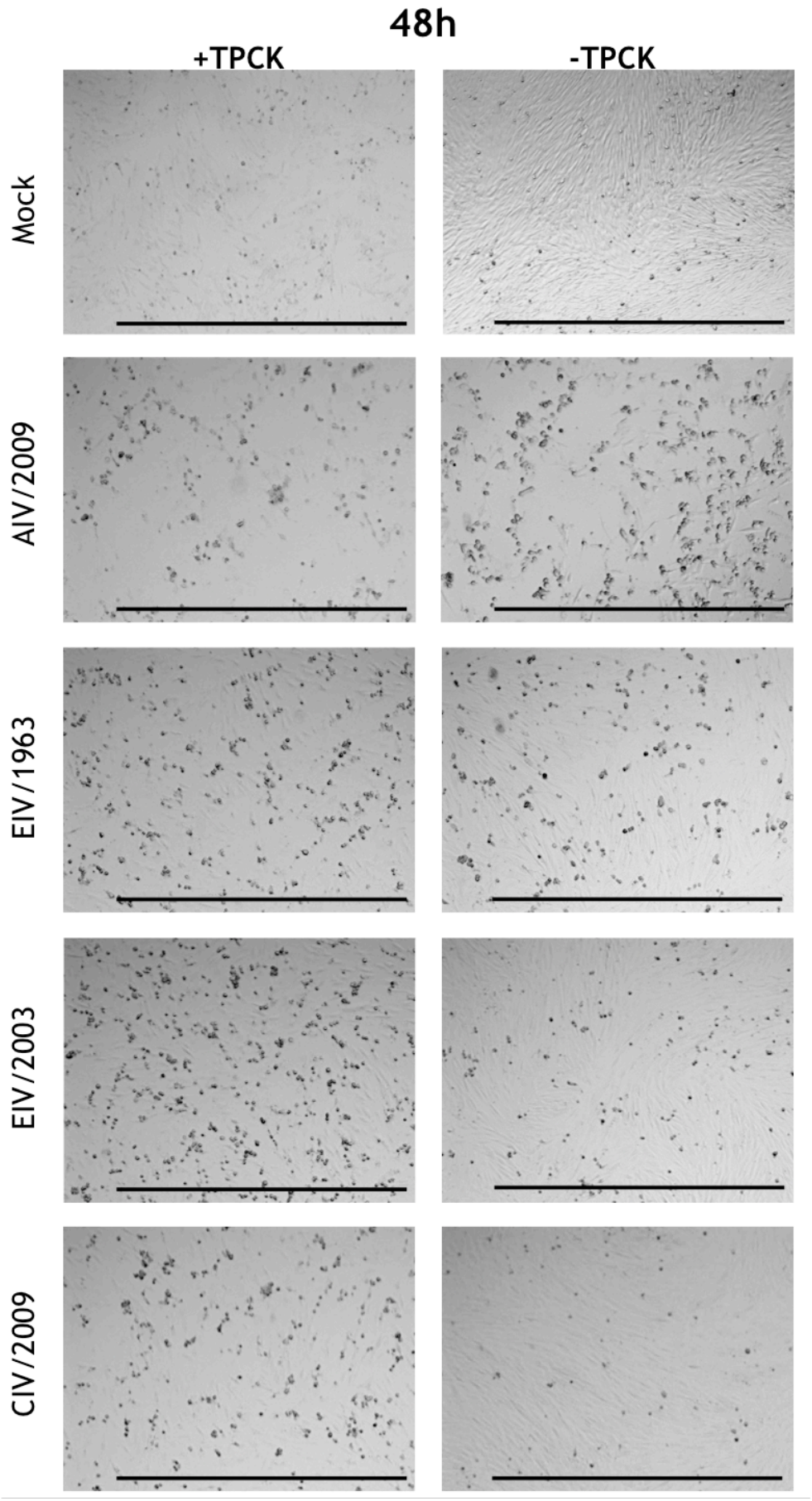

Figure 19: Light microscopy images of E.Derm cells infected in the presence or absence of TPCK trypsin. A panel of viruses were tested: AIV/2009, EIV/1963, EIV/2003 and CIV/2009 at 48 hours post-infection, MOI 0.1 (based on MDCK titre). Horizontal bars represent 1,000µm. (Magnification x4)

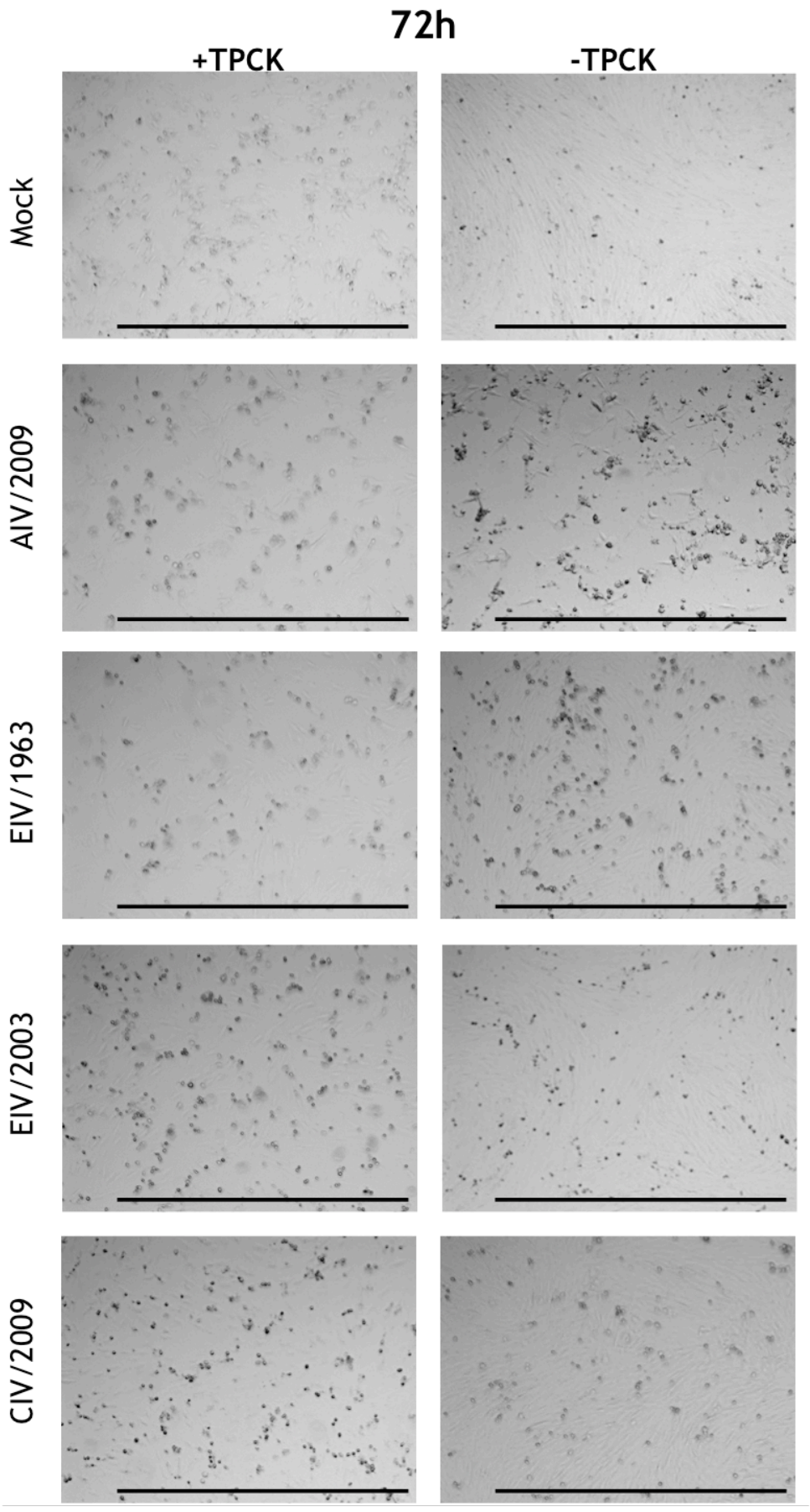

Figure 20: Light microscopy images of E.Derm cells infected in the presence or absence of TPCK trypsin. A panel of viruses were tested: AIV/2009, EIV/1963, EIV/2003 and CIV/2009 at 72 hours post-infection, MOI 0.1 (based on MDCK titre). Horizontal bars represent 1,000µm. (Magnification x4)

3.2.5. Less evolutionary adapted influenza viruses were highly affected by IFN-α pre-treatment before infection

In order to assess the capacity of the selected IAVs to antagonize an antiviral response, viruses were used to infect E.Derm cells that had been pre-treated with 1,000 UI/ml of IFN-α for 24 hours. The antiviral state of the cells was confirmed by infection with a VSV-ΔG-GFP virus (data not shown). Vesicular stomatitis virus (VSV) is a virus that is highly sensitive to IFN and can therefore be used as a control to assess the presence of an IFN response in cells. This particular virus is missing the gene that encodes glycoprotein and is therefore replication incompetent. As VSV is a virus tagged with green fluorescent protein (GFP), infected cells can be easily identified to quantify infection. All of these elements mean that VSV-ΔG-GFP is a very useful virus for testing the antiviral state of cells.

All of the IAV viruses infected fewer cells when grown in E.Derm cells in an antiviral state (**Figure 21, A**), as measured using the Guava Flow Cytometer. Infection with AIV/2009 showed a significant difference (*) in the percentage of pre-treated and untreated infected cells at all of the time-points checked (24h: ~32.6% and ~57.3%, 48h: ~27.6% and ~69.5%, 72h: ~36.8% and ~69% for IFN-α pre-treated and untreated cells respectively). The same pattern was observed for EIV/1963, a significant difference (*) in the percentage of infected cells between IFN-α pre-treated and untreated cells was observed (24h: ~15.2% and ~37.7%, 48h: ~5.3% and ~32.3%, 72h: ~7.2% and ~57.8% for IFN-α pre-treated and untreated cells respectively). CIV/2009 only showed a significant difference (*) between pre-treated and untreated infected cells at 48 hours post-infection (~12.2% and ~23.7% for IFN-α pre-treated and untreated cells respectively). There was no significant difference for EIV/2003 when grown in cells with or without the pre-treatment of IFN-α.

The ratio of infection with IFN-α pre-treatment divided by no IFN-α treatment (+IFN-α/- IFN-α) was compared between viruses (**Figure 21, B**). The closer the ratio was to 1, the less affected the virus was by IFN-α pre-treatment. EIV/2003 was the virus that was least affected by IFN-α pre-treatment as it had the highest ratio of 0.85 at 48 hours post-infection. The virus that was most affected

by IFN-α pre-treatment was EIV/1963, which had the lowest ratio of 0.12 found at 72 hours post-infection. The ratio for AIV/2009, EIV/1963, and CIV/2009 were all shown to be statistically different (*) to the EIV/2003 ratio at all three time-points.

The phenotype of infection was affected by pre-treatment of the E.Derm cells with IFN-α, as can be seen in **Figure 22, Figure 23**, and **Figure 24**. For all of the infections with IAV, there was less cell rounding and detachment in the infections after pre-treatment with IFN-α. Less rounding and detachment was most apparent for AIV/2009 and EIV/1963. For the infection with AIV/2009, very few attached cells remained at 72 hours post-infection. Whereas when the cells were pre-treated with IFN-α and infected with AIV/2009 the monolayer remained, although there were still a lot of dead cells present. At 72 hours post-infection with EIV/1963 there were still cells attached but there was a lot of cell death, which was much decreased in the infection after pre-treatment with IFN-α.

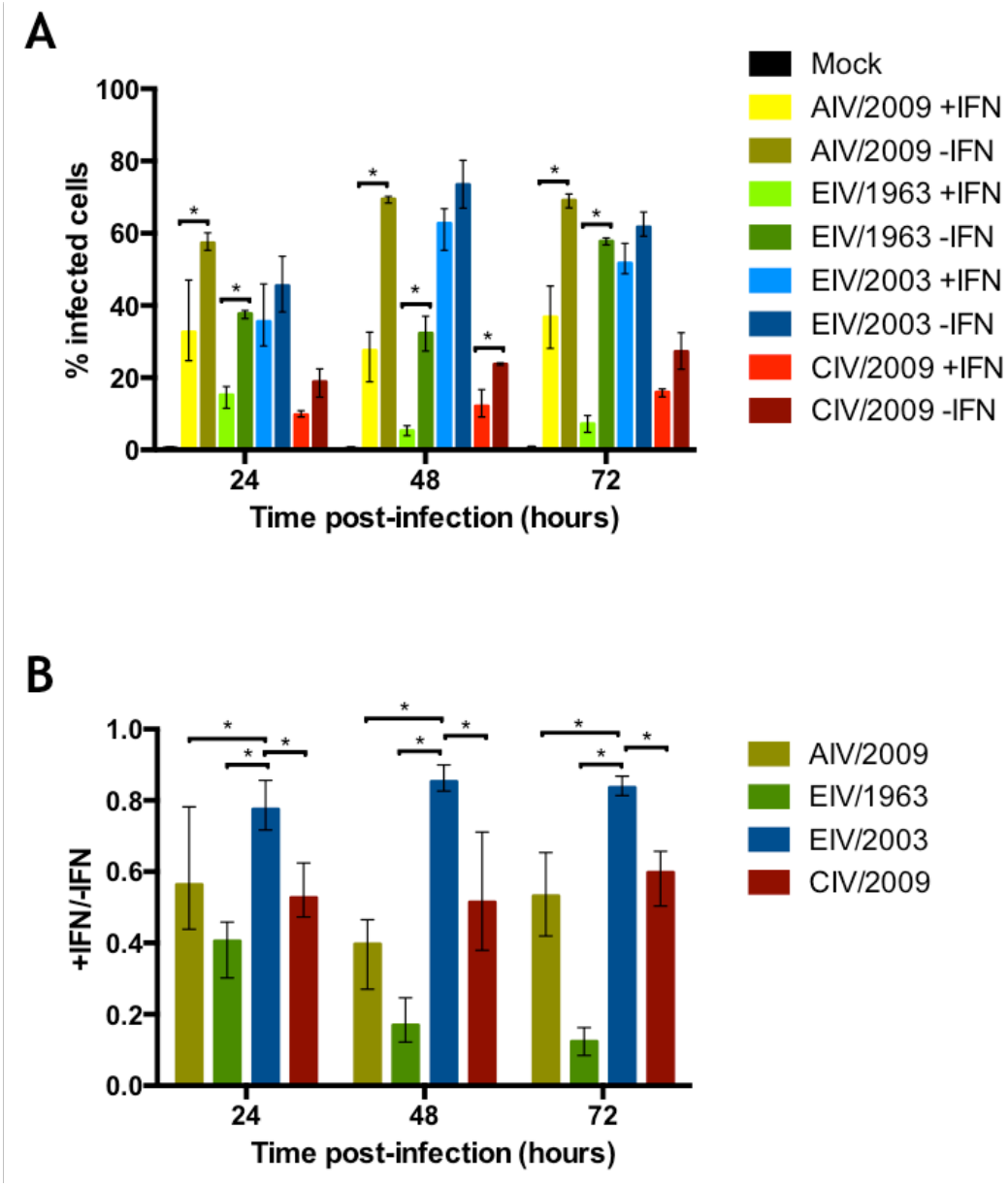

Figure 21: (A) Growth curves of intracellular virus in E.Derm cells infected with AIV/2009, EIV/1963, EIV/2003 and CIV/2009, MOI 0.1 (based on MDCK titre), with and without 24 hours of pre-treatment with 1,000 UI/ml of IFN-α. (B) Ratio of percentage of infected cells with IFN-α pre-treatment, divided by percentage of infected cells without IFN-α pre-treatment. Infected cells were measured using the Guava Flow Cytometer. Experiments were repeated independently three times; error bars indicate the mean with range of the values. For each figure a statistical t-test was carried out, (A) comparing the values in the presence and absence of TPCK trypsin, (B) comparing the values to EIV/2003. Significance is shown with * where $p \leq 0.05$.

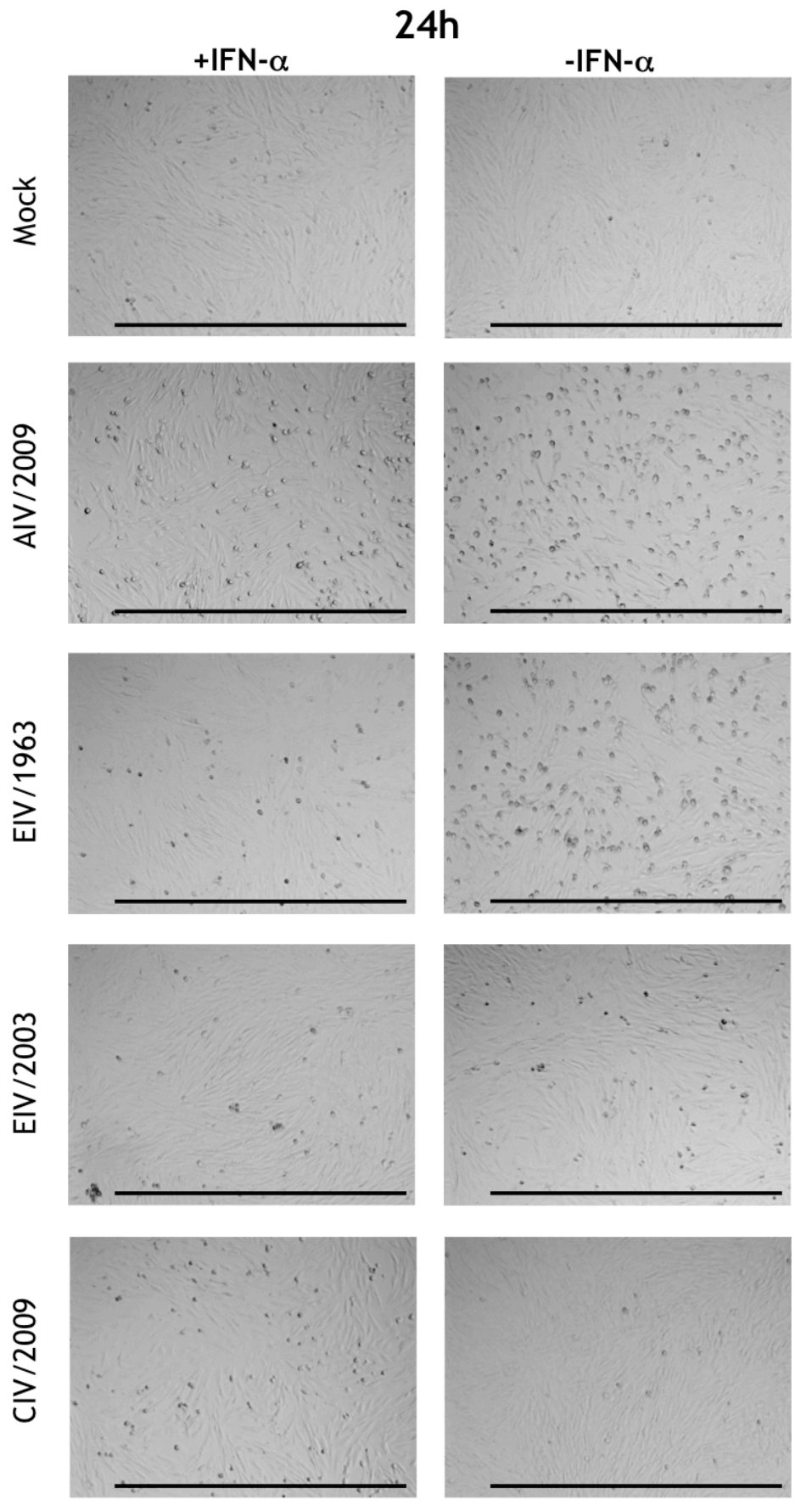

Figure 22: Light microscopy images of E.Derm cells infected with or without 24 hours of pre-treatment with 1,000 UI/ml of IFN-α. A panel of viruses were tested, AIV/2009, EIV/1963, EIV/2003 and CIV/2009 at 24 hours post-infection, MOI 0.1 (based on MDCK titre). Horizontal bars represent 1,000µm. (Magnification x4)

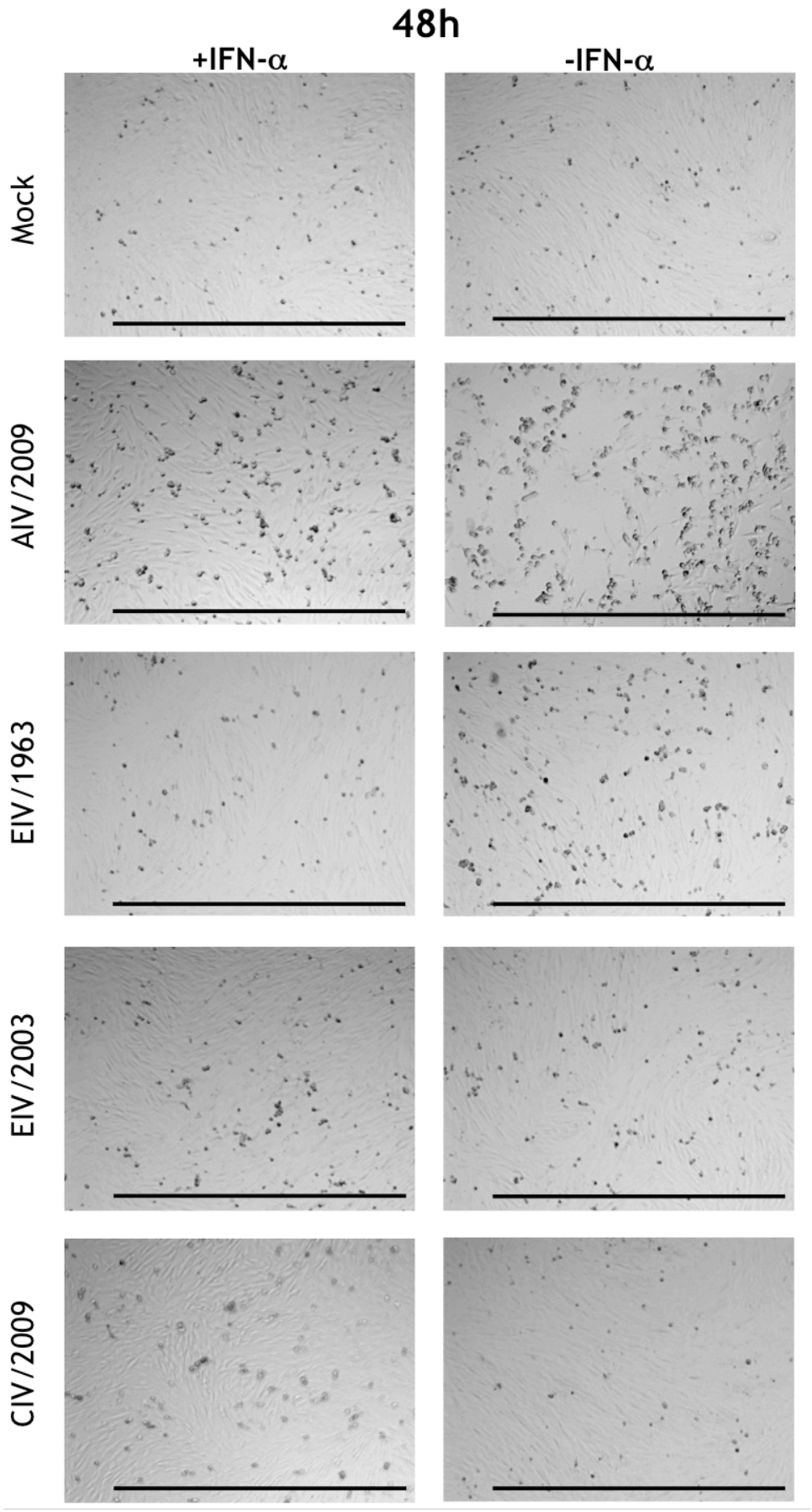

Figure 23: Light microscopy images of E.Derm cells infected with or without 24 hours of pre-treatment with 1,000 UI/ml of IFN-α. A panel of viruses were tested, AIV/2009, EIV/1963, EIV/2003 and CIV/2009 at 48 hours post-infection, MOI 0.1 (based on MDCK titre). Horizontal bars represent 1,000µm. (Magnification x4)

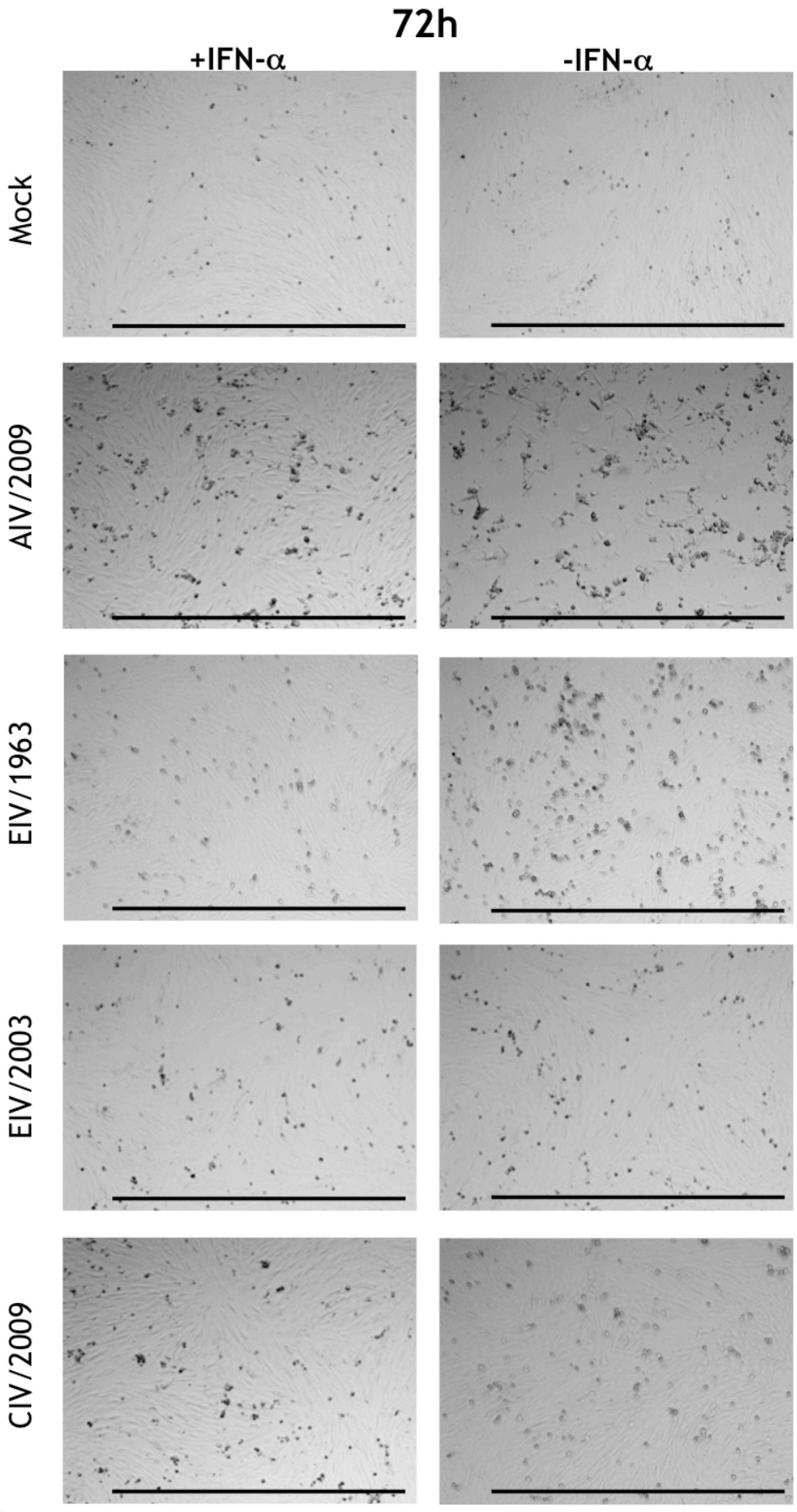

Figure 24: Light microscopy images of E.Derm cells infected with or without 24 hours of pre-treatment with 1,000 UI/ml of IFN-α. A panel of viruses were tested, AIV/2009, EIV/1963, EIV/2003 and CIV/2009 at 72 hours post-infection, MOI 0.1 (based on MDCK titre). Horizontal bars represent 1,000µm. (Magnification x4)

3.3. Discussion

Host barriers to infection with influenza A viruses (IAVs) have not been fully characterized for any hosts, including the horse. It is necessary to understand equine barriers to influenza infection, in order to better prevent cross-species transmission of IAVs to horses. Understanding equine barriers is also important as horses can be used as a model to better identify how IAVs infect humans.

A previously established *ex vivo* tracheal organ culture system (Nunes *et al*. 2010) was used to culture tracheal explants from horses. In this chapter, it was shown that these explants retain the ability to mount an interferon (IFN) response by treating the explants for 24 hours with IFN-α. Mx1 (Myxovirus Resistance Protein 1) was increasingly detected in the epithelial cells, extending to the cells in the lamina propria with higher concentrations of treatment (**Figure 11**). The presence of Mx1 means that studies with influenza infection using the *ex vivo* model are relevant, as they involve the IFN response.

Of note, the horse trachea used for the IFN treatment experiment was from a vaccinated horse and therefore would be resistant to *ex vivo* infection with EIV. Mx1 expression is quite high in the Mock-treated tracheal explants (**Figure 11**), which can be explained as it has been shown to be constitutively expressed in the respiratory tract (Chang *et al*. 1990).

Infection with the repertoire of viruses (EIV/1963, EIV/2003, AIV/2009, and CIV/2009) in the equine tracheal explants demonstrated differing growth kinetics (**Figure 12**). The virus that replicated most efficiently was EIV/2003, which was as expected, as EIV/2003 is the virus that is most adapted to an equine host. AIV/2009 replicated very sporadically, with no virus titre detected on several days of infection. CIV/2009 grew to low titres, which mimics what is reported in nature – CIV cannot infect horses (Yamanaka *et al*. 2012). EIV/1963 grew to lower titres than EIV/2003, but produced a faster decrease in ciliary function, as measured by a coloured bead assay. EIV/2003 also induced a blockage to bead clearance from the explant, meaning that infection was damaging the cilia. AIV/2009 did not cause any reduction in ciliary function, and CIV/2009 only a little at later days of infection. These results suggest that both the AIV/2009 and CIV/2009 viruses did not damage the epithelial cells of the

explants. Overall, the most adapted viruses to equine tracheal explants are the two EIV viruses, with limited replication by CIV/2009. AIV/2009 did not seem to easily replicate in the tracheal explants, suggesting that it is not adapted for replication in an equine host.

The aim of studying *in vitro* infections of E.Derm cells was to have a convenient model to better understand the barriers a virus has to overcome to adapt to its new host. MDCK and E.Derm cells were infected with a panel of four viruses. Virus replication in MDCK cells was very similar between the viruses, except for AIV/2009, which replicated 3-4 logs lower at 72 hours post-infection (**Figure 13, A+B**). Some avian influenza viruses (AIVs) replicate better in eggs rather than in cells, as is the case for this avian virus (Parvin *et al*. 2015). As for virus growth kinetics in E.Derm cells, there was a large distinction between the viruses (**Figure 13, C+D**). CIV/2009 replicated at very low titres, similar to the growth kinetics in the tracheal explants. EIV/1963 was much lower when compared to the titre of EIV/2003, which grew as high as 10^9 PFU/ml. The virus titre and percentage of cells infected of AIV/2009 were contrasting. The virus did not grow to very high titres, yet at 72 hours it had infected the highest percentage of cells out of the panel of viruses tested. An explanation for this may be that the virus could be producing Defective Interfering Particles (DIPs) that would not be detected in a plaque assay, which only detects infectious particles (Frensing *et al*. 2014). AIV/2009 also produced much higher cell death in both MDCKs and E.Derm cells. The virus could possibly be infecting the cells, but producing an abortive infection. Another reason could be that the avian virus does not titrate well on MDCK cells. If this experiment were to be repeated, it would be useful to measure virus production using another method to measure the viral genome load.

It has been extensively shown that proteases are essential for the replication of IAVs (Garten *et al*. 1981; Klenk *et al*. 1975). For a successful second round of replication, exiting virions must have the haemagglutinin (HA) proteins cleaved by proteases. This allows the maturation of the HA enabling it to bind to another new cell. Proteases are naturally present in certain cells, and are one of the factors that lead to tissue tropism by the virus (Steinhauer 1999). Infection of MDCKs requires the addition of an exogenous protease in the form of

TPCK trypsin (Tobita *et al*. 1975). As has previously been shown in this thesis, the correct proteases were present in E.Derm cells for the replication of EIV/2003 without the addition of TPCK trypsin. To test whether the replication of other IAVs would be affected by the addition of TPCK trypsin, and demonstrate that host proteases could be a barrier to infection, the viruses were grown with and without the presence of TPCK trypsin in the infection media. As seen in **Figure 17**, the viruses most affected by the addition of TPCK trypsin were AIV/2009 and CIV/2009. The reason for this could be that both viruses are not adapted to an equine host, and therefore are not evolutionarily modified to use equine proteases to cleave the HA protein. In support of this, the equine viruses (EIV/1963 and EIV/2003) were not positively affected by the addition of exogenous proteases. The lack of a positive affect for the EIVs means that they were already replicating efficiently using equine proteases, to which they were well adapted. **Figure 18**, **Figure 19**, and **Figure 20** show the light microscopy images of infection with and without TPCK trypsin. It is important to remember that E.Derm cells were negatively affected by the presence of TPCK trypsin, causing rounding of cells and detachment, as can be seen in Mock cells at 48 and 72 hours post-infection. However, taking this into account, infection with AIV/2009 and CIV/2009 in the presence of TPCK trypsin induced a marked increase of cell death and monolayer destruction.

One of the greatest barriers to viral infection is the IFN response. In order to study this effect on the panel of viruses, E.Derm cells were pre-treated for 24 hours with IFN-α to establish an antiviral state before being infected (**Figure 21**). All of the viruses were affected negatively, as shown by the ratio of the percentage of regularly infected cells, divided by the percentage of infected cells after pre-treatment with IFN-α. Each virus had a ratio less than one, which means that the viruses infected less cells with IFN-α pre-treatment than without.

As H3N8 AIVs have crossed the host-species barrier to infect the horse on more than one occasion (Morens & Taubenberger 2010; Sovinova *et al*. 1958; Waddell *et al*. 1963), it was important to study the replication of an H3N8 of avian-origin in equine tracheal explants (**Figure 11, A**) and E.Derm cells (**Figure 13, C**). The AIV/2009 virus replicated to higher consistent titres in E.Derm cells

than in tracheal explants, suggesting that a host barrier was present in the *ex vivo* tissue that is not found *in vitro*. When comparing replication with and without the presence of exogenous proteases in the form of TPCK trypsin, AIV/2009 infect a significantly higher percentage of cells when grown in the presence of TPCK trypsin (**Figure 17**). High replication rates in the presence of TPCK trypsin suggests that AIV/2009 could benefit from the presence of an exogenous trypsin, and that equine proteases may not sufficiently cleave the HA of the avian virus. In addition, there was a significant difference when AIV/2009 was grown in cells pre-treated with IFN-α. The AIV/2009 was therefore greatly restricted by an equine IFN response, which would be a significant barrier to infection if this virus ever spilled over into a horse.

The equine virus EIV/1963 is an influenza virus of avian-origin, which may not have had sufficient time to fully adapt to an equine host. In comparison to EIV/2003, the EIV/1963 virus replicated to considerably lower titres in both the tracheal explants and E.Derm cells (**Figure 12, A and Figure 13, C**). The addition of TPCK trypsin to the infection media did not cause a positive increase in viral replication (**Figure 17**). In fact, EIV/1963 infected a higher percentage of cells when not grown in the presence of TPCK trypsin, a phenomenon which was also observed by Capua *et al*. (Capua *et al*. 2013). Treatment with IFN-α significantly inhibited virus growth, meaning that EIV/1963 has not had the time to adapt to counteract the mammalian IFN response (**Figure 13**).

EIV/2003 has had 40 years to adapt to its equine host, and it replicated to the highest titre in equine tracheal explants (**Figure 12, A**) and E.Derm cells (**Figure 13, C**). Interestingly, EIV/2003 was affected least by the pre-treatment of the cells with IFN-α (**Figure 13**). The lack of a pre-treatment effect suggests that EIV/2003 has evolved ways to counter-act the anti-viral response and can replicate to high titres even in the presence of IFN. The main antagonist of the IFN response in IAVs is the non-structural protein (NS1) (Hale, Randall, et al. 2008). The NS1 of EIVs from the H3N8 lineage has evolved over time, and contributed to the adaptation of EIV to the horse (Chauché *et al*. 2017). The addition of TPCK trypsin to the media did not boost the replication kinetics of EIV/2003 (**Figure 17**), revealing that EIV/2003 was already replicating efficiently using equine proteases present in E.Derm cells.

In the case of CIV, it is not known why the virus cannot infect horses after it evolved from an EIV (**Figure 13, A**). The results in this chapter may shed some light onto why this may be. The infection of E.Derm cells with CIV after pre-treatment with IFN-α shows that they are indeed affected, but not as significantly as EIV/1963 (**Figure 13)**. The presence of infected cells is interesting, as CIV/2009 may be more evolved than EIV/1963 to counteract the mammalian anti-viral response, and so be able to replicate at the same relative efficiency after IFN-α pre-treatment. As for the experiment studying the effect of addition of an exogenous protease, this boosted the replication of CIV significantly (**Figure 17**). The boosting effect of adding exogenous protease suggests that the equine proteases are not compatible for the successful replication of CIV. When these were replaced exogenously with TPCK tryspin, the infection was rescued. These results implicate the HA and NA of CIV as determinants of viral restriction, and may give us an indication that the host proteases of horses are the barrier for CIV infection.

This chapter has only looked at the affect of pre-treatment with IFN-α to infection with IAVs. It would be very interesting to look at pre-treatment with IFN-β and IFN-γ to see if similar results are observed, or if IFN-α is the only antagonist to virus replication in equine cells. Future studies could also use reverse genetics to investigate the non-structural protein (NS1) of these IAVs, in order to find out more about the evolution of this IFN antagonist protein and how it affects viral replication.

There are many host barriers present to prevent host species transmission, and this chapter has only looked in more detail at two of these in the context of equine cells. Future research could compare these experiments in a canine cell line such as A72 cells (Feng *et al*. 2015), to determine whether CIV would be the most efficient virus that is least affected by IFN-α pre-treatment and the addition of TPCK trypsin. If such experiments showed these effects they would provide a greater strength to the argument that a virus will perform better within the context of its own host cell line and demonstrate that it has evolved to overcome the species barriers.

Overall, this chapter has looked in detail at two of the equine host barriers to influenza infection and demonstrated their effect on the replication of four different IAVs. EIV/2003, potentially the most highly adapted equine influenza from the panel of viruses, showed the greatest level of resilience to pre-treatment with IFN-α, and does not seem to be limited in replication by cellular proteases. The potentially un-adapted EIV/1963 was highly affected by the IFN response, but cellular proteases do not seem to be a limiting factor for its replication. The next chapter will use transcriptomics to study the gene expression of E.Derm cells upon infection with the two equine viruses.

Acknowledgements

The work involving equine tracheal explants was done as a team with Dr John F. Marshall, Dr Gaelle Gonzalez and Dr Livia V. Patrono. This study was funded by grants from the Horserace Betting Levy Board (HBLB).

Chapter 4

4.Comparative transcriptomics of two evolutionary distinct equine influenza viruses

4.1. Introduction

Influenza A viruses (IAVs) are a significant pathogen of many birds and mammals causing high numbers of mortality. Originating in waterfowl (Kawaoka *et al*. 1988), they have crossed species barriers to infect many other animals such as seals, humans and horses (Geraci *et al*. 1982; Rambaut *et al*. 2008; Oxburgh *et al*. 1994). These cross-species jumps do not occur readily due to within-host barriers against infection with foreign pathogens (Kuiken *et al*. 2006).

The horse is a mammal that has been infected with influenza since at least 1956, when it was first documented (Sovinova *et al*. 1958). An equine influenza virus (EIV) of the subtype H7N7 (H for Haemagglutinin and N for Neurominidase) was shown to infect horses, however this particular EIV is now considered to be extinct. It is thought that the old H7N7 was outcompeted by the new subtype to infect horses. In 1963, horses were first recorded as being infected with a new EIV of avian origin – the H3N8 subtype that led to the extinction of the old H7N7 EIV (Waddell *et al*. 1963). The virus continued to circulate within horse populations and is still present to this day.

After a spillover infection[2], such as occurred with EIV in horses in 1963, the virus must establish onward transmission and infect new susceptible hosts if it is to be maintained within the new species. Therefore, it must quickly adapt and evolve to the novel barriers encountered in a new host. These barriers include sialic acid receptors, innate immunity and protease availability (Kuiken *et al*. 2006).

IAVs are viruses that are able to evolve quickly in order to avoid the adaptive and innate immune responses of the hosts they infect (Steinhauer & Holland 1987). As RNA viruses, they have specific enzymes that drive the viral replication cycle – the RNA-dependent RNA polymerase (RdRp) (Lauring *et al*. 2013; Robert G Webster *et al*. 1992). The RdRp is known to be error-prone, producing a very high mutation rate when replicating the viral genome (Penhoet *et al*. 1971). The random production of beneficial mutations helps the viruses to

[2] A spillover infection is a single event when a pathogen from one species infects another species, and has the potential to result in an outbreak.

escape the immune response or lead to new viral properties. However, evolving the ability for continuous transmission once in a new host species is a significant challenge due to the high number of mutations that can sometimes be required.

The interferon (IFN) response is one of the greatest of the host barriers, turned on when an invading pathogen is detected and inducing neighbouring uninfected cells into an antiviral state (Guidotti & Chisari 2000). An antiviral state is produced by the presence of a cascade of IFN stimulated genes (ISGs) that can defend the cell from viral infection in many different ways (Randall & Goodbourn 2008; Goodbourn *et al*. 2000; Sadler & Williams 2008). For example, one of the most well known influenza ISGs is Mx1 (Myxovirus Resistance Protein 1), a protein that has been shown to inhibit primary transcription, viral mRNA (messenger Ribo Nucleic Acid) translation, and the activity of the viral polymerase (Samuel 1991; Staeheli *et al*. 1986; Verhelst *et al*. 2012). There are different kinds of IFN, such as IFN-β and IFN-γ, but for the purposes of this study we will concentrate on the effects of treatment with IFN-α, which is a type I IFN.

The non-structural protein (NS1) of IAVs in the main antagonist for the IFN response in cells, acting in different ways depending upon the specific virus (Hale, Randall, et al. 2008; Krug et al. 2003). The NS1 of EIV H3N8 has adapted over time through evolution in a mammalian host. The current research aims to study how a virus would control the host IFN response at different time points during its evolutionary history.

A relatively recent tool developed to study the within-host dynamics of infection is the use of high-throughput RNA sequencing (RNA-seq) to examine cellular transcriptomes (Weber 2015). RNA-seq functions by sequencing the cellular RNAs and aligning them to a host genome in order to quantify which genes are being expressed. By comparing the results from an infected group of cells/tissue to control cells/tissue, it is possible to observe which genes are upregulated or downregulated – these are named Differentially Expressed (DE) genes. Different algorithms exist to produce these lists of DE genes such as edgeR and DeqSeq, but for the purpose of this chapter we have used the algorithm called CuffDiff2 (Trapnell *et al*. 2013).

CuffDiff2 works by mapping the RNA-seq reads to a reference genome, and then calculates the transcript abundance to produce an output defined as: Fragments Per Kilobase of transcript per Million mapped reads (FPKM) (Trapnell *et al*. 2013). The FPKM value for the combined replicates of each condition is compared to the FPKM value of the Mock-infected cells. This comparison allows the calculation of the fold change in the gene expression, which is reported as the Log_2FoldChange (Log_2FC). Competing methods such as DeSeq and edgeR may sometimes offer a higher gene-level sensitivity as they use count-based methods, but can produce a higher background of false positives (Seyednasrollah *et al*. 2013). As CuffDiff2 controls for cross-replicate variability and read-mapping ambiguity, there should be less false positives identified.

The aim of this chapter was to analyse the equine cellular response to treatment with IFN-α, and infection with two different H3N8 EIVs of evolutionary distinct origin. The cells used for the transcriptomic analysis were equine dermal (E.Derm) cells, infected with one EIV from when the virus had first infected horses (EIV/1963), and one EIV after 40 years of adaption to its equine host (EIV/2003). Two time-points were analysed, corresponding to one being during the eclipse phase of replication (4 hours), and one after 24 hours of treatment/infection. The gene expression from the IFN-α-treated or infected cells will be compared to the RNA present in Mock-infected cells to quantitatively measure the increase or decrease of gene transcripts in response to the stimulus.

4.2. Results

4.2.1. Proportion of infected E.Derm cells at 4 hours post-infection

E.Derm cells were infected with two different equine influenza viruses, the older EIV/1963 and the newer mammalian adapted EIV/2003. Three separate stocks of each virus were grown, so as to allow for the transcriptomic analyses of viral quasispecies. Two wells were infected in parallel for each experiment, one from which cells were collected for RNA extraction, and one from which cells were collected for immunofluorescent staining and quantification using the Guava Flow Cytometer. Samples were chosen with similar percentage of infected cells, so as to allow for the most unbiased comparison between the two viruses (i.e. if one virus had infected more cells, the transcriptome would be affected differently when compared to a virus that had infected fewer cells). **Figure 25** shows the experimental samples that were selected for RNA extraction and sequencing. For EIV/1963, the average percentage of infected cells was 45.8%, and for EIV/2003 it was 46.2%.

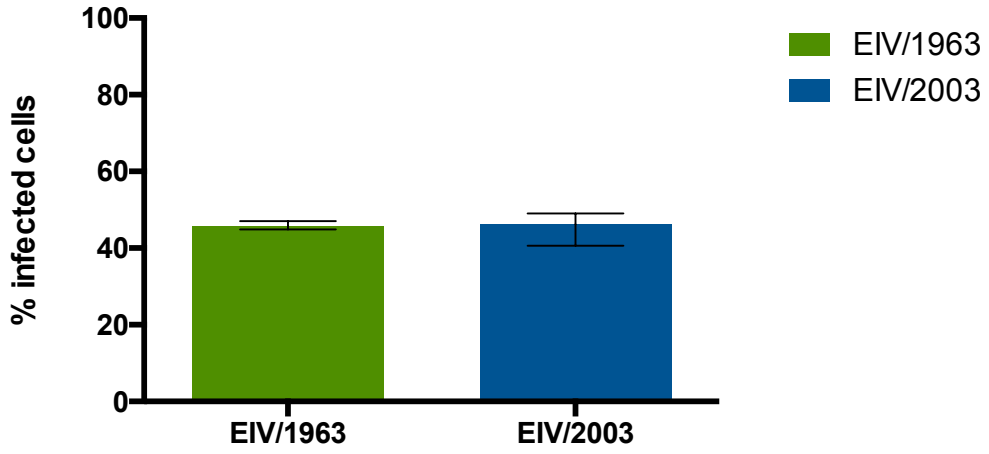

Figure 25: Percentage of infected E.Derm cells with both EIVs at 4 hours post-infection. Infected cells were measured using the Guava Flow Cytometer. Experiments were repeated independently three times; error bars indicate the mean with range of the values.

4.2.2. RNA Quantification and Integrity

The RNA extracted from the Mock, INF-α treated, and EIV-infected E.Derm cells were measured using a Qubit to check the RNA Integrity Number (RIN). Only samples with an RIN of over 8 were accepted for sequencing. The lowest RIN

value was 9.8, with five samples having a RIN of 9.9, and seventeen samples with a RIN of 10.

Table 2: Information regarding the samples sent for sequencing, RIN value and concentration of RNA is provided.

		RNA Integrity Number	Concentration (ng/µl)
Mock 4hours	Repeat 1	10	83.6
	Repeat 2	10	86.3
	Repeat 3	10	144
IFN-a 4hours	Repeat 1	10	62.7
	Repeat 2	10	94.8
	Repeat 3	10	168
EIV/1963 4hours	Repeat 1	10	64.7
	Repeat 2	10	116
	Repeat 3	10	181
EIV/2003 4hours	Repeat 1	10	71.2
	Repeat 2	10	110
	Repeat 3	10	171
Mock 24hours	Repeat 1	10	91.7
	Repeat 2	10	156
	Repeat 3	9.9	242
IFN-a 4hours	Repeat 1	10	67.2
	Repeat 2	10	126
	Repeat 3	9.9	186
EIV/1963 4hours	Repeat 1	9.9	79.7
	Repeat 2	9.9	57.5
	Repeat 3	9.7	109
EIV/2003 4hours	Repeat 1	9.9	129
	Repeat 2	10	114
	Repeat 3	9.8	148

4.2.3. Kraken results after RNASeq

Kraken is a tool that provides the information of how many reads align to pathogens, indicating contamination levels within the samples. These pathogens consist of bacteria, viruses, and archaea. Across the replicates and different conditions, there was a varying percentage of reads that were assigned as belonging to pathogens.

For Mock-infected and IFN-α-treated cells at both 4 hours and 24 hours there was were no hits with pathogens (**Figures 25-30 and 37-42**). At 4 hours post-infection EIV/1963 had 0.8%, 1% and 2% of unaligned reads mapped to viruses (**Figures 31-33**). Of these reads, 99%, 99% and 100% mapped to IAV, respectively. Similarly for EIV/2003, 0.3%, 0.2% and 1% of unmapped reads mapped to viruses (**Figures 34-36**). However, of these hits 90%, 91% and 98% mapped to IAV, respectively. The majority of the rest of the hits aligned to RD114 Retrovirus – 6%, 7% and 2% respectively.

When analysing the unaligned reads at 24 hours post-infection, Kraken assigned 2%, of all three repeats of EIV/1963-infected samples to virus (**Figures 43-45**). Of these, 98%, 98% and 99% were assigned to IAV respectively. However, another 0.9%, 1% and 0.5% were assigned to Orthoretrovirinae respectively. For EIV/2003-infected samples at 24 hours 0.7%, 0.6% and 0.9% of unassigned reads were mapped to viruses, with 98%, 97% and 96% of these hits aligning to IAV respectively (**Figures 46-48**). Again, some hits aligned to RD114 Retrovirus – 2%, 2% and 3% respectively.

Figure 26: All unmapped sequenced reads from Mock 4 hour (Replicate 1) were processed with the Kraken tool. Image shows the level of reads aligned to pathogens: first a summary, and then a closer analysis of the reads aligned to viruses.

Figure 27: All unmapped sequenced reads from Mock 4 hour (Replicate 2) were processed with the Kraken tool. Image shows the level of reads aligned to pathogens: first a summary, and then a closer analysis of the reads aligned to viruses.

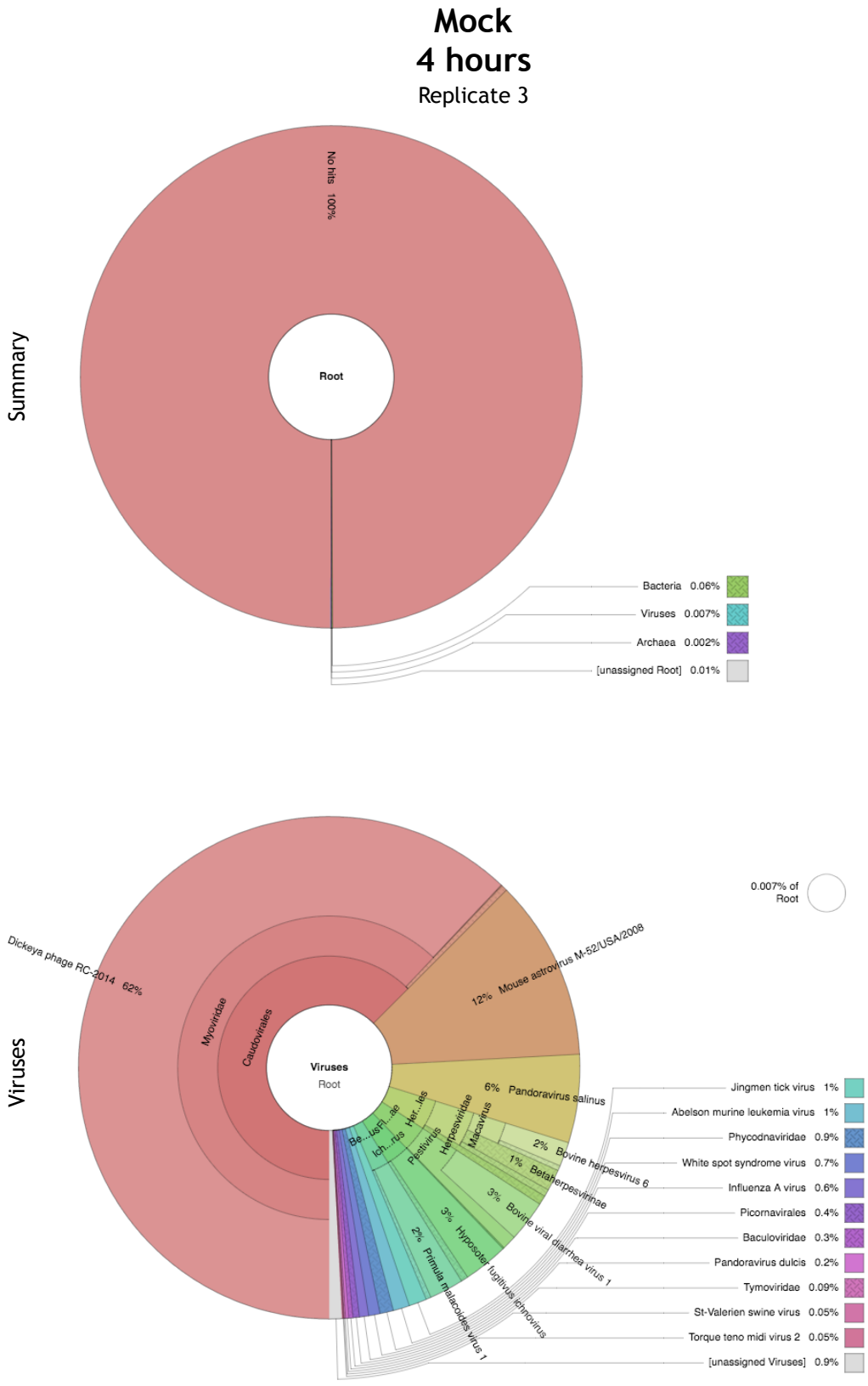

Figure 28: All unmapped sequenced reads from Mock 4 hour (Replicate 3) were processed with the Kraken tool. Image shows the level of reads aligned to pathogens: first a summary, and then a closer analysis of the reads aligned to viruses.

Figure 29: All unmapped sequenced reads from IFN-α 4 hour-treated (Replicate 1) were processed with the Kraken tool. Image shows the level of reads aligned to pathogens: first a summary, and then a closer analysis of the reads aligned to viruses.

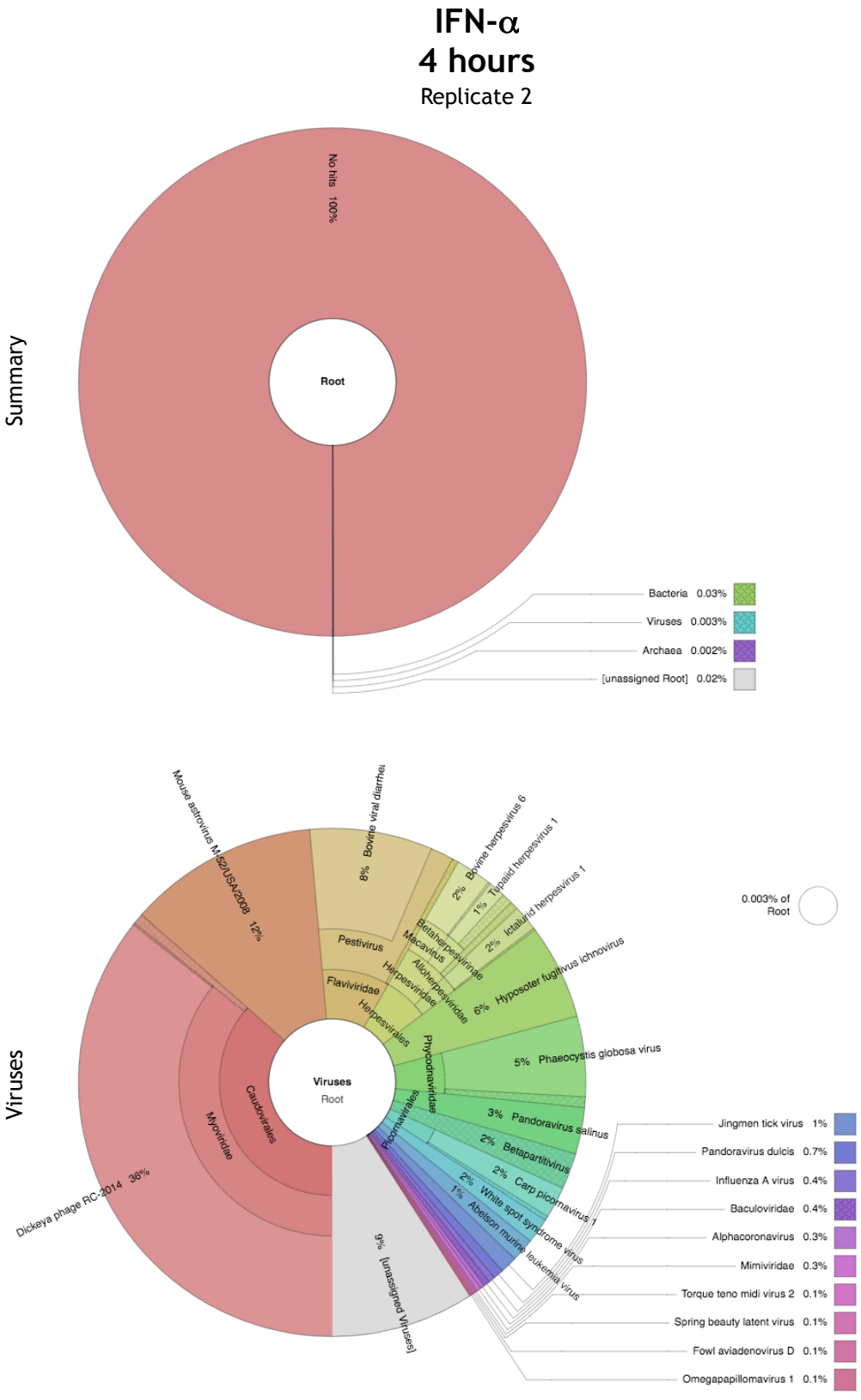

Figure 30: All unmapped sequenced reads from IFN-α 4 hour-treated (Replicate 2) were processed with the Kraken tool. Image shows the level of reads aligned to pathogens: first a summary, and then a closer analysis of the reads aligned to viruses.

Figure 31: All unmapped sequenced reads from IFN-α 4 hour-treated (Replicate 3) were processed with the Kraken tool. Image shows the level of reads aligned to pathogens: first a summary, and then a closer analysis of the reads aligned to viruses.

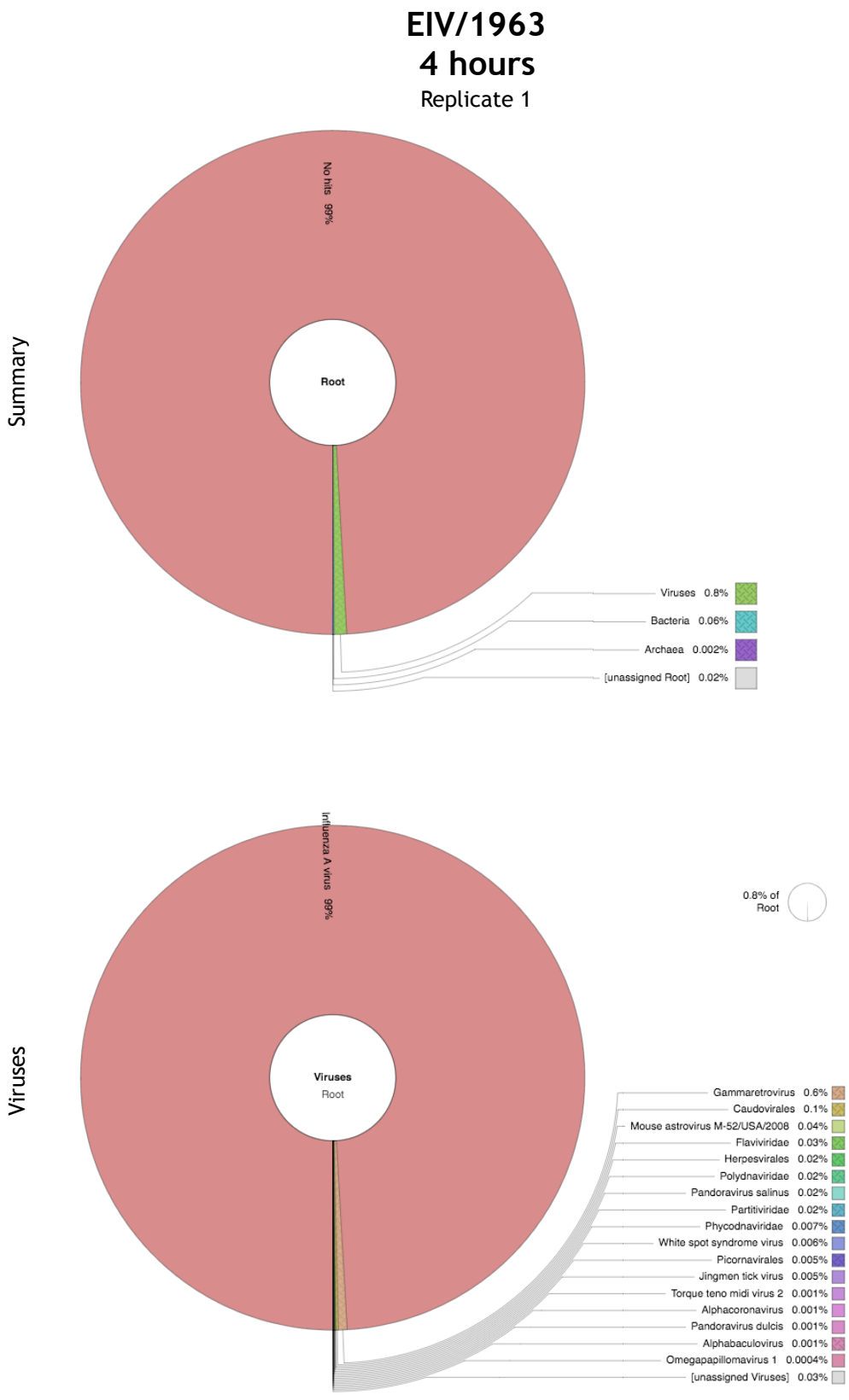

Figure 32: All unmapped sequenced reads from EIV/1963 4 hour-infected (Replicate 1) were processed with the Kraken tool. Image shows the level of reads aligned to pathogens: first a summary, and then a closer analysis of the reads aligned to viruses.

Figure 33: All unmapped sequenced reads from EIV/1963 4 hour-infected (Replicate 2) were processed with the Kraken tool. Image shows the level of reads aligned to pathogens: first a summary, and then a closer analysis of the reads aligned to viruses.

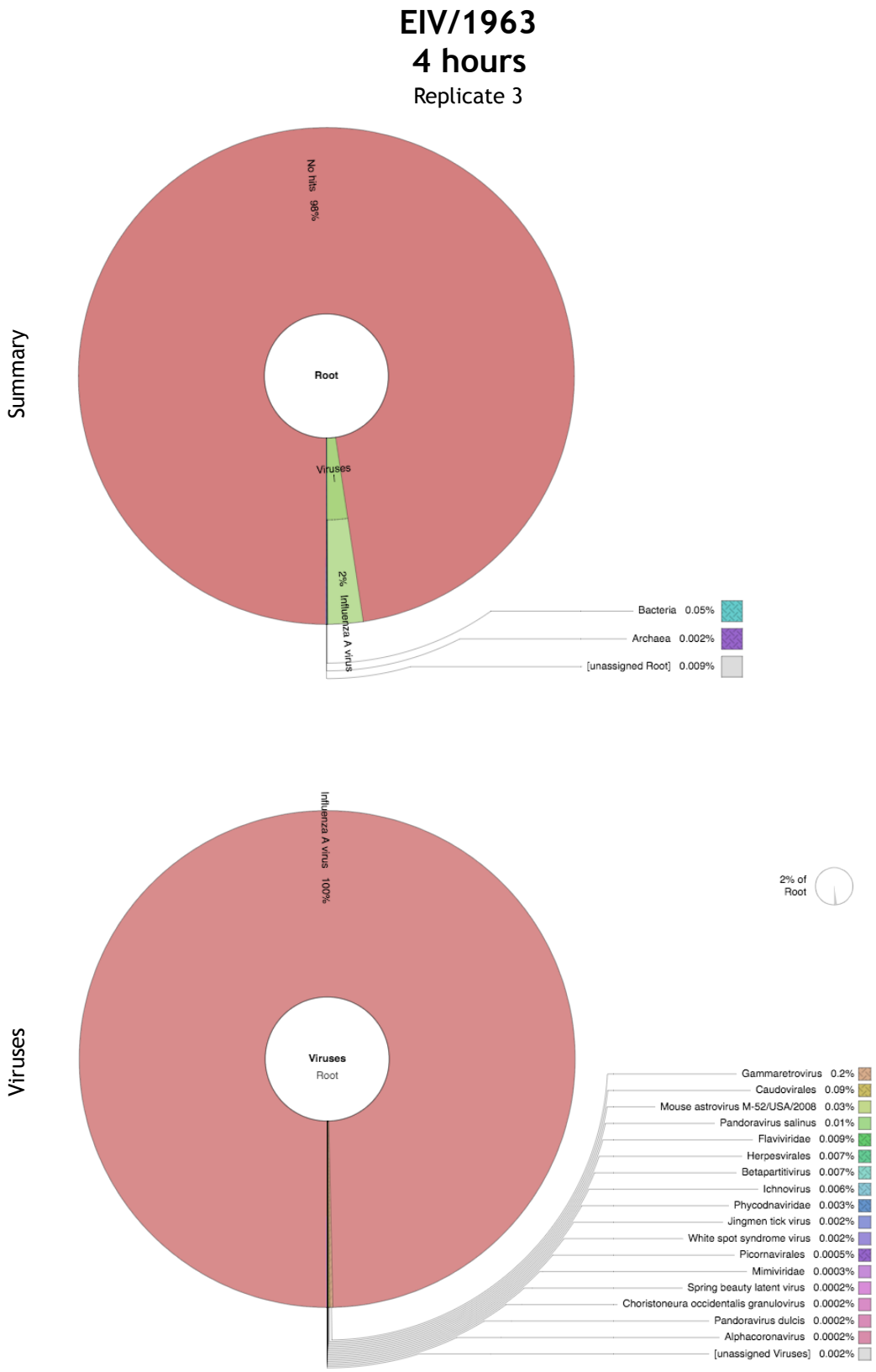

Figure 34: All unmapped sequenced reads from EIV/1963 4 hour-infected (Replicate 3) were processed with the Kraken tool. Image shows the level of reads aligned to pathogens: first a summary, and then a closer analysis of the reads aligned to viruses.

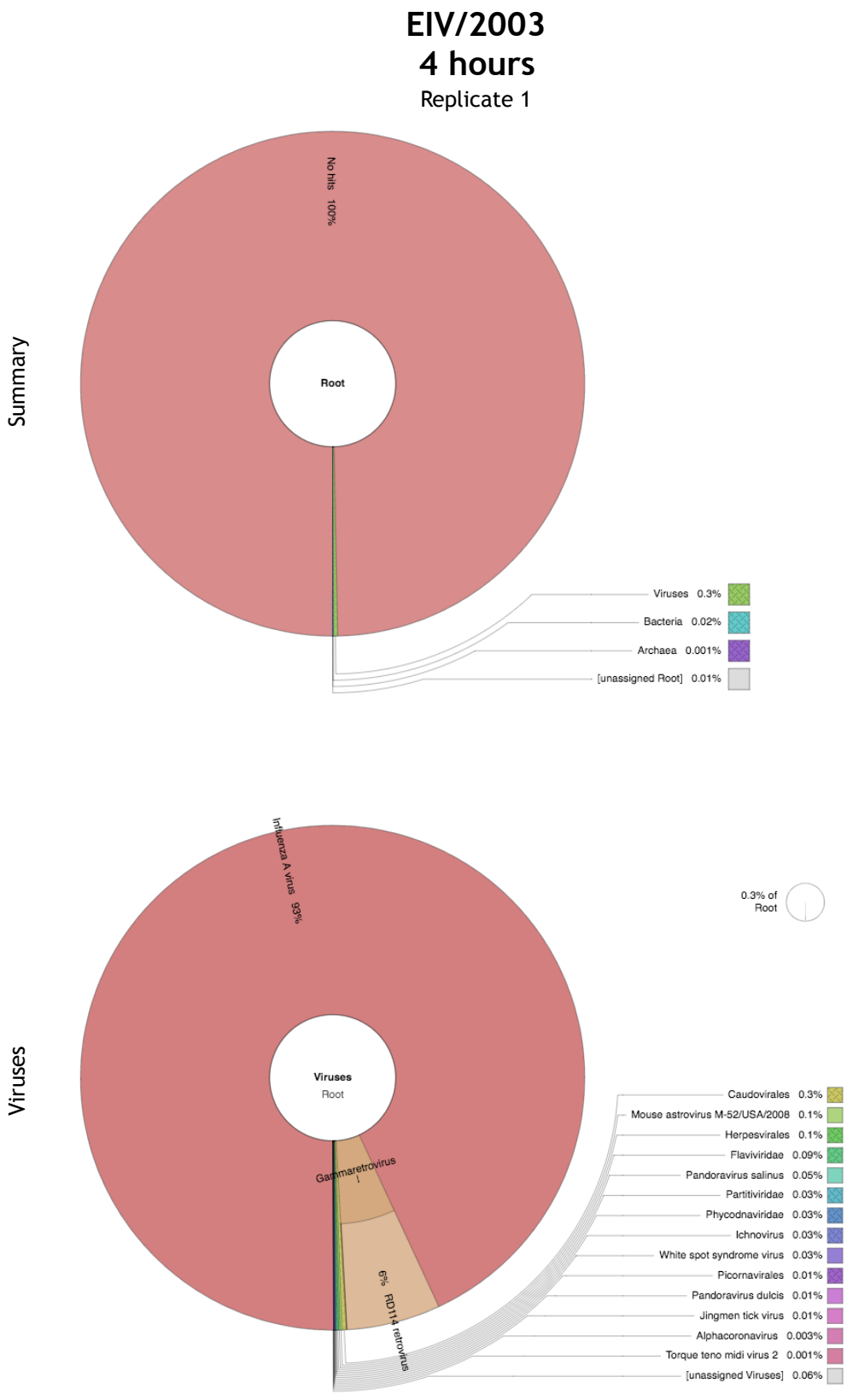

Figure 35: All unmapped sequenced reads from EIV/2003 4 hour-infected (Replicate 1) were processed with the Kraken tool. Image shows the level of reads aligned to pathogens: first a summary, and then a closer analysis of the reads aligned to viruses.

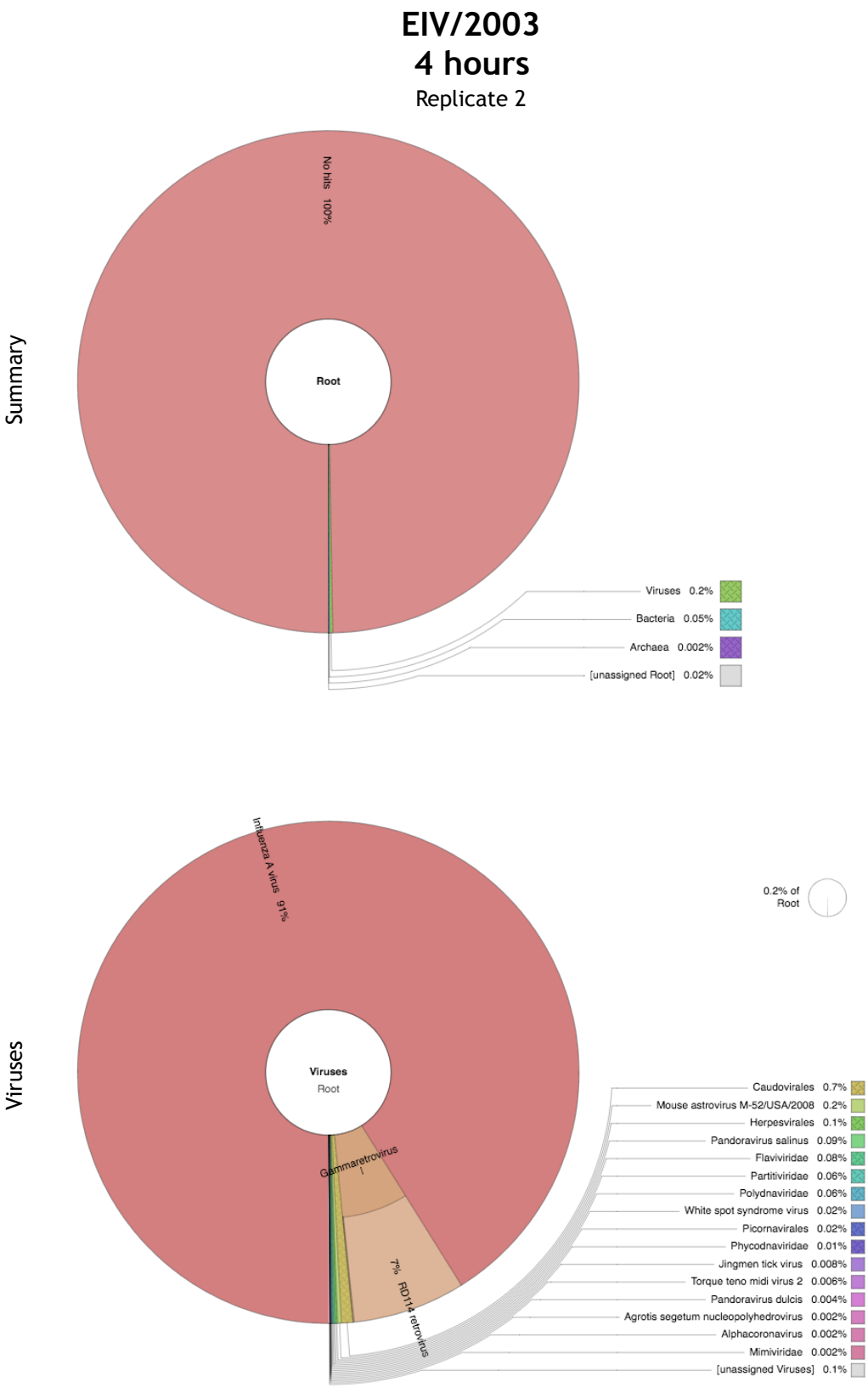

Figure 36: All unmapped sequenced reads from EIV/2003 4 hour-infected (Replicate 2) were processed with the Kraken tool. Image shows the level of reads aligned to pathogens: first a summary, and then a closer analysis of the reads aligned to viruses.

Figure 37: All unmapped sequenced reads from EIV/2003 4 hour-infected (Replicate 3) were processed with the Kraken tool. Image shows the level of reads aligned to pathogens: first a summary, and then a closer analysis of the reads aligned to viruses.

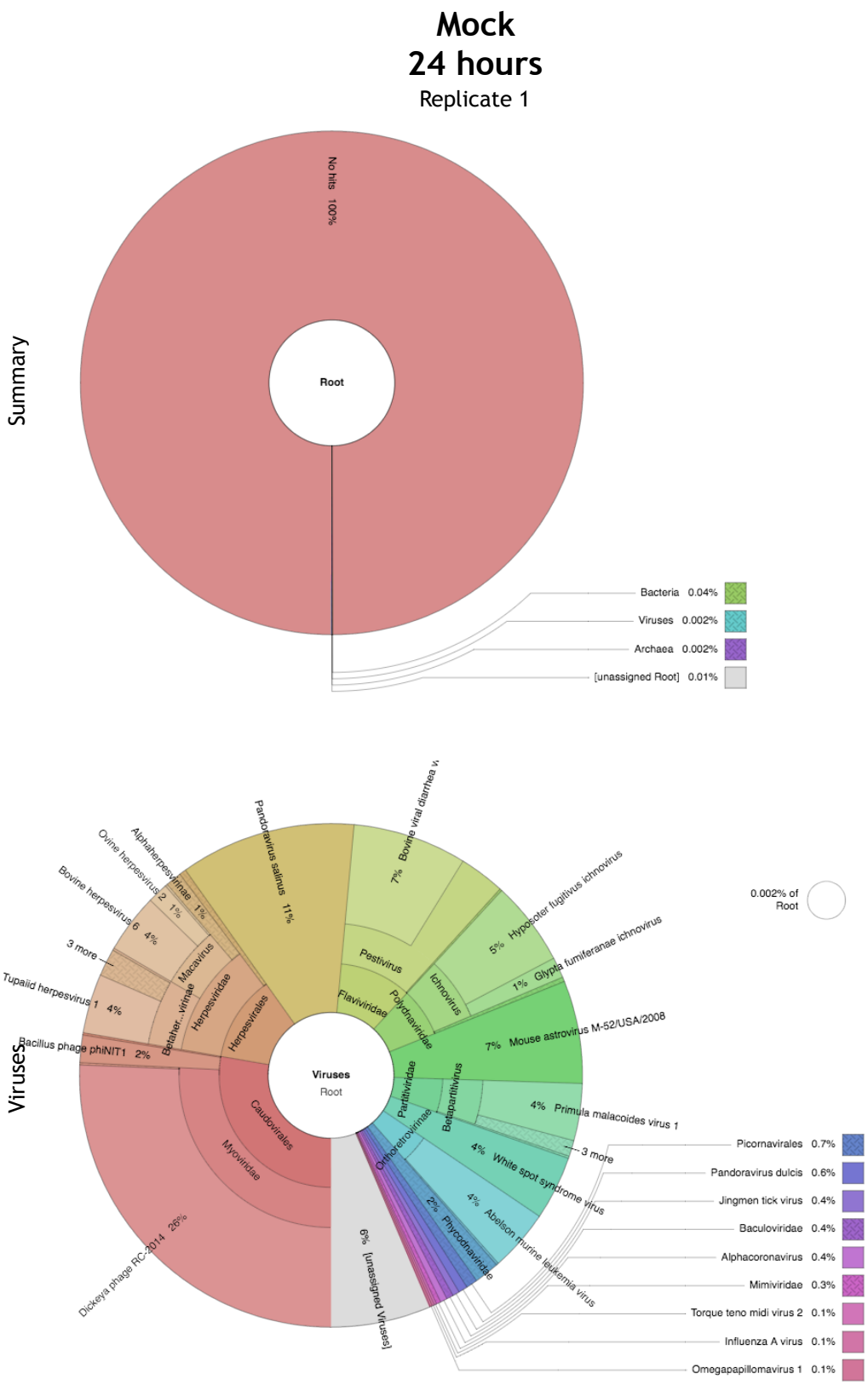

Figure 38: All unmapped sequenced reads from Mock 24 hour (Replicate 1) were processed with the Kraken tool. Image shows the level of reads aligned to pathogens: first a summary, and then a closer analysis of the reads aligned to viruses.

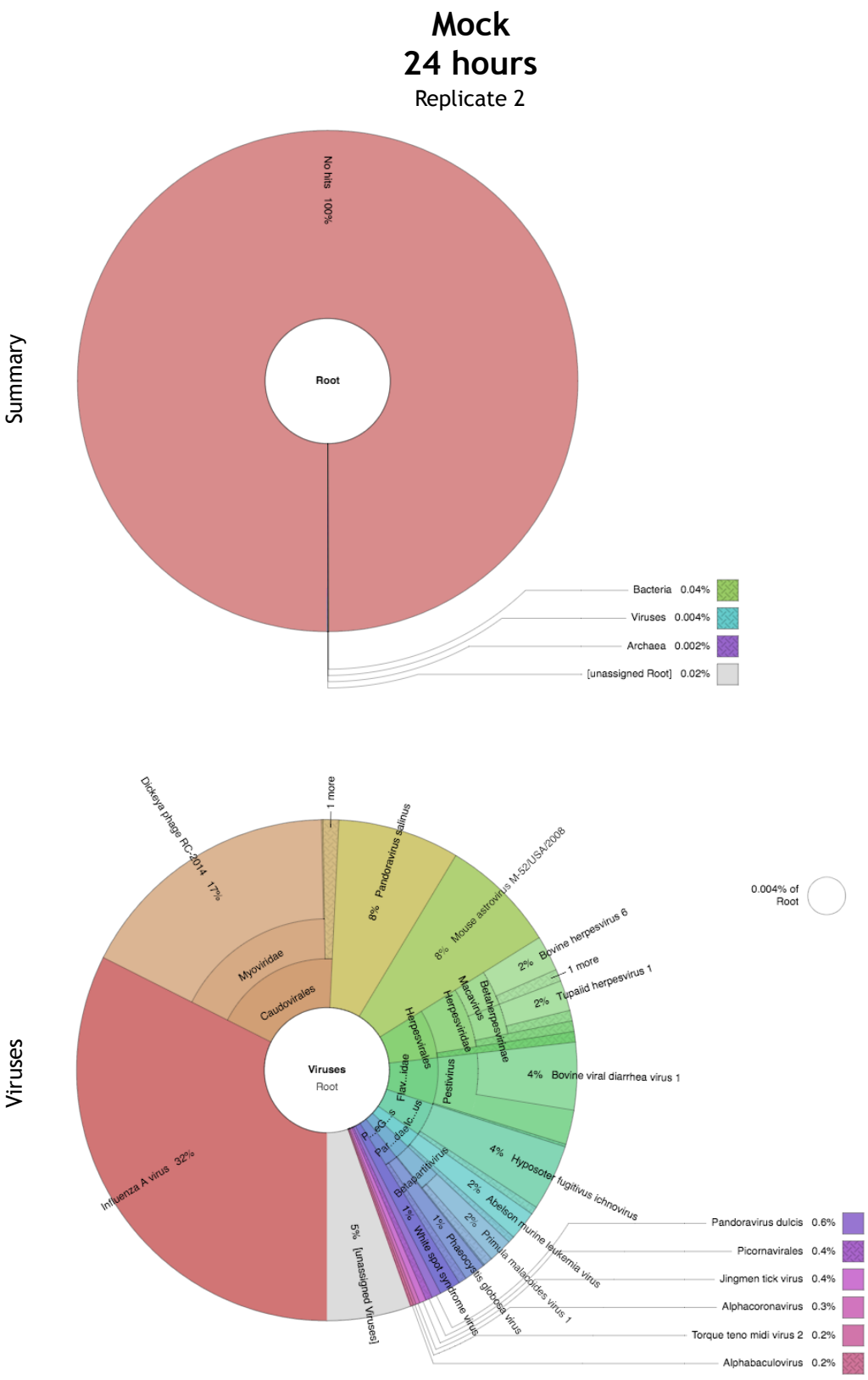

Figure 39: All unmapped sequenced reads from Mock 24 hour (Replicate 2) were processed with the Kraken tool. Image shows the level of reads aligned to pathogens: first a summary, and then a closer analysis of the reads aligned to viruses.

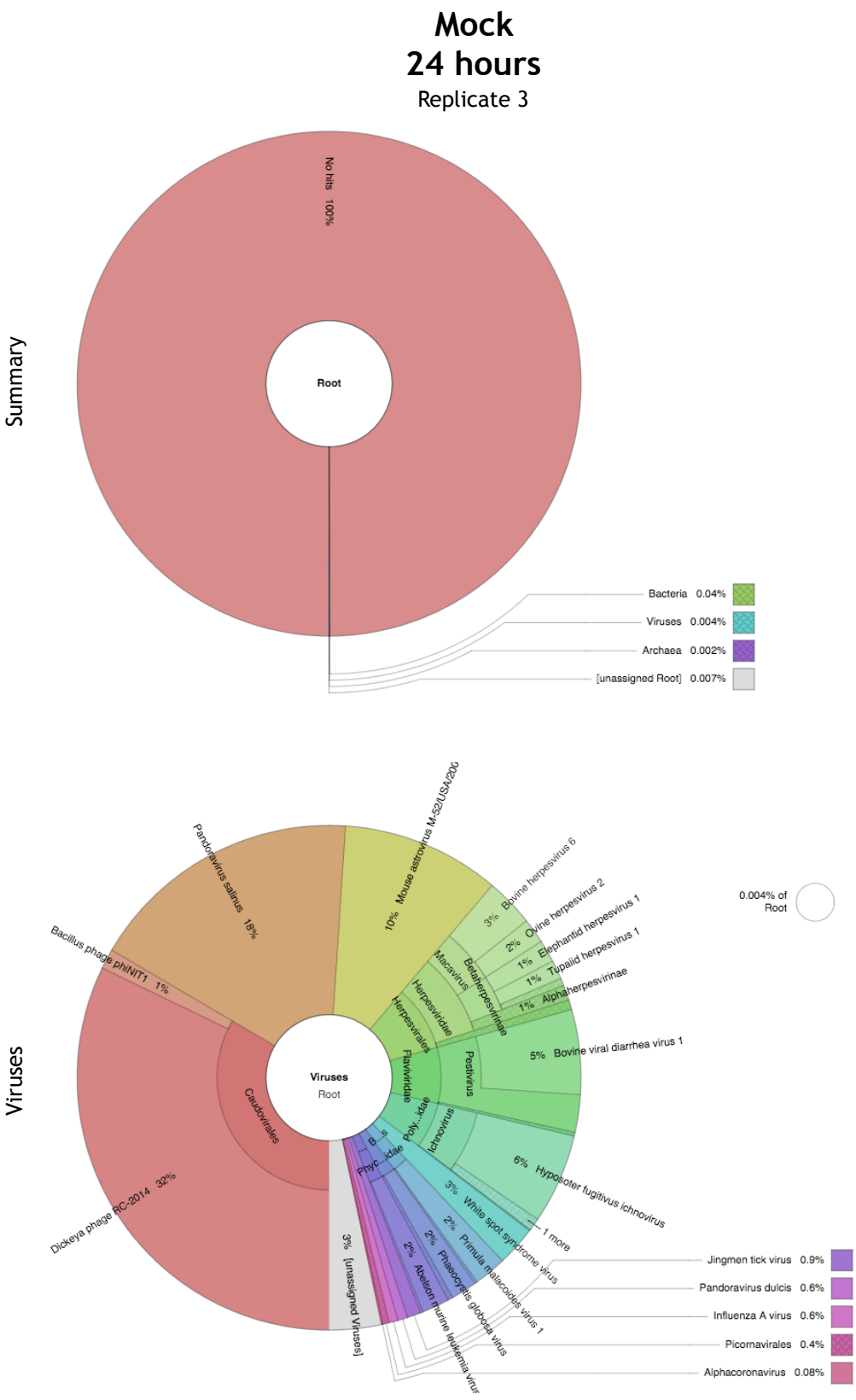

Figure 40: All unmapped sequenced reads from Mock 24 hour (Replicate 3) were processed with the Kraken tool. Image shows the level of reads aligned to pathogens: first a summary, and then a closer analysis of the reads aligned to viruses.

Figure 41: All unmapped sequenced reads from IFN-α 24 hour-treated (Replicate 1) were processed with the Kraken tool. Image shows the level of reads aligned to pathogens: first a summary, and then a closer analysis of the reads aligned to viruses.

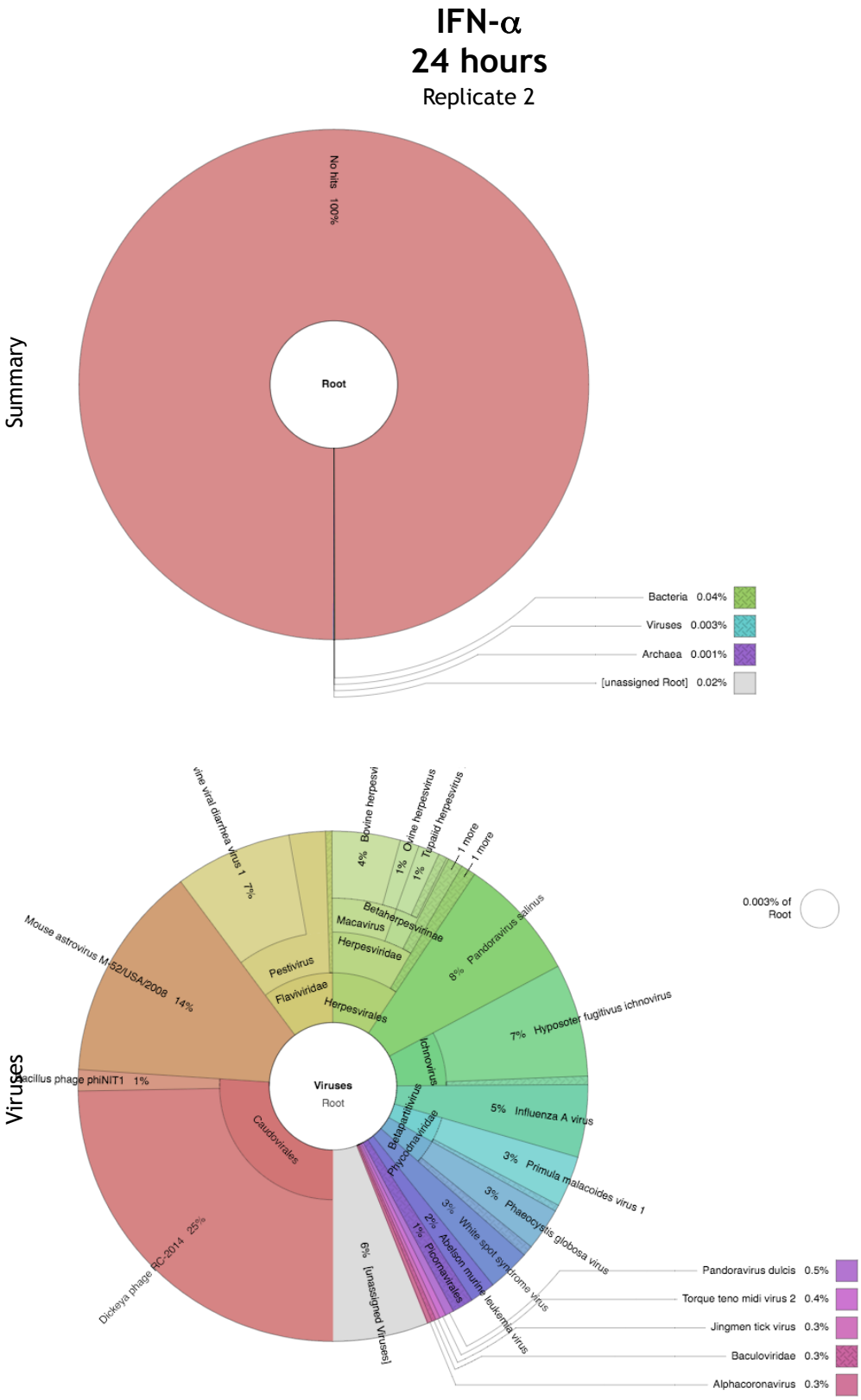

Figure 42: All unmapped sequenced reads from IFN-α 24 hour-treated (Replicate 2) were processed with the Kraken tool. Image shows the level of reads aligned to pathogens: first a summary, and then a closer analysis of the reads aligned to viruses.

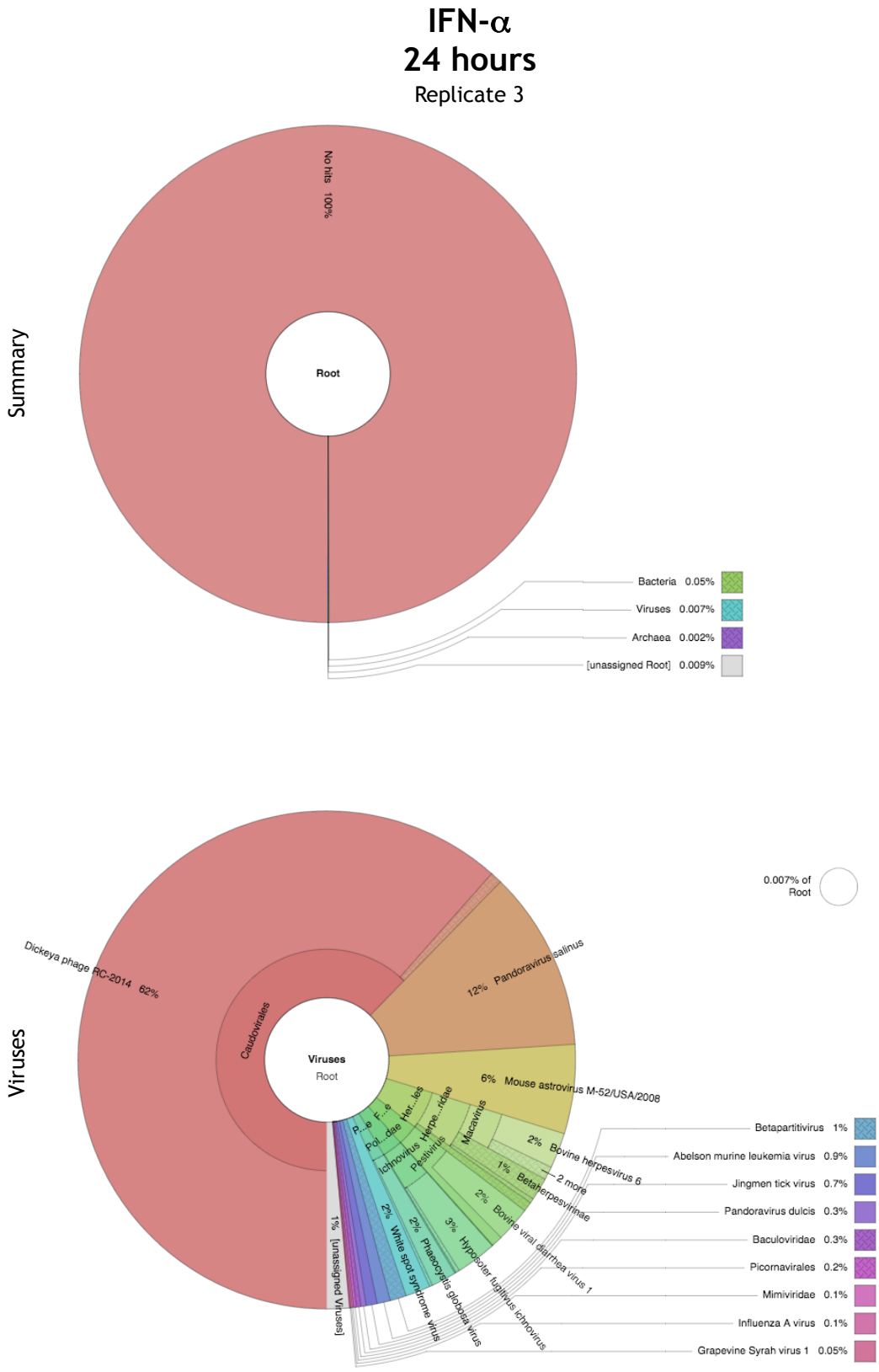

Figure 43: All unmapped sequenced reads from IFN-α 24 hour-treated (Replicate 3) were processed with the Kraken tool. Image shows the level of reads aligned to pathogens: first a summary, and then a closer analysis of the reads aligned to viruses.

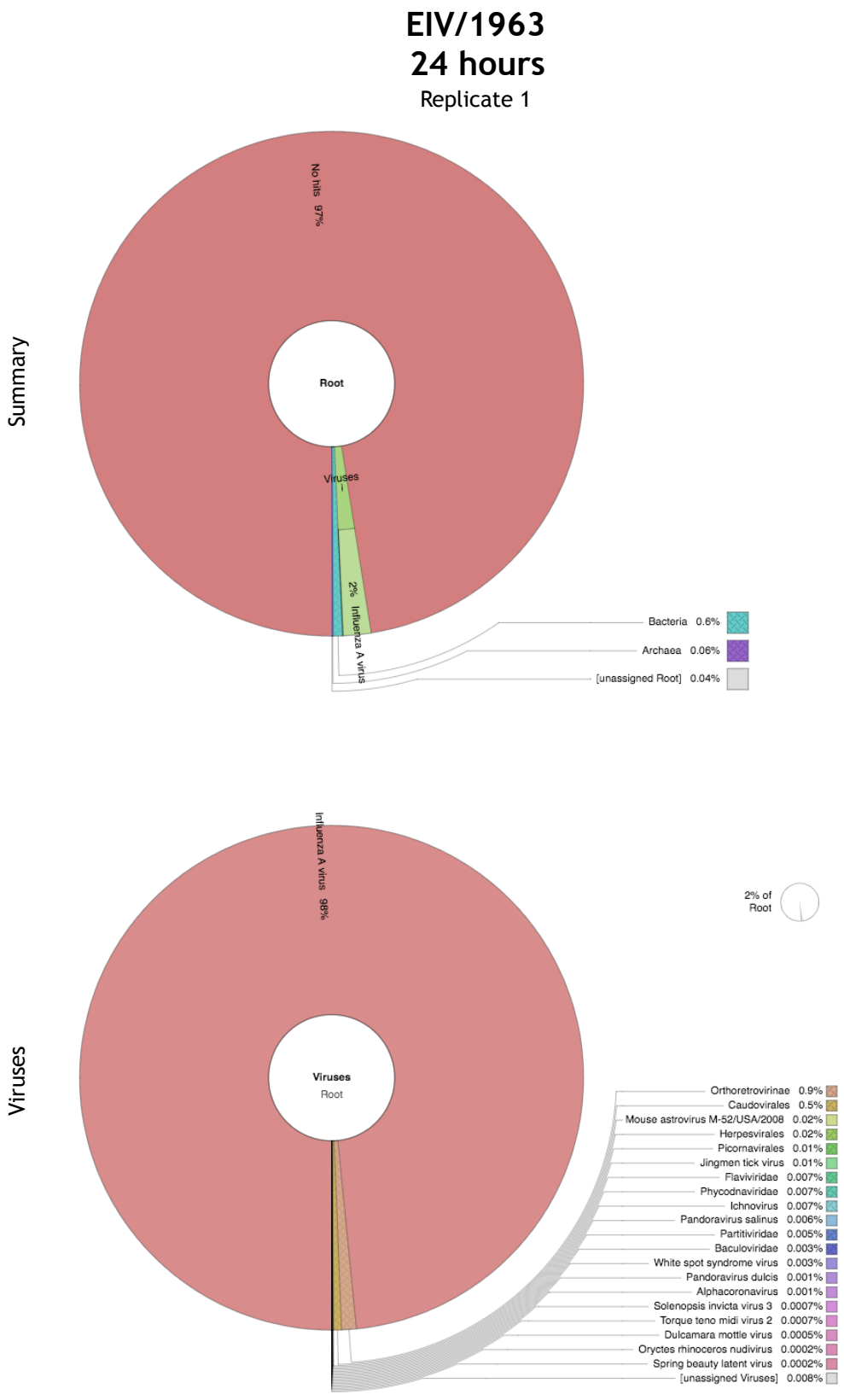

Figure 44: All unmapped sequenced reads from EIV/1963 24hour-infected (Replicate 1) were processed with the Kraken tool. Image shows the level of reads aligned to pathogens: first a summary, and then a closer analysis of the reads aligned to viruses.

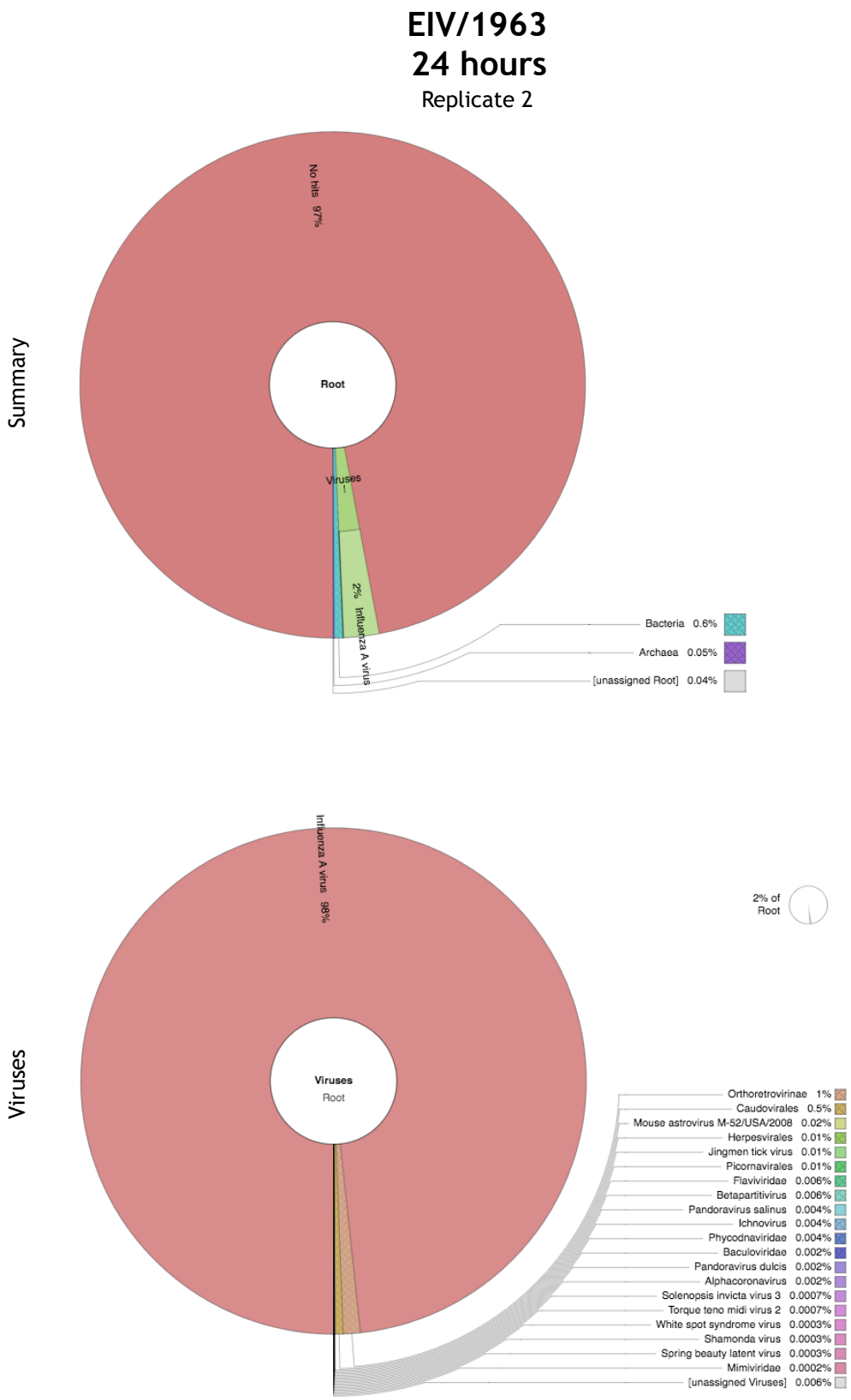

Figure 45: All unmapped sequenced reads from EIV/1963 24hour-infected (Replicate 2) were processed with the Kraken tool. Image shows the level of reads aligned to pathogens: first a summary, and then a closer analysis of the reads aligned to viruses.

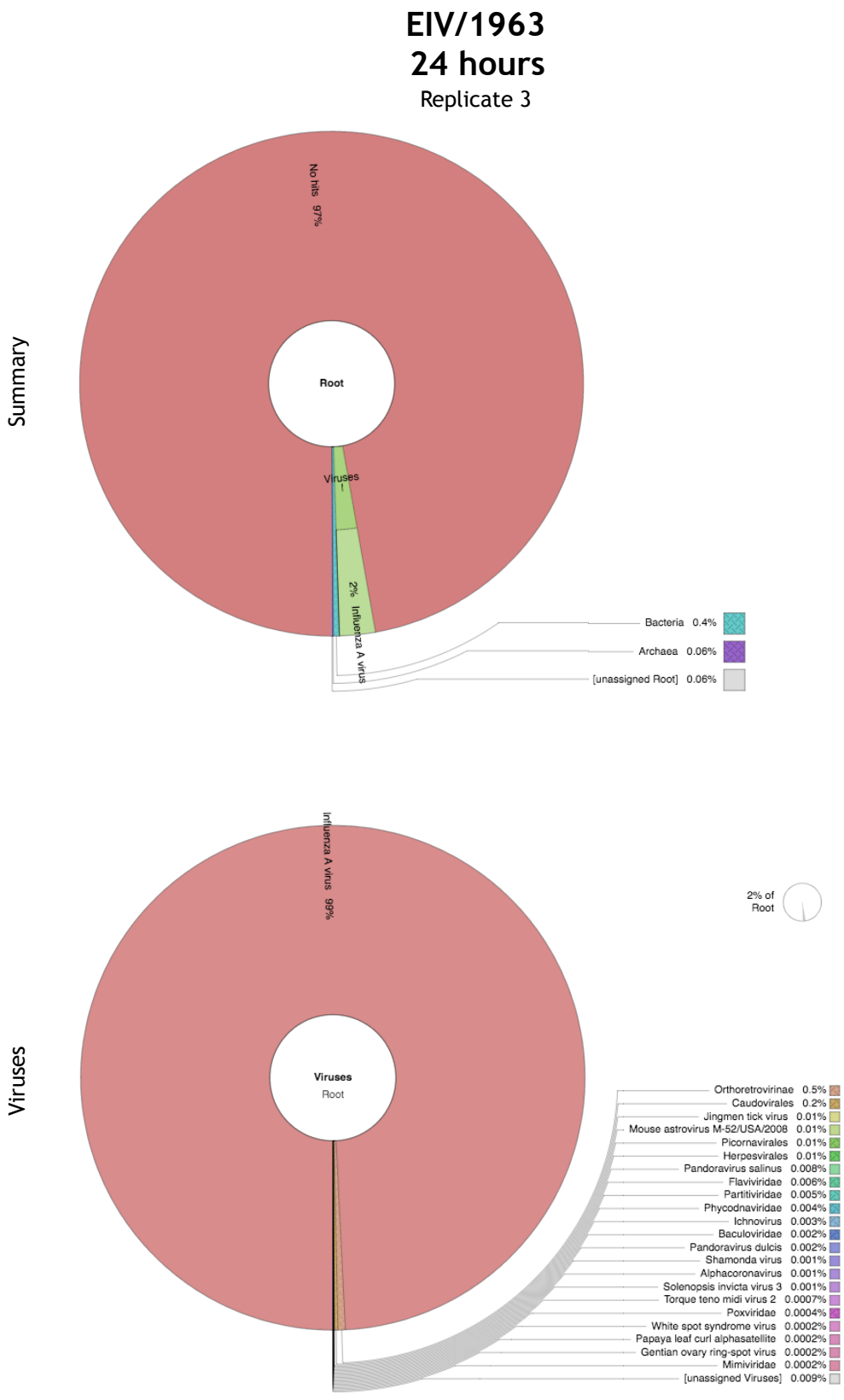

Figure 46: All unmapped sequenced reads from EIV/1963 24hour-infected (Replicate 3) were processed with the Kraken tool. Image shows the level of reads aligned to pathogens: first a summary, and then a closer analysis of the reads aligned to viruses.

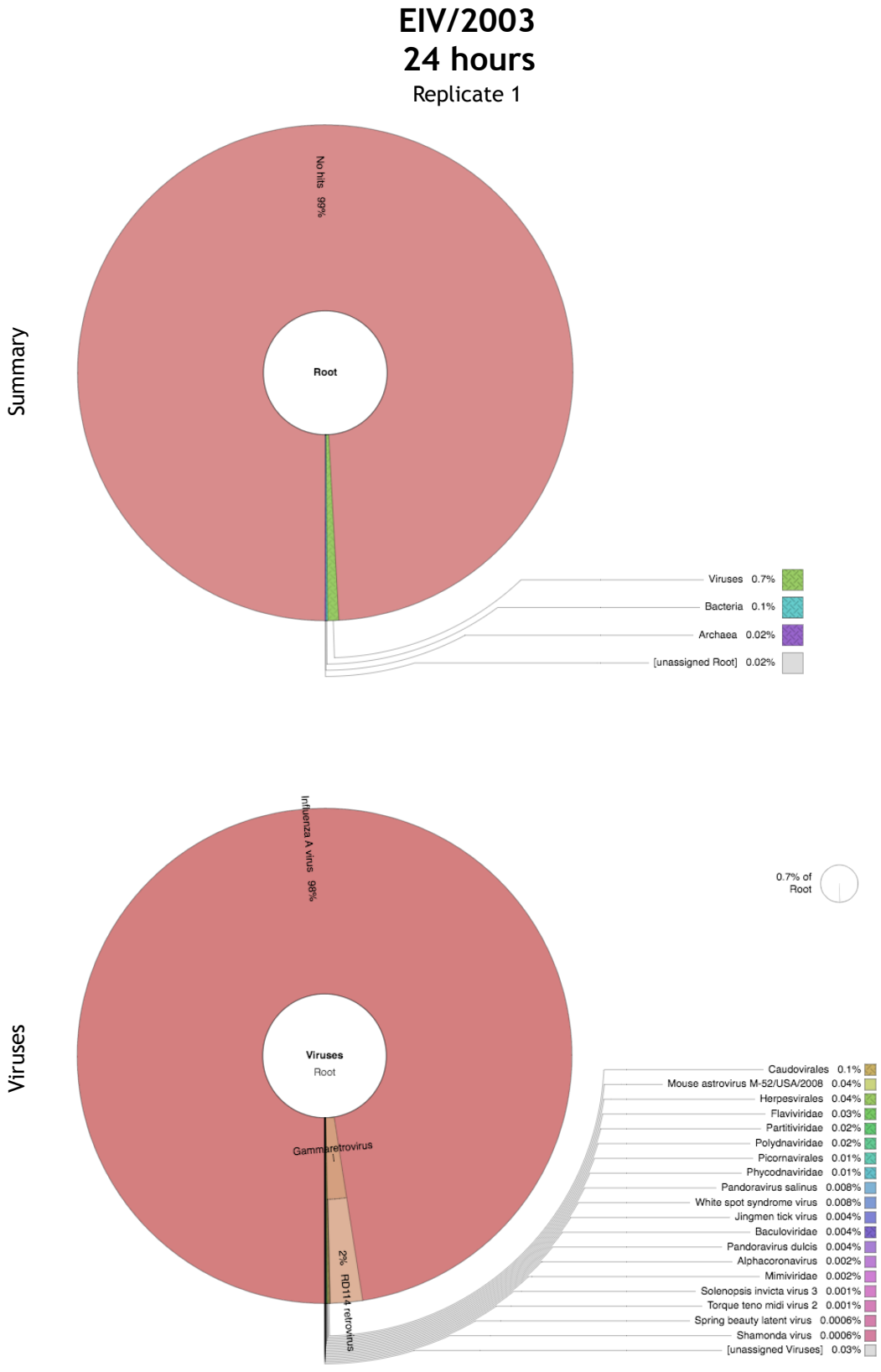

Figure 47: All unmapped sequenced reads from EIV/2003 24hour-infected (Replicate 1) were processed with the Kraken tool. Image shows the level of reads aligned to pathogens: first a summary, and then a closer analysis of the reads aligned to viruses.

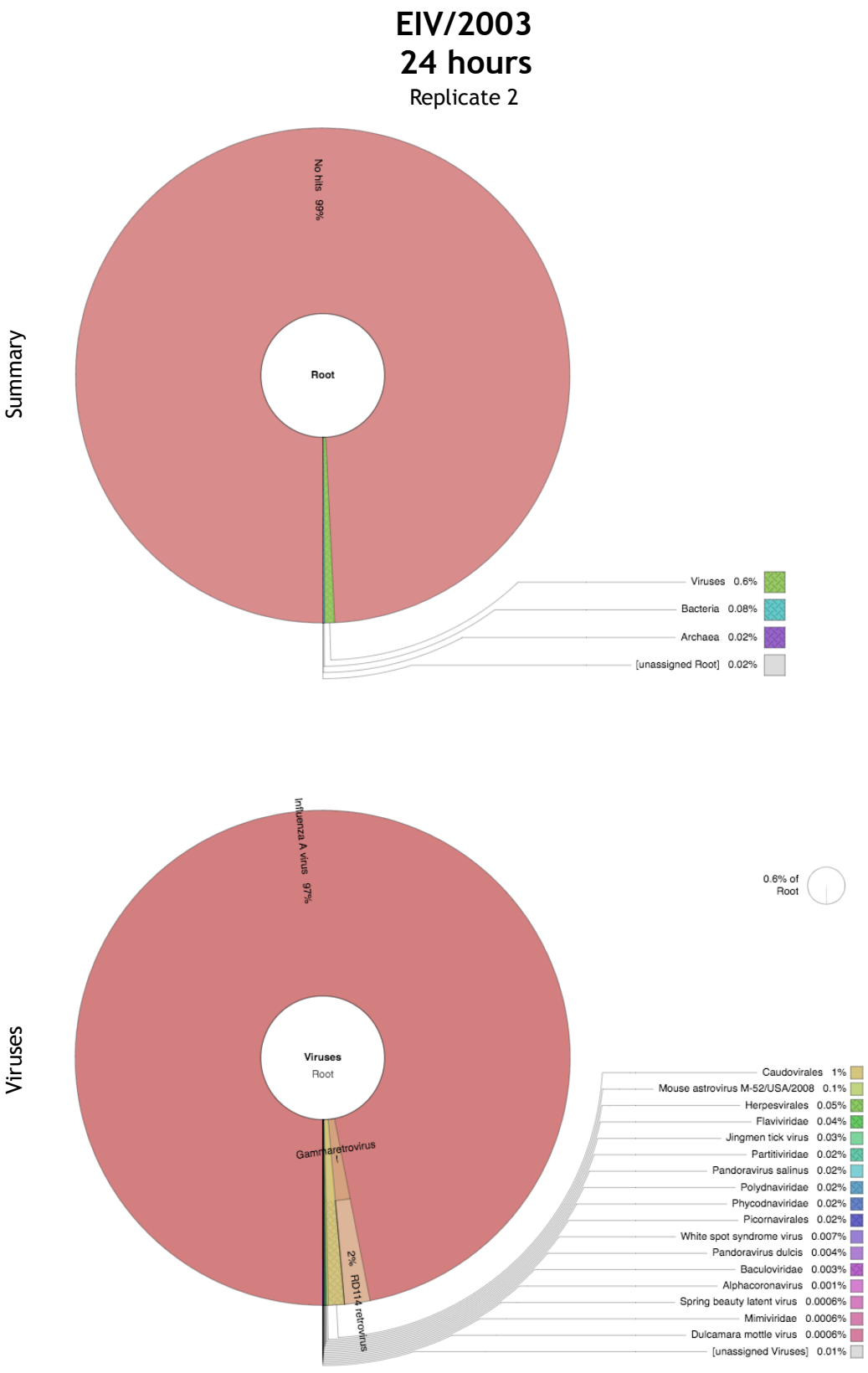

Figure 48: All unmapped sequenced reads from EIV/2003 24hour-infected (Replicate 2) were processed with the Kraken tool. Image shows the level of reads aligned to pathogens: first a summary, and then a closer analysis of the reads aligned to viruses.

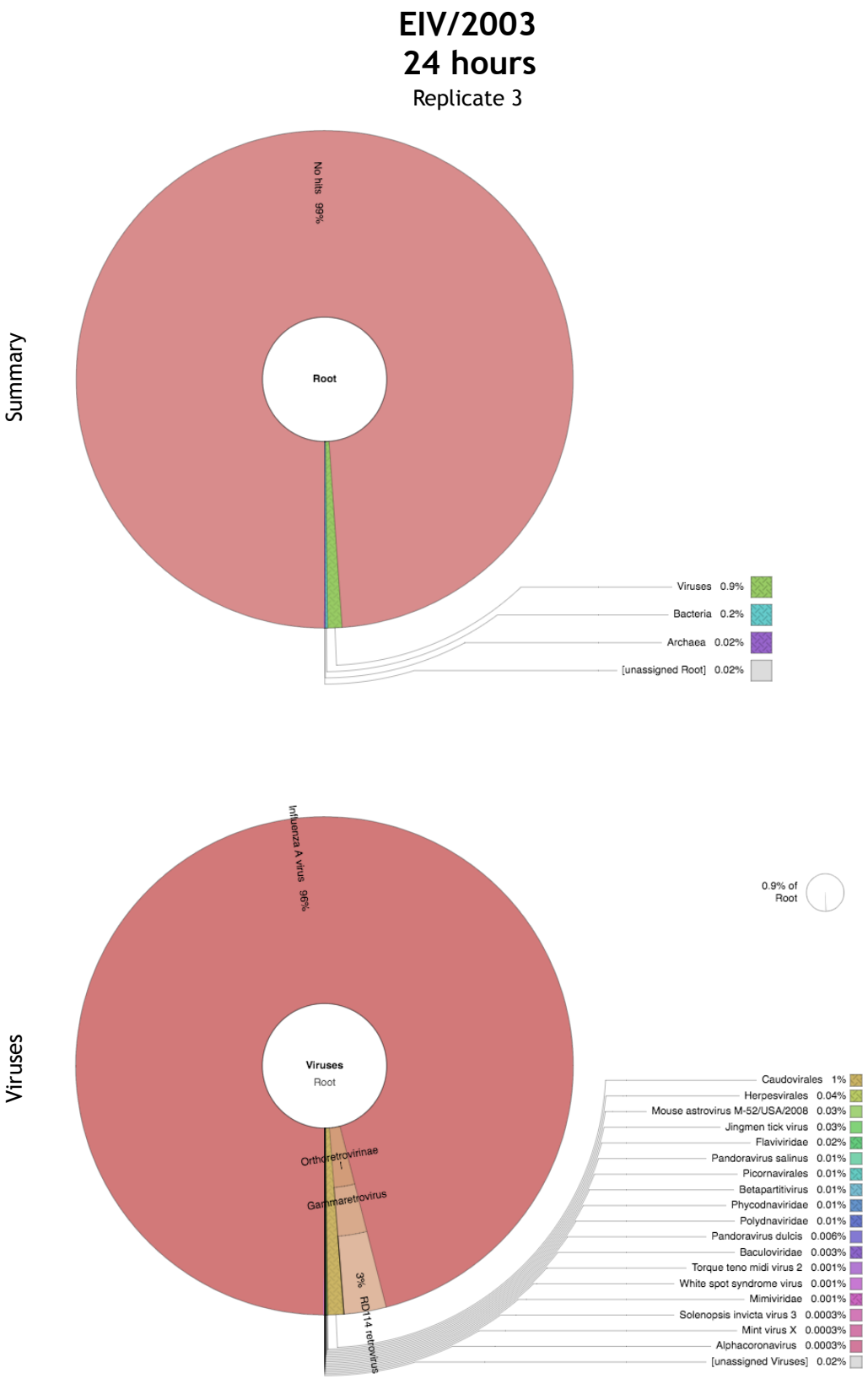

Figure 49: All unmapped sequenced reads from EIV/2003 24hour-infected (Replicate 3) were processed with the Kraken tool. Image shows the level of reads aligned to pathogens: first a summary, and then a closer analysis of the reads aligned to viruses.

4.2.4. Data characterization (MDS, Pearson Cor, Hierarchical clustering)

The overall transcriptomic profile of the four conditions – Mock-infected, IFN-α treated, EIV/1963-infected and EIV/2003-infected were investigated using different distance-based metrics. Multidimensional Scaling (MDS) was first used to examine the Euclidian distances between each transcriptomic profile in two dimensions. As can be seen from **Figure 50** (A), a small triangle indicates 4 hours post-infection samples, and a small circle indicates 24 hours post-infection samples. When samples have a similar transcriptomic profile, they will have a smaller Euclidian distance to one another, and are therefore found closer together. The opposite is true when the samples become divergent, the Euclidian distance between them increases. **Figure 50** (B) shows the sample variation explained by Principle Component (PC) Analysis, and demonstrates how PC1 explains much larger variation than PC2. Therefore, the distance horizontally has a bigger significance than vertical distances.

At 4 hours post-infection Mock-infected and IFN-α treated cells are most similar to each other, with a very small Euclidian distance on the PC1 axis. According to the MDS plot, EIV/1963 is more similar than EIV/2003 to Mock-infected samples when studied using PC1.

When using MDS to study the variation between the samples at 24 hours post-infection, both Mock-infected and IFN-α treated cells have moved slightly on the plot, showing that they have changed slightly when compared to their placement at 4 hours post-infection. They were again very close to each other, meaning that in comparison to the other samples, they were very similar to each other. Both EIV viruses produced infections with very distant Euclidian distances when analyses using MDS. The virus with the largest distance along the PC1 axis from the Mock-infected sample was EIV/1963. This means that the transcriptomic host responses to the two EIV viruses were different overall.

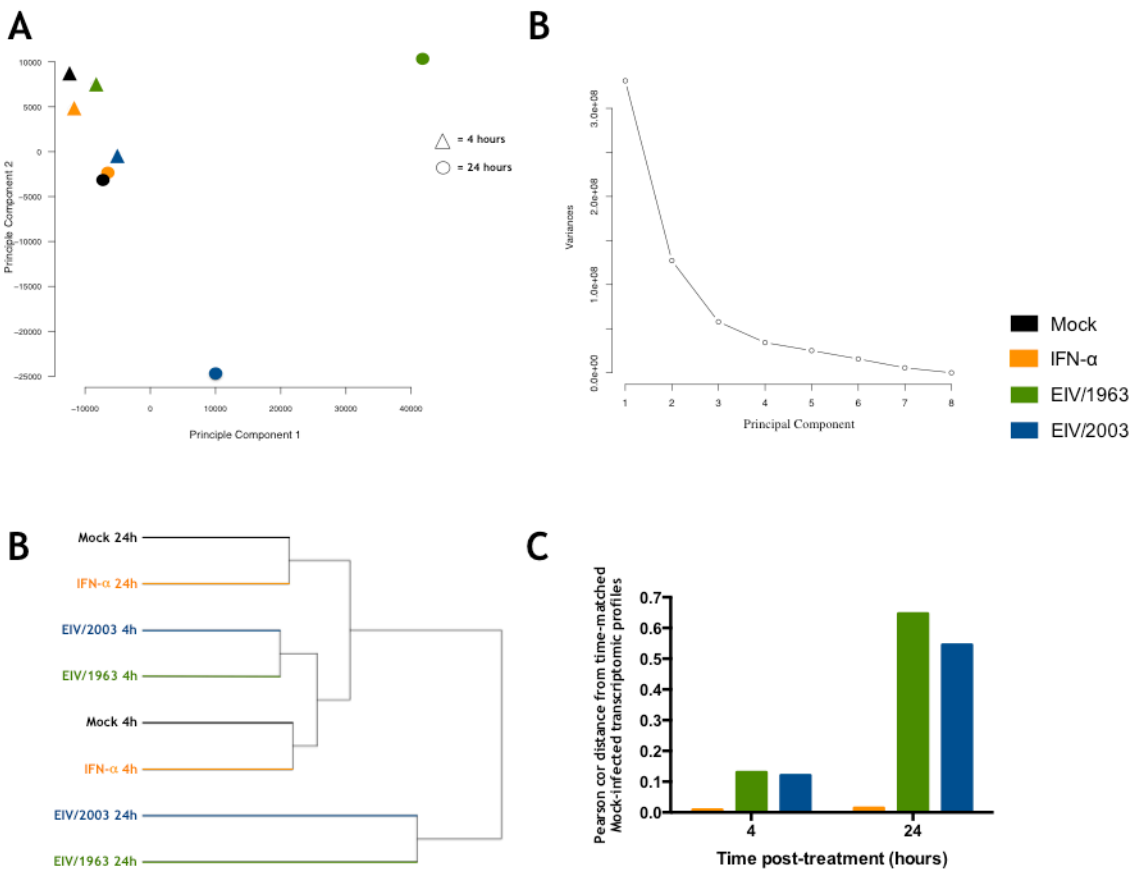

Figure 50: (A) Transcriptomic responses are represented using nonparametric Multidimensional Scaling (MDS) at 4 hours and 24 hours post-infection. Euclidian distance was calculated using the whole normalized transcriptomic data, such that proximity indicates likeness, whereas distance indicates variation, of gene expression profiles. (B) Graph showing variance depending on Principal Component. (C) Hierarchical clustering of Mock, IFN-α treated and EIV infected samples. Distances were calculated using Pearson correlation distance. (D) Distance between Mock-infected samples and IFN-α treatment or EIV-infected samples. The Pearson correlation distance (Pearson cor distance) was calculated as 1 - Pearson correlation coefficient calculated using normalized transcriptomic data.

To further investigate the Euclidean distances (based upon the transcriptomic data), hierarchical clustering was used (**Figure 50, C**). The hierarchical clustering confirmed that the Mock-infected and IFN-α treated transcriptomic profiles were very similar at both 4 hours and 24 hours post-infection. In addition, the clustering demonstrated that EIV/1963 and EIV/2003 infections were more similar to each other than to the Mock-infected and IFN-α treated conditions. The EIV-infected samples were very distant from the other samples at 24 hours post-infection, supporting the evidence from the other plots.

To determine whether the host responses to IFN-α treatment or EIV-infection were closer to the Mock-infected transcriptome, we measured the transcriptomic distance between the samples of each condition at both time-

points (**Figure 50, D**). The IFN-α treated samples had a very small Pearson cor distance from the Mock-infected condition (0.0086 and 0.0143 at 4 hours and 24 hours post-infection, respectively). Infection with either EIV viruses had much larger distances than the IFN-α treatment. The transcriptomic response of EIV/1963 infection compared to the Mock-infected transcriptome was the larger of the two viruses. The Pearson cor distance for EIV/1963 was 0.13 and 0.65 at 4 hours and 24 hours post-infection, respectively, as compared to 0.12 and 0.55 at 4 hours and 24 hours post-infection, respectively, for infection with EIV/2003.

4.2.5. A Log_2FC value of 0.58 is chosen as the threshold for selecting differentially expressed genes for analysis

Using an algorithm such as CuffDiff2 to interpret the RNASeq results produces a large list of DE genes. The DE genes are produced for each condition, where the sample is compared to the Mock-infected results at the same time-point. Comparisons are between samples within a repeat, rather than the average values for all repeats. These must be narrowed down to study the most significantly expressed DE genes. A Q value threshold of ≤0.05 was used to select a list of genes.

A threshold of Log_2FoldChange (Log_2FC) was investigated by creating lists of DE genes with a Log_2FC cut-off of 0.58, 1 and 1.58. These lists of genes were plotted to examine how the thresholds affected the numbers of DE genes (**Figure 51, A**). There was a large difference in the number of DE genes after infection with EIV/1963 between setting the Log_2FC cut-off at 0.58 and 1. These large differences implied that there were a large number of the DE genes of EIV/1963 infection that had a Log_2FC value of between 0.58 and 1. The lists of genes were also entered into Ingenuity Pathway Analysis (IPA) to analyse the Core Pathways that were affected. As can be seen from **Figure 51** (B) the number of pathways affected decreased, with lower P values, upon increasing the Log_2FC threshold. Therefore for all further analyses, a Log_2FC threshold of 0.58 (1.5 Fold Change) was chosen as the threshold for selecting the DE genes to study.

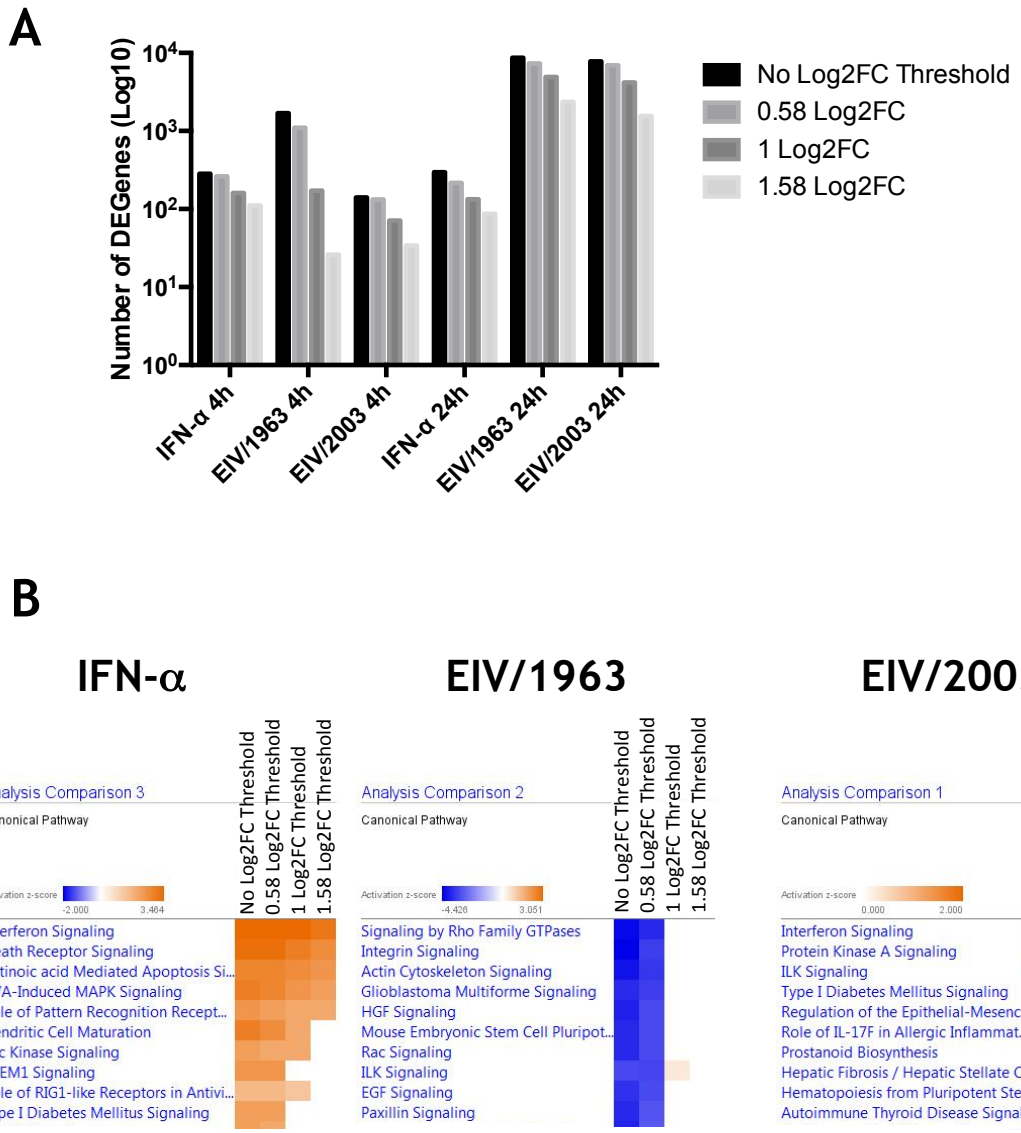

Figure 51: (A) The number of differentially expressed (DE) genes upon application of different Log2FC thresholds. (B) The top 10 Canonical Pathways highlighted by IPA with the different thresholds applied to the list of DE genes at 4 hours.

4.2.6. The number of DE genes between conditions varies greatly

The number of DE genes for each of the conditions varied greatly depending on whether the cells were treated with IFN-α or infected with an EIV. The transcriptome was also dependent upon time; a much larger number of DE genes reported for the infected cells at 24 hours post-infection. As can be seen from **Figure 52**, the number of DE genes upon IFN-α treatment decreased from 4 to 24 hours post-treatment (262 to 216).

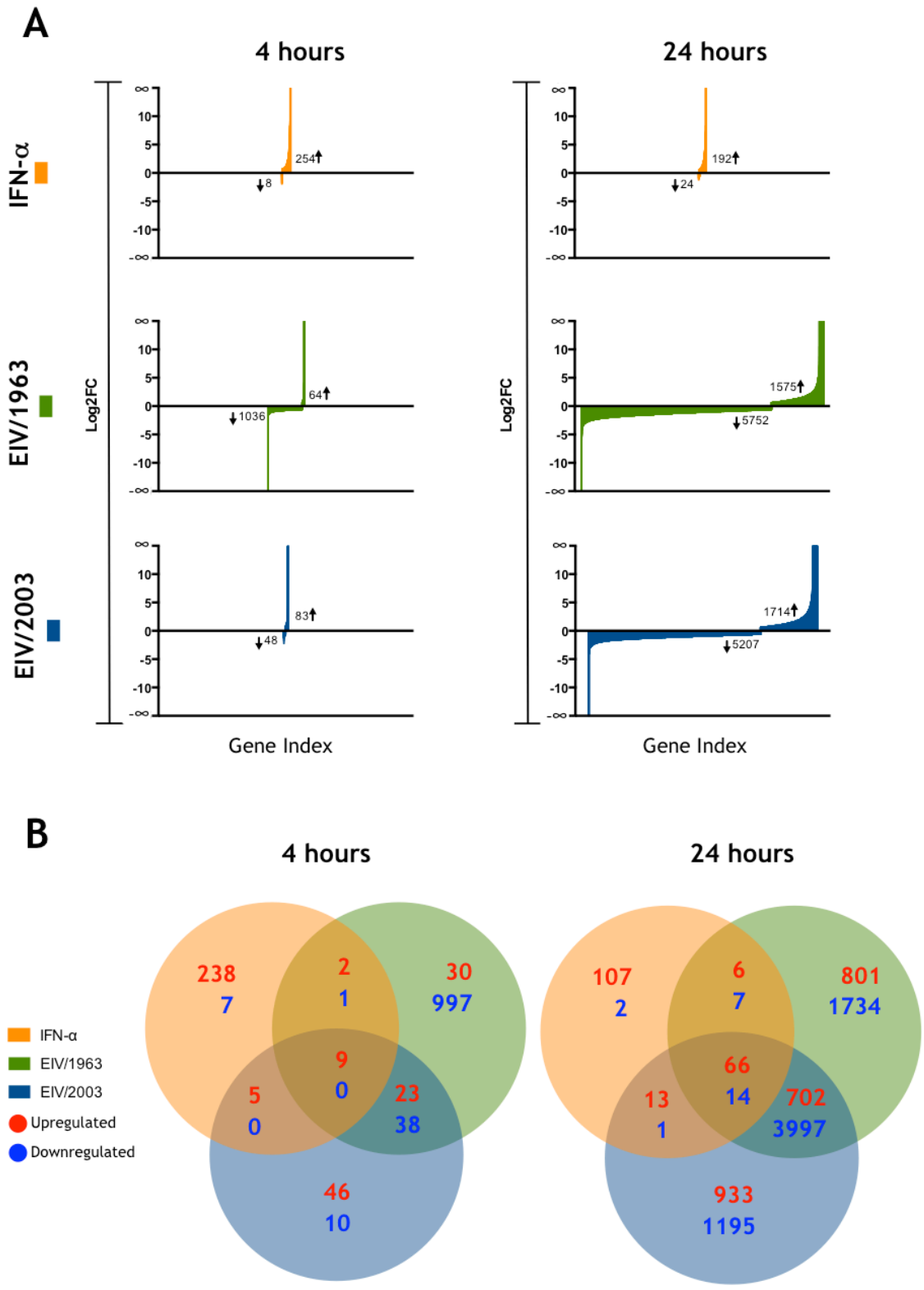

Figure 52: (A) Number of Differentially Expressed (DE) genes for each of the conditions with the Log2FC values shown. The number of upregulated and downregulated DE genes is shown with up and down arrows. (B) Venn diagrams showing the number of DE genes for each condition. Numbers in red correspond to upregulated DE genes, and numbers in blue to downregulated.

The DE genes for each condition were compared using Venn diagrams. As can be seen from **Figure 52**, there were 66 shared upregulated genes for the three conditions at 24 hours post-treatment, as opposed to only 9 shared upregulated genes at 4 hours. There were also 14 downregulated shared genes at 24 hours post-treatment, and none at 4 hours. EIV/2003 shared more genes with IFN-a treated cells at both 4 and 24 hours post-treatment, as opposed to EIV/1963-infected cells.

When analysing the shared DE genes between the two virus infections, there was a greater quantity of shared downregulated DE genes, as opposed to upregulated, at both 4 hours post-infection (38 downregulated, 23 upregulated) and 24 hours post-infection (3,997 downregulated, 702 upregulated).

4.2.7. E.Derm interferome is dynamic over time

The interferome of the horse has not been well-characterised, with many genes not annotated or unknown. E.Derm cells provide the *in vitro* system in which to fully investigate the Interferon Stimulated Genes (ISGs) produced upon treatment with 1,000 UI/ml Universal IFN-α. The two time-points of 4 hours and 24 hours post-treatment allow the study of a dynamic change in the cellular interferome. Cells were collected, RNA extracted, and the transcriptome of the treated cells was compared to the transcriptome of control cells at the same time-point so as to highlight the DE genes.

The DE genes were plotted on a heat map for the two time-points of IFN-α treatment (**Figure 53**). The interferome didn't appear static, but was dynamic and changed over the increase of treatment time. It was possible to observe 224 uniquely DE genes over the course of both time-points (135 and 89 for 4 hours and 24 hours post-treatment, respectively). When considering the downregulated DE genes, there were only eight of these at 4 hours post-treatment (including S1PR1, NR4A2, PER1 and NFATC2), whereas there were twenty-four downregulated DE genes at 24 hours post-treatment (including ND5, SACS, USF3 and PYGO1).

The response of the cells to the exogenous IFN-α developed over the time difference of 20 hours (**Figure 53**). The number of genes that had a Log_2FC of infinity decreased from eight to three with the genes that were no longer expressed being XAF1, SECTM1, TLR3, GBP5 and CCL13. However, it was important to notice that of the three DE genes that had an expression fold change of infinity, they had a higher Fragments Per Kilobase of transcript per Million mapped reads (FPKM) value at 24 hours post-treatment as opposed to 4 hours. For example, PLAC8, Mx2 and BST2 all increased their FPKM value at 24 hours post-treatment from 18.70 to 85.46, 11.83 to 20.82, and 2.11 to 15.65 respectively. The two viruses share 127 DE genes, with well-known interferon stimulated genes (ISGs) such as ISG15, IRF9 and PML all being upregulated.

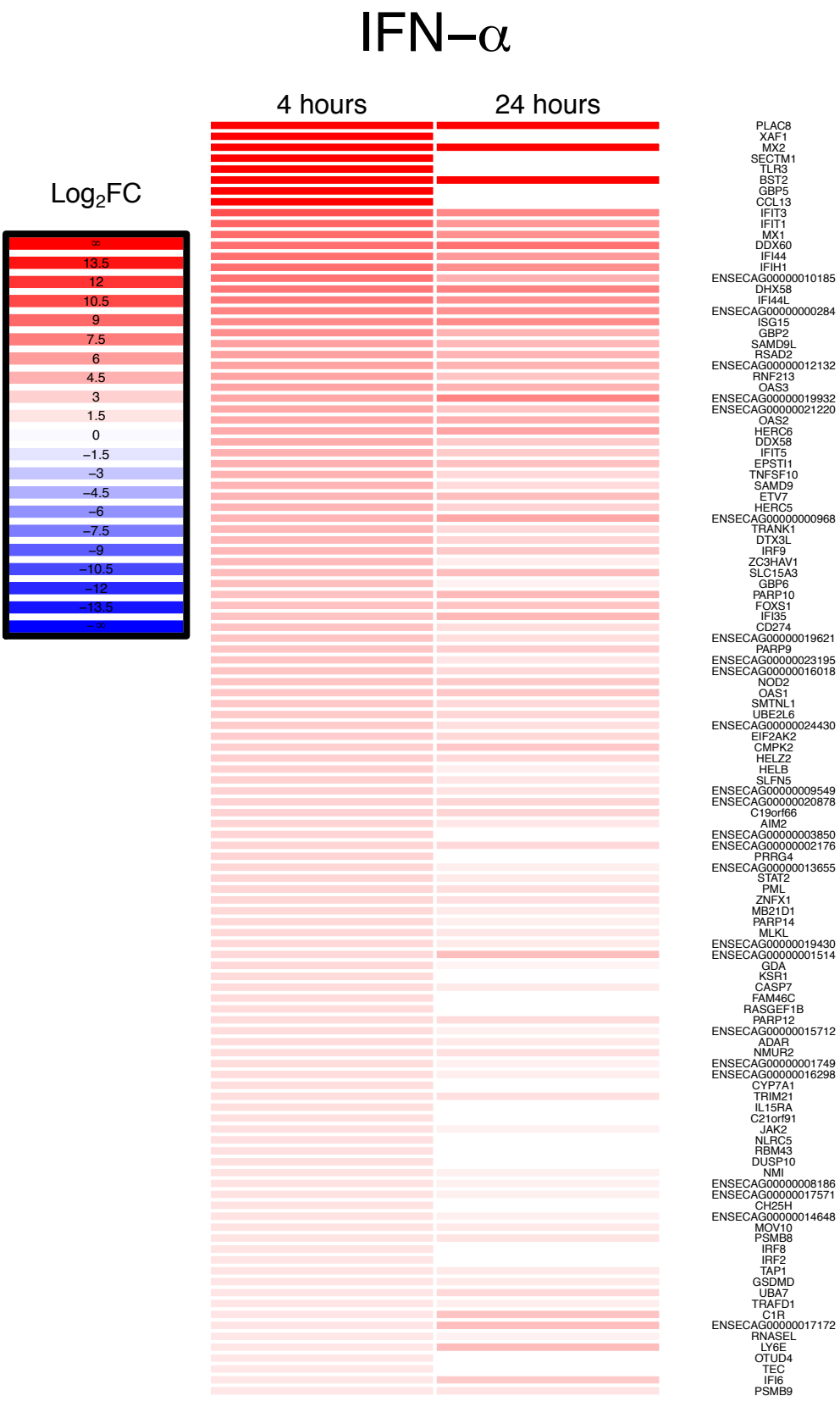
IFN–α
4 hours
24 hours
Log2FC
∞
13.5
12
10.5
9
7.5
6
4.5
3
1.5
0
−1.5
−3
−4.5
−6
−7.5
−9
−10.5
−12
−13.5
−∞
PLAC8
XAF1
MX2
SECTM1
TLR3
BST2
GBP5
CCL13
IFIT3
IFIT1
MX1
DDX60
IFI44
IFIH1
ENSECAG00000010185
DHX58
IFI44L
ENSECAG00000000284
ISG15
GBP2
SAMD9L
RSAD2
ENSECAG00000012132
RNF213
OAS3
ENSECAG00000019932
ENSECAG00000021220
OAS2
HERC6
DDX58
IFIT5
EPSTI1
TNFSF10
SAMD9
ETV7
HERC5
ENSECAG00000000968
TRANK1
DTX3L
IRF9
ZC3HAV1
SLC15A3
GBP6
PARP10
FOXS1
IFI35
CD274
ENSECAG00000019621
PARP9
ENSECAG00000023195
ENSECAG00000016018
NOD2
OAS1
SMTNL1
UBE2L6
ENSECAG00000024430
EIF2AK2
CMPK2
HELZ2
HELB
SLFN5
ENSECAG00000009549
ENSECAG00000020878
C19orf66
AIM2
ENSECAG00000003850
ENSECAG00000002176
PRRG4
ENSECAG00000013655
STAT2
PML
ZNFX1
MB21D1
PARP14
MLKL
ENSECAG00000019430
ENSECAG00000001514
GDA
KSR1
CASP7
FAM46C
RASGEF1B
PARP12
ENSECAG00000015712
ADAR
NMUR2
ENSECAG00000001749
ENSECAG00000016298
CYP7A1
TRIM21
IL15RA
C21orf91
JAK2
NLRC5
RBM43
DUSP10
NMI
ENSECAG00000008186
ENSECAG00000017571
CH25H
ENSECAG00000014648
MOV10
PSMB8
IRF8
IRF2
TAP1
GSDMD
UBA7
TRAFD1
C1R
ENSECAG00000017172
RNASEL
LY6E
OTUD4
TEC
IFI6
PSMB9

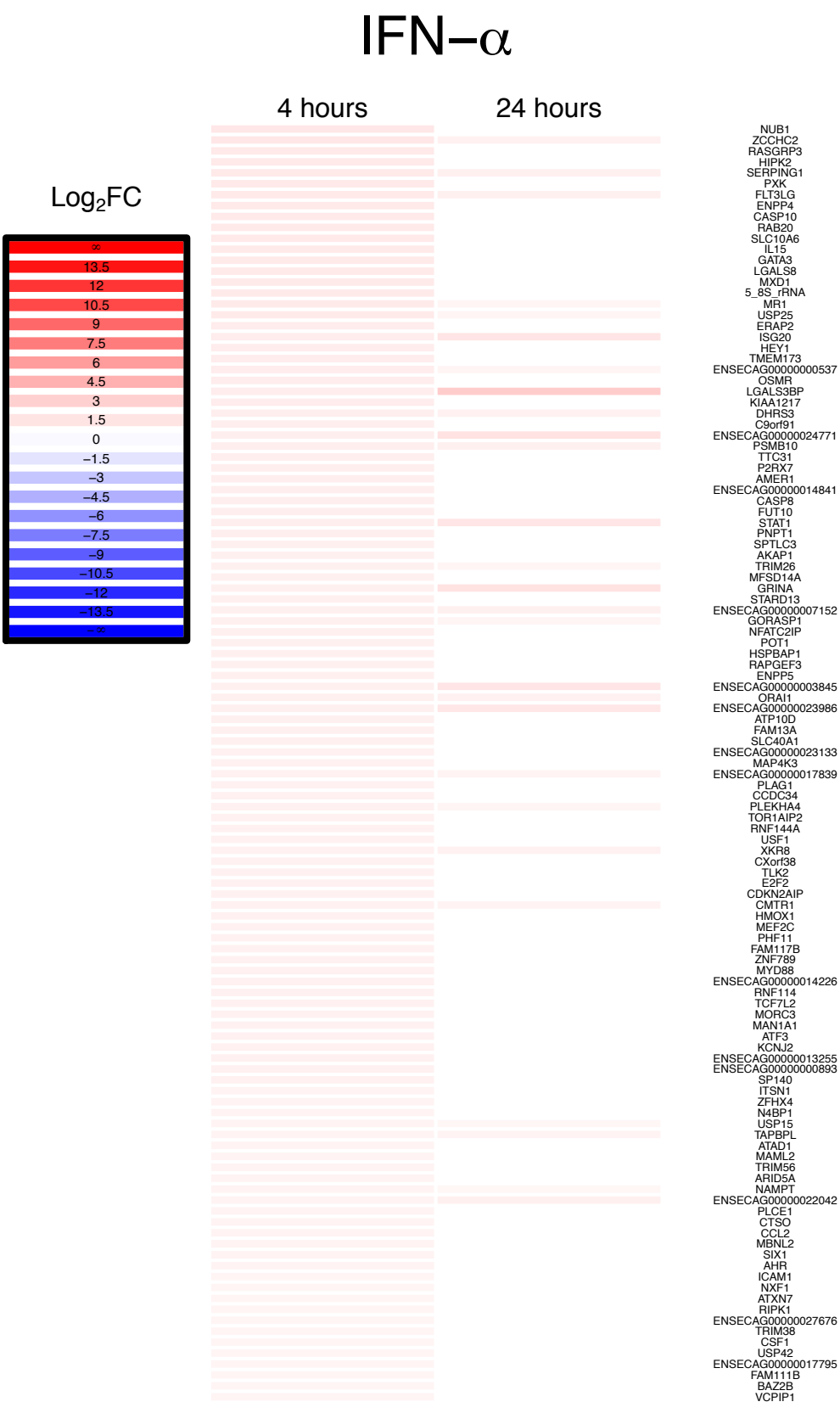
IFN–α
4 hours
24 hours
Log2FC
∞
13.5
12
10.5
9
7.5
6
4.5
3
1.5
0
−1.5
−3
−4.5
−6
−7.5
−9
−10.5
−12
−13.5
−∞
NUB1
ZCCHC2
RASGRP3
HIPK2
SERPING1
PXK
FLT3LG
ENPP4
CASP10
RAB20
SLC10A6
IL15
GATA3
LGALS8
MXD1
5_8S_rRNA
MR1
USP25
ERAP2
ISG20
HEY1
TMEM173
ENSECAG00000000537
OSMR
LGALS3BP
KIAA1217
DHRS3
C9orf91
ENSECAG00000024771
PSMB10
TTC31
P2RX7
AMER1
ENSECAG00000014841
CASP8
FUT10
STAT1
PNPT1
SPTLC3
AKAP1
TRIM26
MFSD14A
GRINA
STARD13
ENSECAG00000007152
GORASP1
NFATC2IP
POT1
HSPBAP1
RAPGEF3
ENPP5
ENSECAG00000003845
ORAI1
ENSECAG00000023986
ATP10D
FAM13A
SLC40A1
ENSECAG00000023133
MAP4K3
ENSECAG00000017839
PLAG1
CCDC34
PLEKHA4
TOR1AIP2
RNF144A
USF1
XKR8
CXorf38
TLK2
E2F2
CDKN2AIP
CMTR1
HMOX1
MEF2C
PHF11
FAM117B
ZNF789
MYD88
ENSECAG00000014226
RNF114
TCF7L2
MORC3
MAN1A1
ATF3
KCNJ2
ENSECAG00000013255
ENSECAG00000000893
SP140
ITSN1
ZFHX4
N4BP1
USP15
TAPBPL
ATAD1
MAML2
TRIM56
ARID5A
NAMPT
ENSECAG00000022042
PLCE1
CTSO
CCL2
MBNL2
SIX1
AHR
ICAM1
NXF1
ATXN7
RIPK1
ENSECAG00000027676
TRIM38
CSF1
USP42
ENSECAG00000017795
FAM111B
BAZ2B
VCPIP1

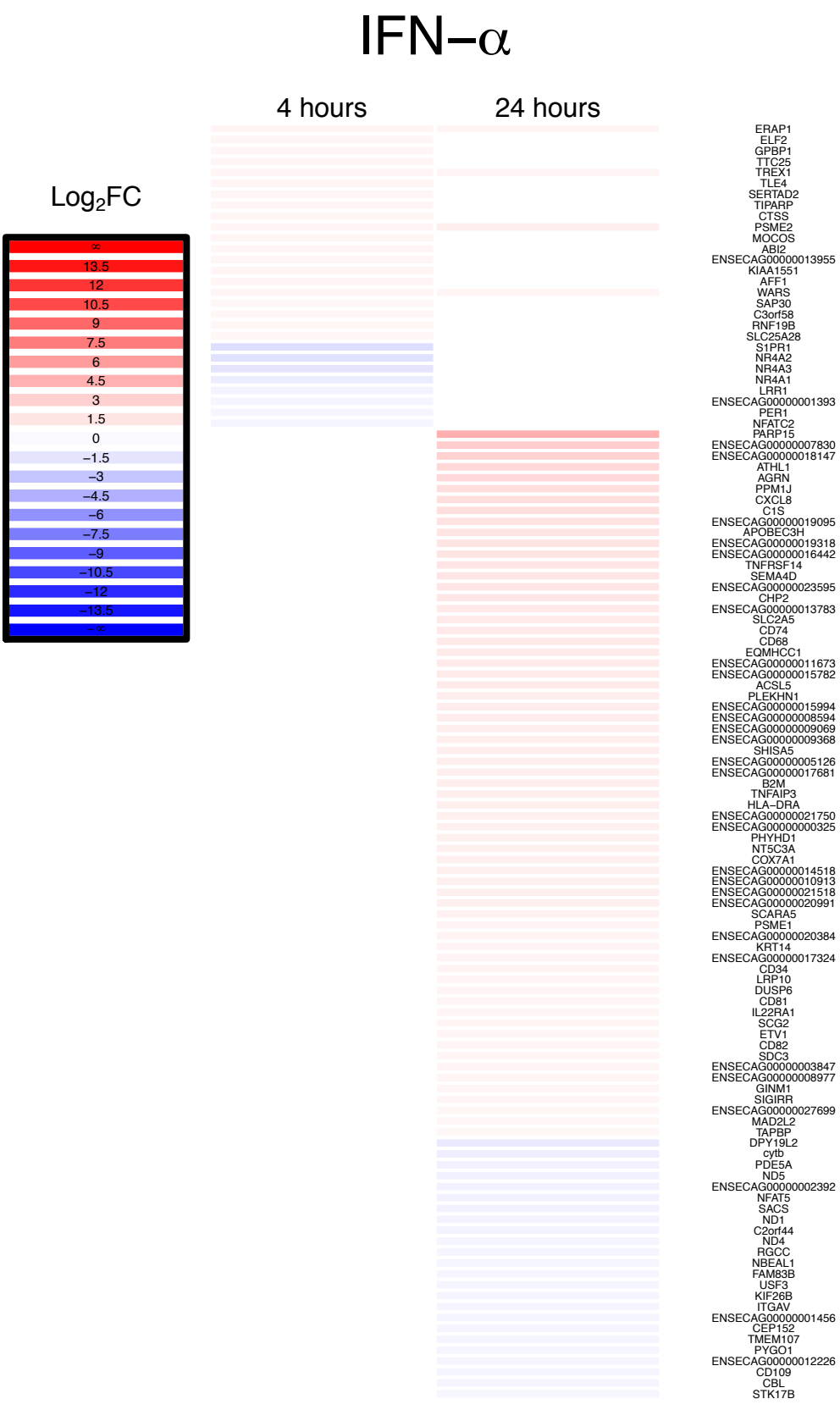

Figure 53: Heat map of Differentially Expressed (DE) genes after 4 and 24 hours IFN-α treatment. Upregulated DE genes are shown in red, downregulated DE genes are shown in blue.

4.2.8. Gene categories

The transcriptomic analysis for each of the virus infections produced an extremely large list of DE genes. At 24 hours post-infection, there were many thousands of genes highlighted for both viruses (**Figure 54**). These genes were categorised into their function using gene ontology (GO) information.

Figure 54 shows the DE genes that were assigned to specified GO categories with their accompanying Log_2FC value. The specified GO categories were defined using descriptive terms returned from Ensembl BioMart.

The difference between the two viruses was more obvious at 4 hours as opposed to 24 hours post-infection, repeating what was already shown (**Figure 54**). In comparison to EIV/2003, more genes were downregulated by the EIV/1963 virus in each of the categories at both time-points. For example, in the "Cytoskeleton or Transport" category, EIV/1963 downregulated 418 genes as compared to 22 for EIV/2003 at 4 hours post-infection. At 24 hours post-infection, the number of downregulated genes for "Cytoskeleton or Transport" increases to 2256 and 2050 for EIV/1963 and EIV/2003 respectively. These results demonstrate that EIV/1963 downregulated the normal cellular functions much more quickly than EIV/2003.

The converse is also true when studying the upregulated DE genes. EIV/2003 caused higher numbers of these genes to be upregulated in almost all the categories as compared to EIV/1963. The exception is the "Unknown function" category where EIV/1963 and EIV/2003 upregulate 28 and 19, and 488 and 409 DE genes at 4 hours and 24 hours post-infection, respectively.

For the "Immune Response" category, differences between EIV/1963 and EIV/2003 were especially apparent at 4 hours post-infection. EIV/1963 downregulated 127 DE genes, as compared to 6 DE genes for EIV/2003. In comparison, when looking at the upregulated DE genes categorised in "Immune Response", the older EIV/1963 upregulated 14 DE genes, when EIV/2003 upregulated 23.

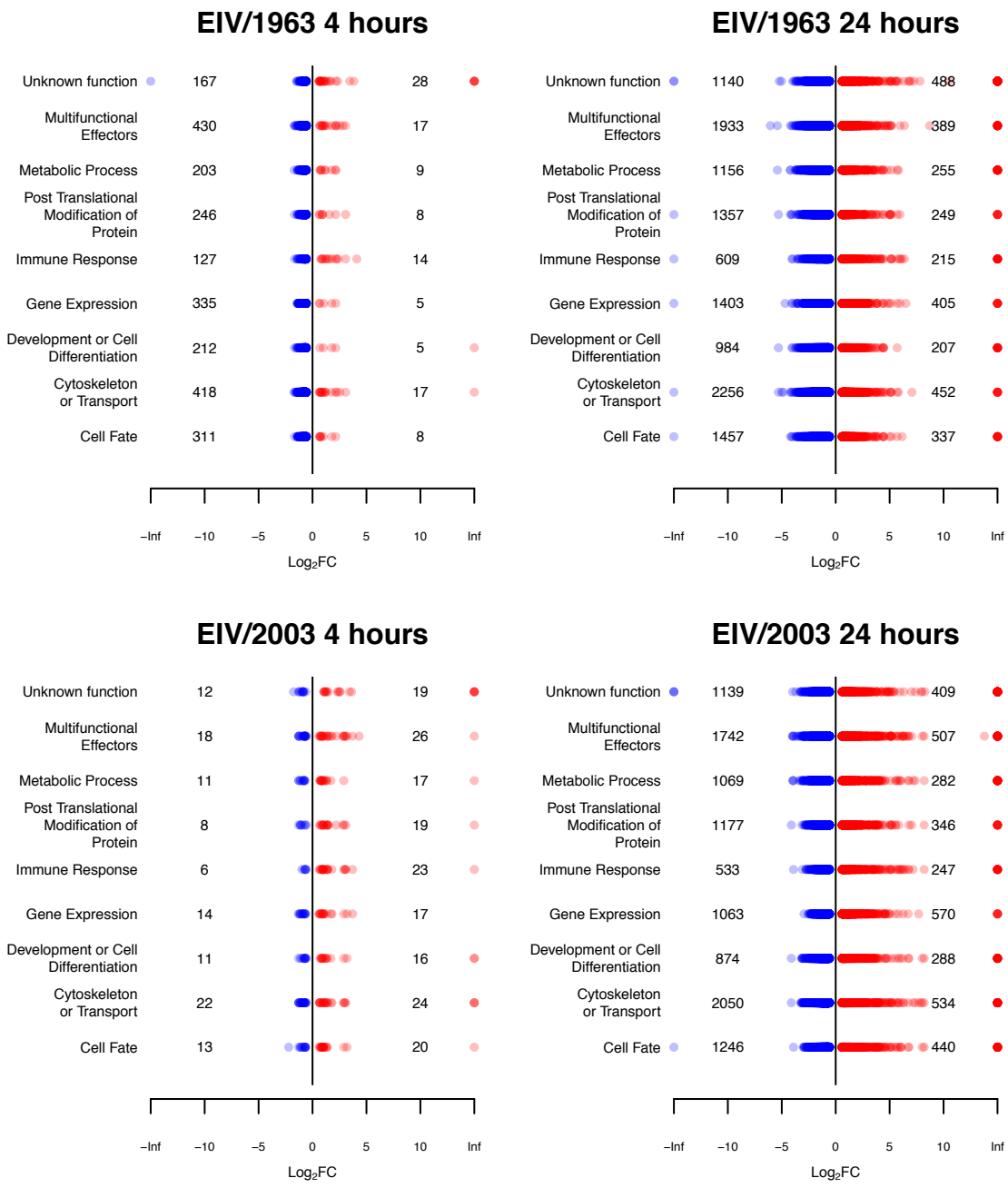

Figure 54: Differentially Expressed (DE) genes categorised based upon their Gene Ontology. Categories were specified based upon search terms returned from the Biomart tool (ensembl). Log_2FC values are provided, red is upregulated and blue is downregulated. All DE Genes were counted for all categories they fell into. The overall total of DE genes found in each category (upregulated and downregulated) is provided.

4.2.9. IFN signaling is manipulated differently by both equine influenza viruses

The IFN signaling pathway was mapped using Ingenuity Pathway Analysis (IPA), and the genes affected were highlighted for the three conditions (IFN-α

treatment, EIV/1963 and EIV/2003 infection) at 4 and 24 hours post-treatment (**Figure 55**).

At 4 hours post-treatment, IPA shows that EIV/1963 downregulated more genes in the IFN pathway than cells infected with EIV/2003 (**Figure 55**). However, the two viruses shared many of the same upregulated IFN genes: IFNα/β, IRF9, IFIT1, Mx1, G1P2 and IFIT3. The downregulated DE genes by EIV/1963, which do not appear to be affected by EIV/2003, were STAT2 and TAP1.

When the IFN pathway at 24 hours post-infection was examined, SOCS1 was upregulated by EIV/1963 but not by EIV/2003. Conversely, IFNRα, IFNR1, TC-PTP and PIAS1 were all downregulated by EIV/1963, but not shown to be affected by EIV/2003. Instead, EIV/2003 downregulated JAK1 and TYK2 while EIV/1963 did not affect these DE genes and both of the viruses downregulated DRIP150. When studying the shared upregulated genes by the two viruses, IFNα/β, IRF9, IFIT1, Mx1, G1P2, IFIT3 also were shared at 4 hours post-infection. IFI35, OAS1, and G1P3 were newly shared upregulated genes for 24 hours post-infection.

When the transcriptome of the IFN-α treated cells was studied with IPA, the exact same genes were highlighted as being upregulated. All of the upregulated genes of the EIV infections were also shared by IFN-α treatment at 4 hours. The extra genes upregulated by IFN-α that were not upregulated by the virus infections at 4 hours post-infection were STAT1, STAT2, JAK2, TAP1, SMB8, IFI35, OAS1, G1P3 and PSMB8. The upregulated genes shared across all three conditions were IRF9, IFIT1, Mx1, G1P2 and IFIT3. At 24 hours post-infection the number of shared upregulated genes increased to include IFI35, OAS1 and G1P3. The only genes highlighted by IPA that were uniquely increased by IFN-α treatment were STAT1, STAT2, JAK2, TAP1, SMB8 and PSMB8. However, at 4 hours post-infection the EIV/1963 virus downregulated TAP1 and STAT2. Overall, EIV/1963 downregulated more genes in the IFN pathway than EIV/2003 especially at 4 hours post-infection.

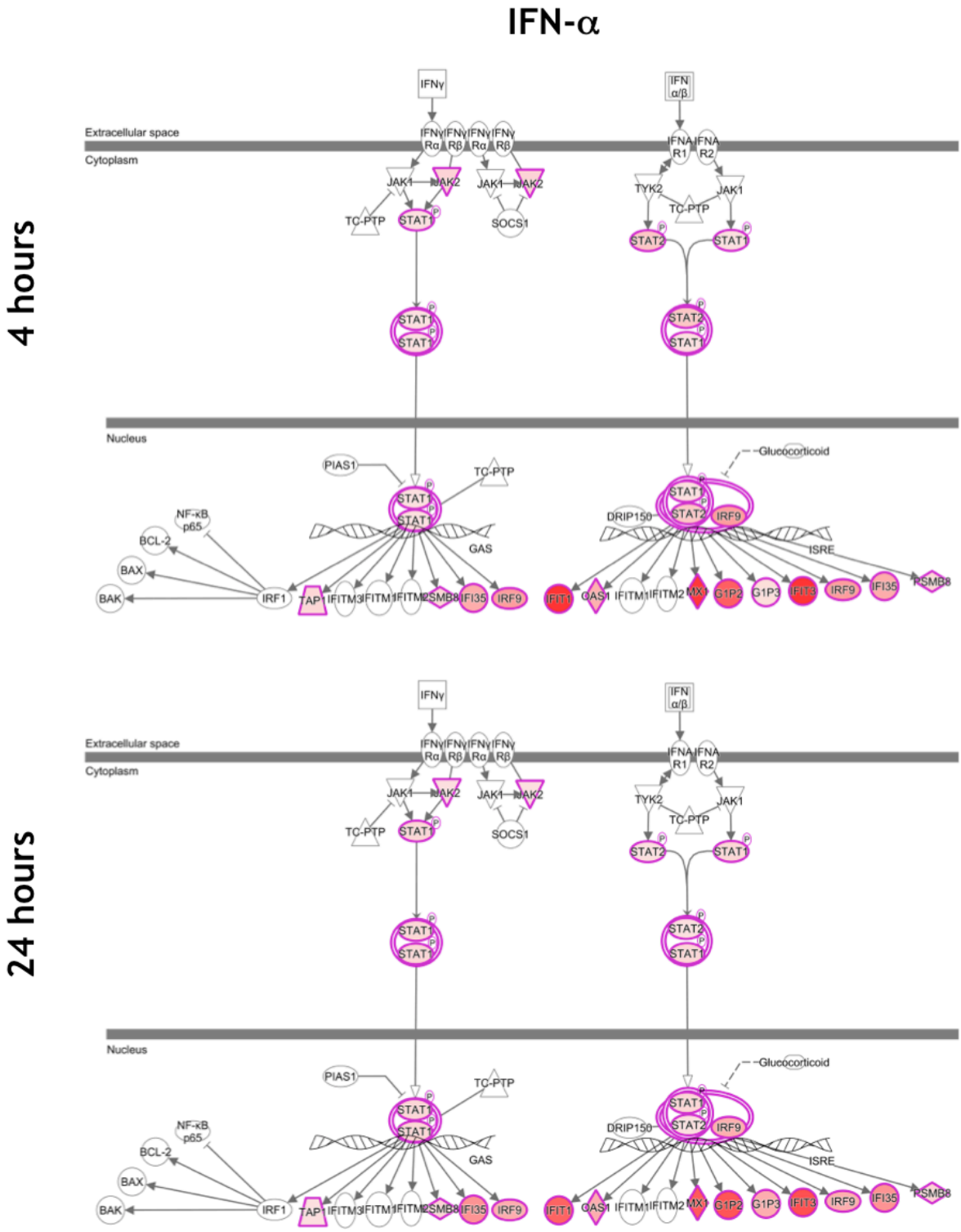

Figure 55: IPA software was used to highlight the affected proteins in the IFN signaling pathway from the list of DE genes for IFN-α treated cells. Both 4 hours and 24 hours results are shown. See Figure 58 for legend.

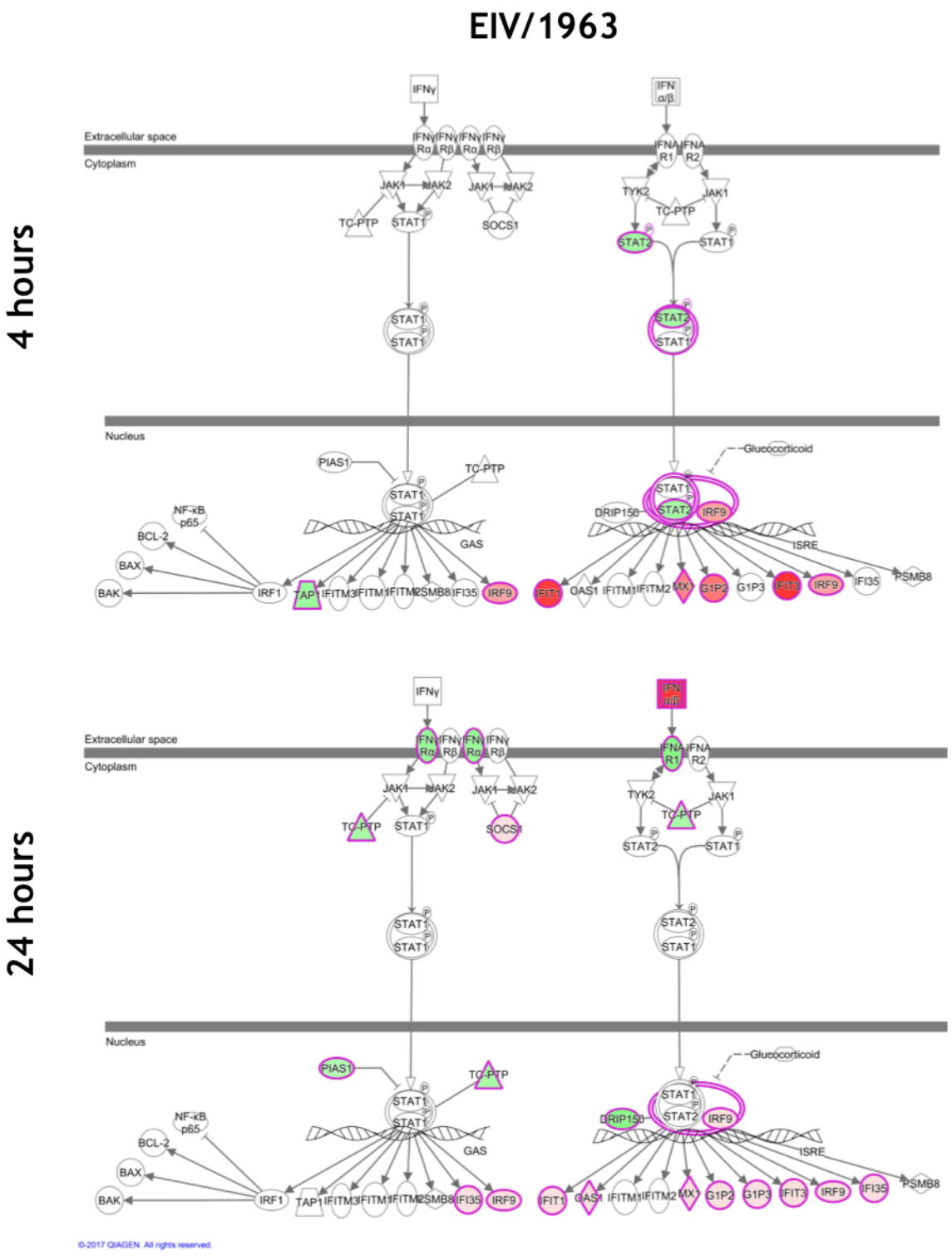

Figure 56: IPA software was used to highlight the affected proteins in the IFN signaling pathway from the list of DE genes for EIV/1963-infected cells. Both 4 hours and 24 hours results are shown. See Figure 58 for legend.

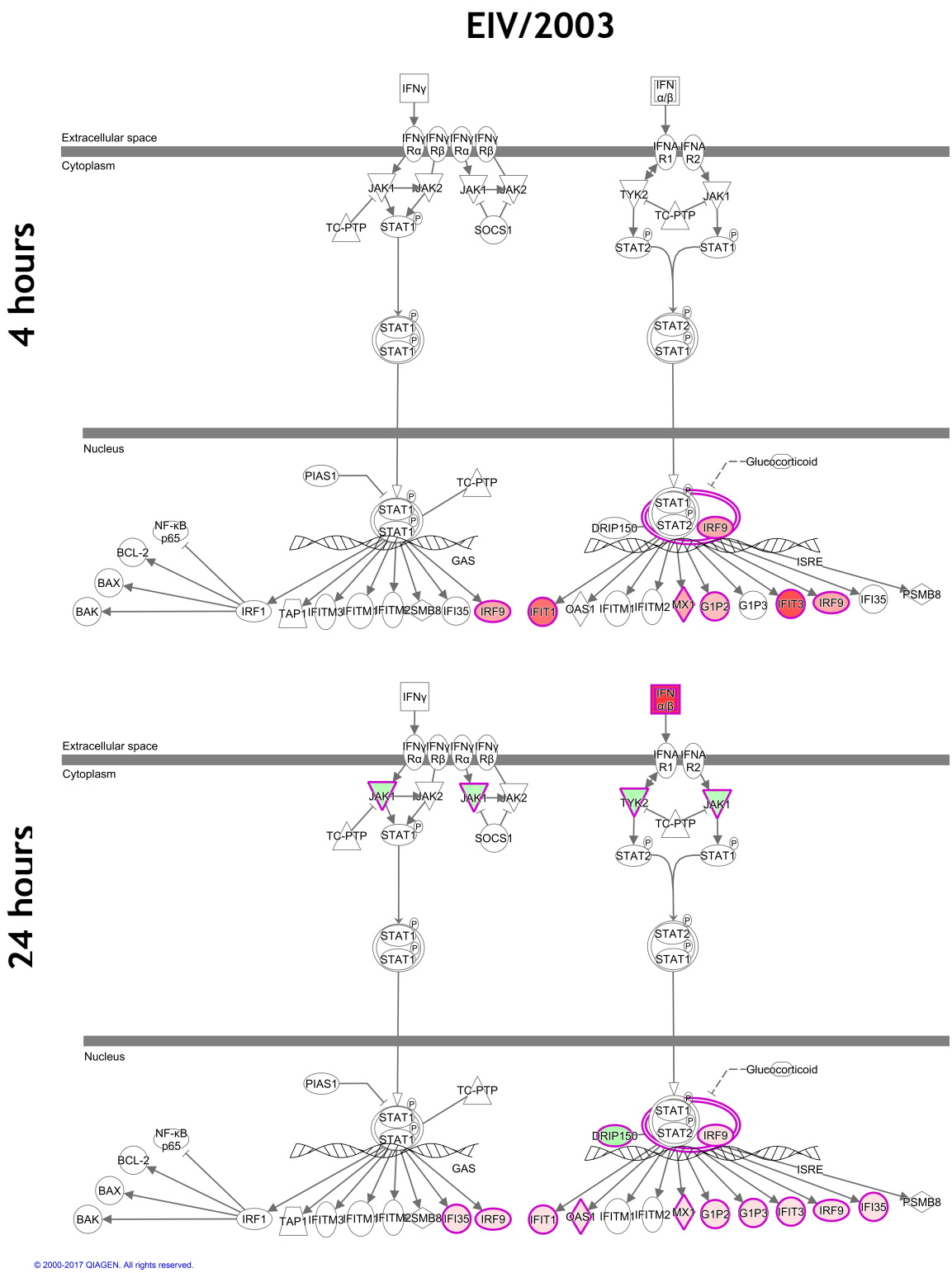

Figure 57: IPA software was used to highlight the affected proteins in the IFN signaling pathway from the list of DE genes for EIV/2003-infected cells. Both 4 hours and 24 hours results are shown. See Figure 58 for legend.

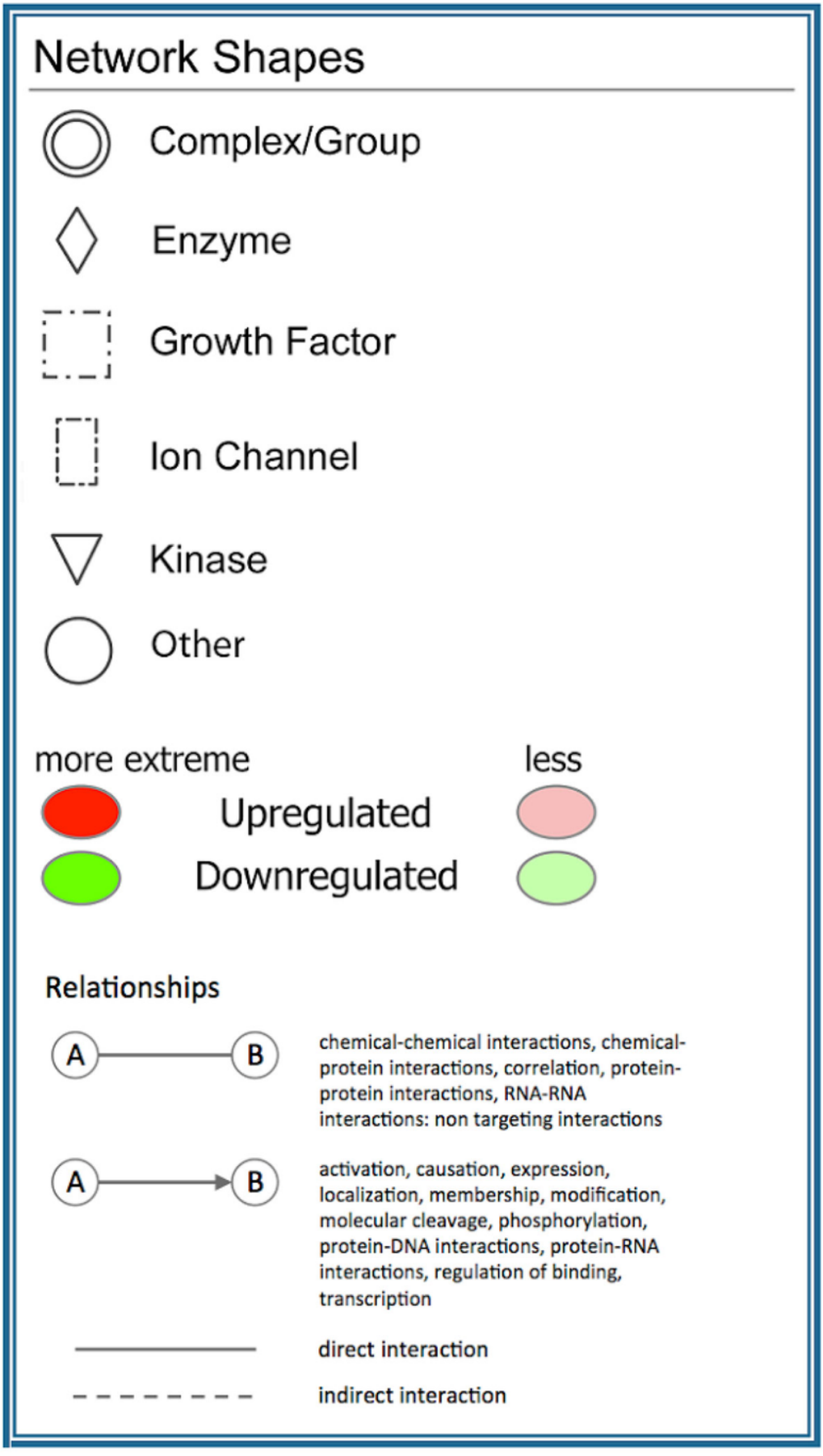

Figure 58: Ingenuity Pathway Analysis legend for pathway analyses (**Figure 55, Figure 56, Figure 57, Figure 59, and Figure 60**).

4.2.10. The eIF2 signaling pathway is affected differently by the two equine influenza viruses

The Eukaryotic Initiation Factor 2 (eIF2) signalling pathway was compared between both evolutionary distinct EIVs. IPA software was used to predict which proteins in the pathway would be affected, either by being up- or downregulated.

At 4 hours post-infection the eIF2 signaling pathway wasn't affected by EIV/2003 and was, therefore, not highlighted by IPA. However, EIV/1963 did affect some of the proteins in this pathway as is shown in **Figure 59**. The older virus downregulated eleven proteins, and upregulated none.

When comparing the two viruses at 24 hours (**Figure 60**), and which proteins they downregulated in the eIF2 signaling pathway, EIV/2003 uniquely downregulated ATF5 and eIF2β, whereas EIV/1963 downregulated ten proteins (CHOP, PERK, HSPA5, GCN2, eIF2α, eIF3, HR1, eIF5, PDK1, ERK1, eIF2β) that the younger virus did not. The two viruses shared nine proteins that were downregulated (TRIB3, SREBP1, XIAP, NOX4, PP1C, eIF4G, PI3K, INSR, SOS).

By observing the upregulated proteins at 24 hours post-infection, it was apparent that EIV/2003 upregulated many more proteins as compared to EIV/1963 (for example AFT3). The two viruses both upregulated five shared proteins (G-actin, CYCLIND1, 40s ribosomal subunit, RAS and 60s ribosomal subunit). The evolutionary older virus, EIV/1963, only upregulated one unique protein (AKT), whereas EIV/2003 upregulated seven (PKR, GADD34, ATF3, N-MYC, C-MYC, VEGFA, eIF3).

4 hours

EIV/1963

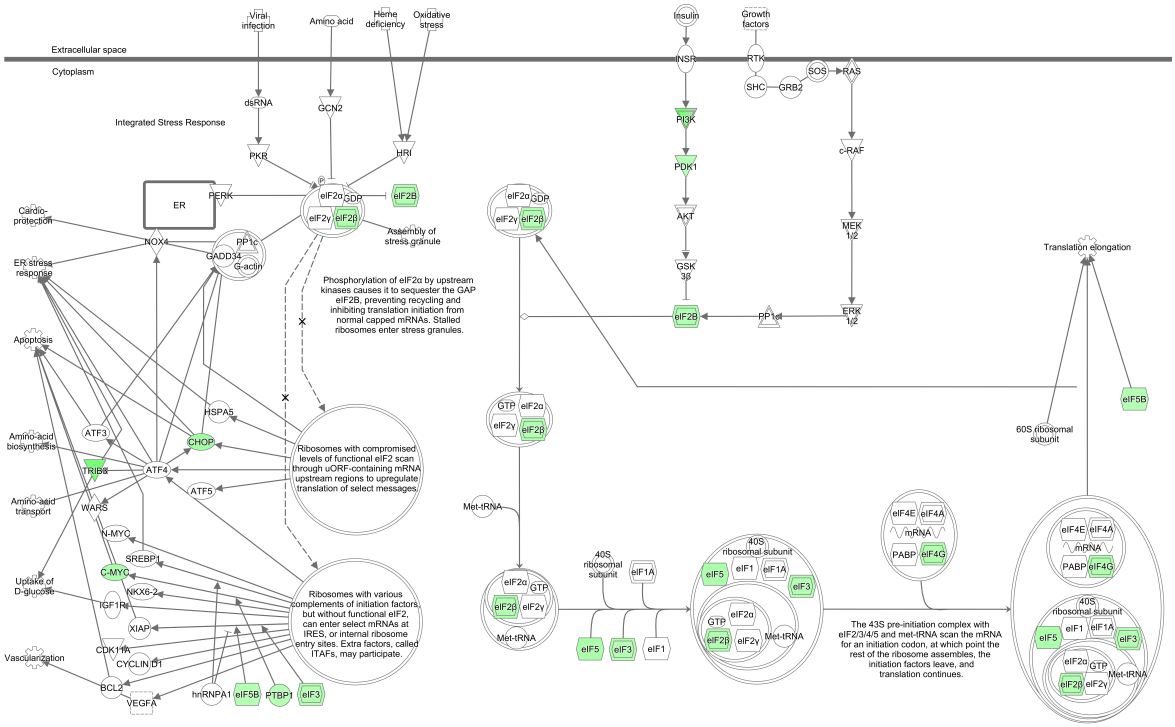

EIV/2003

NA

Figure 59: IPA software was used to highlight the affected proteins in the eIF2 signaling pathway from the list of DE genes for IFN-α treatment, EIV/1963-infected and EIV/2003-infected. The results for 4 hours are shown. See Figure 58 for legend.

24 hours

EIV/1963

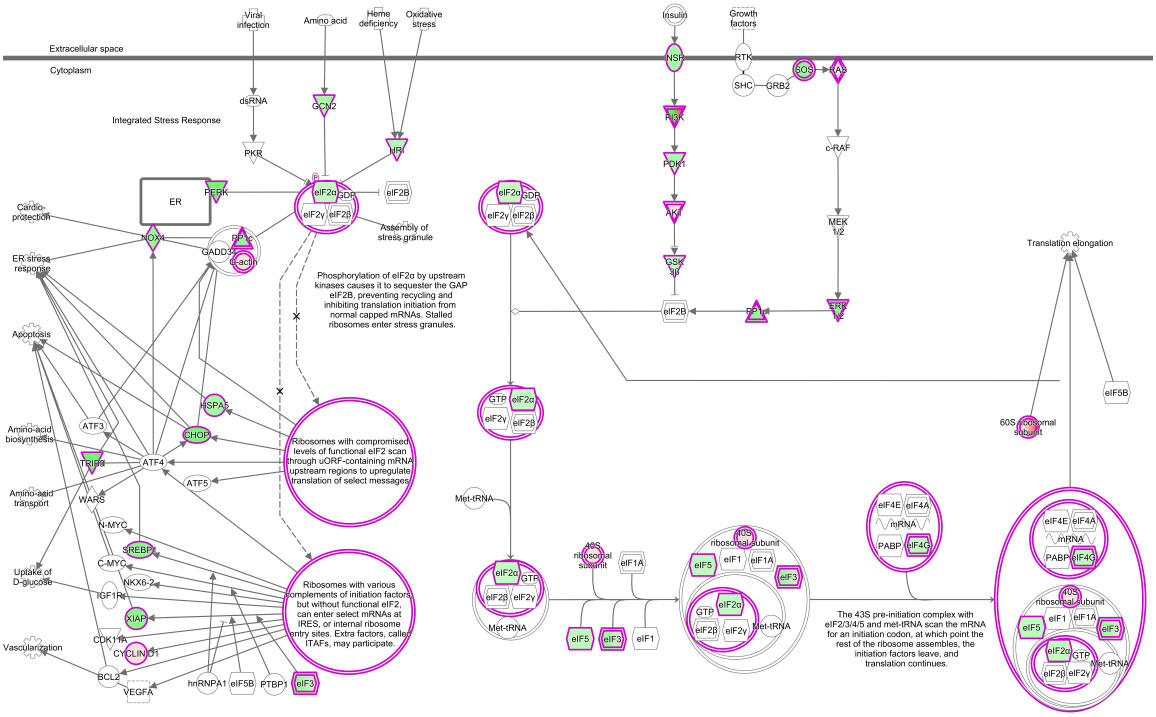

EIV/2003

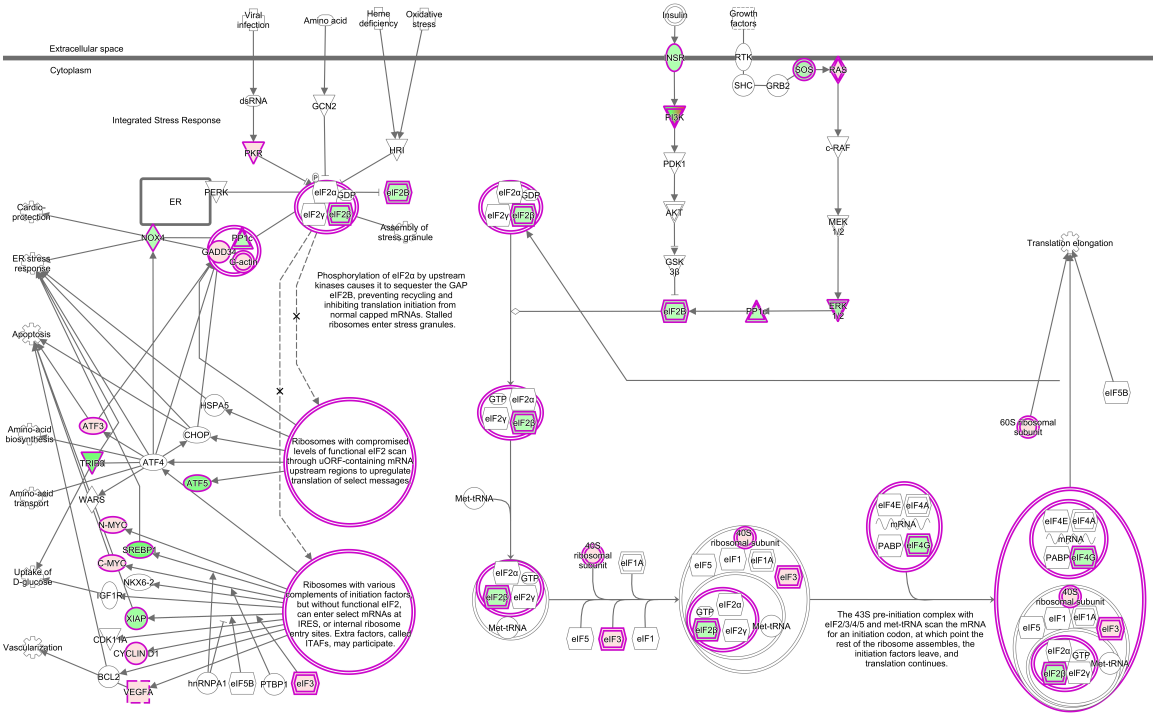

Figure 60: IPA software was used to highlight the affected proteins in the eIF2 signaling pathway from the list of DE genes for IFN-α treatment, EIV/1963-infected and EIV/2003-infected. The results for 24 hours are shown. See Figure 58 for legend.

4.3. Discussion

The way a virus controls the cellular machinery of a host changes over time. These changes over time are not only due to viral evolution, but also due to the evolution of the host. The evolution of the virus and host together is often referred to as an "arms race", where both the virus and the host are trying to evolve more rapidly and efficiently than the other (Daugherty & Malik 2012). To date, studies into how the evolution of influenza affects viral control of the host cell are lacking.

Two evolutionary distinct equine influenza viruses (EIVs) were selected to study in E.Derm cells. They had previously been shown in Chapter 3 to grow very differently in the equine cells (**Figure 13**). The newer evolutionary virus (EIV/2003) grew much more efficiently and to considerably higher titres than the older evolutionary virus (EIV/1963). When both viruses were grown in cells pre-treated with 1,000 UI/ml of IFN-α, EIV/1963 was much more negatively affected than EIV/2003 (**Figure 21**). The difference in how pre-treatment affected the EIV/1963 and EIV/2003 viruses formed the hypothesis that the two EIVs were manipulating the host response in different ways, with the more adapted virus (EIV/2003) being able to overcome IFN-α treatment.

RNASeq is a relatively novel tool that allows for the study of the transcriptome of cells exposed to different conditions (Josset *et al*. 2014; Simon *et al*. 2015; Morrison *et al*. 2014). In this chapter transcriptomics was used to study an equine dermal (E.Derm) cell line upon IFN-α treatment, and infection with two evolutionary distinct EIVs.

Kraken is a useful tool to study the unassigned sequencing reads after alignment to a genome. It allows for the analysis and identification of possible contaminants. This result was reassuring as it was evidence that the samples had not become contaminated with other bacteria or viruses during culture, experimental infection or RNA extraction. For the samples infected with EIV, it was expected that some of the reads for align with IAV as the cells were infected with this virus. However, it was interesting to note that at both 4 hours and 24 hours post-infection that a higher percentage of reads mapped to IAV for infection with EIV/1963. The reason for this could be that EIV/1963 possibly

produces a higher number of RNA transcripts than EIV/2003. More investigation could be carried out to analyse these transcripts separately. Another point of interest was that quite a few of the unassigned read for infection with EIV/2003 that aligned to viruses were shown to be a match for RD114 Retrovirus. This observation was repeated across time-points, and independent repeats just for EIV/2003, which would suggest that this was not a contamination issue. A possible reason could be that some of EIV/2003 transcripts can also be aligned to the genome of the RD114 Retrovirus. This phenomenon was also observed at 24 hours for infected cells with EIV/1963 – a number of reads mapped to Orthoretrovirinae. Possibly there are transcripts produced by EIV/1963 later in infection that align to Orthoretrovirinae, as there were no reads aligned to this other virus at 4 hours post-infection.

The sequencing data were studied using distance-based metrics in order to ascertain how similar the experimental replicates were. The Mock-infected and IFN-α treated cells were shown to be much more similar to each other than the EIV-infected samples at both 4 and 24 hours post-infection. At 24 hours post-infection, the EIV/1963 and EIV/2003 samples were very distant to the Mock-infected samples (**Figure 50**, A). The similarity between the EIV infected cells was confirmed using hierarchical clustering and Pearson cor distance, to show that the EIV-infected cells clustered together and had a greater distance to the Mock-infected cells, as opposed to the IFN-α treated cells that were very close to the Mock samples (**Figure 50, C+D**). Overall, these results demonstrate that the host response to infection with EIVs is highly specific to each virus, although these viruses shared more similarities than to the Mock-infected or IFN-α transcriptomic profiles.

After RNASeq was carried out, the sequencing reads were processed using the CuffDiff2 pipeline to produce a list of upregulated or downregulated genes in the treated/infected cells, when compared to the gene transcripts expressed in the control cells. These genes are referred to as differentially expressed (DE) genes. When determining which of the DE genes to select for further analyses, it was important to use thresholds to choose the most important genes for study. Therefore, a Q value threshold of ≤ 0.05 was used to select the lists of genes. A further threshold was used for the Log_2FoldChange (Log_2FC) range. The effect of

varying the Log_2FC threshold was investigated by creating lists of DE genes with a Log_2FC cut-off of 0.58, 1 and 1.58. As can be seen from **Figure 51**, the number of DE genes began to decrease after a Log_2FC value of 1 was applied. When the lists of DE genes for each of the thresholds for the data at 4 hours post-infection was analysed using Ingenuity Pathway Analysis (IPA) software, there was an obvious decrease in the number of Canonical Pathways highlighted when a Log_2FC threshold of 1 or 1.5 was selected. This loss of IPA data was considered to be an important loss of information and therefore, a Log_2FC value of 0.58 was selected as the threshold. For the rest of the chapter any analyses were carried out using only DE genes with a Log_2FC value larger than 0.58.

It is important to note that the Log_2FC threshold can vary in the literature (0.58 (Eschbaumer *et al*. 2016), 1 (Morrison *et al*. 2014) and 1.58 (Josset *et al*. 2014)) and that this can affect any conclusions made upon investigation of the list of DE genes. To this end, the chosen thresholds, the motivations for their choice, and their possible effects were stated. As the world of RNASeq is still relatively new, this is something that the field will have to reach conclusions on. What are considered liberal and strict thresholds, and how should researchers check whether the correct filters are being applied? These questions are something that will need to be investigated further and may take many years before the research community reaches an agreement.

The number of DE genes was plotted for each of the conditions, with the number of upregulated and downregulated DE genes highlighted by arrows (**Figure 52, A**). The transcriptome for the IFN-α treated cells remained under 300 genes for both time-points studied (4 hours and 24 hours). The stasis of the IFN-α transcriptome is in contrast to the dynamic response of the two EIV-infected transcriptomes over the two time-points. The number of DE genes increased considerably for both viruses, however EIV/1963 affected many more genes than EIV/2003 at 4 hours post-infection (1,100 and 131 respectively). The stasis of the IFN-α treatment demonstrated that the cells were already in a highly responsive state with just 4 hours of treatment.

Venn diagrams were a useful tool for indicating the genes shared by each condition, as well as allowing for the identification of unique genes (**Figure 52,**

B). Interestingly, at both the 4 hours and 24 hours time-points, all three conditions upregulated some IFN stimulated genes (ISGs) that have been shown to be important in relation to influenza infection. These important genes included IRF9, ISG15 and MX1. Four hours post-infection the EIV/1963 virus downregulated a large number of genes (997). Conversely, EIV/2003 appeared to be more selective in the genes that it targets for downregulation, targeting LARP6 (function includes RNA binding and nucleotide binding (Fagerberg *et al*. 2014)) and CCXC5 (function includes sequence-specific DNA binding and signal transducer activity (Fagerberg *et al*. 2014)) among others. EIV/2003 tolerated five genes that were upregulated by IFN-α, one of these includes OAS2 – a gene that has been documented as being important for the innate response to viral infection (Hovanessian *et al*. 1987). At the time-point of 24 hours, the three conditions shared a large number of upregulated genes. The reason for a high number of upregulated genes being shared is that the IFN response has been stimulated by both infections at this later time-point, and a lot of the genes shared are also turned on by IFN-α treatment.

While the number of DE genes for IFN-α treatment did not change over the two time-points, when upregulation and downregulation of the DE genes was studied more closely using a heat map (**Figure 53**), the actual DE genes were vastly different, even though the number of DE genes stayed relatively similar. The analysis of two time-points allowed for the dynamic nature of the response of the E.Derm to IFN-α to be evaluated. At 24 hours post-treatment there were more downregulated genes than at 4 hours. The Fragments Per Kilobase of transcript per Million mapped reads (FPKM) value of some of the DE genes had increased greatly. The results from this chapter have shown the interferome of E.Derm cells to be dynamic over time, rather than a static event. Two time-points of IFN-α treatment were compared (4 and 24 hours) and the number of upregulated and downregulated DE genes (as compared to Mock-infected) decreased at the later time-point. This is a phenomenon that has not been regularly studied. The results of this chapter agreed with a study that investigated IFN treatment over time of Primary Human Hepatocytes (PHH) (Jilg *et al*. 2014). Genes such as IFIT3, IFI1 and Mx1 were shown to be dynamic and had a lower Log2FC value at 24 hours post-treatment. In the study by Jilg *et al*. (Jilg *et al*. 2014), they shared some of the genes that increased expression at 8

hours post-treatment to then decrease at 24 hours post-treatment. However, there wasn't complete concordance between this study and the current Chapter, genes such as Mx2 were shown to increase their FPKM value here and Jilg *et al*. found that the gene decreased at 24 hours. Overall, these findings show that treatment of cells with IFN-α produces a kinetic expression of ISGs that changes over time.

Categories were created based on Gene Ontology (GO) from the online tool Biomart (Ensembl), and the DE genes for the virus-infected conditions were analysed to see which category they fell into (**Figure 54**). The largest differences were observed at 4 hours post-infection, with EIV/1963 downregulating many genes involved with gene expression, as opposed to EIV/2003. EIV/1963 downregulated many more genes than EIV/2003 for all of the eight categories analysed. In addition, the downregulation of more genes by EIV/1963 was true in almost all the categories at 24 hours post-infection, but the difference wasn't as marked as at 4 hours. Therefore, EIV/1963 was controlling the host cellular response to infection in a different way than EIV/2003 especially at 4 hours post-infection. The older, less evolutionary adapted, virus appeared to shut down the cellular functions of the host much faster than EIV/2003. The stronger response by the virus may be required because the virus has not adapted more efficient ways of hiding from the host immune response. It may be that as EIV became more adapted to its host, it was able to target the specific genes required for successful concealment and replication of the virus and didn't require the unconditional downregulation of DE genes.

IPA was used to study the IFN signalling pathway, and predict how the three conditions (IFN-α treatment, EIV/1963-infection and EIV/2003-infection) affected the proteins within this pathway (**Figure 55**). It was interesting that although Jilg *et al*. (Jilg *et al*. 2014) showed that the IFN-α transcriptome was a dynamic event, the proteins highlighted in the IFN signalling pathway were the exact same at 4 hours and 24 hours post-treatment. The kinetic genes in the IFN-α treated cells appear involved in cellular aging and metabolic processes, while the core ISGs remain present across both time-points. The genes that were upregulated by IFN-α treatment were crucial during the interferon response (e.g. STAT1, STAT2, JAK2) and therefore it is of interest that these genes were

not upregulated upon infection with an IAV. In fact, EIV/1963 downregulated STAT2 at 4 hours post-infection, which could be the way that the older virus is manipulating the interferon response to infection. STAT1 isn't phosphorylated without STAT2, and as this process begins the cascade to turn on ISGs it is beneficial for EIV/1963 to target this gene for degradation (Qureshi *et al*. 1996). It is of interest that EIV/2003 downregulated JAK1 at 24 hours post-infection, targeting a gene that is before STAT2 in the IFN-signaling cascade (Uetani *et al*. 2008).

At 24 hours post-infection the two signalling pathways for eIF2 appeared similar, but there were important differences (**Figure 60**). The formation of the heterotrimer consists of three subunits: eIF2α, eIF2β and eIF2γ. EIV/1963 acts to disrupt the eIF2 signalling pathway by downregulating the eIF2α subunit, as opposed to EIV/2003, which downregulates the eIF2β subunit. By decreasing expression of the eIF2α subunit, EIV/1963 is limiting the production of the eIF2 complex, which is required for the initiation of mRNA translation. Therefore, this inhibits protein synthesis. The phosphorylation of eIF2α by PKR is one of the most frequent targets by invading viruses to regulate the host cell (22, 23). EIV/2003 manipulated the eIF2 signaling pathway in a different way by targeting the eIF2β subunit for downregulation. **Figure 60** also demonstrates that EIV/2003 infection caused the upregulation of PKR (Protein Kinase R). As the PKR molecule is very important for downstream antiviral responses, it would be interesting to study the formation of PKR protein to see if the virus targets this molecule post-translationally.

One of the molecules in the eIF2 signaling pathway that EIV/2003 upregulated, and which was not affected by EIV/1963, was AFT3 (Activating Transcription Factor 3) (**Figure 60**). Contrary to its name, AFT3 suppresses rather than activates transcription from promoters with ATF sites. It combats an excessive, and potentially damaging, inflammatory response as it regulates both inflammatory chemokines and cytokines (Khuu *et al*. 2007; Chen *et al*. 1994). Therefore, the fact that EIV/2003 upregulated the expression of this gene could be one of the reasons to explain why this virus was more efficient at replicating in the host cells, and why it can replicate much more efficiently than EIV/1963 after pre-treatment with IFN-α (**Figure 21, D**).

It is understood that IAVs cause host shutdown in order to replicate within a cell (Rivas *et al*. 2016). Nevertheless, the dynamics of how the host shutdown differs between different strains of viruses has not been studied in detail. It has been shown that some IAVs are more selective in the degradation of host transcripts due to the PA-X protein. A study by Khaperskyy *et al*. (Khaperskyy *et al*. 2016), demonstrated that PR8 targeted host RNA polymerase II (Pol II) transcribed mRNAs, while sparing products of Pol I and Pol III. Two additional methods that IAVs can use to shutdown host responses are through inhibition of polyadenylation and export of host mRNAs by NS1 (Krug 2015), or RNA Pol II degradation by the viral RNA-dependent RNA polymerase (RdRp) (Chan *et al*. 2006). In summary, there are three known methods through which IAVs can manipulate the host cellular responses, but it is unclear which of these methods a virus uses and how this is affected by how well adapted the virus has become to its host. A virus that may not have evolved an NS1 that can bind to CPSF30 (the 30-kDa subunit of cleavage and polyadenylation specificity factor, whose function is to carry out in the 3′-end processing of cellular pre-mRNAs, may instead depend more heavily upon methods such as PA-X activity or Pol II degradation. With RNASeq becoming more developed and refined, it will be possible to perform further experiments studying how different evolutionary strains of the same IAV manipulate the host response using these different methods.

Broadly, some of the differences between how the older EIV and the younger EIV control the host response upon infection were dramatic, and yet some of them were subtler. This chapter has highlighted these differences for two very specific EIVs, and it would be interesting to test different EIVs from across the evolutionary time period, to determine whether the method of controlling the host transcriptome evolves over time. In addition, it would be useful to study additional time-points of infection to observe the dynamic change over time. With only having the two time-points of 4 and 24 hours, there are a lot changes in the missing 20 hours between that could provide more information of how the two viruses control the cell. As this chapter describes an observational study, it would be beneficial to further investigate the genes highlighted using mechanistic experiments.

Overall, the research carried out in this chapter was to examine the equine host response to two evolutionary different EIVs. Transcriptomics was used to study the host transcriptome after infection, and compare it to the interferome – the transcriptome present in the cells after treatment with IFN-α. The two viruses were shown to manipulate the host response in distinct ways, with EIV/1963 acting much more strongly than EIV/2003 by downregulating many more genes at both 4 and 24 hours post-infection. The less-adapted virus induces host shutoff by downregulating as many host proteins as possible, causing more cell death (as seen in Chapter 2). Conversely, EIV/2003 appeared more selective in the genes that it targeted for downregulation, in both the IFN-response and general gene expression. The phenotype of infection didn't produce a lot of cell death, yet much higher viral titres were produced when compared to production of EIV/1963 virions. Over the evolution of the two viruses – from first infecting a horse, to 40 years later – the virus has adapted to its mammalian host, through evolution of all the gene segments. It has become adapted and able to target specific cellular functions, replicate in IFN-treated cells, and replicate to high titres. These findings were investigated in more detail by Chauché *et al.* ((Chauché et al. 2017).

A hypothesis is that as the EIV virus adapted to its equine host it evolved to be able to manipulate the cellular response to infection much more efficiently and selectively, without having to downregulate many genes unconditionally. Of course, much more research must be done to investigate this hypothesis and test its strength. But the research described here begins to attempt to understand how viruses spanning 40 decades control the same host in different ways, and these are important experiments that should be continued with other influenza A viruses in other hosts to see if there are similar patterns when an avian virus crosses the species barrier and has to adapt to mammals.

Acknowledgements

This study was funded by grants from the Horserace Betting Levy Board (HBLB). I would like to thank Lily Tong and Gavin Wilkie for sequencing the samples. A special thanks to Quan Gu who ran the CuffDiff2 analysis to provide the list of differentially expressed genes. A big shout-out to Andrew Shaw, who provided

many useful conversations discussing transcriptomics. I would particularly like to acknowledge Joseph Crispell who helped with the creation of some of the figures in R.

Chapter 5

5.General Discussion

5.1. Summary of Findings

Influenza A viruses (IAVs) are viruses that are capable of jumping the host species barriers to infect new hosts. Originally viruses of avian origin, infecting wild waterfowl, they now infect many different mammals such as pigs, whales and humans (Ito *et al*. 1998; Cheung & Poon 2007). Horses have been documented as infected with influenza since 1956, when an IAV was first isolated, but it is believed they were infected much longer before this (Sovinova *et al*. 1958). An H3N8 of avian origin was first detected in horses in 1963 and has since outcompeted the previous equine influenza virus (EIV) of subtype H7N7, to the point where it is now considered extinct.

One of the most interesting aspects of influenza is the way it can manipulate and escape the host immune response allowing it to jump the host species barrier and infect a wide range of hosts (Waddell *et al*. 1963; Lee *et al*. 2010; Anthony *et al*. 2012). The research described in this thesis has concentrated on EIV as a model to study the evolution of a virus over time to its host. The lessons learned from this study can hopefully be applied to study human IAVs and how they adapt over time to human hosts.

The availability of cells to study influenza infection *in vitro* is limited, especially when considering cells from a specific host such as the horse. There are a few human cell lines such as A549 and BEAS-2B, or the widely used MDCK cell line (Lee *et al*. 2010; Gan *et al*. 2015; Seitz *et al*. 2012). However, it was essential to study the infection kinetics of EIV in an appropriate equine cell line in order to reveal the specific host responses to infection. Therefore, Chapter 2 of this thesis describes the characterization of an equine dermal (E.Derm) cell line, specifically for studying infection with IAVs. The infection conditions used, and the replication phase of an equine influenza virus (EIV) was determined.

There was no previous documentation of E.Derm cells being used for infection with influenza. The only papers in a literature search were those involving equine arteritis virus and equine herpesvirus-1 (McCollum 1986; Cullinane *et al*. 1988; Hasebe *et al*. 2009; Telford *et al*. 1992). The conditions to grow influenza *in vitro* usually requires the addition of exogenous proteases for the maturation of the HA of the IAVs (Klenk *et al*. 1975; Seitz *et al*. 2012). Cell

lines can be susceptible to infection with viruses, but this does not necessarily mean that they will be permissive and produce new virions. Therefore, one of the critical purposes of Chapter 2 was to establish if E.Derm cells were permissive to infection with EIVs. An EIV from 2003 (EIV/2003) was used as the test virus, and it was shown that E.Derm cells do allow for the successful replication of an EIV.

A point of interest was whether the cells would have a selective capacity over which IAV would be able to replicate. It is known that after EIV infected dogs, and continued to evolve into Canine Influenza Virus (CIV), this new strain cannot infect horses (Yamanaka *et al*. 2010). Hence, a CIV virus from 2009 (CIV/2009) was used to infect E.Derm cells and was shown to have significantly lower replication efficiency when compared to EIV/2003. The finding that E.Derm cell lines were selective in the viruses that could replicate efficiently was an important result, since it allowed for the investigation into host specific barriers that allow some IAVs to replicate more effectively than others. For example, MDCK cells were permissive to almost all IAVs and they replicate to very high titres in this cell line. So the well-known cell line could not be studied for host barriers to infection, as there appears to be very few. The rest of the experiments in this thesis were based upon the finding that the E.Derm cell line was a relevant equine cell line, and experiments were designed to investigate the host barriers.

An additional finding from the experiments described in Chapter 2 characterising the E.Derm cell line was that an exogenous protease was not required for the successful replication of an EIV. The lack of a necessity for exogenous protease showed that the HA of the virus must be being cleaved by an intrinsic protease present within the E.Derm cells. All further experiments within the thesis did not require the presence of an exogenous protease (specifically Tosyl Phenylalanyl Chloromethyl Ketone (TPCK)-trypsin).

The establishment of the E.Derm cell line meant that specific host barriers to infection with different IAVs could be analysed. Four IAVs were selected for analysis: an avian IAV that has the potential to cross the host species barrier and infect horses (AIV/2009), an un-adapted EIV from 1963 when

horses were first infected (EIV/1963), an EIV from 2003 after 40 years of adaptation to the horse (EIV/2003), and a CIV from 2009 after the virus had become adapted to canine rather than equine hosts (CIV/2009) – all of the H3N8 subtype.

Chapter 3 of this thesis shows the results from the infections with these IAVs in the E.Derm cell line. The overall growth kinetics of the viruses were examined and following this, two host barriers were thoroughly investigated: susceptibility to pre-treatment with IFN-α, and protease cleavage of the haemagglutinin (HA) glycoprotein. To compliment this work, the growth kinetics of the viruses were also studied in *ex vivo* horse trachea in order to compare the *in vitro* results to a more realistic model. The results from the infection in the *ex vivo* system showed that the two EIVs were able to replicate in the system, with EIV/2003 replicating more efficiently than EIV/1963. In addition, AIV/2009 and CIV/2009 replicated to lower titres than the EIV viruses, with AIV/2009 absent on some days of infection.

The *in vitro* infections with the four IAVs demonstrated that the viruses had very different phenotypes in relation to cytopathic effects (CPE) in the cells. AIV/2009 completely destroyed the monolayer of cells and EIV/1963 also killing a lot of cells. Whereas, EIV/2003 produced very little CPE, and CIV/2009 produced even less. When TPCK trypsin was added to the cells during infection to provide an exogenous protease, the virus that was most positively affected was AIV/2009, although CIV/2009 also benefitted. The positive effect of providing an exogenous protease suggests that a barrier to these viruses is the availability of compatible proteases for the haemagglutinin (HA) glycoprotein of the virus. Whereas the two EIVs that are adapted to the equine host were not positively affected by the addition of TPCK trypsin.

The results of pre-treating the E.Derm cells with 1,000 UI/ml of IFN-α for 24 hours and then infecting with the viruses allowed for the assessment of how resilient each virus was to the host immune response. The viruses that were most negatively affected by this pre-treatment were AIV/2009 and EIV/1963. The high negative affect of pre-treatment on these two viruses was interesting since AIV/2009 is an avian virus with no known replication in mammals, and

EIV/1963 was isolated at the very beginning of the H3N8 outbreak in horses meaning that it had recently been an avian virus. Therefore, these two viruses are not adapted to mammals, unlike EIV/2003 and CIV/2009 which have been evolving in a mammalian host for decades and were not majorly affected by pre-treatment with IFN-α.

Overall, the results from Chapter 3 showed that the four viruses appeared to manipulate the cells in different ways. AIV/2009 and EIV/1963 caused more CPE while replicating, and therefore seem to aggressively shutdown cellular pathways. The equine IAVs have an HA that is efficient at replicating in cells with an equine protease, which is particularly interesting in the context of CIV/2009 replicating more efficiently with the addition of an exogenous protease. Therefore, protease availability may be one of the limiting factors that inhibit the canine virus from infecting horses. CIV/2009 appears to have evolved in the canine host and adapted to those proteases, and therefore has shifted efficiency away from equine proteases. Finally, it appears that the IAVs, which have been circulating in mammals for many years and have had time to adapt to their immune response, are able to manipulate the host response after pre-treatment with IFN-α. In contrast, the infection kinetics of AIV/2009 and EIV/1963 decrease when an immune response is already present.

Following the preliminary investigations carried out in Chapter 3 in relation to the growth kinetics and host barriers to infection with a panel of IAVs, it was decided to further investigate the two EIVs within the E.Derm cells. Transcriptomics was used to study how both viruses differ in their manipulation of the host response to infection. In conjunction, other cells were treated with IFN-α in order to investigate the equine interferon (IFN) response in infected and non-infected cells.

The eclipse phase of EIV infection within E.Derm cells was investigated in Chapter 2, and was established as being 7 hours. Therefore, of the two time-points selected for investigation, one was during the eclipse phase (4 hours), and the other was chosen to allow the virus to have several cycles of replication (24 hours). Transcriptomics was used to analyse the cellular transcripts within the cells at these two time-points for four conditions: Mock-infected, IFN-α treated,

EIV/1963-infected and EIV/2003-infected. The CuffDiff2 pipeline was used to produce lists of Differentially Expressed (DE) genes by comparing the transcripts found in each of the conditions to the transcripts in the Mock-infected cells. The DE genes were given a value called Log_2FoldChange (Log_2FC), which could either be positive or negative depending on whether the DE gene was upregulated or downregulated by the condition. When looking at how similar the samples were to each other, distance based metrics were used. It was reassuring to see that replicates of each condition were spaced closely to each other, demonstrating that there was corroboration between the replicates. The closest two conditions were the EIV infected samples.

The equine IFN response has not been studied extremely closely, and so there are many equine ISGs that remain uncategorized, as shown by the genes that did not have a defined "Gene Name". The transcriptomics analysis of the two time-points showed that the IFN response was dynamic, with many genes only differentially expressed at either 4 hours or 24 hours post-treatment. The genes that were present at both time-points also changed their expression levels within the cells. Overall, the results showed some of the highly expressed genes in response to IFN treatment, and these could be analysed further and deemed the "core" equine ISGs.

When the cellular pathways affected by infection were both analysed using gene ontology, it was shown that the two viruses controlled the host cellular responses in different ways. This was most apparent during the eclipse phase when EIV/1963 caused host shutdown and downregulated many DE genes, whereas EIV/2003 affected far fewer genes at 4 hours post-infection. The two viruses also controlled the IFN response in different ways, with EIV/2003 apparently tolerating the presence of more ISGs than the less adapted EIV/1963. The hypothesis at the end of this chapter of results is that the EIV/2003 has had many more years to adapt to its equine host and so has become more efficient at targeting specific genes for downregulation. Whereas, the EIV/1963 has not evolved to replicate efficiently within the host and so must shut down the host cellular pathways in a much more aggressive way.

5.2. Limitations and Future Directions

This thesis describes experiments undertaken mainly using the E.Derm cell line to study equine host barriers to infection with influenza. It is important to discuss the limitations to this research, and possible methods to overcome these restrictions to proceed with future directions.

The first point to address is the equine cell line that was used. It is a fibroblast cell line from the dermis of a horse. In mammals, IAVs naturally infect the respiratory tract of the host. Therefore, artificially infecting a cell line originally from the skin of a horse is not ideal, and it would have been more biologically relevant to have a cell line originating from the respiratory tract, which at the time was not possible. The Murcia group had also tried to culture a primary cell line from the horse trachea with no success. It is important to note that the E.Derm cell line had also been extensively passaged, and senesces after 40 passages according to the information provided by the American Type Culture Collection (ATCC) website. For this reason, cells used for experiments in this thesis were not kept beyond 30 passages. The ATCC additionally noted that "55% of the cells have a chromosome number within + or - 1 of the diploid and modal number" with the "modal number = 64; range = 52 to 145". A highly variable chromosome number of the cells can lead to inconsistencies and cellular abnormalities. Overall, it would be useful to produce an immortalised equine cell line in order to repeat these experiments in a more relevant system, or use the *ex vivo* organ culture system.

The percentage of cells infected at the time of RNA collection could be interpreted as another limitation in two different ways. After a lot of optimising the highest percentage of cells infected at 4 hours post-infection was 46%. It could be argued that this means that 54% of cells were uninfected and that could have dampened the overall transcriptomics signal as they wouldn't be expressing the same genes as infected cells. An additional criticism could be that infecting such a high percentage of cells is not something that would occur naturally to a host during infection in the wild. Normally during infection with a virus, very few virions actually infect a host directly, so having such a high percentage of cells infected during the eclipse phase may not reveal the same DE genes as a lower impact, slower infection as seen *in vivo*. It was decided during the course of this

thesis to pursue the results using a high percentage of infected cells to increase the chance of a unique transcriptomic signal at the short time-point of 4 hours post-infection. The high percentage of infected cells meant that the latest time-point that could be taken was at 24 hours post-infection, as at this point all the cells were dying. It would be useful to compare an infection beginning with a more realistic percentage of infected cells and to follow the infection over a longer time period. Due to time constraints this wasn't investigated for the purpose of this thesis, but could be followed up in the future.

An alternative to transcriptomics of a whole well of cells is to perform single cell transcriptomics. This technique is the study of the transcriptome within a single cell, and would allow the comparison of different cells and their responses. It is reported in the literature that there is a wide variation between the responses of cells to stimuli such as infection and treatment with IFN, therefore this would be an interesting point to study (Shalek *et al*. 2013). It would also overcome the fact that such a high percentage of cells would have to be infected as to have an overall signal, as the infected cells could be selected individually.

The number of replicates used in this thesis for the transcriptomics analysis (and other infections) was three. As with any biological experiment, it is always preferable to have more replicates in order to have a higher statistical power. The limitations of statistics were due to the low sample size, as they assume that the underlying distribution being sampled is a normal distribution and that the variances of the distributions being compared are the same. If more time and resources were available, more replicates would have provided stronger statistical analyses. This is why a lot of comparisons appear to be non-significant. It is interesting that for the bioinformatics tools that were analysing the cellular transcriptome, it was possible to run these with only one sample, but this is highly un-recommended. In the end, three samples were chosen as the minimum for this thesis, but it would be good to repeat more replicates, potentially decreasing the p-value of any DE genes identified. A higher number of replicates was not possible for this research due to time constraints, and the sequencing costs, of preparing additional replicates.

A drawback to using transcriptomics is that this studies the RNA and gene expression of a cell, before the genes were translated into proteins. The overall gene expression of a cell does not fully equate with what is present as proteins, due to the host cell not translating all gene transcripts. It is also important to consider that influenza can cause degradation of gene transcripts before they are formed into proteins. Transcriptomics is also lacking, in that it misses any post-translational modifications. Therefore, it could be argued that transcriptomics alone is not enough to understand how a virus is controlling a cell. Rather, proteomics - the study of the proteins present in cells - could provide a clearer picture of what is occurring. However, proteomics is much more expensive than transcriptomics and requires mass spectrometers. Hence, mechanistic studies are required along with transcriptomics analysis to decipher and fully trust the highlighted results.

There are many different bioinformatics pipelines that can be used for the analysis of transcriptomic data, such as EdgeR and DeqSeq. These are pipelines that use count based tools, rather than CuffDiff2 that estimates expression at transcript-level resolution (Trapnell *et al*. 2013). The tool used in this thesis was CuffDiff2, commonly used for experiments with fewer replicates, as it produces lower numbers of false positives. Ideally, it would have been valuable to analyse the sequencing data using at least two separate pipelines and see which of the DE genes were highlighted in both and strengthen the conclusions drawn. However, the literature shows that there is usually corroboration between the different pipelines (Zhang *et al*. 2014), and so we increased the thresholds in order to select for more statistically significant DE genes.

In order to validate the findings of the *in silico* pipelines, experiments in the literature have used qRT-PCR (quantitative Reverse Transcription Polymerase Chain Reaction) to quantify the RNA expression of a few selected genes within the cells (Ratinier *et al*. 2016; Liu *et al*. 2016). Quantifying the RNA expression could allow for a higher degree of confidence, if the results match up with those found through *in silico* analysis. However, it is not a necessary step nowadays with many tools in place to make the same arguments by cross-validation, which produces all of the standard statistics. It is

also discussed in this paper (Hughes 2009) how pursuit of validation can often be at the expense of a thorough evaluation of the key points of the results. Therefore, it was decided for the purpose of this thesis not to pursue the use of qRT-PCR, and instead use stricter thresholds for selecting the DE genes produced by the transcriptomic analysis in order to reduce the number of false positives DE genes identified.

A lot of the data was gathered from observational studies, and while they do produce a lot of results and interesting areas for development, it would have been ideal to strengthen the claims and hypotheses of this thesis by including follow-up experiments. Techniques such as Western blotting could have been used to study the protein levels present within the cells. Western blotting would have been especially interesting as, has already been stated, transcriptomics only studies the transcripts present within a cell which doesn't always relate directly to the proteins that are translated. Another technique that could have been used to investigate the results more mechanistically would have been reverse genetics. Different biologically active sites of the EIV proteins could have been targeted for mutagenesis, and the interactions of these viruses with the host response could have been studied. These kinds of experiments were not conducted for this thesis due to time constraints, as the setting up of the pipeline from cells to transcriptomics was time consuming. However, it is hoped that other members of the laboratory will continue this work.

The work described in this thesis is a lot of the background work to set up a transcriptomics pipeline using equine cells and IAVs setting the scene for a project to continue on with studying different conditions in the E.Derm cells and using other culture systems.

The *ex vivo* trachea organ culture technique is something that has been perfected in the Murcia lab. Some infections carried out using this system were included in Chapter 4, studying the presence of an IFN response within the tissue. However, it would be very interesting to study the infection of the organ cultures with IAVs using transcriptomics. The results of these experiments could be compared to those described in this thesis to see how realistic the *in vivo* gene expression results were. This thesis was used to primarily investigate

infections in E.Derm cells, as a proof-of-concept and to set up the transcriptomics pipeline for future work. The development of the pipeline included the set up of infections, the RNA extraction and sequencing, the testing of analyses tools for analysing the sequencing reads, and the writing of scripts and creation of figures to visualise the results. If there had been more time the next step could have been to sequence the infected *ex vivo* tracheal organ cultures.

5.3. Final Conclusions

This thesis describes the research that aimed to study influenza infection in a host-specific cell line, in order to establish how IAVs change the way they manipulate a host due to adaptation and evolution.

The aims of this thesis consisted of:

1. Characterization of an equine cell line for the *in vitro* study of EIV

2. Explore equine host barriers to infection with different IAVs

3. Determine the cellular response to infection between two evolutionary distinct equine influenza viruses of the same lineage using transcriptomics

I believe that all of the aims that were stated were achieved, although as has been discussed there remains future work to build upon the findings described here. Collectively, the research carried out in this PhD thesis provided significant tools for the *in vitro* study of EIV, and progress towards understanding how the evolution of an IAV can change how the virus manipulates the host cell. The characterization of an equine cell line, and how to study the specific host barriers and transcriptome, will be important tools for the future advancement of improving the basic knowledge of EIVs, and IAVs in general, and how they evolve over time to manipulate a host.

Chapter 6

6.Materials and Methods

6.1. Materials

6.1.1. Eukaryotic Cell Lines

MDCK — Madin-Darby Canine Kidney Epithelial Cells (Source – ATCC)
Maintained in Dulbecco's Modified Eagle Medium supplemented with 10% fetal bovine serum and 1% penicillin/streptomycin.

E.Derm — Equine dermal cells (NBL-6) (Source – ATCC)
Maintained in Dulbecco's Modified Eagle Medium supplemented with 15% fetal bovine serum, 1% non-essential amino acids and 1% penicillin/streptomycin.

293T — Human embryonic kidney cells (Source – ATCC)
Maintained in Dulbecco's Modified Eagle Medium supplemented with 10% fetal bovine serum and 1% penicillin/streptomycin.

6.1.2. Viruses

Where stated, reverse genetics viruses of equine viruses A/equine/Ohio/1/03 (EIV/2003) and A/equine/Uruguay/1963 (EIV/1963) were used. The canine influenza virus A/canine/New York/dog23/2009 (CIV/2009) was also a reverse genetics virus. The isolate of virus A/equine/Uruguay/1963 was used in the infection of horse tracheal explants, rather than the reverse genetics virus. The virus A/ruddy shelduck/Mongolia/963V/2009 is an avian influenza virus isolate.

6.1.3. Virus Passage History

A/equine/Uruguay/1963:

- Virus Isolate: Origin - NIMR collection. First isolated in eggs, number of further passages unknown.
- Reverse Genetics Virus: Rescued by reverse genetics technique (Passage 1), passaged in MDCK cells (Passage 2), titrated and passaged on MDCK cells to produce separate viral stocks (Passage 3).

A/equine/Ohio/1/03:

- Virus Isolate: Origin - University of Kentucky. First isolated in eggs, number of further passages unknown.
- Reverse Genetics Virus: Rescued by reverse genetics technique (Passage 1), passaged in MDCK cells (Passage 2), titrated and passaged on MDCK cells to produce separate viral stocks (Passage 3)

A/canine/New York/dog23/2009:

- Virus Isolate: Origin – Cornell University. Unknown passage history.
- Reverse Genetics Virus: Rescued by reverse genetics technique (Passage 1), passaged in MDCK cells (Passage 2), titrated and passaged on MDCK cells to produce separate viral stocks (Passage 3)

A/ruddy shelduck/Mongolia/963V/2009:

- Virus Isolate: Origin - State Central Veterinary Laboratory (Mongolia). First isolated in eggs, and passaged another time in eggs. Further passaged three times in MDCK cells.

6.1.4. Horse tracheas

Horse tracheas were sourced from horses provided by the Animal Health Trust (AHT) and one horse was sourced from the Vet School, University of Glasgow (thanks to Nicola Kerbyson).

6.1.5. Plasmids

The full set of 8 plasmids for A/equine/Ohio/1/03 and A/canine/New York/dog23/2009 were a kind gift from Colin Parrish. The full set of 8 A/equine/Uruguay/1963 plasmids were cloned by Alice Coburn, a fellow PhD student in the lab.

The VSV glycoprotein plasmid was kindly provided by Brian Willett.

6.1.6. Reagents

6.1.5.1. Tissue Culture

- DPBS

Dulbecco's Phosphate-Buffered Saline 1X without calcium (Invitrogen, Catalogue Number: 14190-094)

- NEAA

100X MEM Non-Essential Amino Acids Solution (Invitrogen, Catalogue Number: 11140-035)

- 2X MEM

MEM (Temin's modification) (2X), no phenol red (Life Technologies, Catalogue Number: 11935046)

- TPCK

Trypsin from bovine pancreas - TPCK Treated, essentially salt-free, lyophilized powder, ≥10,000 BAEE units/mg protein. (Catalogue Number: T1426-250MG)

- DMEM

Dulbecco's modified Eagle's medium High Glucose GLUAMax Pyruvate (Invitrogen, Catalogue Number: 31966021)

- FBS

(Fetal Bovine Serum), Life Technologies.

- Trypsin

Trypsin EDTA .05% 1X (Invitrogen, Catalogue Number: 25300-054)

- NGS

Normal Goat Serum, New Zealand Origin, Life Technologies (Catalogue Number 16210064)

- OptiMEM

Opti-Minimum Essential Medium (Life Technologies, Catalogue Number: 11058021)

- Poly I:C

Polyinosinic-polycytidylic acid (HMW, 10mg) (Invivogen, Cat Code: tlrl-pic)

- BSA

Bovine Albumin Fraction V (7.5% solution) (Thermo Fisher Scientific, Catalogue Number: 15260037)

- IFN-α

Human Universal Type I Interferon (PBL Assay Science, Catalogue Number: 11200-2-PBL)

- RPMI

Roswell Park Memorial Institute 1640 medium (Invitrogen, Catalogue Number: 21875-034)

- Penicillin/Streptomycin

Invitrogen, Catalogue Number: 15140-122

- L-glut

L-glutamine (Invitrogen, Catalogue Number: 25030-024)

- Fungizone

Gibco™ Amphotericin B (Invitrogen, Catalogue Number: 15290026)

- Polybead® Carboxylate Blue Dyed Microspheres 1.00µm

Polysciences Inc., Cat Number: 19120, 15ml

6.1.5.2. Fixing and staining solutions

- Formalin solution neutral buffered, 10% (diluted to 1% or 4% in PBS, as required) (Sigma-Aldrich, Catalogue Number: HT501128-4L)

- TrueBlue Peroxidase Substrate (200ml) (Insight Biotechnology LTD, Catalogue Number: 5510-0030)
- DAKO System - HRP (DAB+) (Agilent, Product Number: K401011-2)
- Acetone Solution (diluted to 80% in distilled water) (VWR, Catalogue Number: 20066330)
- Phosphate Buffered Saline tablets (Fisher Scientific, Catalogue Number: 1282-1680)

6.1.5.3. Transfection reagents

- TransIT-LT1 Transfection Reagent (Mirus, Catalogue Number: MIR 2300)

6.1.5.4. Virus plaque assay overlay

- Avicel overlay 1.2% (w/v)
  Avicel RC/CL, Microcrystalline cellulose & Sodium carboxymethylcellulose was mixed for a final concentration of 1.2% in 500ml of distilled water. Autoclaved and stored at room temperature until use. Diluted in a 1:1 ratio with 2XMEM, and 1µg/ml of TPCK-trypsin was added prior to use in plaque assays.

6.1.5.5. RNA Extraction and Analysis

- Trizol Reagent (Invitrogen, 15596026)
- Agilent RNA Pico Kit (Agilent Technologies, Catalogue Number: 5067-1513)
- Qubit® RNA BR Assay Kit (Life Technologies; Reference: Q10210)
- RNeasy Mini Kit (Qiagen; Catalogue Number: 74104)
- RNase-Free DNase Set (Qiagen; Cat Number: 79254)
- RNase*Zap*® RNase Decontamination Solution (Ambion, Catalogue Number: AM9782)
- RNase-free Microfuge Tubes (1.5 mL) (Thermo Fisher Scientific, Catalogue Number: AM12400)
- TruSeq Stranded mRNA Library Prep Kit High Throughput (RS-122-2103)
- NextSeq® Sequencing System
- NextSeq® 500/550 High Output Kit v2 (75 cycles, FC-404-2005)

6.1.5.6. Antibodies

Primary Antibodies

- Anti-HA (A kind gift from Colin Parish, dilution 1:2000)
- Polyclonal rabbit anti-NP (Genescript, dilution: 1:500)
- Monoclonal mouse anti-NP, Clone HB65 (European Veterinary Laboratory, dilution 1:1500)
- Monoclonal mouse anti-Mx1 (Mab 143 anti-Mx1, dilution 1:600 (IF) and 1:200 (IHC)), kindly supplied by Georg Kochs

Secondary Antibodies

- Anti-rabbit Alexa Fluor 488, Catalogue Number: ab150077 (Abcam, Dilution 1:2000 for IF and FACS)
- Anti-mouse Alexa Fluor 488, Catalogue Number: A-11001 (Abcam, Dilution 1:2000 for IF and FACS)
- HRP anti-mouse
- Rabbit F(ab')2 anti Mouse IgG:HRP (Human Adsorbed) (Bio-Rad, Catalogue Number: STAR13B)

6.2. Methods

6.2.1. Cell Culture

Cell monolayers were cultured and maintained in 25, 75 or 150cm^2 tissue culture flasks. When cell monolayers reached 90% confluence, they were washed with DPBS and treated with Trypsin EDTA until the cells detached (37°C for all cell lines, except E.Derm which were kept at room temperature). Detached cells were re-suspended in media containing FBS to stop the action of the Trypsin EDTA and centrifuged at 1000 rpm to pellet cells. Pellet was re-suspended in appropriate media. For general maintenance cells were split at a ratio of 1:10, except for E.Derm cells, which were always split 1:2. All cells were kept in a humidified atmosphere with 5% CO2 at 37°C.

6.2.2. Influenza Reverse Genetics

293T cells and MDCK cells were plated in six-well plates one day before transfection using a 2:1 ratio of 293T to MDCK cells. The cell co-cultures were transfected with 300ng of each of eight plasmids containing all the genomic segments of the influenza virus to be rescued. Transfections were performed using TransIT-LT1 according to the manufacturer's instructions. 7.5µl of TransIT-LT1 transfection reagent per 2.5µg of DNA was mixed, incubated at room temperature for 30 minutes, and added to the cells. A day later, media was replaced with DMEM containing 0.3% bovine serum albumin (BSA) and 1µg/ml of TPCK trypsin. After 72 hours of incubation, supernatants were collected and clarified by low-speed centrifugation, aliquoted, stored at −80°C and titrated. This was called termed as passage 0 – P0. The reverse genetics virus was then subsequently passaged on MDCK cells to grow the virus to a high titre.

6.2.3. Experimental Infections

Unless otherwise stated cells were inoculated with virus diluted in infectious media for the required MOI and placed for 1 hour at 37°C. The inoculum was then washed off and replaced with either fresh infectious media or the appropriate regular media. Plates were then placed at 37°C for 60 minutes to allow viral entry, after which the inoculum was washed off and replaced with

fresh regular media.

6.2.4. Virus quantification by plaque assays

Viral titres were determined by standard plaques assays on MDCK cells and revealed by immunostaining of plaques. Cells were plated in 48-well plates and infected upon confluence 18-24 hours later. The inoculum was washed with DPBS after two hours of incubation and the cells were then overlaid with a 1:1 mix of 2XMEM and Avicel (1.2% w/v Stock) supplemented with TPCK trypsin to a concentration of 1µg/ml. Two days after infection cells were fixed in 80% acetone solution for at least 10 minutes at room temperature and then permeabilised with 1% Triton X100 + PBS for 10 minutes at room temperature. A mouse monoclonal anti influenza A NP antibody and Rabbit F(ab')2 anti Mouse IgG:HRP (Human Adsorbed) were used as primary and secondary antibodies, respectively. To visualize the infected cells, True Blue peroxidase substrate was added, and was stopped less than 10 minutes of incubation once colour had developed. Viral titres were calculated by counting blue plaques. Titres were expressed as log10 PFU per millilitre.

PFU/ml = P/(D x V)

P = Plaque number

D = Dilution factor of the well counted

V = Volume of diluted virus added to the well

Virus titrations throughout this thesis are affected by a methodological error,. This error was at the stage of dilution of the virus to be titrated where a multichannel was used to dilute viruses in 96 well plates. Instead of tips being changed in between every dilution, tips were changed between row 4 and 5. This means that virus will have been carried over between wells, and titres will be overestimated. As stated by Chase and Hoel, “errors of this magnitude can result in dramatic increases in the variation of the estimate of the initial concentration” (Chase & Hoel 1975).

Regrettably, it was not possible to repeat these experiments in the time available and, because the degree of systematic error might vary, the ability to make quantitative comparisons between these data is limited. However, it is still possible to describe changes in qualitative terms.

6.2.5. Preparation of working viral stocks

All viruses used in this study were grown in MDCK cells. Cells were infected at an MOI of 0.001 PFU/cell in infectious media containing DMEM, with no FBS, 0.3% BSA and 1 µg/ml of TPCK trypsin. Cells were incubated at 37°C for 1 hour, and then washed with DPBS before replacing with infectious media and incubated at 37°C and 5% CO2. Cells were constantly checked for Cytopathic Effects (CPE) and when this reached 80% of dead cells (usually ~36 hours post-infection) the supernatant from the flasks were removed and centrifuged at 1,000 rpm for 5 minutes at room temperature to pellet any cell debris. The clarified supernatant was then stored in 0.2 ml aliquots at -80°C.

Each virus stock was grown independently so that each independent repeat experiment was carried out with a new virus stock, allowing for the observation of differences in viral quasispecies. This method of virus preparation was considered especially important when carrying out transcriptomic experiments, in case a certain transcriptome was due to a particular viral quasispecies.

6.2.6. Virus infection

To study viral growth kinetics, cells were seeded in 12-well plates at 2×10^5cells/ml. 18-24 hours later the cells were infected with 250µl virus inoculum calculated at the desired viral MOI and diluted in infectious media. After an adsorption period of 1 hour at 37°C, virus inoculum was removed and the cells were washed with DPBS. At desired time points supernatant was collected and cells were harvested for FACS analysis. Viral titres were determined by plaque assay on MDCK cells as described.

6.2.7. Immunofluorescence

Cells were seeded at a density of 2×10^5cells per well of a 12-well plate containing 30mm glass coverslips. 18-24 hours later the cells were infected with virus at the desired MOI diluted in infectious media. At the required time-points the cells were fixed for 30 minutes at room temperature with 4% formalin diluted in DPBS. Cells were then permeabilised for 10 minutes at room temperature in 1% Triton X100 + PBS. Cells were then incubated for 2 hours with

the primary antibody at the required dilution and then washed three times in DPBS to get rid of any unbound antibody. Cells were then incubated for 1 hour in the dark with the secondary antibody and washed again using DPBS. The coverslips were then mounted onto slides using VECTASHIELD mounting solution and stored at 4°C until imaging using a Zeiss 710 Confocal Microscope.

6.2.8. Rescue of VSV-ΔG-GFP virus

293T cells were grown in a $10cm^2$ dish for 60-80% confluence and a transfection mix of 200ul Opti-MEM, 2µg of plasmid containing the missing VSV glycoprotein gene, and 6µl of Trans IT-LT was prepared and incubated at room temperature for 30 minutes before being added to the cells in a drop-wise manner. The next morning the transfection was washed off and the plate was incubated for another 36 hours. After, 293T transfected cells were infected with a previous stock of VSV-ΔG-GFP virus and incubated for a further 16 hours. Supernatant was removed and passed through a 0.45µm filter. VSV-ΔG-GFP virus stock was titrated on E.Derm cells by serially diluting the virus and infecting cells, infected cells were measured by Fluorescence-Activated Cell Sorting (FACS).

6.2.9. IFN Competence Assays

Cells were seeded on a 48-well plate and 18-24 hours later treated with increasing concentrations of Universal IFN-α for 4 hours and 24 hours before being challenged with VSV-ΔG-GFP. Cells were treated for 4 and 24 hours with increasing concentrations of high molecular weight Poly I:C and then challenged with VSV-ΔG-GFP. 16 hours after infection with VSV-ΔG-GFP the cells were fixed in 1% formalin overnight and were counted using the Guava FACS machine to calculate the percentage of infected cells expressing GFP.

6.2.10. FACS Staining

Cells were fixed in 1% formalin at 4°C overnight. After the cells were permeabilised with 1% Triton X100 for 10 minutes, blocked in 10% NGS + PBS for 1 hour, incubated with primary antibody for 2 hours and then washed 3 times with DPBS. The secondary antibody was incubated for 1 hour and washed

another further 3 times before being fixed again in 1% formalin. Antibodies were diluted in 10% NGS + PBS. Cells were then quantified using the Guava FACS machine.

6.2.11. Ex-Vivo Experimental Work

Explant preparation

The whole trachea was aseptically collected upon euthanasia and transported in culture medium consisting of a 1:1 mixture DMEM and Roswell Park Memorial Institute (RPMI) 1640 medium supplemented with penicillin, streptomycin (50 µg/ml, L-glutamine and fungizone (2.5 µg/ml). The tracheas underwent 6 washes over a period of 4 hours in pre-warmed culture medium, being kept at 37°C in a 5% CO2–95% air mixture in a humidified incubator. Extra connective tissue on the cartilage was removed and the tracheas were opened up and cut into six strips that were each cut into square explants of approximately 0.5cm by 0.5cm. The explants were then placed on square pieces of sterile filter paper on top of agarose plugs in 6-well plates mimicking the air interface found in the respiratory tract of the living animal, and kept for up to seven days in 5% CO2 and 37°C in a humidified incubator.

Experimental infections

Explants were infected with a dose of 200 PFU 24 hours after explant preparation (designated as time 0). Culture medium was used for mock-infected explants. Inoculated explants were sampled for, histology and viral replication at 6 hours and every 24 hours post-infection for five days.

Quantification of virus present in infected explants was carried out by immersion of the explants in 0.5 ml of sterile DPBS followed by vortexing for at least five minutes. The supernatant was then quantified by plaque assays as described above.

Interferon Assay

For the IFN assay of horse explants, inoculation with Universal Type I IFN Alpha was carried out by placing increasing concentrations of Universal IFN, diluted in 10µl of DMEM, onto the explants for 24 hours.

6.2.12. Immunohistochemistry

Explants were fixed in 10% (v/v) buffered formalin and paraffin embedded. Subsequently, 4µm paraffin sections were cut and tissue sections were deparaffinised and hydrated using standard procedures. Antigen retrieval was performed using citrate buffer followed by pressure cooker heating. In order to quench endogenous peroxidase, sections were permeabilised with 1% Triton x100 for 10 minutes, and then incubated in a peroxidase blocking buffer for 10 minutes. Sections were incubated overnight at 4°C with either of the following primary antibodies diluted in 10% normal goat serum: polyclonal rabbit anti-NP or monoclonal mouse anti-Mx1. Immunohistochemistry was performed with DAKO supervision system, which included an HRP labelled polymer that is conjugated to secondary antibodies - either an anti-mouse of anti-rabbit secondary depending on primary antibody used, and slides were counterstained with Mayer's haematoxylin. Histological images were taken using cell^D software (Olympus).

6.2.13. Experimental Work Involving Transcriptomics

6.2.13.1. RNA Extraction

Add 1ml of TRIzol®Reagent to the well of a 12-well plate and pipette up and down several times to lyse cells. Incubate the homogenized sample for 5 minutes at room temperature and then add 0.2 mL of chloroform per 1mL of TRIzol®Reagent used for homogenization. Shake tube vigorously by hand for 15 seconds and then incubate for 2–3 minutes at room temperature. Centrifuge the sample at 12,000 × g for 15 minutes at 4°C. Carefully remove the aqueous phase of the sample and avoid contaminating with any of interphase or organic layer. Then add 230ul of 100% ethanol to aqueous phase and mix and add to a column from the RNeasy Mini Kit and centrifuge for 30 seconds at maximum speed. Perform one wash with RW1 buffer from RNeasy Mini Kit and at this point for the complete removal of DNA from sample, use the RNase-Free DNase Set in conjunction. After the DNase I step, continue with the washing steps of the RNeasy Mini Kit. Finally elute in 30ul of nuclease free water.

6.2.13.2. Qubit

The Qubit® 2.0 Fluorometer (Life Techonologies) is used as a precise way to measure RNA concentration within a sample. The Qubit® RNA BR Assay Kit was used as per the manufacturer's instructions.

6.2.13.3. Bioanalyser

Before sending the samples to sequence, the Agilent 2100 Bioanalyzer was used for the analysis of RNA purity by separating the nucleic acid fragments based on their size by electrophoresis. The Agilent RNA Pico Kit was used as per the manufacturer's instructions. Only samples with a RNA Integrity Number (RIN) above or equal to 8 were sequenced.

6.2.13.4. Sequencing

Each sample (Mock, IFN-α, EIV/1963 and EIV/2003) was set up independently three times, and sequenced on separate Illumina runs, with 24 samples being carried out in total. On average, ~28 million reads/sample was generated, Phred quality >30 (A Phred quality score is a measure of the quality of the identification of the nucleobases generated by automated DNA sequencing). Libraries for the samples were prepared using TruSeq Stranded mRNA Library Prep Kit High Throughput (RS-122-2103). Each library was made from 300ng total RNA /per sample and NextSeq® Sequencing System was used, with each sequencing run containing 16 Libraries. NextSeq® 500/550 High Output Kit v2 (75 cycles, FC-404-2005) Cartridges were used.

6.2.13.5. Sequencing quality and assembly

Bioinformatics analysis was performed using the FastQC software (http://www.bioinformatics.babraham.ac.uk/projects/fastqc) to check the RNA-Seq reads quality. Kraken (REF) was used to check the contamination of samples. TopHat2 is a fast splice junction mapper for RNA-Seq reads. It aligns RNA-Seq reads to mammalian-sized genomes using the ultra high-throughput short read aligner Bowtie2, and then analyses the alignment results to identify splice junctions between exons. In the present research, we align the short reads to the *Equus caballus* genome (Equ Cab 2), downloaded via Ensembl (Ensembl

genome browser 84) April 2016. In total, 89.4% of the sequence reads assembled to the reference genome.

6.2.13.6. Differential expression and pathway analysis

CuffDiff2 is a program in the Cufflinks package (v2.2.1). It adopts an algorithm that controls cross-replicate variability and read-alignment ambiguity by using a model for fragment counts based on a beta negative binomial distribution. It can identify differentially expressed transcripts and genes, differential splicing and promoter-preference changes, which returns far more statistically significant differentially expressed genes than microarray analysis. CuffDiff2 was used to identify Differentially Expressed (DE) genes (genes with Benjamini Hochberg *P*-value ≤ 0.05 were considered significant).

6.2.13.7. Data Analysis

Transcriptomics data was analysed using Ingenuity Pathway Analysis (IPA) (https://analysis.ingenuity.com/) software to visualise pathways and produce figures. R Version 3.2.3 (RTeam 2017) was used to produce some figures, as was GraphPad Prism (Anon n.d.).

Chapter 7

7. References

Alberts, B. et al., 2014. Chapter 24: The Adaptive Immune System. In *Molecular Biology of the Cell. 4th edition*. New York.

Ambrose, C.S. & Levin, M.J., 2012. The rationale for quadrivalent influenza vaccines. *Human Vaccines and Immunotherapeutics*, 8(1), pp.81–88.

Anderson, T.C. et al., 2012. Serological evidence of H3N8 canine influenza-like virus circulation in USA dogs prior to 2004. *The Veterinary Journal*, 191(3), pp.312–316. Available at: http://dx.doi.org/10.1016/j.tvjl.2011.11.010.

Ank, N., West, H. & Paludan, S.R., 2006. IFN-λ: Novel Antiviral Cytokines. *Journal of Interferon & Cytokine Research*, Vol. 26, N.

Anon, Graphpad Prism version 6.00. Available at: https://www.graphpad.com/scientific-software/prism/.

Anthony, S.J. et al., 2012. Emergence of Fatal Avian Influenza in New England Harbour Seals. *mBio*, 3(4), pp.1–10.

Audsley, J.M. & Tannock, G.A., 2004. The role of cell culture vaccines in the control of the next influenza pandemic. *Expert Opinion on Biological Therapy*, 4(5), pp.709–717.

Baird, T. & Wek, R., 2012. Eukaryotic initiation factor 2 phosphorylation and translational control in metabolism. *Advances in Nutrition*, 3(3), pp.307–321. Available at: http://dx.doi.org/10.3945/an.112.002113.

Barba, M. & Daly, J., 2016. The Influenza NS1 Protein: What Do We Know in Equine Influenza Virus Pathogenesis? *Pathogens*, 5(3), p.57. Available at: http://www.mdpi.com/2076-0817/5/3/57.

Bouvier, N.M. & Palese, P., 2008. The biology of influenza viruses. *Vaccine*, 86(12), pp.3279–3288.

Capua, I. et al., 2013. Influenza A viruses grow in human pancreatic cells and cause pancreatitis and diabetes in an animal model. *Journal of Virology*, 87(1), pp.597–610.

Chan, A.Y. et al., 2006. Influenza virus inhibits RNA polymerase II elongation. *Virology*, 351(1), pp.210–217.

Chang, K.C. et al., 1990. The influenza resistance murine Mx1 gene is constitutively expressed in the epithelia of the gastrointestinal, respiratory and uterine tracts. *Journal of Cell Science*, 97 (Pt 3), pp.497–502. Available at: http://www.ncbi.nlm.nih.gov/pubmed/2074268.

Chase, G.R.. & Hoel, D.G.., 1975. Serial Dilutions : Error Effects and Optimal Designs. *Biometrika*, 62(2), pp.329–334.

Chauché, C. et al., 2017. Mammalian adaptation of an avian influenza A virus involves stepwise changes in NS1. *Journal of Virology*, 92(5), p.JVI.01875-17. Available at: http://jvi.asm.org/lookup/doi/10.1128/JVI.01875-17.

Chen, B.P. et al., 1994. ATF3 and ATF3 delta Zip. Transcriptional repression versus activation by alternatively spliced isoforms. *The Journal of biological chemistry*, 269(22), pp.15819–15826.

Chen, H. et al., 2009. Critical role for constitutive type I interferon signaling in the prevention of cellular transformation. *Cancer Science*, 100(3):449.

Cheung, T.K.W. & Poon, L.L.M., 2007. Biology of influenza A virus. *Annals of the New York Academy of Sciences*, 1102, pp.1–25.

Choppin, P., Murphy, J. & Tamm, I., 1960. Studies of two kinds of virus particles which comprise influenza A2 virus strains. III Morphological characteristics: Independence of morphological and functional traits. *Journal of Experimental Medicine*, 112:945–95.

Couceiro, J.N.S.S., Paulson, J.C. & Baum, L.G., 1993. Influenza virus strains selectively recognize sialyloligosaccharides on human respiratory epithelium; the role of the host cell in selection of hemagglutinin receptor specificity. *Virus Research*, 29, pp.155–165.

Crawford, P.C. et al., 2005. Transmission of Equine Influenza Virus to Dogs. *Science*, 310(5747), pp.482–485. Available at: http://www.sciencemag.org/cgi/doi/10.1126/science.1117950.

Cullinane, A.A., Rixon, F.J. & Davison, A.J., 1988. Characterization of the genome of equine herpesvirus 1 subtype 2. *Journal of General Virology*, 69(1988), pp.1575–1590.

Daly, J.M. et al., 2008. Transmission of equine influenza virus to english foxhounds. *Emerging Infectious Diseases*, 14(3), pp.461–464.

Daugherty, M.D. & Malik, H.S., 2012. Rules of Engagement : Molecular Insights from Host-Virus Arms Races. *Annual Review of Genetics*.

Desmyter, J., Melnick, J.L. & Rawls, W.E., 1968. Defectiveness of Interferon Production and of Rubella Virus Interference in a Line of African Green Monkey Kidney Cells (Vero). *Journal of Virology*, 2(10), pp.955–61. Available at: http://www.ncbi.nlm.nih.gov/pubmed/4302013%5Cnhttp://www.pubmedcentral.nih.gov/articlerender.fcgi?artid=PMC375423.

Eschbaumer, M. et al., 2016. Transcriptomic Analysis of Persistent Infection with Foot-and-Mouth Disease Virus in Cattle Suggests Impairment of Apoptosis and Cell-Mediated Immunity in the Nasopharynx. *PLoS ONE*, pp.1–30.

Fagerberg, L. et al., 2014. Analysis of the Human Tissue-specific Expression by Genome-wide Integration of Transcriptomics and Antibody-based. *Molecular and Cellular Proteomics*, (2), pp.397–406.

Feng, K.H. et al., 2015. Equine and Canine Influenza H3N8 Viruses Show Minimal Biological. *Journal of Virology*, 89(13), pp.6860–6873.

Frensing, T. et al., 2014. Impact of defective interfering particles on virus replication and antiviral host response in cell culture-based influenza vaccine production. *Applied Microbiology and Biotechnology*, 98(21), pp.8999–9008.

Gack, M.U. et al., 2010. Influenza A virus NS1 targets the ubiquitin ligase TRIM25 to evade recognition by RIG-. *Cell*, 5(5), pp.439–449.

Gale, M. & Katze, M.G., 1998. Molecular mechanisms of interferon resistance

mediated by viral-directed inhibition of PKR, the interferon-induced protein kinase. *Pharmacology and Therapeutics*, 78(1), pp.29–46.

Gambaryan, A. et al., 2005. Receptor specificity of influenza viruses from birds and mammals: New data on involvement of the inner fragments of the carbohydrate chain. *Virology*, 334, pp.276–283.

Gan, H. et al., 2015. Transcription Factor Runx3 Is Induced by Influenza A Virus and Double-Strand RNA and Mediates Airway Epithelial Cell Apoptosis. *Scientific Reports*, 5(April), p.17916. Available at: http://www.ncbi.nlm.nih.gov/pmc/articles/PMC4672321/pdf/srep17916.pdf.

Gao, R. et al., 2013. Human Infection with a Novel Avian-Origin Influenza A (H7N9) Virus. *New England Journal of Medicine*, 368(20), pp.1888–1897. Available at: http://www.nejm.org/doi/10.1056/NEJMoa1304459.

Garten, W. et al., 1981. Proteolytic activation of the influenza virus hemagglutinin: The structure of the cleavage site and the enzymes involved in cleavage. *Virology*, 115(2), pp.361–374.

Gaush, C.R. & Smith, T.F., 1968. Replication and plaque assay of influenza virus in an established line of canine kidney cells. *Applied Microbiology*, 16(4), pp.588–594.

Geraci, J.R. et al., 1982. Mass Mortality of Harbor Seals: Pneumonia Associated with Influenza A Virus. *Science*, 215(4536), pp.1129–1131.

Gilbert, M. et al., 2012. Highly Pathogenic Avian Influenza Virus among Wild Birds in Mongolia. *PLoS ONE*, 7(9), pp.1–9.

Goodbourn, S., Didcock, L. & Randall, R.E., 2000. Interferons: cell signalling, immune modulation, antiviral response and virus countermeasure. *Journal of General Virology*, v.81(2000), p.2341.2364.

Gregersen, J.-P. et al., 2011. Safety of MDCK cell culture-based influenza vaccines. *Future microbiology*, 6(2), pp.143–152.

Guidotti, L.G. & Chisari, F. V, 2000. Cytokine-mediated control of viral infections. *Virology*, 273(2), pp.221–7. Available at: http://www.ncbi.nlm.nih.gov/pubmed/10915592%5Cnhttp://linkinghub.elsevier.com/retrieve/pii/S0042682200904422.

Guo, Y. et al., 1992. Characterization of a new avian-like influenza A virus from horses in China. *Virology*, 188, 245–2.

Guo, Y. et al., 1991. Evolution of Influenza A Virus Nucleoprotein Genes : Implications for the Origins of HlNi Human and Classical Swine Viruses. *Journal of Virology*, 65(7), pp.3704–3714.

Guo, Y. et al., 1995. Seroepidemiological and molecular evidence for the presence of two H3N8 equine influenza viruses in China in 1993-94. *Journal of General Virology*, 76(8), pp.2009–2014.

Guu, T.S.Y., Zheng, W. & Tao, Y.J., 2012. Chapter 11: Bunyavirus: Structure and Replication. In *Viral Molecular Machines*. pp. 245–266.

Hale, B. et al., 2006. Influenza A virus NS1 protein binds p85beta and activates phosphatidylinositol-3-kinase signaling. *Proceedings of the National Academy of Sciences of the United States of America*, 19;103(38).

Hale, B.G., Barclay, W.S., et al., 2008. Structure of an avian influenza A virus NS1 protein effector domain. *Virology*, 378(1), pp.1–5.

Hale, B.G., Randall, R.E., et al., 2008. The multifunctional NS1 protein of influenza A viruses. *Journal of General Virology*, 89(10), pp.2359–2376.

Harder, T.C. & Vahlenkamp, T.W., 2010. Influenza virus infections in dogs and cats. *Veterinary Immunology and Immunopathology*, 134(1–2), pp.54–60. Available at: http://dx.doi.org/10.1016/j.vetimm.2009.10.009.

Hare, D. et al., 2016. The importance of physiologically relevant cell lines for studying virus-host interactions. *Viruses*, 8(11), pp.1–10.

Hasebe, R. et al., 2009. Infectious entry of equine herpesvirus-1 into host cells through different endocytic pathways. *Virology*, 25(4), pp.1163–306.

Hause, B. et al., 2014. Characterization of a novel influenza virus strain in cattle and swine: proposal for a new genus in the Orthomyxoviridae family. *MBio*, 5(2), pp.1–10. Available at: http://dx.doi.org/10.1128/mBio.00031-14.

Hay, A. et al., 2001. The evolution of human influenza viruses. *Philosophical transactions of the Royal Society of London. Series B, Biological sciences*, 356(1416), pp.1861–70. Available at: http://www.pubmedcentral.nih.gov/articlerender.fcgi?artid=1088562&tool=pmcentrez&rendertype=abstract.

Heldt, F.S. et al., 2013. Multiscale Modeling of Influenza A Virus Infection Supports the Development of Direct-Acting Antivirals. *PLoS Computational Biology*, 9(11).

Hoffmann, H.-H., Schneider, W.M. & Rice, C.M., 2015. Interferons and viruses: an evolutionary arms race of molecular interactions. *Trends in Immunology*, 36(3), p.Pages 124-138.

Hovanessian, A.G. et al., 1987. Identification of 69-kd and 100-kd forms of 2-5A synthetase in interferon-treated human cells by specific monoclonal antibodies. *EMBO Journal*, 6(5), pp.1273–1280.

Hughes, T.R., 2009. “Validation” in genome-scale research. *Journal of Biology*.

Ilyushina, N.A. et al., 2012. Comparative study of influenza virus replication in MDCK cells and in primary cells derived from adenoids and airway epithelium. *Journal of Virology*, 86(21), pp.11725–34. Available at: http://www.pubmedcentral.nih.gov/articlerender.fcgi?artid=3486302&tool=pmcentrez&rendertype=abstract.

Isaacs, B.A. & Lindenmann, J., 1957. Virus interference: I. The Interferon. *Cancer Journal for Clinicians*.

Ito, T. et al., 1997. Differences in Sialic Acid-Galactose Linkages in the Chicken Egg Amnion and Allantois Influence Human Influenza Virus Receptor Specificity and Variant Selection. *Jorunal of Virology*, 71(4), pp.3357–3362.

Ito, T. et al., 1998. Molecular basis for the generation in pigs of influenza A viruses with pandemic potential. *Journal of Virology*, 72, 7367–7.

Jackson, A. et al., 1996. A human respiratory-tissue organ culture incorporating an air interface. *American Journal of Respiratory and Critical Care Medicine*, 153:1130–1.

Jackson, D. & Lamb, R.A., 2008. The influenza A virus spliced messenger RNA M mRNA3 is not required for viral replication in tissue culture. *Journal of General Virology*, 89(0 12), pp.3097–3101.

Jagger, B.W. et al., 2012. An overlapping protein-coding region in influenza A virus segment 3 modulates the host response. *Science*, 337(6091), pp.199–204.

Jang, Y. et al., 2005. Development of rhinovirus study model using organ culture of turbinate mucosa. *Journal of Virological Methods*, 125:41–47.

Jilg, N. et al., 2014. Kinetic differences in the induction of interferon stimulated genes by interferon-α and interleukin 28B are altered by infection with hepatitis C virus. *Hepatology*, 59(4), pp.1250–1261. Available at: http://doi.wiley.com/10.1002/hep.26653.

Johnson, N.P.A.S. & Mueller, J., 2002. Updating the Accounts : Global Mortality of the 1918-1920 " Spanish " Influenza Pandemic Updating the Accounts : Global Mortality of the 1918 – 1920 " Spanish " Influenza Pandemic. *Bulletin of the History of Medicine*, 76(1), pp.105–115.

Josset, L. et al., 2014. Transcriptomic Characterization of the Novel Avian-Origin Influenza A (H7N9) Virus: Specific Host Response and Responses Intermediate between Avian (H5N1 and H7N7) and Human (H3N2) Viruses and Implications for Treatment Options. *mBio*, 5(7), pp.1–12.

Katze, M.G. & Krug, R.M., 1984. Metabolism and expression of RNA polymerase II transcripts in influenza virus-infected cells. *Molecular and Cellular Biology*, 4, 2198–20.

Kaverin, N. V & Webster, R.G., 1995. Impairment of Multicycle Influenza Virus Growth in Vero (WHO) Cells by Loss of Trypsin Activity. *Journal of Virology*, 69(4), pp.2700–2703.

Kawaoka, Y. et al., 1988. Is the gene pool of influenza viruses in shorebirds and gulls different from that in wild ducks? *Virology*, 163(1), pp.247–250.

Khaperskyy, D.A. et al., 2016. Selective Degradation of Host RNA Polymerase II Transcripts by Influenza A Virus PA-X Host Shutoff Protein. *PLoS Pathogens*, pp.1–25.

Khuu, C.H. et al., 2007. Activating transcription factor 3 (ATF3) represses the expression of CCL4 in murine macrophages. *Molecular Immunology*, 44(7), pp.1598–1605.

Kilbourne, E.D. et al., 2002. The total influenza vaccine failure of 1947 revisited: Major intrasubtypic antigenic change can explain failure of vaccine in a post-World War II epidemic. *Proceedings of the National Academy of Sciences of the United States of America*, 99(16), pp.10748–

10752.

Klenk, H.D. et al., 1975. Activation of influenza A viruses by trypsin treatment. *Virology*, 68(2), pp.426–439.

Kochs, G. et al., 2009. Strong interferon-inducing capacity of a highly virulent variant of influenza A virus strain PR8 with deletions in the NS1 gene. *Journal of General Virology*, 90(12), pp.2990–2994.

Kochs, G., Garcia-Sastre, A. & Martinez-Sobrido, L., 2007. Multiple anti-interferon actions of the influenza A virus NS1 protein. *Journal of Virology*, 81, 7011–2.

Krug, R.M., 2015. Functions of the Influenza A Virus NS1 Protein In Antiviral Defense. *Current Opinion in Virology*, (12), pp.1–6.

Krug, R.M. et al., 2003. Intracellular warfare between human influenza viruses and human cells: The roles of the viral NS1 protein. *Virology*, 309(2), pp.181–189.

Kuiken, T. et al., 2006. Host Species Barriers to Influenza Virus Infections. *Science*, (April), pp.394–398.

Lamb, R.A. & Krug, R.M., 2001. Orthomyxoviridae: The Viruses and Their Replication. In D. M. K. & P. & M. Howley, eds. *Fields Virology*. Lippincott Williams & Wilkins, Philadelphia.

Lamb, R.A. & Pinto, L.H., 2006. The proton selective ion channels of influenza A and B viruses. In Y. Kawaoka, ed. *Influenza Virology: Current Topics*. Caister Academic Press., pp. 65–93.

Larner, A.C., Chaudhuri, A. & Darnell, J.E., 1986. Transcriptional Induction by Interferon. New protein(s) determine the extent and length of the induction. *The Journal of biological chemistry*, 2(7), pp.453–459.

Lauring, A.S., Frydman, J. & Andino, R., 2013. The role of mutational robustness in RNA virus evolution. *Nature Reviews Microbiology*, 11(5), pp.327–336. Available at: http://dx.doi.org/10.1038/nrmicro3003.

Lee, C.W. et al., 2008. Evaluation of chicken-origin (DF-1) and quail-origin (QT-6) fibroblast cell lines for replication of avian influenza viruses. *Journal of Virological Methods*, 153(1), pp.22–28.

Lee, C.W. & Saif, Y.M., 2009. Avian influenza virus. *Comparative Immunology, Microbiology & Infectious Diseases*, 32, 301–31.

Lee, D.C.W. et al., 2010. Differential replication of avian influenza H9N2 viruses in human alveolar epithelial A549 cells. *Virology Journal*, pp.1–5.

Li, J., Ding, S.C. & Cho, H., 2013. A Short Hairpin RNA Screen of Interferon-Stimulated Genes Identifies. *American Society for Microbiology*, 4(3), pp.e00385-13. Available at: http://eutils.ncbi.nlm.nih.gov/entrez/eutils/elink.fcgi?dbfrom=pubmed&id=23781071&retmode=ref&cmd=prlinks%5Cnpapers3://publication/doi/10.1128/mBio.00385-13.

Li, S. et al., 2010. Avian-origin H3N2 canine influenza A viruses in Southern

China. *Infection, Genetics and Evolution*, 10(8): 128.

Lin, C. et al., 2001. Cultures of equine respiratory epithelial cells and organ explants as tools for the study of equine influenza virus infection Brief Report. *Archives of Virology*, pp.2239–2247.

Liu, P. et al., 2016. Transcriptome analysis of genes responding to NNV infection in Asian seabass epithelial cells. *Fish and Shellfish Immunology*, 54, pp.342–352. Available at: http://dx.doi.org/10.1016/j.fsi.2016.04.029.

Lu, Y. et al., 1995. Binding of the influenza virus NS1 protein to double-stranded RNA inhibits the activation of the protein kinase that phosphorylates the elF-2 translation initiation factor. *Virology*, 214(1), pp.222–228.

Marc, D., 2014. Influenza virus non-structural protein NS1: Interferon antagonism and beyond. *Journal of General Virology*, 95(2014), pp.2594–2611.

Masters, J.R. & Stacey, G.N., 2007. Changing medium and passaging cell lines. *Nature Protocols*, 2(9), pp.2276–2284.

McCollum, W., 1986. Responses of horses vaccinated with avirulent modified-live equine arteritis virus propagated in the E. Derm (NBL-6) cell line to nasal inoculation with virulent virus. *American Journal of Veterinary Research*, Sep;47(9):

Morens, D.M. & Fauci, A.S., 2007. The 1918 influenza pandemic: insights for the 21st century. *The Journal of Infectious Diseases*, 195(7), pp.1018–1028. Available at: http://jid.oxfordjournals.org/content/195/7/1018.full.pdf.

Morens, D.M. & Taubenberger, J.K., 2010. An avian outbreak associated with panzootic equine influenza in 1872: an early example of highly pathogenic avian influenza? *Influenza and other Respiratory Viruses*, pp.373–377.

Morrison, J. et al., 2014. H7N9 and other pathogenic avian influenza viruses elicit a three-pronged transcriptomic signature that is reminiscent of 1918 influenza virus and is associated with lethal outcome in mice. *Journal of Virology*, 88(18), pp.10556–68. Available at: http://www.pubmedcentral.nih.gov/articlerender.fcgi?artid=4178843&tool=pmcentrez&rendertype=abstract.

Munoz-Fontela, C. et al., 2005. Resistance to viral infection of super p53 mice. *Oncogene*, 21;24(18):

Murcia, P.R. et al., 2010. Intra- and interhost evolutionary dynamics of equine influenza virus. *Journal of Virology*, 84(14), pp.6943–54. Available at: http://jvi.asm.org/content/84/14/6943.full.

Murcia, P.R., Wood, J.L.N. & Holmes, E.C., 2011. Genome-scale evolution and phylodynamics of equine H3N8 influenza A virus. *Journal of Virology*, 85(11), pp.5312–22. Available at: http://www.pubmedcentral.nih.gov/articlerender.fcgi?artid=3094979&tool=pmcentrez&rendertype=abstract.

Naffakh, N. et al., 2000. Genetic analysis of the compatibility between polymerase proteins from human and avian strains of influenza A viruses. *Journal of General Virology*, 81(5), pp.1283–1291.

Neumann, G., Noda, T. & Kawaoka, Y., 2009. Emergence and pandemic potential of swine-origin H1N1 influenza virus. *Nature*, 459, pp.931–939.

Noda, T. et al., 2006. Architecture of ribonucleoprotein complexes in influenza A virus particles. *Nature*, 439(7075), pp.490–492. Available at: http://www.nature.com/doifinder/10.1038/nature04378.

Nunes, S.F. et al., 2010. An ex vivo swine tracheal organ culture for the study of influenza infection. *Influenza and other Respiratory Viruses*, 4(1), pp.7–15.

Oxburgh, L. et al., 1994. Evolution of H3N8 equine influenza virus from 1963 to 1991. *Virus Research*, 34, pp.153–165.

Parvin, R. et al., 2015. Differential replication properties among H9N2 avian influenza viruses of Eurasian origin. *Veterinary Research*, 46(1), pp.1–11. Available at: http://dx.doi.org/10.1186/s13567-015-0198-8.

Payungporn, S. et al., 2008. Influenza A virus (H3N8) in dogs with respiratory disease, Florida. *Emerging Infectious Diseases*, 14(6), pp.902–908.

Pecoraro, H.L. et al., 2013. Comparison of the infectivity and transmission of contemporary canine and equine H3N8 influenza viruses in dogs. *Veterinary Medicine International*, 2013.

Penhoet, E. et al., 1971. RNA-Dependent RNA Polymerase Activity in Influenza Virions. *Proceedings of the National Academy of Sciences of the United States of America*, 68(6), pp.1369–1371.

Petri, T., Patterson, S. & Dimmock, N.J., 1982. Polymorphism of the NS1 proteins of type A influenza virus. *Journal of General Virology*, 61(2), pp.217–231.

Pinto, L.H., Holsinger, L.J. & Lamb, R.A., 1992. Influenza virus M2 protein has ion channel activity. *Cell*, 69, pp.517–528.

Pleschka, S., 2013. Overview of Influenza Viruses. *Current Topics in Microbiology and Immunology*.

Plotch, S.J. et al., 1981. A unique cap(m7GpppXm)-dependent influenza virion endonuclease cleaves capped RNAs to generate the primers that initiate viral RNA transcription. *Cell*, 23, pp.847–58.

Plotch, S.J. & Krug, R.M., 1977. Influenza virion transcriptase: synthesis in vitro of large, polyadenylic acid-containing complementary RNA. *Journal of Virology*, 21, pp.24–34.

Portela, A. & Digard, P., 2002. The influenza virus nucleoprotein: a multifunctional RNA-binding protein pivotal to virus replication. *Journal of General Virology*, 83, pp.723–34.

Priestnall, S. et al., 2009. Quantification of mRNA encoding cytokines and chemokines and assessment of ciliary function in canine tracheal epithelium during infection with canine respiratory coronavirus (CRCoV). *Veterinary Immunology and Immunopathology*, 127:38–46.

Qureshi, S.A. et al., 1996. Function of Stat2 protein in transcriptional activation by alpha interferon. *Molecular and cellular biology*, 16(1), pp.288–93.

Available at: http://www.pubmedcentral.nih.gov/articlerender.fcgi?artid=231002&tool=pmcentrez&rendertype=abstract.

Ragimbeau, J. et al., 2003. The tyrosine kinase Tyk2 controls IFNAR1 cell surface expression. *EMBO Journal*, 22(3), pp.537–547.

Rambaut, A. et al., 2008. The genomic and epidemiological dynamics of human influenza A virus. *Nature*, 453(7195), pp.615–619.

Randall, R.E. & Goodbourn, S., 2008. Interferons and viruses: An interplay between induction, signalling, antiviral responses and virus countermeasures. *Journal of General Virology*, 89(1), pp.1–47.

Ratinier, M. et al., 2016. Bluetongue virus NS4 protein is an interferon antagonist and a determinant of virus virulence. *Journal of Virology*, 44(March), p.JVI.00422-16. Available at: http://jvi.asm.org/lookup/doi/10.1128/JVI.00422-16.

Reddel, R., 2010. Senescence: an antiviral defense that is tumor suppressive? *Carcinogenensis*.

Rivailler, P. et al., 2010. Evolution of canine and equine influenza (H3N8) viruses co-circulating between 2005 and 2008. *Virology*, 408(1), pp.71–79. Available at: http://dx.doi.org/10.1016/j.virol.2010.08.022.

Rivas, H.G., Schmaling, S.K. & Gaglia, M.M., 2016. Shutoff of host gene expression in influenza A virus and herpesviruses: Similar mechanisms and common themes. *Viruses*, 8(4), pp.1–26.

Robinson, M.D., McCarthy, D.J. & Smyth, G.K., 2009. edgeR: A Bioconductor package for differential expression analysis of digital gene expression data. *Bioinformatics*, 26(1), pp.139–140.

Ronni, T. et al., 1997. Regulation of IFN-alpha/beta, MxA, 2',5'-oligoadenylate synthetase, and HLA gene expression in influenza A-infected human lung epithelial cells. *Journal of Immunology*, 158(5), pp.2363–74. Available at: http://www.ncbi.nlm.nih.gov/pubmed/9036986.

Rossman, J. & Lamb, R., 2011. Influenza virus assembly and budding. *Virology*, 15;411(2):

RTeam, R.D.C., 2017. R: A Language and Environment for Statistical Computing. *R Foundation for Statistical Computing*. Available at: https://www.r-project.org/.

Sadler, A.J. & Williams, B.R.G., 2008. Interferon-inducible antiviral effectors. *Nature Reviews Immunology*, 8(7), pp.559–568.

Salk, J.E. & Suriano, P.C., 1949. Importance of antigenic composition of influenza virus vaccine in protecting against the natural disease. *American Journal of Public Health*, 39, pp.345–355.

Samuel, C.E., 1991. Antiviral Actions of Interferon Cellular Proteins and Their Surprisingly Interferon-Regulated Selective Antiviral Activities. *Virology*, 11.

Scheuner, D. et al., 2006. Double-stranded RNA-dependent protein kinase

phosphorylation of the alpha-subunit of eukaryotic translation initiation factor 2 mediates apoptosis. *The Journal of biological chemistry*, 28;281(30).

Seitz, C. et al., 2010. High yields of influenza A virus in Madin-Darby canine kidney cells are promoted by an insufficient interferon-induced antiviral state. *Journal of General Virology*, 91(7), pp.1754–1763.

Seitz, C. et al., 2012. Trypsin promotes efficient influenza vaccine production in MDCK cells by interfering with the antiviral host response. *Applied Microbiology and Biotechnology*, 93(2), pp.601–611.

Seladi-Schulman, J., Steel, J. & Lowen, A.C., 2013. Spherical Influenza Viruses Have a Fitness Advantage in Embryonated Eggs, while Filament-Producing Strains Are Selected In Vivo. *Journal of Virology*, 87 no.

Selman, M. et al., 2012. Adaptive mutation in influenza A virus non-structural gene is linked to host switching and induces a novel protein by alternative splicing. *Emerging Microbes and Infections*, 1(0), p.0. Available at: http://dx.doi.org/10.1038/emi.2012.38.

Seyednasrollah, F., Laiho, A. & Elo, L.L., 2013. Comparison of software packages for detecting differential expression in RNA-seq studies. *Briefings in Bioinformatics*, 16(1), pp.59–70.

Shalek, A.K. et al., 2013. Single-cell transcriptomics reveals bimodality in expression and splicing in immune cells. *Nature*, 498(7453):

Sharp, G.B. et al., 1997. Coinfection of Wild Ducks by Influenza A Viruses: Distribution Patterns and Biological Significance. *Journal of Virology*, 71(8), pp.6128–6135.

Shope, R.E., 1931. Swine influenza: I. Experimental transmission and pathology. *The Journal of Experimental Medicine*, 54(3), pp.349–59. Available at: http://www.pubmedcentral.nih.gov/articlerender.fcgi?artid=2131998&tool=pmcentrez&rendertype=abstract.

Simon, P.F. et al., 2015. Highly pathogenic H5N1 and novel H7N9 influenza A viruses induce more profound proteomic host responses than seasonal and pandemic H1N1 strains. *Journal of Proteome Research*, 14(11), pp.4511–4523.

Smith, W. et al., 1933. A Virus obtained from influenza patients. *Reviews in Medical Virology*, 5(4), pp.187–191.

Solórzano, A. et al., 2005. Mutations in the NS1 Protein of Swine Influenza Virus Impair Anti-Interferon Activity and Confer Attenuation in Pigs. *Journal of Virology*, 79(12), pp.7535–7543.

Song, D. et al., 2008. Transmission of Avian Influenza Virus (H3N2) to Dogs. *Emerging Infectious Diseases*, 14(5), pp.741–746.

Sovinova, O. et al., 1958. Isolation of a virus causing respiratory disease in horses. *Acta Virologica*, Jan-Mar(2(1)), pp.52–61.

Staeheli, P. et al., 1986. Mx Protein: Constitutive Expression in 3T3 Cells Transformed with Cloned Mx cDNA Confers Selective Resistance to Influenza

Virus. *Cell*, 44(1), pp.147–158.

Steinhauer, D.A. & Holland, J.J., 1987. Rapid evolution of RNA viruses. *Annual Review of Microbiology*, 41:409–33.

Steinhauer, D. a, 1999. Role of hemagglutinin cleavage for the pathogenicity of influenza virus. *Virology*, 258(1), pp.1–20.

Su, S. et al., 2013. Avian-origin H3N2 canine influenza virus circulating in farmed dogs in Guangdong, China. *Infection, Genetics and Evolution*, 14, pp.444–449.

Subbarao, K. & Katz, J., 2000. Avian influenza viruses infecting humans. *Cellular and molecular life sciences : CMLS*, 57(12), pp.1770–1784.

Suzuki, Y. et al., 2000. Sialic Acid Species as a Determinant of the Host Range of Influenza A Viruses. *Journal of Virology*, 74(24), pp.11825–11831.

Telford, E.A. et al., 1992. The DNA Sequence of Equine Herpesvirus-1. *Virology*, 79(July 1991), pp.1197–1203.

Tobita, K. et al., 1975. Plaque assay and primary isolation of influenza A viruses in an established line of canine kidney cells (MDCK) in the presence of trypsin. *Medical Microbiology and Immunology*, 162(1), pp.9–14. Available at: http://www.ncbi.nlm.nih.gov/entrez/query.fcgi?db=pubmed&cmd=Retrieve&dopt=AbstractPlus&list_uids=1214709.

Tong, S. et al., 2013. New World Bats Harbor Diverse Influenza A Viruses. *PLoS Pathogens*, 9(10).

Trapnell, C. et al., 2013. Differential analysis of gene regulation at transcript resolution with RNA-seq. *Nature Biotechnology*, 31(1), pp.46–53. Available at: http://dx.doi.org/10.1038/nbt.2450.

Tu, J. et al., 2009. Isolation and molecular characterization of equine H3N8 influenza viruses from pigs in China. *Archives of Virology*, pp.887–890.

Uetani, K. et al., 2008. Influenza A virus abrogates IFN-γ response in respiratory epithelial cells by disruption of the Jak/Stat pathway. *European Journal of Immunology*, 38(6), pp.1559–1573.

Ulfert, R. et al., 2014. Uncoupling of the dynamics of host–pathogen interaction uncovers new mechanisms of viral interferon antagonism at the single-cell level. *Nucleic Acids Research*, 42, p.109.

Verhelst, J. et al., 2012. Interferon-Inducible Protein Mx1 Inhibits Influenza Virus by Interfering with Functional Viral Ribonucleoprotein Complex. *Journal of Virology*, 86(24), pp.13445–13455.

Waddell, G., Teigland, M. & Sigel, M., 1963. A new influenza virus associated with equine respiratory disease. *Journal of the American Veterinary Medical Association*, (Sep 15, 143), pp.587–90.

Weber-Gerlach, M. & Weber, F., 2016. To Conquer the Host, Influenza Virus Is Packing It In: Interferon-Antagonistic Strategies beyond NS1. *Journal of Virology*, 90(19), pp.8389–8394.

Weber, A.P.M., 2015. Discovering new biology through RNA-Seq. *Plant Physiology*, 169(3):, pp.1524–31.

Webster, R.G., 1993. Are equine 1 influenza viruses still present in horses? *Equine Veterinary Journal*, 25(6), pp.537–538.

Webster, R.G. et al., 1992. Evolution and ecology of influenza A viruses. *Microbiological reviews*, 56(1), pp.152–79. Available at: http://www.ncbi.nlm.nih.gov/pubmed/1579108%5Cnhttp://www.pubmedcentral.nih.gov/articlerender.fcgi?artid=PMC372859.

Webster, R.G. et al., 1992. Evolution and Ecology of Influenza A Viruses. *Microbiological Reviews*, 56(1), pp.152–179.

White, D.O. & Cheyne, I.M., 1966. Early Events in the Eclipse Phase of Influenza and Parainfluenza Virus Infection. *Virology*, 29(1), pp.49–59.

Whittaker, G. & Digard, P., 2006. Entry and intracellular transport of influenza virus. In *Influenza virology: current topics*. p. Kawaoka Y, editor. Norfolk: Caister Academic Press.

van Wielink, R. et al., 2011. MDCK cell line with inducible allele B NS1 expression propagates delNS1 influenza virus to high titres. *Vaccine*, 29:6976–69.

Wise, H.M. et al., 2009. A Complicated Message: Identification of a Novel PB1-Related Protein Translated from Influenza A Virus Segment 2 mRNA. *Journal of Virology*, 83(16), pp.8021–8031. Available at: http://jvi.asm.org/cgi/doi/10.1128/JVI.00826-09.

Wise, H.M. et al., 2009. Identification of a Novel Splice Variant Form of the Influenza A Virus M2 Ion Channel with an Antigenically Distinct Ectodomain. *Journal of Virology*, 83(16).

World Health Organization, 2018. http://www.who.int/mediacentre/factsheets/fs211/en/. Available at: http://www.who.int/mediacentre/factsheets/fs211/en/.

Wright, P.F., Neumann, G. & Kawaoka, Y., 2007. Orthomyxoviruses. In *Fields Virology*. pp. 1691–1740.

Wurzer, W. et al., 2003. Caspase 3 activation is essential for neuroprotection in preconditioning. *Proc Natl Acad Sci U S A*, 100(2), pp.715–720. Available at: http://www.ncbi.nlm.nih.gov/entrez/query.fcgi?cmd=Retrieve&db=PubMed&dopt=Citation&list_uids=12522260.

Yamanaka, T. et al., 2010. Infectivity and pathogenicity of canine H3N8 influenza A virus in horses. *Influenza and other Respiratory Viruses*, 4(6), pp.345–351.

Yamanaka, T. et al., 2012. No evidence of horizontal infection in horses kept in close contact with dogs experimentally infected with canine influenza A virus (H3N8). *Acta Veterinaria Scandinavica*, 54, p.25. Available at: http://www.ncbi.nlm.nih.gov/entrez/query.fcgi?cmd=Retrieve&db=PubMed&dopt=Citation&list_uids=22506984%5Cnhttp://www.actavetscand.com/content/pdf/1751-0147-54-25.pdf.

Yamayoshi, S. et al., 2016. Identification of a Novel Viral Protein Expressed from the PB2 Segment of Influenza A Virus. *Journal of Virology*, 90(1), pp.444–456. Available at: http://jvi.asm.org/lookup/doi/10.1128/JVI.02175-15.

Yondon, M. et al., 2014. Equine Influenza A (H3N8) Virus Isolated from Bactrian Camel, Mongolia. *Emerging Infectious Diseases*, 20(12), pp.2012–2015.

Zanin, M. et al., 2015. Pandemic swine H1N1 influenza viruses with almost undetectable neuraminidase activity do not transmit via aerosols in ferrets and are inhibited by human mucus, but not swine mucus. *Journal of Virology*, 89(11), p.JVI.02537-14. Available at: http://www.ncbi.nlm.nih.gov/pubmed/25810540%5Cnhttp://jvi.asm.org/lookup/doi/10.1128/JVI.02537-14.

Zhang, Z.H. et al., 2014. A comparative study of techniques for differential expression analysis on RNA-seq data. *PLoS ONE*, 9(8).

Zhou, Z. et al., 2007. Type III interferon (IFN) induces a type I IFN-like response in a restricted subset of cells through signaling pathways involving both the Jak-STAT pathway and the mitogen-activated protein kinases. *Journal of Virology*, 81(14):774.

Zurlo, J., Rudacille, D. & Goldberg, A.M., 1996. The three Rs: the way forward. *Environmental Health Perspectives*, 104(8): 87.